Methods in
Molecular Biology 2175

Springer Protocols

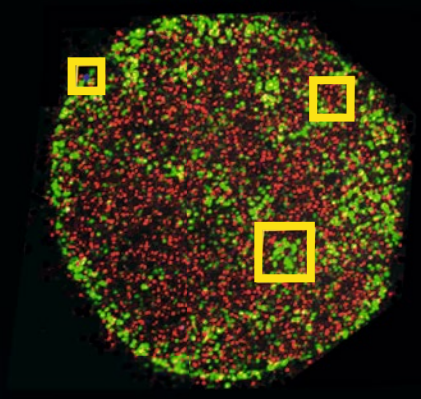

Ronald Hancock *Editor*

The Nucleus

Third Edition

Humana Press

METHODS IN MOLECULAR BIOLOGY

Series Editor
John M. Walker
School of Life and Medical Sciences
University of Hertfordshire
Hatfield, Hertfordshire, UK

For further volumes:
http://www.springer.com/series/7651

For over 35 years, biological scientists have come to rely on the research protocols and methodologies in the critically acclaimed *Methods in Molecular Biology* series. The series was the first to introduce the step-by-step protocols approach that has become the standard in all biomedical protocol publishing. Each protocol is provided in readily-reproducible step-by-step fashion, opening with an introductory overview, a list of the materials and reagents needed to complete the experiment, and followed by a detailed procedure that is supported with a helpful notes section offering tips and tricks of the trade as well as troubleshooting advice. These hallmark features were introduced by series editor Dr. John Walker and constitute the key ingredient in each and every volume of the *Methods in Molecular Biology* series. Tested and trusted, comprehensive and reliable, all protocols from the series are indexed in PubMed.

The Nucleus

Third Edition

Edited by

Ronald Hancock

Biosystems Group, Biotechnology Center, Silesian University of Technology, Gliwice, Poland

Humana Press

Editor
Ronald Hancock
Biosystems Group, Biotechnology Center
Silesian University of Technology
Gliwice, Poland

ISSN 1064-3745 ISSN 1940-6029 (electronic)
Methods in Molecular Biology
ISBN 978-1-0716-0762-6 ISBN 978-1-0716-0763-3 (eBook)
https://doi.org/10.1007/978-1-0716-0763-3

Cover Illustration Caption: Single molecule localization image of a section of a nucleus labeled with an ALU-specific oligonucleotide (red) and an antibody against H3K9me3 (heterochromatin, green) (see Chapter 6 by Hausmann et al).

This Humana imprint is published by the registered company Springer Science+Business Media, LLC, part of Springer Nature.
The registered company address is: 1 New York Plaza, New York, NY 10004, U.S.A.

Preface

This third edition of *The Nucleus* presents recently developed and detailed protocols for those working on the cell nucleus, including some less well-explored aspects. The volumes in this series are designed primarily for researchers, but when recalling my own experience as a PhD student which included visits to all the neighboring laboratories to see the most recent methods at work, they should also help students and postdocs to be aware of available methodologies when planning their projects.

I thank the authors who contributed to this book for their friendly and timely collaboration, and Joanna Rzeszowska and Andrzej Świerniak for their support during its preparation.

Gliwice, Poland ***Ronald Hancock***

Contents

Contributors

David Anchel • *Genetics and Genome Biology Program, The Hospital for Sick Children, Toronto, ON, Canada*

Eugene A. Arifulin • *Belozersky Institute of Physico-Chemical Biology, Lomonosov Moscow State University, Moscow, Russia*

Michael D. Bartoschek • *Department of Biology II and Center for Integrated Protein Science Munich (CIPSM), Human Biology and BioImaging, Ludwig-Maximilians-Universität München, Munich, Germany*

Lutz Berwanger • *IUF-Leibniz Research Institute of Environmental Medicine at Heinrich-Heine-University Duesseldorf, Duesseldorf, Germany*

Marco Biggiogera • *Laboratory of Cell Biology and Neurobiology, Department of Biology and Biotechnology, University of Pavia, Pavia, Italy*

Arnold J. Boersma • *DWI-Leibniz Institute for Interactive Materials, Aachen, Germany*

Reagan W. Ching • *Genetics and Genome Biology Program, The Hospital for Sick Children, Toronto, ON, Canada; Department of Epigenetics, Max Planck Institute of Immunobiology and Epigenetics, Freiburg, Germany*

Alexey I. Chizhik • *Third Institute of Physics – Biophysics, Georg August University, Göttingen, Germany*

Anna M. Chizhik • *Third Institute of Physics – Biophysics, Georg August University, Göttingen, Germany*

Laure Crabbe • *LBCMCP, Centre de Biologie Integrative (CBI), CNRS, Université de Toulouse, Toulouse, France*

Jörg Enderlein • *Third Institute of Physics – Biophysics, Georg August University, Göttingen, Germany; Multiscale Bioimaging: from Molecular Machines to Networks of Excitable Cells (MBExC), Georg August University, Göttingen, Germany*

Jiří Fajkus • *Laboratory of Functional Genomics and Proteomics, National Centre for Biomolecular Research, Faculty of Science, Masaryk University, Brno, Czech Republic; Mendel Centre for Plant Genomics and Proteomics, Central European Institute of Technology, Masaryk University, Brno, Czech Republic; Institute of Biophysics, Academy of Sciences of the Czech Republic, v.v.i., Brno, Czech Republic*

Ingo Gregor • *Third Institute of Physics – Biophysics, Georg August University, Göttingen, Germany*

Michael Hausmann • *Kirchhoff Institute for Physics, University of Heidelberg, Heidelberg, Germany*

Peter Hemmerich • *Leibniz Institute on Aging-Fritz Lipmann Institute, Jena, Germany*

Georg Hildenbrand • *Kirchhoff Institute for Physics, University of Heidelberg, Heidelberg, Germany*

Urszula Jankowska • *Laboratory of Proteomics and Mass Spectrometry, Malopolska Centre of Biotechnology, Jagiellonian University, Krakow, Poland*

Narain Karedla • *Third Institute of Physics – Biophysics, Georg August University, Göttingen, Germany*

Sylwia Kedracka-Krok • *Department of Physical Biochemistry, Faculty of Biochemistry, Biophysics and Biotechnology, Jagiellonian University, Krakow, Poland*

Ralph H. Kehlenbach • *Department of Molecular Biology, GZMB, University Medical Center of Göttingen, Georg August University, Göttingen, Germany*
Zachary Klase • *Department of Pharmacology and Physiology, Drexel University College of Medicine, Philadelphia, PA, USA*
Matthias Krufczik • *Kirchhoff Institute for Physics, University of Heidelberg, Heidelberg, Germany*
Jin-Ho Lee • *Kirchhoff Institute for Physics, University of Heidelberg, Heidelberg, Germany*
Heinrich Leonhardt • *Department of Biology II and Center for Integrated Protein Science Munich (CIPSM), Human Biology and BioImaging, Ludwig-Maximilians-Universität München, Munich, Germany*
Yuan Li • *Department of Infectious Diseases and Vaccines, MRL, Merck & Co. Inc., West Point, PA, USA*
Peng Mao • *School of Molecular Biosciences, Washington State University, Pullman, WA, USA*
Raul Martínez-Zaguilán • *Department of Cell Physiology and Molecular Biophysics, Texas Tech University Health Sciences Center, Lubbock, TX, USA*
Sara N. Mouton • *European Research Institute for the Biology of Ageing, University of Groningen, University Medical Center Groningen, Groningen, The Netherlands*
Janine Pfaff • *Department of Molecular Biology, GZMB, University Medical Center of Göttingen, Georg August University, Göttingen, Germany*
Annette Piechulek • *IUF-Leibniz Research Institute of Environmental Medicine at Heinrich-Heine-University Duesseldorf, Duesseldorf, Germany*
Anna R. Poetsch • *St. Anna Children's Cancer Research Institute, Vienna, Austria*
Daja Ruhlandt • *Third Institute of Physics – Biophysics, Georg August University, Göttingen, Germany*
Luca Sardo • *Department of Infectious Diseases and Vaccines, MRL, Merck & Co. Inc., West Point, PA, USA*
Šárka Schořová • *Laboratory of Functional Genomics and Proteomics, National Centre for Biomolecular Research, Faculty of Science, Masaryk University, Brno, Czech Republic*
Petra Procházková Schrumpfová • *Laboratory of Functional Genomics and Proteomics, National Centre for Biomolecular Research, Faculty of Science, Masaryk University, Brno, Czech Republic; Mendel Centre for Plant Genomics and Proteomics, Central European Institute of Technology, Masaryk University, Brno, Czech Republic*
Souad R. Sennoune • *Department of Cell Physiology and Molecular Biophysics, Texas Tech University Health Sciences Center, Lubbock, TX, USA*
Eugene V. Sheval • *Belozersky Institute of Physico-Chemical Biology, Lomonosov Moscow State University, Moscow, Russia; Department of Cell Biology and Histology, Faculty of Biology, Lomonosov Moscow State University, Moscow, Russia*
Stella Siciliani • *Laboratory of Cell Biology and Neurobiology, Department of Biology and Biotechnology, University of Pavia, Pavia, Italy*
Aaron Sievers • *Kirchhoff Institute for Physics, University of Heidelberg, Heidelberg, Germany*
Bozena Skupien-Rabian • *Department of Physical Biochemistry, Faculty of Biochemistry, Biophysics and Biotechnology, Jagiellonian University, Krakow, Poland*
Michal Sobecki • *Institute of Anatomy, University of Zurich, Zurich, Switzerland*
Dmitry V. Sorokin • *Laboratory of Mathematical Methods of Image Processing, Faculty of Computational Mathematics and Cybernetics, Lomonosov Moscow State University, Moscow, Russia*

Enes Ugur • *Department of Biology II and Center for Integrated Protein Science Munich (CIPSM), Human Biology and BioImaging, Ludwig-Maximilians-Universität München, Munich, Germany*

David Umlauf • *LBCMCP, Centre de Biologie Integrative (CBI), CNRS, Université de Toulouse, Toulouse, France*

Yegor S. Vassetzky • *Koltzov Institute of Developmental Biology of the Russian Academy of Sciences, Moscow, Russia; UMR9018, CNRS, Institut de Cancérologie Gustave Roussy, Université Paris-Saclay, Villejuif, France*

Liesbeth M. Veenhoff • *European Research Institute for the Biology of Ageing, University of Groningen, University Medical Center Groningen, Groningen, The Netherlands*

Anna von Mikecz • *IUF-Leibniz Research Institute of Environmental Medicine at Heinrich-Heine-University Duesseldorf, Duesseldorf, Germany*

John J. Wyrick • *School of Molecular Biosciences, Washington State University, Pullman, WA, USA; Center for Reproductive Biology, Washington State University, Pullman, WA, USA*

Lorena Zannino • *Laboratory of Cell Biology and Neurobiology, Department of Biology and Biotechnology, University of Pavia, Pavia, Italy*

Chapter 1

Live-Cell Imaging and Analysis of Nuclear Body Mobility

Dmitry V. Sorokin, Eugene A. Arifulin, Yegor S. Vassetzky, and Eugene V. Sheval

Abstract

The cell nucleus contains different domains and nuclear bodies, whose position relative to each other inside the nucleus can vary depending on the physiological state of the cell. Changes in the three-dimensional organization are associated with the mobility of individual components of the nucleus. In this chapter, we present a protocol for live-cell imaging and analysis of nuclear body mobility. Unlike other similar protocols, our image analysis pipeline includes non-rigid compensation for global motion of the nucleus before particle tracking and trajectory analysis, leading to precise detection of intranuclear movements. The protocol described can be easily adapted to work with most cell lines and nuclear bodies.

Key words Nucleus, Nuclear body, Mobility, Interphase prenucleolar bodies, Particle tracking, Global non-rigid motion compensation

1 Introduction

The cell nucleus contains numerous structures referred to as nuclear bodies (NBs) [1]. The most known example of a NB is the nucleolus [2]. NBs concentrate coding and non-coding RNAs, as well as proteins which are necessary for genome functioning. Their position and mobility within the nucleus play an important role in the regulation of genome functions [3]; at the same time, few studies on the NB mobility exist as this is a challenging task. Here we describe a simple and robust protocol to study the mobility of NBs *in vivo*, and we discuss technical problems and ways to solve them using an example of experimentally induced NBs, interphase prenucleolar bodies (iPNBs). iPNBs are formed in interphase nuclei from partially disassembled nucleoli when cells return to isotonic conditions after a hypotonic shock (4). iPNBs contain different nucleolar proteins including NPM1 (B23 or nucleophosmin) [4–7], NCL (C23 or nucleolin) [8], and pre-rRNAs [7]. In contrast to the majority of other NBs, a large number (several

Ronald Hancock (ed.), *The Nucleus*, Methods in Molecular Biology, vol. 2175, https://doi.org/10.1007/978-1-0716-0763-3_1,

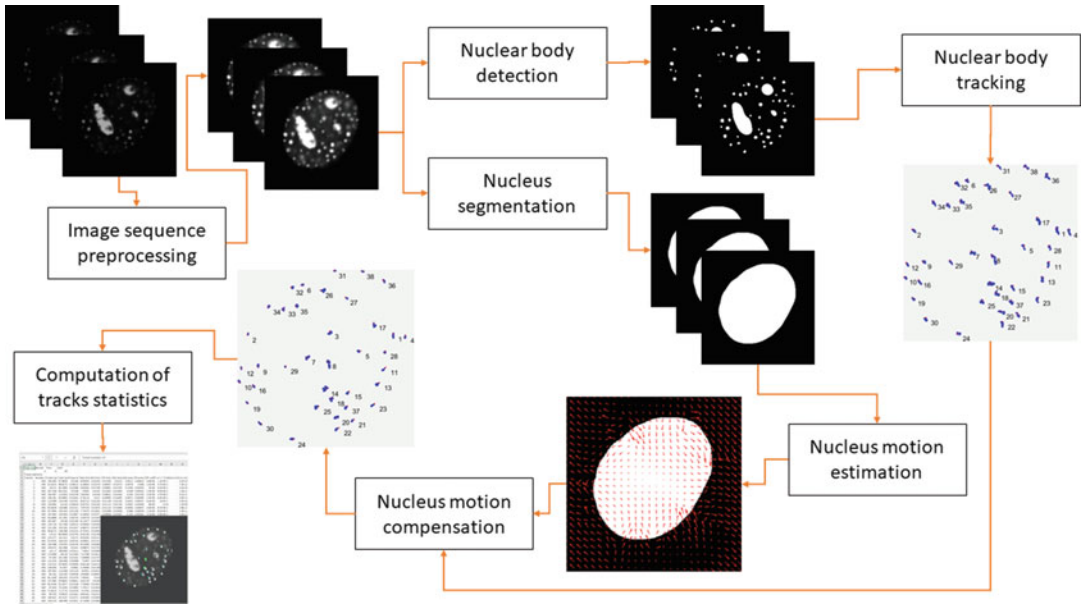

Fig. 1 The pipeline for NB mobility analysis

hundred per nucleus) of iPNBs appear simultaneously, and they are uniformly distributed within the nuclear space [7].

The analysis of NB mobility is a complex problem, as living cells move and deform during image acquisition. The observed motions consist of two components: a local motion of the NBs and a global motion of the nucleus (displacement and deformation) that should be compensated for prior to NB mobility analysis. The global motion of the nucleus can be ignored if the nucleus is relatively immobile and the time of observation is short, but correct description of intranuclear motility is impossible without compensation for global mobility of the nucleus before particle tracking and trajectory analysis. Here, we describe a pipeline for analysis of NB mobility that allows plotting the trajectories of the NBs within the nucleus taking into account the global movement of the nucleus (*see* Fig. 1).

We describe a 2D contour-based image registration protocol for compensation of the motion and deformation of the nucleus in fluorescence microscopy time-lapse sequences [9]. Our pipeline also allows to classify the observed NB motion into simple diffusion (Brownian diffusion), constrained diffusion, or directed (flow) diffusion [10]. The NB tracking pipeline is freely available at https://gitlab.com/dsorokin.msk/mmb-ipnb-tracking. It should be stressed that the approach described here may be adapted for the mobility analysis of other types of NBs or discrete nuclear compartments.

2 Materials

2.1 Cells and Cell Culture

1. The HeLa cell line used here was originally obtained from the Russian Cell Culture Collection (Institute of Cytology of the Russian Academy of Sciences, Saint Petersburg, Russia) (*see* **Note 1**). Cells are grown in Dulbecco's modified Eagle's medium (DMEM) supplemented with alanine-glutamine, 10% fetal calf serum, and an antibiotic and antimycotic mixture.
2. Hank's balanced salt solution.
3. Plasmid GFP-NPM WT (GFP-nucleophosmin), a gift from Dr. X.W. Wang [11] (also available as plasmid no. 17578 from Addgene, http://www.addgene.org).
4. Lipofectamine 2000 Transfection Reagent (Thermo Fisher Scientific).
5. Ventilated T25 flasks.
6. 35-mm dishes with a coverslip (MatTek).
7. 15 mL centrifuge tubes.

2.2 Microscopy

1. Nikon C2 scanning confocal microscope mounted on a motorized inverted microscope (Eclipse Ti-E, Nikon) (*see* **Note 2**).
2. CO_2 incubator.

2.3 Image Analysis Software

1. NIS-Elements Microscope Imaging Software (Nikon) (*see* **Note 2**).
2. FIJI (https://fiji.sc/).
3. ICY (http://icy.bioimageanalysis.org/).
4. Matlab (MathWorks) with DIPimage toolbox (http://www.diplib.org).
5. Excel (Microsoft).
6. NB tracking pipeline (https://gitlab.com/dsorokin.msk/mmb-ipnb-tracking).

3 Methods

3.1 Cell Culture

HeLa cells are maintained in DMEM supplemented with alanine-glutamine, 10% fetal calf serum, and an antibiotic and antimycotic mixture. Approximately 10^5 cells are seeded onto 35 mm Petri dishes with a glass bottom. Cells are then transfected with the GFP-NPM WT plasmid using Lipofectamine 2000 reagent according to the manufacturer's instructions (*see* **Note 3**).

3.2 Induction of iPNB Formation (See Note 4)

All operations should be carried out at 37 °C unless indicated otherwise.

1. Prepare the hypotonic solution (20% Hank's solution) (*see* **Note 5**). Use at least 5 mL of hypotonic solution pre-warmed to 37 °C per one 35 mm Petri dish.
2. Remove the growth medium from the Petri dish and briefly wash cells with ~2 mL of the hypotonic solution.
3. Incubate cells in a second change of the hypotonic solution (~2 mL) for 15 min at 37 °C in the CO_2 incubator.
4. Wash cells with complete growth medium and then incubate cells in the complete growth medium for ~20 min at 37 °C in the CO_2 incubator (*see* **Note 6**).

3.3 Live-Cell Imaging

1. Use an inverted confocal microscope suitable for live experiments, i.e., equipped with a humidified thermostatic chamber with CO_2 level maintenance.
2. Use a high-aperture objective, e.g., Nikon Plan Apo VC 60/1.40 Oil or equivalent.
3. Identify transfected cell and focus in the center of the nucleus.
4. Capture a time-lapse movie. Use the following parameters as a starting point and adjust them if needed: scale factor 0.05 μm/pixel, FPS 2 frames/s, duration 2 min.
5. Use FIJI software or the microscope software provided to export the captured movie into multipage TIFF format.

3.4 Image Analysis

The input image sequences should be in the multipage TIFF format. All further operations are performed in Matlab, except for the iPNB tracking which is performed using freely available ICY software with the Spot Tracking plugin [12]. The Matlab code, including precompiled libraries, can be downloaded at https://gitlab.com/dsorokin.msk/mmb-ipnb-tracking. The detailed description of the pipeline and the adjustable parameters can be found in the *main_script.m* file. The pipeline is shown in Fig. 1 and is described in more detail below:

1. Image sequence preprocessing (*preprocessSequence.m*). At this stage, we equilibrate image intensities of every frame. As a result, the image intensities of all frames should be within the same range.
2. Nucleus segmentation (*nucleusSegmentation.m*). Here we segment the nucleus (identify the contours) using a threshold-based approach. The threshold type and other parameters can be adjusted depending on the data.
3. Nuclear body detection (*findNuclearBodies.m*). At this stage we segment the nuclear bodies using a combination of a threshold-based approach for larger bodies (e.g., nucleoli) and a blob detection-based approach [13] for smaller bodies (e.g., iPNBs) (*see* Fig. 2).

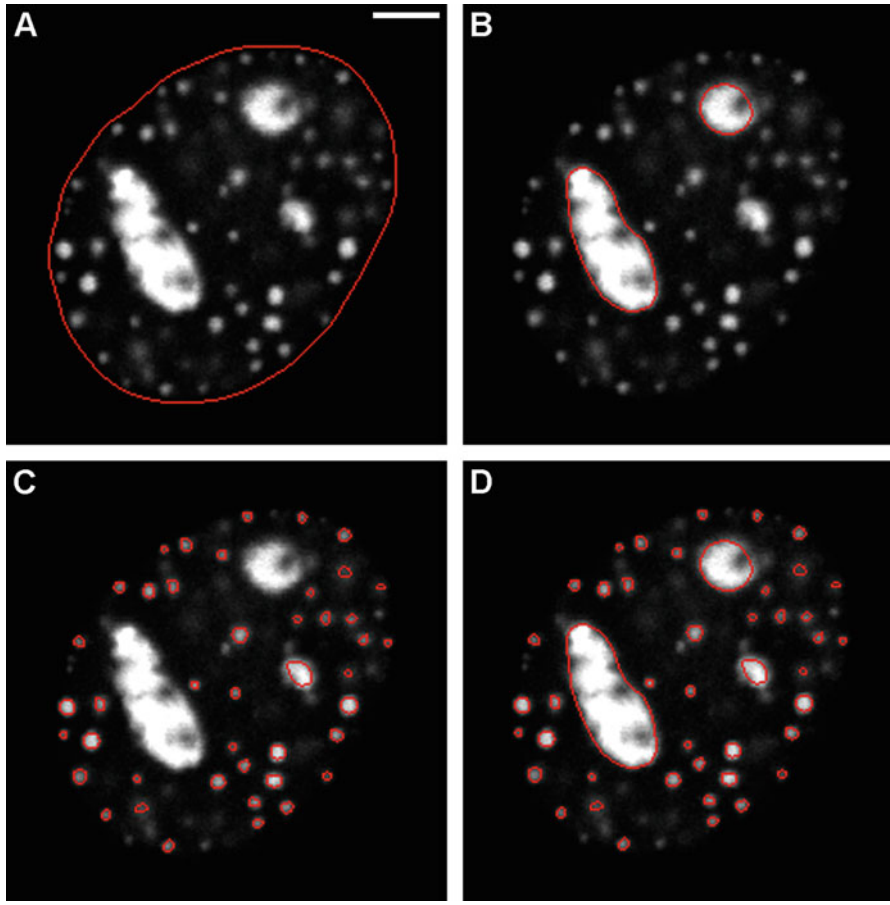

Fig. 2 Representative images of nucleus segmentation (**a**), nucleolus detection by a threshold-based approach (**b**); iPNB detection by a blob detection-based approach (**c**); resulting NB detection (**d**). Scale bar = 5 μm

4. Nuclear body tracking using the ICY Spot Tracking plugin:
   (a) Import the results of the previous step ("∗*_spots_ICY.txt*") into the ICY software using Plugins → Spot Detection Import and Export → Import.
   (b) Track using the Spot Tracking plugin: choose spots imported in the previous step as Detection set, Estimate parameters, Run tracking.
   (c) Export the tracking results from Track Manager to "∗*_tracks.xml*" using File → Save As...
5. Convert the tracks to Matlab format and postprocess by joining adjacent subtracks (*convertTracksToMatlab.m*).
6. Nucleus motion compensation and application of the obtained deformation fields to track coordinates (*compensateGlobalMotion.m*). At this stage the nucleus motion is estimated using the non-rigid elasticity-based approach. The motion obtained is applied to the NB tracks to compensate for motion of the nucleus (*see* Fig. 3 for comparison between the original and compensated NB tracks).

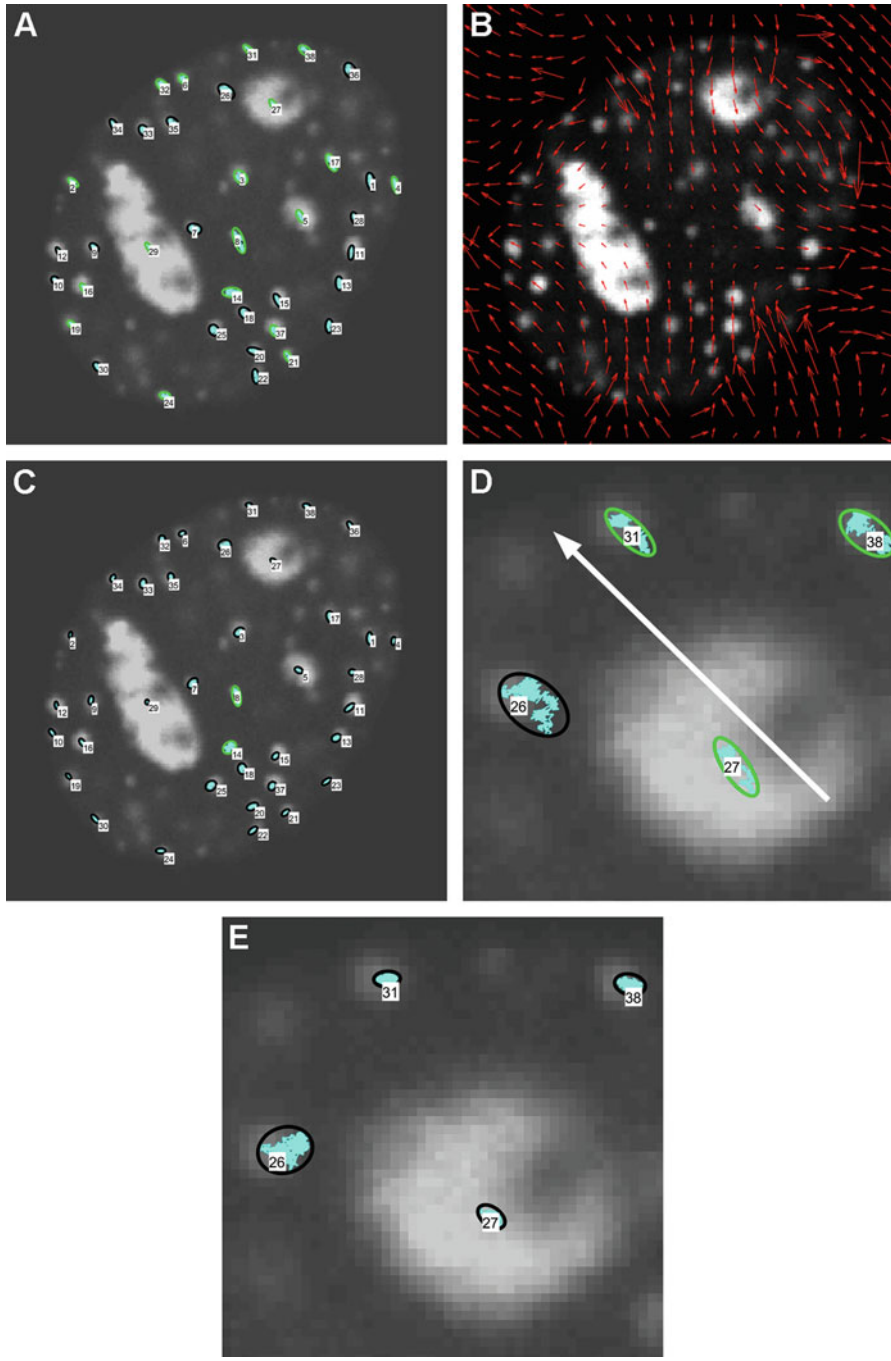

Fig. 3 Example of non-rigid compensation for global nucleus motion. The analysis pipeline outputs the first frame of a microscopy image sequence with the tracks depicted on it by enclosing ellipses of different colors corresponding to the iPNB motion types (black, constrained diffusion; green, simple diffusion). (**a**) iPNB tracks plotted over the first frame of the image sequence without compensation for nucleus nonrigid motion; (**b**) the compensating deformation field plotted over the image (the length of the vectors and spacing between them are enlarged for better visibility); (**c**) iPNB tracks after compensation for the nucleus motion; (**d** and **e**) are enlarged fragments of (**a**) (non-compensated motion) and (**c**) (compensated motion), respectively. The dominant direction of iPNB motion, which is a result of global nucleus motion, is indicated by an arrow in (**d**). Scale bar = 5 μm in (**a–c**) and 1 μm in (**d**) and (**e**)

	A	B	C	D	E	F	G	H	I	J	K	L	M	N	O
1	Total numb	Normal	Flow	Conf											
2		2	0	36											
3	Tracks statistics:														
4	TrackID	Number Of	X start (px)	Y start (px)	Ellipse Area	Total dist. (	AVG Dist-p	STD Dist-p	AVG Veloc	AVG area (r	STD area (n	Diff. coeff.	v or L * 10^	Motion type	Error norm
5	1	400	195,3834	97,88288	0,019598	8,959345	0,022454	0,013038	0,022398	0,0512	0,008126	6,91E-09	1,13E-05	C	3,24E-10
6	2	400	52,64243	98,82746	0,006139	6,298344	0,015785	0,009371	0,015746	0,0576	0,005997	2,39E-09	5,66E-06	C	7,34E-12
7	3	400	133,3104	95,29854	0,025885	6,820622	0,017094	0,008908	0,017052	0,1056	0,004554	3,96E-09	6,24E-06	C	3,2E-10
8	4	400	207,4278	99,22006	0,010796	7,859096	0,019697	0,010623	0,019648	0,048	0,005415	2,5E-09	8,41E-06	C	1,26E-12
9	5	400	163,4668	114,6327	0,013781	5,823617	0,014596	0,00812	0,014559	0,264	0,011548	3,18E-09	4,68E-06	C	6,13E-11
10	6	400	106,181	50,09653	0,010521	6,781144	0,016995	0,009946	0,016953	0,0672	0,005848	2,4E-09	6,51E-06	C	5,61E-12
11	7	400	110,5988	120,4475	0,027614	8,63713	0,021647	0,011359	0,021593	0,0432	0,003468	6,26E-09	1E-05	C	3,48E-10
12	8	400	130,9818	124,4902	0,048155	8,637007	0,021647	0,01113	0,021593	0,0592	0,004394	8E-09	1,6	N	1,41E-09
13	9	400	63,06494	130,0888	0,012408	7,873186	0,019732	0							
14	10	400	44,76647	145,4341	0,011561	7,743746	0,019408	0							
15	11	400	187,9928	130,6556	0,018966	6,26934	0,015713	0							
16	12	400	46,68883	131,5653	0,007445	5,954788	0,014924	0							
17	13	400	181,6667	145,5801	0,021687	8,11677	0,020343	0							
18	14	400	129,7188	151,458	0,044139	9,595627	0,024049	0							
19	15	400	152,2964	154,2643	0,014374	6,683717	0,016751	0							
20	16	400	58,81734	148,4984	0,012245	6,754414	0,016928	0							
21	17	400	176,2204	86,90581	0,027562	8,651954	0,021684	0							
22	18	400	135,477	161,0121	0,027199	8,502639	0,02131	0							
23	19	400	52,97048	166,4254	0,007433	6,908306	0,017314	0							
24	20	400	140,4978	179,4535	0,023763	8,310954	0,020829	0							
25	21	400	156,6735	181,9078	0,013105	6,988724	0,017516	0							
26	22	400	142,1702	189,9094	0,016107	7,963098	0,019958	0							
27	23	400	176,9683	166,2799	0,014625	7,227894	0,018115	0							
28	24	400	97,39301	201,3686	0,014424	7,008978	0,017566	0							
29	25	400	122,3246	169,0078	0,029975	7,046701	0,017661								
30	26	400	124,314	55,06349	0,040586	9,631284	0,024139	0							
31	27	400	148,3952	61,93705	0,009199	4,784838	0,011992	0							
32	28	400	187,6533	114,6381	0,011261	8,035101	0,020138								
33	29	400	90,19204	129,3359	0,005482	3,959661	0,009924	0							
34	30	400	66,10481	185,6555	0,014792	7,58281	0,019005	0							
35	31	400	137,0833	35,8645	0,006507	6,621448	0,016595	0							
36	32	400	95,31061	52,26768	0,013281	7,70636	0,019314	0							
37	33	400	87,63397	73,3294	0,018932	7,755171	0,019437	0							
38	34	400	72,93154	71,2773	0,010791	6,4762	0,016231	0							
39	35	400	99,70296	70,85252	0,01401	8,901622	0,02231	0							
40	36	400	185,6414	45,31066	0,013706	6,644051	0,016652	0							
41	37	400	150,4146	168,499	0,019212	6,71838	0,016838	0							
42	38	400	164,4793	36,46553	0,010244	7,323825	0,018355	0							

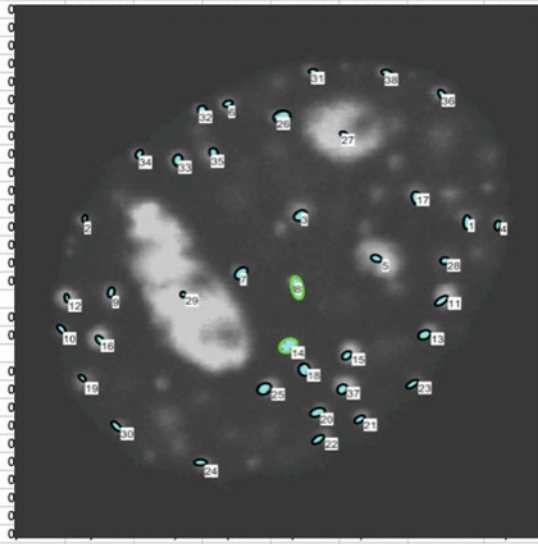

Fig. 4 Example of track visualization and output statistics in an Excel file as a result of the NB tracking pipeline (https:/gitlab.com/dsorokin.msk/mmb-ipnb-tracking)

7. Compute track statistics and determine the motion type and pattern for each NB (*analyzeTracksMotionType.m*) (*see* **Note 7** and Fig. 4).

4 Notes

1. Different adherent cultured cells may be used for analysis of NB mobility. Suspension cells can be immobilized on polylysine-coated slides or grown in soft agar.
2. Other microscopy systems may be used for image recording. The input image sequences should be in the multipage TIFF format.
3. The approach described here can be applied to other types of NBs. If the work is carried out with other NBs, then a plasmid coding for a fluorescent form of the most abundant proteins of these NBs should be used.
4. This step is necessary only for iPNBs. It should be omitted when studying other NBs.

5. iPNBs formation may start during hypotonic treatment if 20% Hank's solution is used (unpublished data). It appears that HeLa cells can adapt to hypotonic conditions, which leads to iPNB formation before the return to isotonic conditions. We believe that this cannot substantially influence NB dynamics, but, nevertheless, it is possible to use 10% Hank's solution (10 min) instead of 20% solution. In this case, the more robust hypotonic conditions do not allow cells to adapt.
6. The optimal time for the start of iPNB imaging is 25–35 min after the return to isotonic conditions. At this stage, the number of iPNBs is substantially reduced [7], facilitating the imaging and analysis of iPNBs tracks. Cells can be incubated directly on the microscope stage, if the thermostatic chamber allows to control both CO_2 and temperature. In this case, it is necessary to work in the darkroom (or at least to turn off the light immediately after mounting the Petri dish inside the thermostatic chamber). The mobility of other NBs may be registered immediately after mounting the Petri dish on the microscope stage. The optimal duration of live-cell imaging depends on the specific experimental conditions and the type of NB studied. It is also possible to acquire images of several cells in one experiment.
7. The mean square displacement (MSD) curve analysis approach described in [10] is used for classification of NB motion patterns. Briefly, the motion can be classified into three types: simple diffusion (Brownian diffusion), constrained diffusion, and directed diffusion (flow). To determine the type of motion represented by the trajectory, we found the best fit for the calculated MSD using the analytical expressions for the different diffusion models [14] with localization uncertainty described in [15]. Fitting of analytical curves to experimental data obtained from track analysis can be performed using the Nelder-Mead optimization method [16]. The analysis pipeline outputs the first frame of microscopy image sequence with the tracks depicted on it enclosed in ellipses of different colors corresponding to the iPNB motion type (black, constrained diffusion; green, simple diffusion; cyan, directed diffusion). It also outputs the statistics of the tracks including track length, iPNB initial position (px), track enclosing ellipse area (micron^2), total traveled distance (micron), average distance per frame (micron), standard deviation of distance per frame (μm), average velocity (μm/s), diffusion coefficient ($\mu m^{2/s} * 10^{-5}$), particle diffusion velocity ($\mu m/s * 10^{-3}$), or confinement area ($\mu m^2 * 10^{-3}$) depending on the type of motion. An example of the output statistics in an Excel file is shown in Fig. 4.

Acknowledgments

We are grateful to Dr. X.W. Wang for the GFP-NPM WT-expressing plasmid. This work was supported by the Russian Science Foundation (17-11-01279 to DVS for image analysis) and the Russian Foundation for Basic Research (project 18-54-16002 to EVS for cell preparation and microscopy).

References

1. Dundr M (2012) Nuclear bodies: multifunctional companions of the genome. Curr Opin Cell Biol 24:415–422. https://doi.org/10.1016/j.ceb.2012.03.010
2. Iarovaia OV, Minina EP, Sheval EV et al (2019) Nucleolus: a central hub for nuclear functions. Trends Cell Biol. https://doi.org/10.1016/j.tcb.2019.04.003
3. Arifulin EA, Musinova YR, Vassetzky YS et al (2018) Mobility of nuclear components and genome functioning. Biochemistry (Mosc) 83 (3):690–700. https://doi.org/10.1134/S0006297918060068
4. Zatsepina OV, Dudnic OA, Todorov IT et al (1997) Experimental induction of prenucleolar bodies (PNBs) in interphase cells: interphase PNBs show similar characteristics as those typically observed at telophase of mitosis in untreated cells. Chromosoma 105:418–430
5. Musinova YR, Lisitsyna OM, Golyshev SA et al (2011) Nucleolar localization/retention signal is responsible for transient accumulation of histone H2B in the nucleolus through electrostatic interactions. Biochim Biophys Acta 1813:27–38. https://doi.org/10.1016/j.bbamcr.2010.11.003
6. Musinova YR, Kananykhina EY, Potashnikova DM et al (2015) A charge-dependent mechanism is responsible for the dynamic accumulation of proteins inside nucleoli. Biochim Biophys Acta 1853:101–110. https://doi.org/10.1016/j.bbamcr.2014.10.007
7. Musinova YR, Lisitsyna OM, Sorokin DV et al (2016) RNA-dependent disassembly of nuclear bodies. J Cell Sci 129:4509–4520. https://doi.org/10.1242/jcs.189142
8. Pellar GJ, DiMario PJ (2003) Deletion and site-specific mutagenesis of nucleolin's carboxy GAR domain. Chromosoma 111:461–469. https://doi.org/10.1007/s00412-003-0231-y
9. Sorokin DV, Peterlik I, Tektonidis M et al (2018) Non-rigid contour-based registration of cell nuclei in 2-D live cell microscopy images using a dynamic elasticity model. IEEE Trans Med Imaging 37:173–184. https://doi.org/10.1109/TMI.2017.2734169
10. Arifulin EA, Sorokin DV, Tvorogova AV et al (2018) Heterochromatin restricts the mobility of nuclear bodies. Chromosoma 127:529–537. https://doi.org/10.1007/s00412-018-0683-8
11. Wang W, Budhu A, Forgues M et al (2005) Temporal and spatial control of nucleophosmin by the Ran-Crm1 complex in centrosome duplication. Nat Cell Biol 7:823–830. https://doi.org/10.1038/ncb1282
12. Chenouard N, Bloch I, Olivo-Marin J-C (2013) Multiple hypothesis tracking for cluttered biological image sequences. IEEE Trans Pattern Anal Mach Intell 35:2736–3750. https://doi.org/10.1109/TPAMI.2013.97
13. Foltánková V, Matula P, Sorokin D et al (2013) Hybrid detectors improved time-lapse confocal microscopy of PML and 53BP1 nuclear body colocalization in DNA lesions. Microsc Microanal 19(2):360–369. https://doi.org/10.1017/S1431927612014353
14. Daumas F, Destainville N, Millot C et al (2003) Confined diffusion without fences of a g-protein-coupled receptor as revealed by single particle tracking. Biophys J 84:356–366. https://doi.org/10.1016/S0006-3495(03)74856-5
15. Michalet X (2010) Mean square displacement analysis of single-particle trajectories with localization error: Brownian motion in an isotropic medium. Phys Rev E Stat Nonlin Soft Matter Phys 82:041914. https://doi.org/10.1103/PhysRevE.82.041914
16. Nelder JA, Mead R (1965) A simplex method for function minimization. Comput J 7 (4):308–313. https://doi.org/10.1093/comjnl/7.4.308

Chapter 2

Laser Targeted Oligo Ligation (LTOL) to Identify DNA Sequences in the Vicinity of a Single Subnuclear Structure in a Single Cell

David Anchel and Reagan W. Ching

Abstract

Gene loci are organized around nuclear substructures, forming gene hubs which provide a level of transcriptional control. To date, most techniques used to investigate the genes in these hubs have been based on using material from bulk cells. This makes identifying specific gene associations difficult. Here we describe the Laser Targeted Oligo Ligation (LTOL) technique that was developed to identify DNA sequences around a single subnuclear structure on a single-cell basis by targeting these regions with two-photon irradiation.

Key words Nuclear organization, Subnuclear structures, Gene hubs, Single cell, Microscopy, Sequencing

1 Introduction

Research studying the structure and function of the nucleus has shown that it is a highly organized organelle. When performing immunofluorescence microscopy experiments on nuclear proteins, it was observed that some proteins localized into distinct foci such as the nucleolus, PML bodies, and Cajal bodies [1, 2]. Not only do nuclear proteins form distinct subnuclear structures in the nucleus, the development and use of DNA fluorescence in situ hybridization (FISH) and chromosome paints have shown that individual chromosomes are also organized as discrete chromosome territories [3, 4]. By combining immunofluorescence labeling of nuclear domains with DNA FISH (immunoFISH), it is observed that certain gene loci are associated with specific nuclear domains, for example the *TP53* gene with PML bodies and the *U2* gene loci with Cajal bodies [5, 6]. One could propose that these nuclear domains could be functioning as gene hubs. The gene hub model is supported by the observations that the nucleus can be partitioned into

Ronald Hancock (ed.), *The Nucleus*, Methods in Molecular Biology, vol. 2175, https://doi.org/10.1007/978-1-0716-0763-3_2,

substructures via a liquid-liquid phase separation mechanism, and this partitioning may also contribute to regulation of gene clusters [7, 8].

Crucial to the testing of the "gene hub" model is the ability to detect multiple loci that converge at a shared nuclear body. Gene hubs can be detected using immunoFISH, but the drawbacks are twofold: Firstly, one needs an *a priori* idea of what gene loci to probe for, and secondly the limited resolution of optical microscopy where DNA elements within 50–100 kbp are not resolved [9]. The development of chromatin conformation capture techniques, from 3C to Hi-C, has enabled scientists to probe into the organization of genes in 3D space at the molecular level. How the 3D gene organization is mediated by a nuclear protein of interest was addressed by the development of Chromatin Interaction Analysis with Paired-End Tag Sequencing (ChIA-PET) [10]. One drawback of ChIA-PET is that it cannot distinguish gene interactions with a protein in a particular nuclear domain or with a protein dispersed throughout the nucleus. To overcome this drawback ImmunoTRAP, which deposits biotin onto chromatin immediately adjacent to a subnuclear structure or compartment, was developed to identify gene interactions around a specific nuclear domain, in this case the PML body [11].

The techniques mentioned above have all provided great insights into the organization of the nucleus, but they produce a model of an average nucleus since they require combining millions of cells to provide a sample to probe for chromatin interactions. Early RNA FISH studies and more recent single-cell studies have observed differences in transcriptional regulation in different cells [12, 13], suggesting that there may be differences in the organization of gene hubs between individual cells. In addition to cell-to-cell variation, for a given type of nuclear domain there exists variation within a single cell. The presently available techniques do not allow for the dissection of those "unique" nuclear domains that, by virtue of their unique size or composition, cannot be biochemically distinguished from other structures within the same cell. Because such nuclear domains occur in cell lines with concomitant genome-wide dysregulation [14], we have hypothesized that the presence of these "aberrant" bodies may be linked to dysregulation of multiple loci that are convergent upon them [15]. Thus, Laser Targeted Oligo Ligation (LTOL) was developed for the identification of DNA sequences around a single nuclear domain in a single cell [16]. This is accomplished by using two-photon irradiation to create localized DNA damage around a nuclear structure of interest, ligating specific probes to the damaged DNA ends, and then isolating and amplifying the ligated DNA from individual cells (*see* Fig. 1). Results of LTOL studies of HLBs and PML bodies are reported in [16].

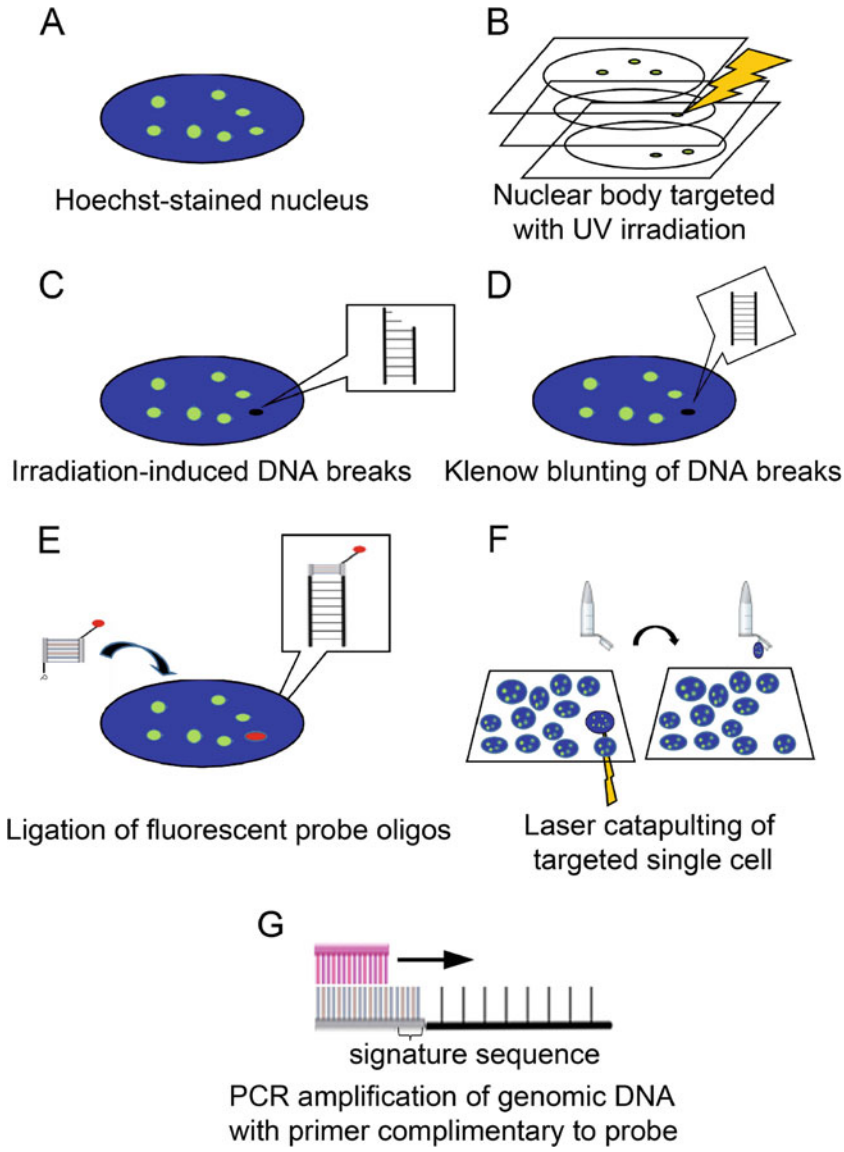

Fig. 1 A brief schematic of the LTOL method. (**a**) A nuclear substructure of interest is immunolabeled and DNA is stained with Hoechst dye. (**b**) A *z*-stack of images of the immunolabeled structure is recorded, and the structure is then bleached by two-photon irradiation. (**c**) The bleaching results in DNA double strand breaks (DSBs) around the substructure of interest. (**d**) The cells are incubated with Klenow enzyme to blunt-end these DSBs. (**e**) A fluorescent blunt-ended oligo containing a priming site for subsequent amplification is ligated to the ends of the Klenow-filled genomic DNA. (**f**) Single cells are located and isolated into lysis buffer using Laser Microdissection Pressure Catapulting. (**g**) The lysed cells are subjected to repeated rounds of PCR amplification with primers complementary to the ligated fluorescent probe (adapted from [16] with permission from Springer Nature)

2 Materials

2.1 PEN (Polyethylene Naphthalate) Coverslips (See Subheading 3.1)

1. PEN film: 1.35 μm thickness (P.A.L.M. Microlaser Technologies, Bernried, Germany).
2. Round 25 mm ∅ coverslips.
3. Diamond-tipped knife.
4. Acid-free rubber cement (Best-Test).

2.2 Immunolabeling and Laser Targeting

1. 10× phosphate buffered saline (10× PBS): 1.37 mM NaCl, 27 mM KCl, 100 mM Na_2HPO_4, 18 mM KH_2PO_4. Weigh 80 g NaCl, 2 g KCl, 14.4 g Na_2HPO_4, and 2.4 g KH_2PO_4, dissolve in 800 mL of water, and adjust pH to 7.4. Make up to 1 L.
2. 1× PBS.
3. Sealed, humid chamber protected from light for incubating coverslips.
4. 4% paraformaldehyde in 1× PBS (fixation buffer).
5. 0.1% (v/v) Triton X-100 in 1× PBS (permeabilization buffer).
6. Blocking oligo: 5′-GCG CTA GAC C*G GTC TAG CGC-3′; *= internal Cy5 conjugate (*see* **Note 1**).
7. Antibodies: the primary anti-Histone Locus Body (HBL) antibody is mouse anti-NPAT (Abcam), and the secondary antibody is conjugated with Alexa 488 [16].
8. 0.5 μg/mL Hoechst 32258 in PBS (DNA stain).
9. Confocal fluorescence microscope: LSM510 META (Zeiss) equipped with excitation laser lines at 458, 488, and 514 nm and a Chameleon Ultra laser (Coherent, Santa Clara, CA, USA).

2.3 Oligo Ligation

1. Klenow fragment.
2. Klenow buffer: 70 mM Tris–HCl pH 7.5, 70 mM $MgCl_2$, 1 M dithioerythritol supplemented with 2.5 mM each of dGTP, dATP, dCTP, and dTTP.
3. ISOL buffer: 1× T4 DNA ligase buffer supplemented with 15% PEG 8000, 0.5 mM ATP, and 0.05 mg/mL bovine serum albumin (BSA).
4. T4 DNA ligase.
5. 20× SSC: 3 M NaCl, 300 mM trisodium citrate. Dissolve 175.3 g of NaCl and 88.2 g of trisodium citrate in 800 mL of water. Make up to 1 L and adjust the pH to 7.0.
6. 0.1% Tween 20 in 2× SSC; low stringency wash buffer.
7. 0.5× SSC: high stringency wash buffer.

8. 5% Hematoxylin in PBS, filtered 0.2 μm.
9. Nuclease-free water.
10. 100%, 70%, and 90% ethanol diluted with nuclease-free water.
11. Targeting oligos: forward strand—5′-(Cy3)AGT GGG ATT CTT GCT GTC AGT TAG CTG-3′, reverse strand—5′-CAG CTA ACT GAC AG(ddC)-3′ (The underlined subsequence is a "signature" used to differentiate amplicons that originate from bona fide ligation of targeting oligo as opposed to those that originate from mispriming events; *see* **Note 2**).

2.4 Microdissection and DNA Extraction and Amplification

1. PALM Laser-Catapulting Microdissecting Microscope (Zeiss).
2. DNA extraction buffer: 0.5 μL of 10× One-Phor-All-Buffer-Plus (GE Healthcare), 0.13 μL of 10% Tween 20, 0.13 μL of 10% Igepal CA-630, 0.13 μL of proteinase K (10 mg/mL).
3. Titanium Taq polymerase kit (Takara Bio).
4. Amplification oligo: 5′-AGT GGG ATT CTT GCT GTC AGT TA-3′.

3 Methods

3.1 Preparation of PEN Coverslips

1. Etch a small "keystone" shape ~2 mm^2 in area into a round coverslip using a diamond knife.
2. Cut PEN film into approximately 18 × 18 mm square pieces. Float these on nuclease-free water in a Petri dish.
3. Take an etched coverslip and gently submerge it underneath a floating PEN sheet. Lift the coverslip out of the water with the PEN film centered over the etched keystone. It is important that the PEN film be flush with the coverslip surface; bumps or bubbles of water indicate an excess of water underneath the film which may prevent successful microdissection later.
4. Dry the "PEN coverslips" overnight in an oven at 60 °C. The next day, apply rubber cement to the border of the film and let it cure overnight at room temperature. Inspect the PEN film to ensure that there are no raised regions that may contain trapped water. Only proceed with those coverslips whose PEN film is adequately flush with the coverslip surface.
5. Irradiate the PEN coverslips with the UV lamp inside a laminar flow hood for 30 min. The coverslips are now ready for plating cells.

3.2 Immunolabeling Subnuclear Structures and Laser Targeting

The following incubations of coverslips are done in a sealed humid chamber and protected from light. To further prevent evaporation, place a coverslip over the cells and seal it with a plastic adhesive; this can be peeled off after the incubation and the coverslip can be floated off with PBS.

1. Plate cells on PEN coverslips and let them grow overnight. Take care to plate cells at a sufficiently low density if single-cell microdissection is desired (*see* **Note 3**).
2. The next day, perform a quick wash of the coverslips with PBS to remove medium. Fix the cells for 10 min in fixation buffer and then wash them for 5 min with PBS. Repeat the wash two more times for a total of three washes.
3. Permeabilize the cells for 5 min in permeabilization buffer and then wash 3 × 5 min with PBS.
4. Ligate the blocking oligo to blunt DNA ends at endogenous DSBs [17] to prevent the ends from providing substrates for subsequent probe ligation and amplification. Incubate the coverslips for 30 min at 37 °C in Klenow buffer with Klenow fragment (100 U/mL) and wash 3 × 5 min in PBS. Next, incubate for 10 min in ISOL buffer and then in ISOL buffer with addition of T4 DNA ligase (100 U/mL) and the blocking oligo (35 μg/mL). After 18 h at room temperature, wash the coverslips 3 × 5 min with low stringency wash buffer at 42 °C and then 3 × 5 min at 60 °C with high stringency wash buffer.
5. Immunolabel the subnuclear structure of interest with the appropriate antibody. For example, to label Histone Locus bodies (HLBs) [7], incubate coverslips with a primary anti-HLB antibody diluted in PBS for 1 h at room temperature and then wash 3 × 5 min in PBS.
6. Incubate the coverslips with the secondary Alexa 488-conjugated antibody diluted in PBS for 1 h at room temperature. Wash 3 × 5 min with PBS.
7. Incubate the cells with Hoechst 32258 to label DNA and cover the coverslips with aluminum foil to avoid exposure to light.
8. Locate the keystone on a coverslip at 10× magnification using the LSM510 META confocal microscope and take a low magnification image at an excitation wavelength of 488 nm.
9. Identify a cell or cells of interest within the keystone on this image and annotate them (mark them with arrows on the image) in order to identify them during following steps.
10. Change the magnification to 63×, visualize a chosen cell or cluster of cells within the keystone, and take a high magnification image under 488 nm excitation using a pinhole size corresponding to an optical section of 0.7 μm.
11. Using the LSM 510 photobleaching software, draw around regions of interest (ROIs) to control the path of the Chameleon laser which will target them using the ROI function to direct a 750 nm two-photon pulse to induce localized DNA damage. It is essential to minimize the time from the initial 63× 488 nm image to the two-photon pulse(s) in order to

reduce effects of stage drift, and especially when multiple ROIs are to be targeted it is advisable to employ a macro for this step (*see* **Note 4**). Optimize the laser settings by altering the transmission power and the number of iterations per pixel; we have optimal results using a 1 s pulse at ~900 mW with AOM attenuation set at 4%.

12. Take a fluorescence image at 488 nm to confirm that the correct subnuclear structure was targeted; if so, the Alexa 488 immunofluorescence signal will have been bleached by the two-photon irradiation.

3.3 Oligo Ligation to DNA in the Targeted Region

Take care throughout these procedures to minimize exposure of the samples to direct light.

1. Ligate the targeting oligo in the same manner as the blocking oligo (*see* Subheading 3.2, **step 4**). Incubate the coverslip with Klenow fragment in Klenow buffer for 1 h to prepare the damaged DNA around the subnuclear structure of interest for oligo ligation, and then wash in PBS 3 × 5 min.
2. Incubate the coverslip in ISOL buffer for 10 min and replace this with fresh ISOL buffer containing T4 DNA ligase (100 U/mL) and the double-stranded oligo at a final concentration of 0.29 nM. After 18 h at room temperature, wash 3 × 5 min with low stringency buffer at 42 °C and 3 × 5 min with high stringency buffer at 60 °C.
3. Visualize the efficiency of ligation under a fluorescence microscope (the double-stranded oligos contain an internal Cy3 fluorophore) (*see* Fig. 2) and the level of background signal. Annotate low magnification images of the targeted cell(s) to indicate their location for the subsequent microdissection.
4. Incubate the cells in hematoxylin solution for 2 min and wash them in nuclease-free water for 30 s. Dehydrate the cells in a

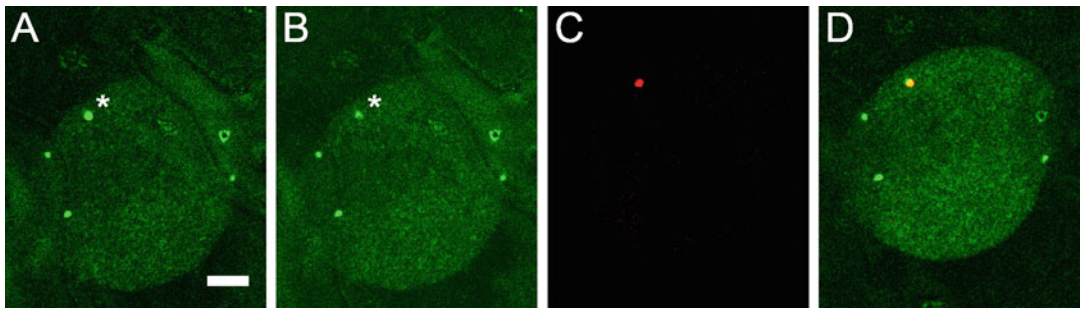

Fig. 2 LTOL of a single Histone Locus Body (HLB). (**a**) HLBs were immunolabeled (green) and targeted with two-photon irradiation. (**b**) Note the loss of fluorescence of the single HLB after photobleaching (asterisk). (**c**) After ligating the fluorescent oligo probe, a fluorescent focus can be seen (red). (**d**) This focus colocalizes with the bleached HLB body. Scale bar 5 μm. (Adapted from [16] with permission from Springer Nature)

series of increasing concentrations of ethanol (70%, 90%, 100%) for 2 min at each step. After the final 100% ethanol, allow the coverslips to air dry for 1 h at room temperature.

3.4 Laser Microdissection Pressure Catapulting of Single Cells and DNA Extraction and Amplification

1. Under the low magnification objective of the PALM microscope, identify the keystone etched into the coverslip that encloses the region containing the targeted cells by referring to the annotated image taken at the time of laser targeting. The cells that were annotated on the low magnification confocal image are located using the 40× objective used for microdissection [18] (*see* **Note 5**).
2. Catapult single cells into the cap of an inverted 200 μL Eppendorf tube containing 4.5 μL of DNA extraction buffer [19] (*see* **Note 6**).
3. Close the tubes, still in the inverted position with the sample in the cap, and incubate them for 16 h in a thermocycler with the lid set at 42 °C and the block set at 70 °C. Invert the tube, spin the contents of the lid down into the tube, and heat to 80 °C to inactivate proteinase K.
4. Amplify the targeted DNA. Make the extracted DNA to 50 μL using a Titanium Taq polymerase kit and perform PCR with these settings: (1) 72 °C for 1 min; (2) 68 °C for 3 min; (3) 94 °C for 40 s; (4) 57 °C for 30 s; (5) 68 °C for 90 s; (6) repeat **steps 3–5** for a total of 14 cycles, increasing each step by 1 s every cycle; (7) 94 °C for 40 s; (8) 57 °C for 30 s; (9) 68 °C for 105 s; (10) repeat **steps 7–9** for a total of eight cycles, increasing each step by 1 s every cycle; (11) 94 °C for 40 s; (12) 65 °C for 30 s; (13) 68 °C for 113 s; (14) repeat **steps 11–13** for a total of 22 cycles, increasing each step by 1 s every cycle; (15) 68 °C for 3 min and 40 s.
5. Clone the resultant amplicons for downstream sequencing applications, together with appropriate controls (*see* **Note 7**).

4 Notes

1. The sequence of the blocking oligo is designed to not contain sequences complementary to the primers used for amplification.
2. The targeting oligo contains the priming site for the amplification oligo used for PCR amplification.
3. If non-adherent cells will be studied, the PEN film needs to be coated with poly-L-lysine or poly-L-ornithine in order for the cells to adhere.
4. Stage drift may occur during the time required for manually selecting targets or multiple ROIs comprised of only a single

pixel. We developed a visual basic macro (available from the authors upon request) from that described in [20] that utilizes user-defined pixel "masks" (binary arrays corresponding to each pixel in the imaging field) as input and closes the laser beam between targeted pixels to avoid leaving a track of laser damage outside the intended volume. An ImageJ macro was adapted to create a binary mask of an image from a user-controlled threshold that captures the immunofluorescence signals for the structures of interest and prompts the user to choose which coordinate corresponding to the center of mass of each thresholded object to include in the resultant binary image array, which is used as input for the microscope macro to open the laser only at those coordinates that correspond to the centers of the structures of interest. Thus, from a scan of the immunofluorescence image the structures of interest can be quickly targeted and stage drift is minimized. Further, because the laser line for immunofluorescence (typically Alexa 488) is separated from that of the 2-photon bleaching laser (750 nm), their focal planes differ due to chromatic aberration. These differences are adjusted before each session using reflected light from the coverslip surface as an alignment reference. For session-to-session variability in the scanning mirror speed, prior to each session an *x-y* coordinate offset is added to the microscope macro, calculated by imaging chromocenters labeled by an H3K9me3 antibody in mouse embryonic fibroblast cells, which offer large targets so that localized 2-photon irradiation creates a clear bleached hole that can be compared to the original target coordinates. Target several chromocenters in different areas of the imaging field (typically the four corners and center) and note the differences in x and y values between the center of the bleach spot (xr,yr) and the original targeting coordinates (xt,yt). Plots of xr vs. xt (yr vs. yt) fit well to linear functions fxr->xt (fyr->yt), and so the user-defined targeting coordinates are first offset before they are input to the microscope targeting macro. This greatly reduces targeting errors and provides sufficient accuracy to consistently direct the laser spot to within the diameter of single nuclear bodies.

5. When cutting the PEN membrane prior to catapulting, take care to extend the cut area well beyond the cell on one side so that the pulse can be directed at the center of the membrane fragment without ablating the cell itself.
6. Ensure that the lysis buffer forms a droplet in the center of the Eppendorf tube cap to minimize the distance that a catapulted cell needs to travel and thus maximize the range of capturable trajectories. The trajectory is affected by where the pulse is directed and small variations can send cells to dry regions of the Eppendorf tube cap; pulses aimed at the edge typically

catapult cells at oblique angles and they miss the bubble of lysis buffer, whereas pulses directed at the center are catapulted normal to the coverslip surface. With all these measures in place, catapulting efficiencies (i.e., intact cells verified to be floating in the lysis buffer) of ~90% can be achieved for adherent cells.

7. Ideal positive controls are HLBs, frequently colocalized with the histone gene clusters on chromosomes 6p22.1 and 1q21.2 [21] and detectable by an antibody to their constituent protein NPAT [22, 23]. Negative controls should include non-targeted cells from the same coverslip and a lysis buffer-only control. An agarose gel should be run to confirm the lack of amplicons in negative controls; these may arise due to mispriming and can be disregarded if they do not contain the "signature" sequence in the targeting oligos (*see* Subheading 2.3, **item 11**). *See* [16] for details of LTOL studies of HLBs and PML bodies.

Acknowledgments

This work was funded by operating grants from the Natural Sciences and Engineering Research Council of Canada and the Canadian Institutes of Health Research. We would like to sincerely thank D.P. Bazett-Jones for his guidance and mentorship throughout our scientific careers.

References

1. Spector DL (2001) Nuclear domains. J Cell Sci 114:2891–2893
2. Staněk D, Fox AH (2017) Nuclear bodies: news insights into structure and function. Curr Opin Cell Biol 46:94–101. https://doi.org/10.1016/j.ceb.2017.05.001
3. Cremer T, Cremer M (2010) Chromosome territories. Cold Spring Harb Perspect Biol 2: a003889. https://doi.org/10.1101/cshperspect.a003889
4. Fritz AJ, Sehgal N, Pliss A, Xu J, Berezney R (2019) Chromosome territories and the global regulation of the genome. Genes Chromosomes Cancer 58:407–426. https://doi.org/10.1002/gcc.22732
5. Carmo-Fonseca M, Pepperkok R, Carvalho MT, Lamond AI (1992) Transcription-dependent colocalization of the U1, U2, U4/U6, and U5 snRNPs in coiled bodies. J Cell Biol 117:1–14. https://doi.org/10.1083/jcb.117.1.1
6. Sun Y, Durrin LK, Krontiris TG (2003) Specific interaction of PML bodies with the TP53 locus in Jurkat interphase nuclei. Genomics 82:250–252
7. Hnisz D, Shrinivas K, Young RA, Chakraborty AK, Sharp PA (2017) A phase separation model for transcriptional control. Cell 169:13–23. https://doi.org/10.1016/j.cell.2017.02.007
8. Strom AR, Emelyanov AV, Mir M, Fyodorov DV, Darzacq X, Karpen GH (2017) Phase separation drives heterochromatin domain formation. Nature 547:241–245. https://doi.org/10.1038/nature22989
9. Trask B, Pinkel D, van den Engh G (1989) The proximity of DNA sequences in interphase cell nuclei is correlated to genomic distance and permits ordering of cosmids spanning 250 kilobase pairs. Genomics 5:710–717
10. Fullwood MJ, Han Y, Wei C-L, Ruan X, Ruan Y (2010) Chromatin interaction analysis using paired-end tag sequencing. Curr Protoc Mol Biol Chapter 21:Unit 21.15.1–Unit 21.1525. https://doi.org/10.1002/0471142727.mb2115s89

11. Ching RW, Ahmed K, Boutros PC, Penn LZ, Bazett-Jones DP (2013) Identifying gene locus associations with promyelocytic leukemia nuclear bodies using immuno-TRAP. J Cell Biol 201:325–335. https://doi.org/10.1083/jcb.201211097
12. Levsky JM, Shenoy SM, Pezo RC, Singer RH (2002) Single-cell gene expression profiling. Science 297:836–840. https://doi.org/10.1126/science.1072241
13. Pijuan-Sala B, Guibentif C, Göttgens B (2018) Single-cell transcriptional profiling: a window into embryonic cell-type specification. Nat Rev Mol Cell Biol 19:399–412. https://doi.org/10.1038/s41580-018-0002-5
14. Lee K-H, Chang M-Y, Ahn J-I, Yu D-H, Jung S-S, Choi J-H, Noh Y-H, Lee Y-S, Ahn M-J (2002) Differential gene expression in retinoic acid-induced differentiation of acute promyelocytic leukemia cells, NB4 and HL-60 cells. Biochem Biophys Res Commun 296:1125–1133. https://doi.org/10.1016/s0006-291x(02)02043-0
15. Torok D, Ching RW, Bazett-Jones DP (2009) PML nuclear bodies as sites of epigenetic regulation. Front Biosci (Landmark Ed) 14:1325–1336
16. Anchel D, Ching RW, Cotton R, Li R, Bazett-Jones DP (2016) A novel single-cell method to identify the genetic composition at a single nuclear body. Sci Rep 6:29191. https://doi.org/10.1038/srep29191
17. Didenko VV, Ngo H, Baskin DS (2003) Early necrotic DNA degradation: presence of blunt-ended DNA breaks, 3′ and 5′ overhangs in apoptosis, but only 5′ overhangs in early necrosis. Am J Pathol 162:1571–1578. https://doi.org/10.1016/S0002-9440(10)64291-5
18. Schütze K, Lahr G (1998) Identification of expressed genes by laser-mediated manipulation of single cells. Nat Biotechnol 16:737–742. https://doi.org/10.1038/nbt0898-737
19. https://cf.gu.se/digitalAssets/1241/1241399_PALM_brochure.pdf
20. Pham HH, Gourevich I, Jonkman JEN, Kumacheva E (2007) Polymer nanostructured material for the recording of biometric features. J Mater Chem 17:523–526. https://doi.org/10.1039/B614491H
21. Zhao J, Kennedy BK, Lawrence BD, Barbie DA, Matera AG, Fletcher JA, Harlow E (2000) NPAT links cyclin E-Cdk2 to the regulation of replication-dependent histone gene transcription. Genes Dev 14:2283–2297. https://doi.org/10.1101/gad.827700
22. Bongiorno-Borbone L, De Cola A, Vernole P, Finos L, Barcaroli D, Knight RA, Melino G, De Laurenzi V (2008) FLASH and NPAT positive but not Coilin positive Cajal Bodies correlate with cell ploidy. Cell Cycle 7:2357–2367. https://doi.org/10.4161/cc.6344
23. Nizami Z, Deryusheva S, Gall JG (2010) The Cajal body and histone locus body. Cold Spring Harb Perspect Biol 2:a000653. https://doi.org/10.1101/cshperspect.a000653

Chapter 3

Visualizing Chromatin Modifications in Isolated Nuclei

Yuan Li, Zachary Klase, and Luca Sardo

Abstract

Modifications in chromatin structure are traditionally monitored by biochemical assays that provide average measurements of static events in a population of cells. Microscopy provides a method by which single cells or nuclei can be observed. Traditionally, microscopy has been used to image the nucleus by the application of immunostaining to chemically fixed samples or the use of exogenously expressed fluorescent proteins. This method represents an approach to observe changes in endogenous proteins relating to chromatin structure in real time. Here we describe a method for isolating transcriptionally and enzymatically active nuclei from live cells and visualizing events using fluorescently labeled antibodies. This method allows the observation of real time changes in chromatin architecture and can be used to observe the effects of drugs on nuclei while under microscopic observation.

Key words Nucleus, Chromatin, Histone, Acetylation, Microscopy

1 Introduction

The nucleus is a highly specialized organelle found in every eukaryotic cell. It performs two major functions: first, it stores the cell's hereditary material, and second, it coordinates the cell's activities including growth, intermediary metabolism, protein synthesis, and reproduction. A distinction between the active and accessible euchromatin and the more inert heterochromatin was first described in 1928 [1]. Our knowledge about chromatin compartmentalization and accessibility for DNA replication, repair, and transcription has since deepened and generated a vast scientific literature [2]. In addition to the crucial role of epigenetic modifications (acetylation, methylation, and ubiquitination) and their positions in chromatin regulation [3], DNA accessibility is also governed by histone spatial localization and interactions with nuclear architecture [4].

Multiple lines of evidence suggest that epigenetics play an important role in cell development, oncogenesis, and viral pathogenesis [5–7], and it is thus critical that techniques are available to

Ronald Hancock (ed.), *The Nucleus*, Methods in Molecular Biology, vol. 2175, https://doi.org/10.1007/978-1-0716-0763-3_3,

monitor these chromatin alterations. Traditionally, chromatin immunoprecipitation (ChIP)-based assays are widely used for studying chromatin modifications. The data generated from these biochemical genomic assays offer averages of cells but cannot query changes in real time in a single cell. Consequently, they are unable to gain vital spatial and temporal information on alterations contributing to chromatin regulation. Fixation of the specimen is the method of choice for immunostaining procedures used in most microscopy methods, but this prevents observations of sequential events. The visualization of chromatin structure in a single cell has benefited from modern optical microscopy techniques and the advent of super-resolution methods [8]. Although the resolution of diffraction-limited objects has been improved, imaging the endogenous chromatin in real time still remains a hurdle. Focusing on imaging intact cells, a promising approach has been reported to track changes in real time for histones targeted by fluorescence-conjugated monoclonal Fab fragments [9]. In living cells, super-resolution microscopy has been taken advantage of to obtain higher resolution images of chromatin by transiently or stably expressing tagged histones [9–12]. Since in living cells the membranes of both the cytoplasm and the nucleus act as barriers and limit the penetration of reagents or antibodies into the nucleus, alternative microscopy approaches to quantitatively study changes of the endogenous chromatin in an unfixed nucleus are desirable, especially for high- and super-resolution microscopy techniques.

We have thus developed a tool to visualize chromatin changes at the single-nucleus level [13]. This method benefits from isolating transcriptionally competent nuclei from cells. Immunofluorescent labeling of unfixed nuclei allows to generate images of endogenous proteins relevant to the histone code, transcription machinery, and nuclear architecture (*see* Fig. 1). By using spinning disk confocal and instant structured illumination microscopy (iSIM), we have mapped several chromatin and nuclear

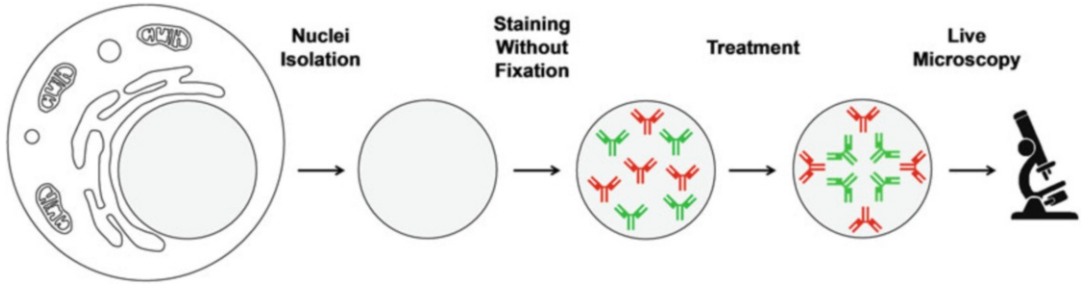

Fig. 1 Flowchart of the method. Live, unfixed cells are treated with lysis buffer to disrupt cytoplasmic and nuclear membranes. The remaining lamin-encased nuclei are then stained with fluorochrome-labeled antibodies prior to live imaging by confocal microscopy

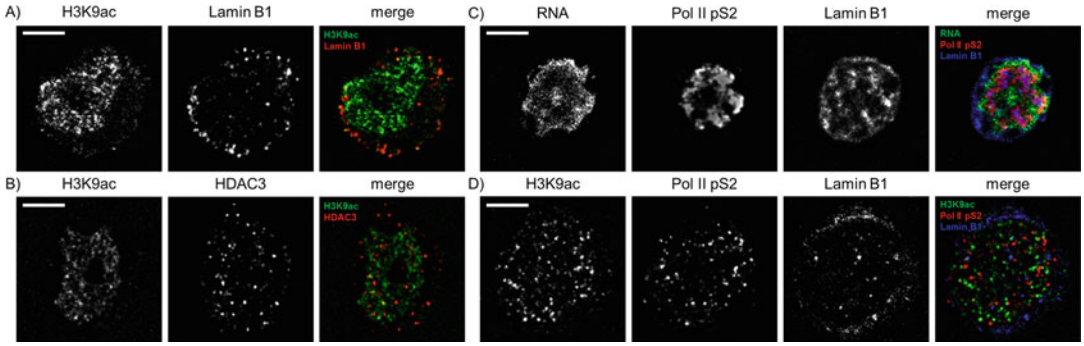

Fig. 2 Images of endogenous nuclear proteins and nucleic acids by confocal microscopy. Nuclei isolated from TZM-bl cells were co-stained for the given nuclear targets and imaged by confocal microscopy (**a–d**). Deconvolved confocal equatorial *z*-series of representative nuclei are shown. Scale bars 5 μm

architectural markers at high resolution (*see* Fig. 2). We have successfully applied this technique to obtain quantitative information on chromatin remodeling dynamics in single unfixed nuclei treated with histone deacetylase inhibitors [13].

For isolating nuclei, both the commercial method used here and the custom protocol which we developed [13] are based on hypotonic lysis and yield nuclei lacking the nuclear envelope and nuclear pore complexes. This benefits downstream experiments in three ways: (a) increasing the optical resolution of nuclear structures, which can be visualized without the presence of cytoplasm and organelles which normally interfere with imaging of the nucleus; (b) increasing the size exclusion limit of the nuclear lamina to allow rapid diffusion of antibodies, dyes, and compounds into the nuclei that enables immunofluorescence staining; and (c) avoiding fixation and permeabilization steps to yield nuclei that are transcriptionally and enzymatically active [13].

2 Materials

The procedures described in this protocol requires the use of standard laboratory equipment (biosafety cabinet, pipettors, benchtop centrifuges, cell counter) and consumables (cell culture flasks and dishes, pipettes).

2.1 Cells and Cell Culture

1. TZM-bl cells (NIH-AIDS Reagent Program, NIH, Bethesda, USA) (*see* **Note 1**).
2. Growth medium: DMEM supplemented with 10% heat-inactivated fetal bovine serum (FBS), penicillin 100 units/mL, streptomycin 100 μg/mL, and L-glutamine 0.4 mg/mL.
3. Culture vessels: 75 cm^2 culture flasks or 55 cm^2 round dishes.

4. 1× Phosphate Buffered Saline (PBS).
5. Trypsin-EDTA solution.
6. Automated cell counter.
7. Suberanilohydroxamic acid (Vorinostat) (SAHA, Sigma), a histone deacetylase inhibitor: 1 mM stock solution in DMSO (*see* **Note 2**).
8. Biosafety cabinet, centrifuges.

2.2 Isolation of Nuclei

1. Nuclei isolation kit: Nuclei EZ Prep Nuc-101 (Sigma) (*see* **Note 3**).

2.3 Immunolabeling, Imaging, and Image Analysis

1. 5% FBS in 1× PBS (5% FBS/PBS): prepare fresh and store at 4 °C.
2. Antibodies: *see* Table 1 for suppliers and immunolabeling conditions.
3. Fluorescent RNA stain: SYTO RNA Select green (ThermoFisher).

Table 1
Antibodies and immunolabeling conditions

Antibody	Dilution	Supplier	Cat. no.
Ms mAb to Histone H3 acetyl K9	1:10,000–1:50,000	Abcam	ab12179
Rb pAb to RNA polymerase II (phospho S2)	1:10,000–1:50,000	Abcam	ab5095
Rb pAb to Histone H3	1:100–1:1000	Abcam	ab61251
Goat pAb to Lamin B1	1:100	Abcam	ab156829
Rb pAb to Lamin B1	1:1000	Abcam	ab16048
Ms mAb to KMT1A/SUV39H1	1:100	Abcam	ab12405
Rb pAb to HDAC3	1:5000	Abcam	ab7030
Ms pAb to CBFβ	1:100	Abcam	ab167382
Rb pAb to RUNX1/AML1	1:1000	Abcam	ab23980
Ms mAb to Histone H3 trimethyl K9	1:100	Abcam	ab184677
Ms mAb to Histone H3 trimethyl K27	1:1000	Abcam	ab6002
Ms mAb to β-Actin	1:200	Sigma-	A1978
Alexa Fluor 488 rabbit anti-goat IgG	1:1000	Thermo Fisher	A11078
Alexa Fluor 555 rabbit anti-goat IgG	1:1000	Thermo Fisher	A21431
Alexa Fluor 488 goat anti-mouse IgG	1:1000–1:2000	Thermo Fisher	A11001
Alexa Fluor 555 goat anti-rabbit IgG	1:1000	Thermo Fisher	A21429
Donkey anti-goat IgG-PerCp-Cy5.5	1:100	Santa Cruz	sc-45102

4. Chambered coverglasses (Nunc Lab-Tek).
5. Confocal laser scanning microscope.
6. Image analysis software: ImageJ (imagej.nih.gov/ij/download/) or a custom MATLAB image analysis script.

3 Methods

3.1 Isolation of Nuclei

1. We passage TZM-bl cells 3–5 times after thawing cells preserved in liquid nitrogen; early passages occasionally do not replicate with the expected doubling time of 24 h. We normally passage cells three times a week to prevent overgrowth; this practice increases the cells' health. We use passages between 5 and 20 and passage them with a 1:2 ratio the day before seeding them. Count cells accurately with an automated cell counter.
2. Start from at least 5×10^6 cells to obtain enough nuclei for one experimental condition. Aspirate the medium without disturbing the cells.
3. Wash the cells with 10 mL of 1× PBS, add 2 mL of 0.25% trypsin-EDTA solution, and incubate for 5 min at 37 °C. Add 8 mL of growth medium and transfer the cells to a 15 mL conical tube (*see* **Note 4**).
4. Pellet the cells at 500 × *g*, 5 min, 4 °C, and remove the supernatant.
5. Resuspend and wash the pellet with 10 mL of ice-cold 1× PBS.
6. Collect the cells by centrifugation at 500 × *g*, 5 min, 4 °C, and remove the supernatant without disturbing the cell pellet. This initial wash is followed by two identical cell lysis steps that yield purified nuclei.
7. Follow the section "Procedure for Suspension Cell Lines" from the Sigma Nuclei Isolation Kit from point 2 to the end (*see* **Note 5**). Add 4 mL of lysis buffer to the cell pellet, resuspend the cells, and set them on ice for 5 min. The buffer should facilitate lysis of the plasma membrane and liberate the nuclei into solution.
8. Pellet the nuclei at 500 × *g*, 5 min, 4 °C, remove the supernatant, and repeat the preceding step to increase the yield of purified nuclei.
9. Centrifuge the nuclei at 500 × *g*, 5 min, 4 °C, and resuspend them in storage buffer; we modify the instructions in the Sigma kit and triturate the pellet of nuclei more than ten times.

10. Aliquot 50 μL volumes of the nuclear suspension into microcentrifuge tubes to allow multiple staining experiments and avoid multiple rounds of freezing/thawing. Each staining condition described below requires 10 μL of purified nuclei.
11. Freeze the nuclei at −80 °C.

3.2 Labeling Nuclei

1. Aliquot 990 μL of 5% FBS/PBS in microcentrifuge tubes, add 10 μL of isolated nuclei, and set on ice. Repeat the operation for each labeling condition.
2. To visualize total RNA, add the cell-permeant stain SYTO RNA Select directly to the nuclei at 50–500 nM for 20 min, wash the nuclei twice, and resuspend them in ice-cold 5% FBS/PBS.
3. For immunolabeling, add the primary antibody(ies) in 5% FBS/PBS to the suspension of nuclei to obtain the desired dilution, vortex gently, and set the samples on ice for 1 h (*see* Table 1 and **Note 6** for antibody concentrations and troubleshooting).
4. Include controls without primary antibodies to determine the fluorescence background for imaging; the signal will be generated only by the secondary fluorophore-conjugated antibody.
5. Pellet the nuclei at 500 × *g* for 5 min at room temperature and carefully remove the primary antibody-containing solution with a pipette without disturbing the pellet. Add 1 mL of ice-cold 5% FBS/PBS to the pellet and vortex to wash and resuspend the nuclei. Wash the nuclei twice and resuspend them in 1 mL of ice-cold 5% FBS/PBS.
6. Add secondary antibodies conjugated with fluorescent dyes in 5% FBS/PBS to the nuclei to the desired concentration and set on ice for 1 h.
7. To identify changes in subnuclear compartmentalization due to drug treatment, for example, co-label the nuclei to detect histone modifications, transcription factors, or structural components (e.g., the lamina).
8. Repeat the washes described in Subheading 3.2, **step 5** and resuspend the nuclei in the storage buffer of the EZ Prep Kit.
9. The immunolabeled nuclei are ready for imaging or can be stored at −20 °C. It is preferable to examine nuclei immediately after labeling, as the fluorescent signals are degraded over time during storage at −20 °C.
10. To combine non-immunofluorescence staining with antibody staining, for example for visualization of total RNA, add SYTO RNA Select to the nuclei 20 min before the end of the incubation with the secondary antibody and proceed with the washes in Subheading 3.2, **step 5**.

3.3 Confocal Microscopy, Image Acquisition, and Analysis

1. Seed a 10 μL drop of labeled nuclei at the center of a lidded and chambered coverglass. This support benefits the imaging in three ways: it conveniently allows a maximum of eight staining conditions on the same slide; it avoids sample cross contamination; and it reduces evaporation of the specimens.
2. Allow the nuclei to sit on the slide for 1 h before imaging to allow them to settle by gravity and sit stably on the coverglass.
3. Turn on the microscope at least 1 h prior to imaging to allow laser sources to warm up and system stabilization.
4. Define the *z*-stage position and step size to acquire images of entire nuclei. Define the acquisition parameters including exposure time, gain, laser power, and Airy units for each condition of illumination.
5. Perform imaging tests to verify stage stability to exclude significant *x*, *y*, *z* drifting. The two previous steps allow multiple location and time-lapse movies with negligible *x*-*y*-*z* drift in our experience.
6. Before performing time-lapse experiments where specimens are illuminated repeatedly, define the illumination parameters to exclude significant loss of signal due to photobleaching and verify that no alteration of the room illumination or aeration occurs during time-lapse acquisitions.
7. Perform imaging and store the raw data for processing.
8. Determine the coordinates and intensity of diffraction-limited spots by MATLAB-based image analysis software [13].
9. Use ImageJ to prepare images for presentation: adjust the lookup tables according to the background controls (no primary antibody), crop regions of interest, and insert scale bars.
10. If required, perform statistical comparisons to evaluate effects of drugs.

4 Notes

1. The protocol described here can be adapted to any type of mammalian cell. We have used it successfully for a variety of cell lines as well as for primary blood immune cells and primary CNS-derived cells.
2. To examine effects of inhibiting histone deacetylation, grow cells for 48 h in medium supplemented with the inhibitor suberanilohydroxamic acid. Harvest cells, count them, aliquot 3×10^6 cells into 15 mL conical tubes, and gently pelleted

them at 500 × *g*, 4 °C for 3–5 min. Resuspend the cells in growth medium containing 1 μM suberanilohydroxamic acid or DMSO alone as a vehicle control and seed them in 75 cm^2 flasks or 55 cm^2 dishes. This allows to seed and treat cells at the same time.

3. In order to minimize exposure to trypsin, we carefully monitor the state of attachment to the surface and remove the trypsin before the cells lift off from the plastic, followed by adding growth medium. This little nuance should significantly reduce the amount of trypsin carried over.
4. We tested detaching cells by scraping as suggested in the EZ Prep Kit instructions, but the yield was poor. We therefore trypsinize and follow the protocol for isolating nuclei from cells in suspension.
5. An alternative protocol for isolating nuclei which we have developed is described in [13, 14].
6. We recommend testing a range of antibody concentrations lower and higher (generally centered around 1:1000) than those recommended by the supplier, observing all conditions under the microscope. We recommend conditions that yield a ≥20-fold increase in labeling intensity over background.

Acknowledgments

This work was supported by NIH grant 1DP2DA044550 and the W. W. Smith Charitable Trust.

References

1. Heitz E (1928) Das Heterochromatin der Moose. I Jahrb Wiss Bot 69:762–818
2. Harr JC, Gonzalez-Sandoval A, Gasser SM (2016) Histones and histone modifications in perinuclear chromatin anchoring: from yeast to man. EMBO Rep 17:139–155
3. Jenuwein T, Allis CD (2001) Translating the histone code. Science 293:1074–1080
4. Benedetti R, Conte M, Altucci L (2015) Targeting histone deacetylases in diseases: where are we? Antioxid Redox Signal 23:99–126
5. Brien GL, Valerio DG, Armstrong SA (2016) Exploiting the epigenome to control cancer-promoting gene-expression programs. Cancer Cell 29:464–476
6. Milavetz BI, Balakrishnan L (2015) Viral epigenetics. Methods Mol Biol 1238:569–596
7. Zhu J, Adli M, Zou JY et al (2013) Genome-wide chromatin state transitions associated with developmental and environmental cues. Cell 152:642–654
8. Lakadamyali M, Cosma MP (2015) Advanced microscopy methods for visualizing chromatin structure. FEBS Lett 589:3023–3030
9. Kimura H, Hayashi-Takanaka Y, Stasevich TJ et al (2015) Visualizing posttranslational and epigenetic modifications of endogenous proteins in vivo. Histochem Cell Biol 144:101–109
10. Ricci MA, Manzo C, García-Parajo MF et al (2015) Chromatin fibers are formed by heterogeneous groups of nucleosomes in vivo. Cell 160:1145–1158
11. Smeets D, Markaki Y, Schmid VJ et al (2014) Three-dimensional super-resolution microscopy of the inactive X chromosome territory reveals a collapse of its active nuclear compartment harboring distinct Xist RNA foci. Epigenetics Chromatin 7:8

12. Wombacher R, Heidbreder M, van de Linde S et al (2010) Live-cell super-resolution imaging with trimethoprim conjugates. Nat Methods 7:717–719
13. Sardo L, Lin A, Khakhina S et al (2017) Real-time visualization of chromatin modification in isolated nuclei. J Cell Sci 130:2926–2940
14. Farrell RE (2010) Analysis of nuclear RNA. In: RNA methodologies. A laboratory guide for isolation and characterization, 4th edn. Elsevier/Academic Press, San Diego

Chapter 4

Dual-Color Metal-Induced Energy Transfer (MIET) Imaging for Three-Dimensional Reconstruction of Nuclear Envelope Architecture

Alexey I. Chizhik, Anna M. Chizhik, Daja Ruhlandt, Janine Pfaff, Narain Karedla, Ingo Gregor, Ralph H. Kehlenbach, and Jörg Enderlein

Abstract

The nuclear envelope, comprising the inner and the outer nuclear membrane, separates the nucleus from the cytoplasm and plays a key role in cellular functions. Nuclear pore complexes (NPCs) are embedded in the nuclear envelope and control transport of macromolecules between the two compartments. Recently, it has been shown that the axial distance between the inner nuclear membrane and the cytoplasmic side of the NPC can be measured using dual-color metal-induced energy transfer (MIET). This chapter focuses on experimental aspects of this method and discusses the details of data analysis.

Key words Metal-induced energy transfer, Nuclear envelope, Nuclear pore complex, Optical microscopy, Plasmonics, Super-resolution microscopy

1 Introduction

Localization of fluorophores with accuracy that goes far beyond the dimensions of the diffraction-limited focal spot has become routine, due to numerous microscopy methods that have been developed in recent decades. A resolution of the order of tens of nanometers in the focal plane is easily available and some techniques even allow to localize with an accuracy as high as just a few nanometers [1–3]. Measurement of the axial position of an emitter has been a more challenging task and typically has led to an order of magnitude worse accuracy. The only methods which achieve nanometer resolution along the optical axis in fluorescence microscopy are interferometric PALM (iPALM) [4] and 4Pi-STORM [5], but at the cost of requiring an exceptionally complex and difficult to operate interferometric setup. We have recently developed a simpler method to precisely measure distances of fluorescent molecules from a surface, which is termed metal-induced energy transfer

Ronald Hancock (ed.), *The Nucleus*, Methods in Molecular Biology, vol. 2175, https://doi.org/10.1007/978-1-0716-0763-3_4,

(MIET) [6]. Since MIET works only within ~200 nm over the substrate surface, it has been mostly applied for profilometry of basal cell membranes (that is, close to the surface of the microscope slide) or localization of proteins in focal adhesions. Recently, it has been shown that its working range suffices to measure the distance between the inner nuclear membrane (INM) and the outer nuclear membrane (ONM) throughout the whole basal area of the nuclear membrane and to reconstruct its 3D architecture [7].

The nucleus of eukaryotic cells is surrounded by the INM and the ONM, which fuse at the level of the nuclear pore complexes (NPCs). These large protein complexes serve as gates for transport of macromolecules between the nucleus and the cytoplasm (for reviews *see* [8, 9]). NPCs comprise an (almost) symmetric core structure close to the INM and ONM with filaments that emanate into the cytoplasm and into the nucleus, where they form a basket-like structure [10]. In human cells, the NPC has a diameter of ~120 nm and a height of the core structure of ~80 nm. Considering the nuclear and cytoplasmic filaments, an axial height of ~150–200 nm can be reached. The NPC consists of ~30 different proteins, nucleoporins or Nups, which all occur in copy numbers of eight or multiples of eight [11]. Some of these are symmetrically arranged and found on both sides (nuclear and cytoplasmic) of the NPC. One example for a nucleoporin that exclusively localizes to the cytoplasmic side of the NPC is Nup358, a very large protein of 358 kDa [12], which was suggested to function as an assembly or disassembly platform for nuclear import or export complexes, respectively [13–15].

The space between the INM and the ONM has a typical width of 30–50 nm [16–18]. Several hundred proteins that are enriched at the INM have been identified, mostly by proteomic screens [19, 20]. One of the best-described is Lap2β (lamina-associated polypeptide 2β, also referred to as thymopoietin β). Lap2β, a protein of 452 amino acids, contains a single transmembrane domain close to the C-terminal end and interacts with the nuclear lamina underneath the INM [21, 22]. A precise localization of a protein of interest to the INM or the ONM (or to the nuclear or the cytoplasmic side of the NPC) is difficult because of the small distance between the two membranes, and typically requires immuno-electron microscopy as a high-resolution method [12, 23]. For this, rather harsh fixation procedures are required that are very different from those used in fluorescence microscopy. DSTORM [24] and STED microscopy [25] have been used to analyze the structure of the NPC at a lateral resolution of about 20 nm. In a recent paper, Yang and co-workers used single-point fluorescence recovery after photobleaching (FRAP) in conjunction with single-molecule localization (SML) for measuring the lateral INM-ONM distance in an equatorial section through the nucleus to be 36–40 nm [26], exploiting the high lateral resolution of SML.

Recently, Chizhik et al. used Lap2β and Nup358 as proteins with defined localizations at the INM and the cytoplasmic side of the NPC, respectively, and determined the axial distance between the two proteins by dual-color MIET [6, 7, 27, 28]. The nanometer axial resolution of MIET allowed for measuring the distance between the INM and ONM throughout the whole basal area of the nuclear membrane. In this chapter, we focus on experimental details of that study which show the simplicity of MIET and should allow researchers to use it for other biological studies.

2 Materials and Methods

2.1 MIET Substrate Preparation

For MIET measurements, glass cover slides (thickness 170 μm) are coated with the following multilayer structure: 2 nm Ti, 15 nm Au, 2 nm Ti, and 10 nm SiO_2. The metal and silica films can be prepared by vapor deposition onto a cleaned cover slide using an electron beam source (Univex 350; Leybold, Cologne, Germany) under high vacuum conditions (~10^{-6} mbar). During vapor deposition, film thickness should be monitored using an oscillating quartz unit.

2.2 Cell Culture and Immunofluorescence

Here we describe the method for HeLa cells using antibodies against Nup358 and Lap2β (*see* **Note 1**); other cell types and combinations of antibodies might need minor modifications of the procedure. HeLa P4 cells [29] are grown in DMEM (Gibco) supplemented with 10% calf serum (Gibco), 100 U/mL penicillin, 100 μg/mL streptomycin, and 2 mM L-glutamine (Gibco) under 5% CO_2 at 37 °C. For indirect immunofluorescence followed by MIET analysis, cells should be seeded onto metal-coated glass coverslips (*see* Subheading 2.1) and incubated until they reach 70% confluency. After washing with PBS, fixation with 3.7% (v/v) formaldehyde in PBS for 10 min and permeabilization with 0.5% Triton X-100 in PBS for 5 min at room temperature, the cells are blocked with 2% BSA in PBS for 30 min. They are then incubated with rabbit anti-Lap2β (Millipore 06-1002, 1:100) and goat anti-Nup358 [13, 30] (1:500) in PBS with 2% BSA for 2 h. After three washing steps with PBS the cells are incubated with cross-absorbed secondary antibodies (Molecular Probes, 1:1000 in PBS with 2% BSA) for 1 h. As secondary antibodies we use goat anti-rabbit AlexaFluor 633 and donkey anti-goat AlexaFluor 488 for samples of type I, and goat anti-rabbit Alexa 488 and donkey anti-goat Alexa 633 for samples of type II. After three final washing steps with PBS and one with H_2O, samples are mounted in Mowiol 4-88 (Calbiochem) for further analysis.

2.3 MIET Measurements

Photoluminescence measurements can be performed using a standard confocal microscope with a fluorescence lifetime imaging (FLIM) extension. In our study, the measurements are done with

a homebuilt confocal microscope equipped with an objective lens of high numerical aperture (Apo N, 60× oil, 1.49 NA, Olympus, Hamburg, Germany). A pulsed, linearly polarized white light laser (SC400-4-20, Fianium, UK; pulse width ~50 ps, repetition rate 20 MHz) equipped with a tunable filter (AOTFnC-400.650-TN, Pegasus Optik, Wallenhorst, Germany) served as excitation source. We use the 488 nm and 635 nm wavelengths for fluorescence excitation. The light is reflected by a non-polarizing beamsplitter towards the objective, and the back-scattered excitation light is blocked with long-pass filters (EdgeBasic BLP01-488R, Semrock, NY, USA) for the green channel and BLP01-635R (Semrock) for the red channel. An additional band-pass filter (BrightLine FF01-550/88, Semrock) is used for A488 measurements. Emission light is focused onto the active area of an avalanche photodiode (PDM Series, MicroPhoton Devices, Bolzano, Italy), and data recording is performed with a multichannel picosecond event timer (HydraHarp 400, PicoQuant, Berlin, Germany). Samples are scanned with a focused laser spot using a piezo nano-positioning stage (P-562.3CD, Physik Instrumente, Karlsruhe, Germany). Photoluminescence spectra of A488 and A633 molecules inside the cells are recorded using a spectrograph (SR 303i, Andor Technology, Belfast, UK) equipped with a CCD camera (iXon DU897 BV, Andor) (*see* Fig. 1).

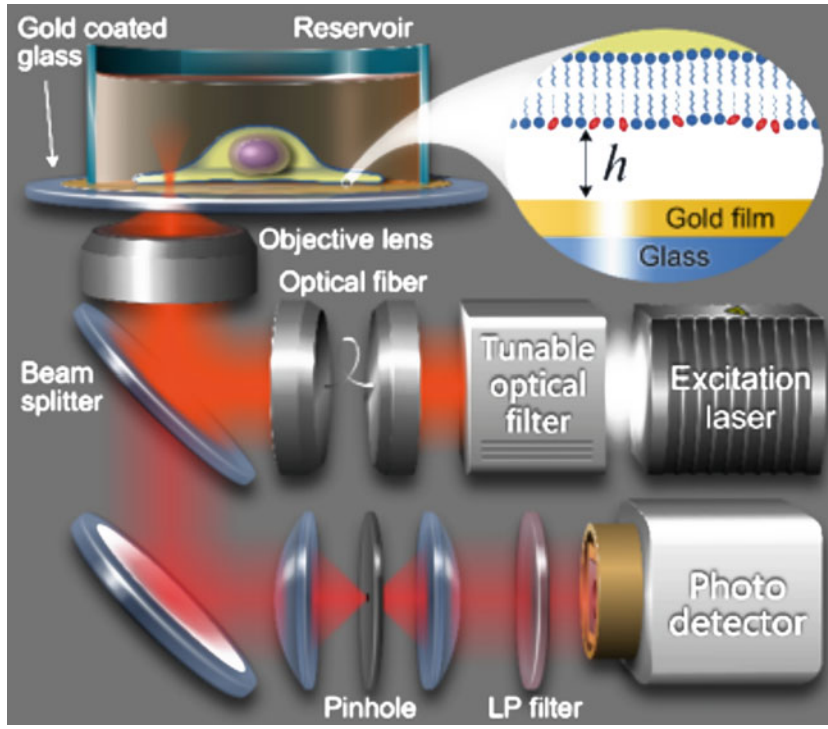

Fig. 1 Scheme of the confocal microscope for MIET measurements. LP is a long-pass optical filter

2.4 Fluorescence Lifetime Data Evaluation

In our study [7], we recorded fluorescence photons in time-tagged, time-resolved mode, which allows gathering all photons from a single pixel and sorting them into a histogram according to their arrival time after the last laser pulse. These time-correlated single-photon counting (TCSPC) histograms are corrected for detector and electronics dead-time effects [31], and finally an average decay rate is extracted from each histogram. The lifetimes used in the calculations are always the inverse values of these average decay rates. In our previous work [6] we found an empirical relationship between the number of photons N, the lifetime τ, and the uncertainty of the lifetime, namely $\sigma_\tau \approx 4.8\tau/\sqrt{N}$. Using the MIET calibration curves described in Subheading 2.6, this value can be translated to a height uncertainty for each pixel. In this chapter, however, we always show distributions of height values from many different pixels, which is why we do not take the height uncertainty of each single pixel into account.

2.5 MIET Measurements and Data Evaluation

In a MIET measurement, the sample of interest should be placed on a substrate that is coated with a thin, semitransparent metal film. The electromagnetic near field of fluorescent emitters close to the metal couples to surface plasmons of the metal film, thus transferring energy from excited molecules to the metal. This leads to a decrease in the emitter's fluorescence lifetime τ, which can be measured using a FLIM. Up to a distance of ~150–200 nm above the metal, there exists a monotonic relationship between the distance h of an emitter to the metal surface and its fluorescence lifetime τ, yielding an unambiguous measure for an emitter's distance from the surface (*see* Fig. 2). The relationship between lifetime and distance can be used to directly convert the FLIM image into a height profile using a MIET calibration curve, as described in the following section.

2.6 MIET Calibration Curves and Axial Localization

For the calculation of MIET calibration curves, a detailed knowledge of the optical parameters of the sample is required (*see* **Note 2**). In all our MIET measurements the sample consisted of a glass cover slide (refractive index $n = 1.52$) coated with 2 nm titanium, 15 nm gold (*see* **Note 3**), 2 nm titanium, and 10 nm silicon dioxide (*see* **Note 4**) ($n = 1.5$), and finally the cell in its mounting medium (Mowiol). In our study, the wavelength-dependent refractive indices of the metal layers were taken from [32], while the mean refractive index of a HeLa cell was assumed to be 1.37 [33, 34]. At first glance, it is unclear whether the complex structure of a cell with different refractive indices in various cell compartments, the cytosol, and the plasma membrane has to be taken into account for an accurate MIET measurement. The refractive index of the plasma membrane has been reported as $n = 1.46$ [35] or $n = 1.48$ [36], while that of the nuclei of four different cell lines, including HeLa cells, has been determined as $n = 1.36$ [34], and values for the

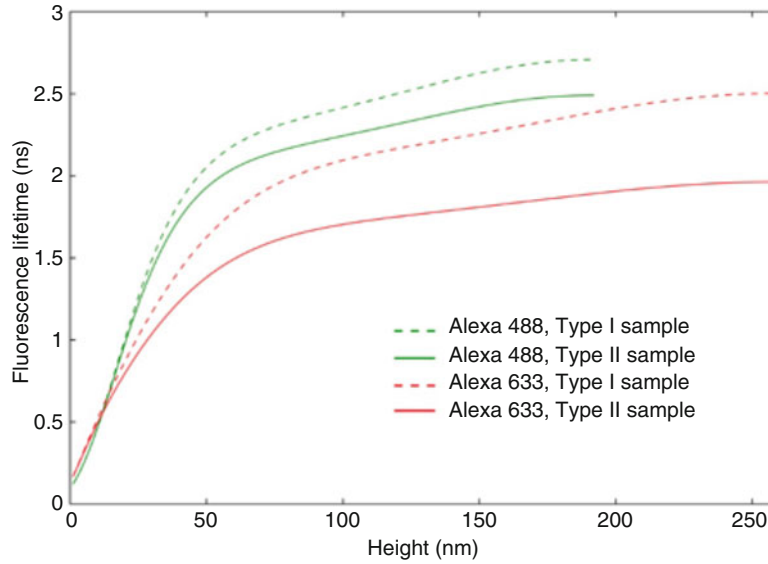

Fig. 2 MIET calibration curves for A633 on the outer nuclear membrane (red solid curve) or inner nuclear membrane (red dashed curve) and for A488 on the inner nuclear membrane (green solid curve) or outer nuclear membrane (green solid curve). The height is measured from the interface between silica and cell medium

cytosol range between 1.36 and 1.39 [35, 37, 38]. In order to estimate the magnitude of the effect these different refractive indices have on the MIET result, MIET calibration curves were calculated for three different situations: (a) a homogeneous refractive index of $n = 1.37$ everywhere above the SiO_2 spacer, (b) a 10 nm thick layer of Mowiol (the refractive index seems to vary from batch to batch; we used $n = 1.49$ as reported in most of publications) between the SiO_2 spacer and the cell with $n = 1.37$, and (c) a homogeneous refractive index of $n = 1.37$ almost everywhere, except for a 6 nm thick lipid bilayer ($n = 1.46$) situated 2 nm below the fluorescent label of the inner nuclear membrane or 2 nm above the fluorescent label of the outer nuclear membrane. The results for the average height distance between the INM and the ONM, calculated as described here, are shown in Table 1.

The results show no significant difference between the three sample geometries. Therefore, we decided to use the simplest situation (a) for all further calculations.

As described in [6], both the quantum yield and the lifetime of the dye in the same surroundings as in the MIET measurement, but without the presence of the metal layer (termed the "free space quantum yield" and "free space lifetime"), are needed for calculating the MIET calibration curves. Both quantities can be determined with the help of a metal nanocavity, as explained in the following Subheading 2.7. Previous measurements found the

Table 1
Type I samples consist of Lap2β labeled with Alexa 633 and Nup358 labeled with Alexa 488, whereas in type II samples the fluorophores are switched (*see* Note 5)

Sample	(a)	(b)	(c)
INM-A488, ONM-A633 (type I)	31 ± 16 nm	29 ± 15 nm	31 ± 16 nm
INM-A633, ONM-A488 (type II)	35 ± 19 nm	35 ± 18 nm	34 ± 19 nm

Table 2
Lifetimes of the dyes conjugated to different antibodies and quantum yields in the cell environment (*see* Note 6)

Sample	Measured lifetime τ [ns]	Calculated QY Φ [–]
gA488 (ONM, sample type I)	2.6	0.59
rbA633 (INM, sample type I)	2.4	0.47
rbA488 (INM, sample type II)	2.4	0.54
gA633 (ONM, sample type II)	1.9	0.37

quantum yield of A488 in water (refractive index $n_0 = 1.33$) to be $\Phi_0 = 0.94$, with a lifetime of $\tau_0 = 4.4$ ns [39]. Since the manufacturer did not publish the quantum yield of A633, we measured it and obtained $\Phi_0 = 0.59$, $\tau_0 = 3.2$ ns in water. However, when a dye is placed in a different medium, the nonradiative decay rate of the excited state can change unpredictably, while we assume that the radiative decay rate changes with the refractive index n of the surrounding medium as described by the empty-cavity model [40]. By measuring the lifetime τ of the dye in the cell (in the absence of any metal layers), the quantum yield Φ in this new environment can be calculated *via*:

$$\Phi = \Phi_0 \cdot \frac{\tau}{\tau_0} \cdot \frac{n^5}{n_0^5} \cdot \frac{\left(2n_0^2 + 1\right)^2}{\left(2n^2 + 1\right)^2}$$

We measured samples without a metal coating and averaged over all pixels within one cell to get an estimate of the lifetimes τ of the dyes conjugated to the different antibodies and in the cell environment. With $n = 1.37$, we arrive at the following Table 2.

Using these values for Φ and τ and assuming the layered structure (a) described above, MIET calibration curves for the four different cases were calculated using MIET_GUI software, custom-written MATLAB routines available for free download in the form of a graphical user interface (https://projects.gwdg.de/projects/miet). Finally, these curves were used to convert measured lifetime values from the metal-coated samples into height values (where $h = 0$ corresponds to the interface between silicon dioxide and the cell medium) (*see* Fig. 2).

2.7 Quantum Yield Measurements

To maximize the accuracy of the measurements, we performed fluorescence quantum yield measurements using our recently developed absolute metal nanocavity method [39] (*see* Fig. 3). The metal nanocavity consists of two mirrors with sub-wavelength spacing. The bottom mirror was prepared by vapor deposition of a 30 nm silver film (*see* Subheading 2.1) onto a commercially available cleaned microscope glass coverslip (thickness 170 μm). The top mirror was prepared by vapor deposition of a 60 nm-thick silver film onto the surface of a plano-convex lens

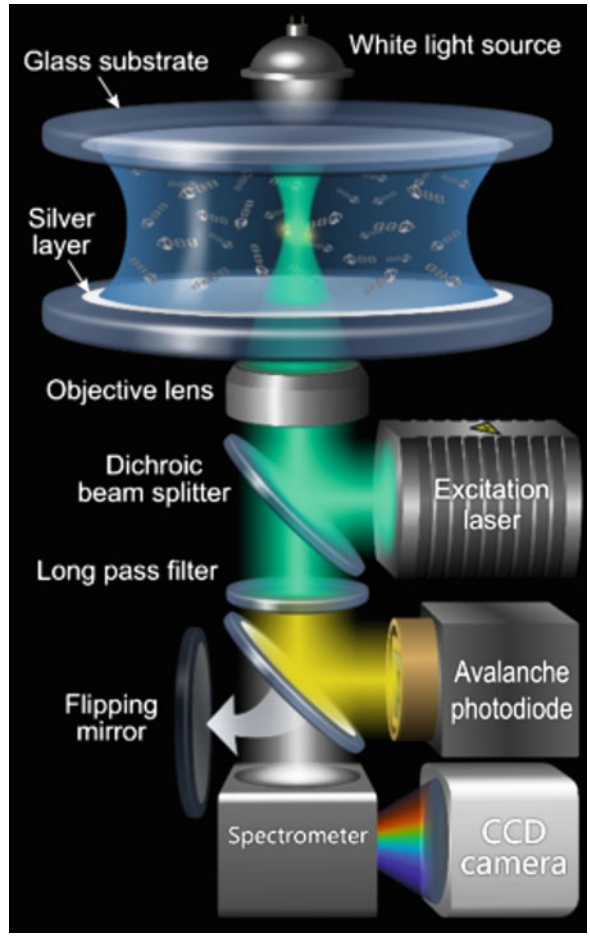

Fig. 3 Experimental setup for quantum yield measurements. The nanocavity consists of two silver layers, deposited on the glass surface. The upper layer is sputtered on the surface of a plano-convex lens, which allows one to tune the cavity length by moving the cavity in a horizontal plane. It should be noted that within the focal spot of a diffraction-limited objective lens, the cavity acts as a plane-parallel resonator

(focal length 150 mm) under the same conditions. The spherical shape of the upper mirror allowed for reversibly tuning the cavity length by moving the laser focus laterally away from or towards the contact point between the lens and the cover slide. It should be noted that across the size of the diffraction-limited laser focus, the cavity can be considered to be a plane-parallel resonator. For a detailed presentation of the theoretical background, *see* [39].

3 Notes

1. Lap2β as a marker for the INM [22] and Nup358 as a marker for the cytoplasmic side of the NPC (*i.e.,* in approximation also for the ONM [41]) were labeled with antibodies coupled to two different organic dyes that allowed us to spectrally separate their signals. To assess the quality of our protein detection procedure, we first analyzed the localization of our proteins of interest by conventional confocal microscopy. HeLa cells were fixed and subjected to standard indirect immunofluorescence, detecting Nup358 and LAP2β within a horizontal plane through the center of the nucleus. Accordingly, a clear rim staining was observed for both proteins, characteristic for nucleoporins or proteins associated with the nuclear envelope. Hence, the two proteins and our specific antibodies seem very appropriate for a MIET approach.
2. One of the key prerequisites of MIET imaging is a precise characterization of the fluorophores in the absence of a metal film (free space parameters). In particular, the emission spectra, fluorescence lifetimes, and quantum yields are required. Therefore, we determined the above parameters for AlexaFluor 488 (A488) and AlexaFluor 633 (A633) dyes under conditions close to those in our samples, allowing the calculation of exact calibration curves for our samples (*see* Fig. 2).
3. Smoothness of the metal layers is crucial for correct measurements of fluorophore height using MIET and of quantum yield using a metal nanocavity. High roughness induces a hardly predictable character of fluorescence modulation when a molecule is located close to a metal film. Besides high purity of the substrate surface, one should also correctly adjust the metal deposition parameters of the evaporation machine. The key parameter is the deposition rate, which ideally should not exceed 0.1 nm/s. The predeposition power should also be adjusted so that the initial deposition rate does not exceed the above value.

4. For MIET imaging, cells are seeded on metal-coated substrates. To use the same sample preparation procedures as for glass surfaces used for standard immunofluorescence, we coat the gold layer with a 10 nm-thick silica (SiO_2) layer. For better adhesion of the gold layer to the glass and the SiO_2 layer, 2 nm thick intermediate titanium layers are added. Focusing the excitation light with a 1.49 NA objective lens onto the metal film allows us to excite only molecules that are located within an ~200 nm distance above the sample surface that is within the working range of MIET. As a result, only fluorescence from the basal nuclear membrane is detected. Out of focus fluorescence is filtered out by a confocal pinhole.
5. To verify the reliability of MIET measurements, two types of samples were examined: sample type I consists of Lap2β labeled with A633 and Nup358 labeled with A488, whereas in sample type II the fluorophores were switched.
6. Although Lap2β is expected to localize predominantly to the INM, a small proportion could be found at the ONM as well, *e.g.,* prior to translocation of the protein *via* the NPC to the INM. This could lead to Förster Resonance Energy Transfer (FRET) between A488 and A633 at locations on the ONM where the distance between Lap2β and Nup358 would be within FRET range, that is near or closer than 5 nm for the two dyes. Because FRET opens an additional de-excitation pathway for the donor (A488), this may lead to a decrease of its fluorescence lifetime. However, for MIET measurements, a reduction of fluorescence lifetime due to FRET would lead to wrong height values. To exclude any impact of FRET, fluorescence lifetime measurements of A488 were done after photobleaching of A633. Once the acceptor molecules are bleached, they cannot receive energy from the donor anymore, which results in a complete suppression of FRET.

Acknowledgments

This work was supported in part by the Deutsche Forschungsgemeinschaft (DFG) through the Cluster of Excellence "Center for Nanoscale Microscopy and Molecular Physiology of the Brain (CNMPB)." A.I.C. and D.R. are grateful to the DFG for financial support *via* SFB 937 (project A14). N.K. is grateful to the DFG for financial support of his position *via* SFB 860 (project A06). R.H.K. and J.P. acknowledge funding by the DFG through SFB1190 (project P07).

References

1. Hell SW (2009) Microscopy and its focal switch. Nat Methods 6:24–32. https://doi.org/10.1038/nmeth.1291
2. Huang B, Bates M, Zhuang X (2009) Super-resolution fluorescence microscopy. Annu Rev Biochem 78:993–1016. https://doi.org/10.1146/annurev.biochem.77.061906.092014
3. Godin AG, Lounis B, Cognet L (2014) Super-resolution microscopy approaches for live cell imaging. Biophys J 107:1777–1784. https://doi.org/10.1016/j.bpj.2014.08.028
4. Shtengel G, Galbraith JA, Galbraith CG, Lippincott-Schwartz J, Gillette JM, Manley S, Sougrat R, Waterman CM, Kanchanawong P, Davidson MW, Fetter RD, Hess HF (2009) Interferometric fluorescent super-resolution microscopy resolves 3D cellular ultrastructure. Proc Natl Acad Sci U S A 106:3125–3130. https://doi.org/10.1073/pnas.0813131106
5. Aquino D, Schonle A, Geisler C, Middendorff CV, Wurm CA, Okamura Y, Lang T, Hell SW, Egner A (2011) Two-color nanoscopy of three-dimensional volumes by 4Pi detection of stochastically switched fluorophores. Nat Methods 8:353–359. http://www.nature.com/nmeth/journal/v8/n4/abs/nmeth.1583.html#supplementary-information
6. Chizhik AI, Rother J, Gregor I, Janshoff A, Enderlein J (2014) Metal-induced energy transfer for live cell nanoscopy. Nat Photonics 8:124–127. https://doi.org/10.1038/nphoton.2013.345
7. Chizhik AM, Ruhlandt D, Pfaff J, Karedla N, Chizhik AI, Gregor I, Kehlenbach RH, Enderlein J (2017) Three-dimensional reconstruction of nuclear envelope architecture using dual-color metal-induced energy transfer imaging. ACS Nano 11:11839–11846. https://doi.org/10.1021/acsnano.7b04671
8. Beck M, Hurt E (2017) The nuclear pore complex: understanding its function through structural insight. Nat Rev Mol Cell Biol 18:73–89. https://doi.org/10.1038/nrm.2016.147
9. Dickmanns A, Kehlenbach RH, Fahrenkrog B (2015) Nuclear pore complexes and nucleocytoplasmic transport: from structure to function to disease. In: Kwang WJ (ed) International review of cell and molecular biology, vol 320. Academic Press, Cambridge, pp 171–233. https://doi.org/10.1016/bs.ircmb.2015.07.010
10. Lin DH, Hoelz A (2019) The structure of the nuclear pore complex (an update). Annu Rev Biochem 88:725–783. https://doi.org/10.1146/annurev-biochem-062917-011901
11. Ori A, Toyama BH, Harris MS, Bock T, Iskar M, Bork P, Ingolia NT, Hetzer W, Beck M (2015) Integrated transcriptome and proteome analyses reveal organ-specific proteome deterioration in old rats. Cell Syst 1:224–237. https://doi.org/10.1016/j.cels.2015.08.012
12. Yokoyama N, Hayashi N, Seki T, Pante N, Ohba T, Nishii K, Kuma K, Hayashida T, Miyata T, Aebi U, Fukui M, Nishimoto T (1995) A giant nucleopore protein that binds Ran/TC4. Nature 376(6536):184–188
13. Hutten S, Flotho A, Melchior F, Kehlenbach RH (2008) The Nup358-RanGAP complex is required for efficient importin α/β-dependent nuclear import. Mol Biol Cell 19:2300–2310. https://doi.org/10.1091/mbc.E07-12-1279
14. Hutten S, Wälde S, Spillner C, Hauber J, Kehlenbach RH (2009) The nuclear pore component Nup358 promotes transportin-dependent nuclear import. J Cell Sci 122:1100–1110. https://doi.org/10.1242/jcs.040154
15. Ritterhoff T, Das H, Hofhaus G, Schröder RR, Flotho A, Melchior F (2016) The RanBP2/RanGAP1∗SUMO1/Ubc9 SUMO E3 ligase is a disassembly machine for Crm1-dependent nuclear export complexes. Nat Commun 7:11482. https://doi.org/10.1038/ncomms11482
16. Cain NE, Starr DA (2015) SUN proteins and nuclear envelope spacing. Nucleus 6:2–7. https://doi.org/10.4161/19491034.2014.990857
17. Franke WW, Scheer U, Krohne G, Jarasch ED (1981) The nuclear envelope and the architecture of the nuclear periphery. J Cell Biol 91:39s–50s
18. Feldherr CM, Akin D (1990) The permeability of the nuclear envelope in dividing and nondividing cell cultures. J Cell Biol 111:1–8. https://doi.org/10.1083/jcb.111.1.1
19. Schirmer EC, Florens L, Guan T, Yates JR, Gerace L (2003) Nuclear membrane proteins with potential disease links found by subtractive proteomics. Science 301:1380–1382
20. Wilkie GS, Korfali N, Swanson SK, Malik P, Srsen V, Batrakou DG, de las Heras J, Zuleger N, ARW K, Florens L, Schirmer EC (2011) Several novel nuclear envelope transmembrane proteins identified in skeletal muscle have cytoskeletal associations. Mol Cell

Proteomics 10:M110.003129. https://doi.org/10.1074/mcp.M110.003129

21. Foisner R, Gerace L (1993) Integral membrane proteins of the nuclear envelope interact with lamins and chromosomes, and binding is modulated by mitotic phosphorylation. Cell 73:1267–1279
22. Furukawa K, Panté N, Aebi U, Gerace L (1995) Cloning of a cDNA for lamina-associated polypeptide 2 (LAP2) and identification of regions that specify targeting to the nuclear envelope. EMBO J 14:1626–1636
23. Cordes VC, Reidenbach S, Rackwitz H-R, Franke WW (1997) Identification of protein p270/Tpr as a constitutive component of the nuclear pore complex–attached intranuclear filaments. J Cell Biol 136:515–529
24. Löschberger A, van de Linde S, Dabauvalle M-C, Rieger B, Heilemann M, Krohne G, Sauer M (2012) Super-resolution imaging visualizes the eightfold symmetry of gp210 proteins around the nuclear pore complex and resolves the central channel with nanometer resolution. J Cell Sci 125:570–575. https://doi.org/10.1242/jcs.098822
25. Göttfert F, Wurm CA, Mueller V, Berning S, Cordes VC, Honigmann A, Hell SW (2013) Coaligned dual-channel STED nanoscopy and molecular diffusion analysis at 20 nm resolution. Biophys J 105:L01–L03. https://doi.org/10.1016/j.bpj.2013.05.029
26. Mudumbi KC, Schirmer EC, Yang W (2016) Single-point single-molecule FRAP distinguishes inner and outer nuclear membrane protein distribution. Nat Commun 7:12562. https://doi.org/10.1038/ncomms12562. https://www.nature.com/articles/ncomms12562#supplementary-information
27. Karedla N, Chizhik AI, Gregor I, Chizhik AM, Schulz O, Enderlein J (2014) Single-Molecule Metal-Induced Energy Transfer (smMIET): resolving nanometer distances at the single-molecule level. ChemPhysChem 15:705–711. https://doi.org/10.1002/cphc.20130076028
28. Baronsky T, Ruhlandt D, Brückner BR, Schäfer J, Karedla N, Isbaner S, Hähnel D, Gregor I, Enderlein J, Janshoff A, Chizhik AI (2017) Cell–substrate dynamics of the epithelial-to-mesenchymal transition. Nano Lett 17(5):3320–3326. https://doi.org/10.1021/acs.nanolett.7b01558
29. Charneau P, Mirambeau G, Roux P, Paulous S, Buc H, Clavel F (1994) HIV-1 reverse transcription A termination step at the Center of the Genome. J Mol Biol 241:651–662. https://doi.org/10.1006/jmbi.1994.1542
30. Pichler A, Gast A, Seeler JS, Dejean A, Melchior F (2002) The nucleoporin RanBP2 has SUMO1 E3 ligase activity. Cell 108:109–120. https://doi.org/10.1016/S0092-8674(01)00633-X
31. Isbaner S, Karedla N, Ruhlandt D, Stein SC, Chizhik A, Gregor I, Enderlein J (2016) Dead-time correction of fluorescence lifetime measurements and fluorescence lifetime imaging. Opt Express 24:9429–9445. https://doi.org/10.1364/OE.24.009429
32. Rakić AD, Djurišić AB, Elazar JM, Majewski ML (1998) Optical properties of metallic films for vertical-cavity optoelectronic devices. Appl Optics 37:5271–5283. https://doi.org/10.1364/AO.37.005271
33. Lue N, Choi W, Popescu G, Yaqoob Z, Badizadegan K, Dasari RR, Feld MS (2009) Live cell refractometry using Hilbert phase microscopy and confocal reflectance microscopy. J Phys Chem A 113:13327–13330. https://doi.org/10.1021/jp904746r
34. Schürmann M, Scholze J, Müller P, Guck J, Chan CJ (2016) Cell nuclei have lower refractive index and mass density than cytoplasm. J Biophotonics 9:1068–1076. https://doi.org/10.1002/jbio.201500273
35. van Manen H-J, Verkuijlen P, Wittendorp P, Subramaniam V, van den Berg TK, Roos D, Otto C (2008) Refractive index sensing of green fluorescent proteins in living cells using fluorescence lifetime imaging microscopy. Biophys J 94:L67–L69. https://doi.org/10.1529/biophysj.107.127837
36. Beuthan J, Minet O, Helfmann J, Herrig M, Müller G (1996) The spatial variation of the refractive index in biological cells. Phys Med Biol 41:369–382
37. Choi W, Fang-Yen C, Badizadegan K, Oh S, Lue N, Dasari RR, Feld MS (2007) Tomographic phase microscopy. Nat Methods 4:717–719. http://www.nature.com/nmeth/journal/v4/n9/suppinfo/nmeth1078_S1.html
38. Curl CL, Bellair CJ, Harris T, Allman BE, Harris PJ, Stewart AG, Roberts A, Nugent KA, Delbridge LMD (2005) Refractive index measurement in viable cells using quantitative phase-amplitude microscopy and confocal microscopy. Cytometry A 65A:88–92. https://doi.org/10.1002/cyto.a.20134
39. Chizhik AI, Gregor I, Ernst B, Enderlein J (2013) Nanocavity-based determination of absolute values of photoluminescence quantum yields. ChemPhysChem 14:505–513. https://doi.org/10.1002/cphc.201200931

40. Schuurmans FJP, Vries PD, Lagendijk A (2000) Local-field effects on spontaneous emission of impurity atoms in homogeneous dielectrics. Phys Lett A 264:472–477. https://doi.org/10.1016/S0375-9601(99)00855-5
41. von Appen A, Kosinski J, Sparks L, Ori A, DiGuilio AL, Vollmer B, Mackmull M-T, Banterle N, Parca L, Kastritis P, Buczak K, Mosalaganti S, Hagen W, Andres-Pons A, Lemke EA, Bork P, Antonin W, Glavy JS, Bui KH, Beck M (2015) In situ structural analysis of the human nuclear pore complex. Nature 526:140–143. https://doi.org/10.1038/nature1538

Chapter 5

Studying Proton Gradients Across the Nuclear Envelope

Raul Martínez-Zaguilán and Souad R. Sennoune

Abstract

The existence of nuclear pore complexes in the nuclear envelope has led to the assumption that ions move freely from the cytosol into the nucleus, and that the molecular mechanisms at the plasma membrane that regulate cytosolic pH also regulate nuclear pH. Furthermore, studies to measure pH in the nucleus have produced contradictory results, since it has been found that the nuclear pH is either similar to the cytosol or more alkaline than the cytosol. However, most studies of nuclear pH have lacked the rigor needed to understand pH regulation in the nucleus. A major problem has been the lack of *in situ* titrations in the nucleus and cytosol, since the intracellular environment is different in the cytosol and nucleus and the behavior of fluorescent pH probes is different in these environments. Here we present a method that uses the fluorescence of SNARF-1 that labels both cytosol and nucleus. Using ratio imaging microscopy, regions of interest corresponding to the nucleus and cytosol to perform steady-state pH measurements followed by *in situ* titrations, to correctly assign pH in those cellular domains.

Key words Nucleoplasmic pH, Cytosolic pH, Fluorescence, Ratio imaging, SNARF-1

1 Introduction

It has been generally accepted that the nuclear envelope allows free movement of ions and small molecules in and out the nucleus because of the existence of the large diameter (30 nm) nuclear pore complexes [1–5]. Consequently, it has been concluded that pH regulation in the nucleus depends on pH regulatory mechanisms at the plasma membrane. However, the flow of ions into the nucleus has been shown to be tightly regulated by ion channels and primary transporting systems such as Na^+/K^+-ATPase and, more recently, by vacuolar H^+-ATPase in the nuclear envelope [6–15]. Several studies have demonstrated the existence of Na^+, K^+, Ca^{2+}, and H^+ gradients between the cytosol and the nucleoplasm [8, 15–20].

The nucleus supports fundamental biological processes including transcription, DNA replication, DNA repair, and chromatin remodeling [1, 2, 21]. pH is an important regulator of gene expression and epigenetic modulation and is fundamental for

Ronald Hancock (ed.), *The Nucleus*, Methods in Molecular Biology, vol. 2175, https://doi.org/10.1007/978-1-0716-0763-3_5,

regulation of cellular functions since the activity of all proteins and enzymes is exquisitely controlled by pH [21–24]. Surprisingly, very few functional studies of pH regulation in the nucleus exist in the literature. The existence of transporters, pumps, and channels in the nuclear envelope has been shown [25, 26], but only a few functional studies have been performed, including patch clamp studies of K^+, Ca^{2+}, and Cl^- channels [10–12, 15]. The significance of V-H^+-ATPase in the nuclear membranes for pH regulation independently of the cytosol has been demonstrated recently [17].

There are many reasons to emphasize the need to perform studies of nuclear pH. There is evidence that changes in [H^+] regulate DNA structure as well as interactions with DNA-binding proteins [31]. Acidic domains are found near double- as well as single-stranded nucleic acids, thus controlling the structure of DNA's major and minor grooves. The [H^+] in the vicinity of DNA mapped by the Poisson-Boltzmann approximation shows three regions of high H^+ concentration and two localized in the major groove, which may be important in regulating interactions between proteins and nucleic acids [31]. These studies are also relevant to understanding the interactions of proteins and noncarcinogenic and carcinogenic molecules with or near the DNA. The presence of V-ATPase in the inner nuclear membrane might be critical for higher order chromosome structure and regulation of enzymes involved in gene expression [17]. The existence of sub-compartments within the nucleus is thought to optimize the efficacy of nuclear functions by establishing specialized microenvironments [2, 32]. The formation of intranuclear tubules with only the inner nuclear membrane and of reticular structures with both nuclear membranes has the potential to contribute to nuclear ion homeostasis that modulates local pH microdomains that regulate DNA structure, gene transcription, epigenetics, and the cell cycle [33].

Recent studies have shown that V-H^+-ATPases located in both inner and outer nuclear membranes are responsible for the generation of inward and outward H^+ gradients, which may promote the coupled transport inward and outward of organic and inorganic molecules across the nuclear membranes as well as transport via proton-coupled transporting mechanisms [17]. For example folates, essential for DNA synthesis and DNA methylation, are transported across the plasma membrane by folate receptors and proton-coupled folate transport (PCFT) [34–37]; the source of protons used to transport folates into the nucleus has not been clarified, but could be generation of H^+ gradients via V-H^+-ATPases. Another example is the co-transport of glucose transporter GLUT-12 and H^+ in the perinuclear area of MCF7 breast cancer cells and human prostate cancer cells [38, 39]. Our recent unpublished observations indicate that glucose is transported into the nucleus to provide energy via glycolysis, further emphasizing

the need to better understand nuclear pH. The significance of inward and outward H^+ gradients and their relationship to transport of macromolecules into the nucleus requires further investigation.

Studies to evaluate nuclear pH have provided contradictory results that the nucleoplasm pH is either similar to the cytosol or that there is a significant pH gradient between them, i.e., nuclear pH is more alkaline than the cytosol [27–29]. These different findings in studies that use ratiometric approaches may be explained by the failure to perform *in situ* titrations in discrete regions corresponding to the cytoplasm and nucleus, where the microenvironments are different and a fluorescent probe may be susceptible to environmental conditions, e.g., viscosity and protein binding [17]. Evaluation of pH has used either a single calibration curve *in vitro* or *in situ*, or averaging of *in situ* calibration curves for nucleus and cytosol [27–30]. The need to perform *in situ* titration in each region of interest (ROI) is emphasized by the demonstration here that using a single pK_a, R_{min}, and R_{max} for all cell types, or even within the same cell type in nucleus and cytosol, results in under- or overestimation of pH in these cellular compartments (pK_a is the negative base-10 logarithm of the acid dissociation constant (Ka) of a solution, R_{min} is the ratio of fluorescence observed when the dye is fully protonated, and R_{max} is the ratio when the dye is fully unprotonated). In this chapter we describe how to perform *in situ* calibration for nucleus and cytosol and to determine the pH in these regions accurately using the dual emission ratiometric probe SNARF-1 AM (seminaphtorhodafluor-1-acetoxymethylester) [17].

2 Materials

2.1 Solutions

Prepare all buffers and solutions using ultra-pure water prepared by purifying deionized water using a MilliQ system to obtain a resistivity of 18.2 MΩ cm at 25 °C (*see***Note 1**).

1. Cell superfusion buffer (CSB): 0.44 mM KH_2PO_4, 110 mM NaCl, 0.35 mM Na_2HPO_4, 1.3 mM $CaCl_2$, 1 mM $MgSO_4$, 5.4 mM KCl, 25 mM HEPES, 5 mM glucose, 2 mM glutamine. Dissolve 0.06 g KH_2PO_4, 6.4295 g NaCl, 0.0497 g Na_2HPO_4, 0.1911 g $CaCl_2$, 0.1204 g $MgSO_4$, 0.4026 g KCl, 5.957 g HEPES, 0.901 g glucose, and 0.2923 g glutamine in 1 L of H_2O, adjust pH to 7.4 using NaOH [17, 40, 41] (*see***Note 2**).
2. High K^+ buffer: 5 mM glucose, 2 mM glutamine, 10 mM HEPES, and 10 mM bicine. Dissolve 0.901 g glucose, 0.2923 g glutamine, 2.383 g HEPES, 1.952 g MES, and 1.632 mM bicine in 1 L of H_2O. Adjust the pH to a value

ranging from 5.5 to 8.5 using NaOH [40]. The three organic buffers used here are selected based on their pK_a to ensure proper buffering from pH 5.5 to 8.5. Their pK_as at 37 °C are: MES 5.97; HEPES 7.31; and bicine 8.0440 [42] (*see***Notes 3** and **4**).

3. Valinomycin.
4. Nigericin.
5. SNARF-1 AM (seminaphtorhodafluor-1-acetoxymethylester) (ThermoFisher): 7 mM stock solution in anhydrous DMSO, store as aliquots at −20 °C.
6. DAPI solution: 1.5 μg/mL.
7. Phosphate-free detergent: 500 μL of 2% Contrad 70 (Decon Labs) in milliQ water, add 1 L of distilled water.

2.2 Equipment and Software

1. Petri dishes ∅ 30 and 60 mm.
2. Sterile round coverslips: ∅ 25 mm, thickness 0.15 or 0.17 mm depending on the optical system [17] (*see* Subheading 2.1, **item 4** and **Note 5**).
3. Cell chamber for ∅ 25 mm coverslips (Attofluor, ThermoFisher).
4. Cell chamber holder (PDMI-2; Greenvale, NY).
5. Peristaltic perfusion pump (Masterflex L/S Digital Standard Drive 7523-50 with MFlex silicone tubing, #13 for inlet and #14 for outlet (Cole-Parmer)).
6. Mini shaker (Grant Bio PS-3D, Fisher) or rocking platform (Bellco) (optional) (*see***Note 6**).
7. Inverted fluorescence microscope (Olympus IX70 with a 60× 1.4 NA oil-immersion objective, or similar).
8. High-speed filter changer and liquid guided optical fiber to deliver the light (Lambda DG4; Sutter Instruments, Novato, CA, USA).
9. Frame transfer CCD camera coupled to an intensifier (Pentamax ADC 5 MHZ, Princeton Instruments).
10. Longpass fluorescence filter set: XF05-2 DAPI excitation 365QM35, dichroic 400DCLP, and emission filter 400 ALP (Omega Optical, Brattleboro, VT, USA).
11. Imaging software: Metafluor (Molecular Devices) or other software that allows to select ROI for image capture.
12. SigmaPlot (version 10.0 or higher).

3 Methods

3.1 Cells and Cell Growth

1. The approach described here can be used with any adherent cell type; non-adherent cells such as lymphocytes can be attached by coating coverslips with polylysine. We use prostate cancer cells (DU-147, LNCaP, CL-1 and CL-2) and prostate epithelial cells (RWPE-1) (provided by Dr. Stephanie Filleur, Urology Department, TTUHSC, Lubbock, TX). Cell lines are maintained in culture for no more than 12 passages.
2. Grow DU-147, LNCaP, and CL-2 cells in RPMI medium supplemented with 5% fetal bovine serum (FBS) and RWPE-1 cells in Keratinocyte-SFM medium with bovine pituitary extract and epidermal growth factor (Gibco) in 5% CO_2 at 37 °C.
3. Maintain cells in T75 flasks and pass them once a week by plating 1×10^5 cells in 14 mL of growth medium [17]. In contrast to the parental LNCaP cells, CL-2 cells are highly tumorigenic and exhibit invasive phenotypes.
4. Prepare 100 mm ∅ petri dishes containing 6 sterile round coverslips (25 mm ∅, thickness 0.15 mm (#1) or 0.17 mm (#1.5) depending on the optical system) (*see***Note 5**) [17]. You can use either thickness for most recent microscope objectives with a high (>1.2) numerical aperture, but for super-resolution use only 0.17 mm (#1.5) to minimize optical aberration.
5. Add 10 mL of growth medium and 3–5 $\times 10^5$ cells (depending on the type and doubling time), gently mix, and arrange the coverslips to avoid overlap (*see***Note 5**). Using a sterile 1 mL pipette tip, press each coverslip down gently for 3–5 s to prevent them from floating or sticking to each other.
6. Grow the cells in the CO_2 incubator for 48–72 h to reach 70–80% confluency (*see***Note 7**).

3.2 Intracellular Loading of the pH Fluoroprobe SNARF-1

Perform these experiments in a biological laminar flow hood to maintain sterility.

1. Transfer a coverslip into a 30 mm ∅ petri dish containing 2 mL of CSB using sterile conditions.
2. Add SNARF-1 to the medium to 7 μM and incubate in the 37 °C incubator for 30 min, a time sufficient for hydrolysis of the acetoxymethyl ester form of SNARF-1 [42] (*see***Note 8**).
3. Aspirate the medium using a pasteur pipette and a very low vacuum to avoid detaching the cells. Add 2 mL of CSB to wash out nonhydrolyzed dye and incubate for 15 min.

4. Transfer the coverslip to the cell chamber; use sterile tweezers with a fine tip and push the coverslip up gently from the edge to avoid breakage.

3.3 Fluorescence Measurements of Cytosolic and Nuclear pH

The most common method to visualize the dual-emission ratiometric probe SNARF is using a single excitation wavelength (e.g., 534 nm) and collecting the emission signals at two wavelengths (584 nm and 644 nm). This requires a rapid filter changer containing the two 40 nm bandpass emission filters and located between the light path exiting the side port of the microscope and the CCD camera. In this case, the ratio 644/584 is used to monitor pH. However, because SNARF-1 can be excited at three wavelengths (488 nm, 514 nm, and 534 nm) it is also feasible to excite at 534 nm and 488 nm to obtain the largest dynamic range, and collect the signal using a single emission filter (600 nm long bandpass). This approach uses an inverted microscope, a frame transfer CCD camera coupled to an intensifier, and a device to rapidly change excitation wavelengths with a liquid guided optical fiber to deliver the light [17].

1. Transfer the cell chamber to the holder maintained at 37 °C on the microscope stage.
2. Keep all buffers at 37 °C in an adjacent water bath.
3. Superfuse the cells continuously with CSB at 3.0 mL/min (*see***Note 9**).
4. Image the cells using a 60× oil-immersion objective (1.4 NA). We use 100 ms exposures to obtain a high signal-to-noise ratio.
5. Using the imaging software, acquire an image and select two ROI of similar dimensions, one cytosolic and one nuclear, for each cell (up to 10–15 cells in the optical field of view) (*see***Notes 10** and **11**).
6. For steady-state pH measurements, obtain ratio images of cytosol and nucleus (530 nm and 488 nm) with 100 ms exposure at 5 s intervals for 5–10 min.

3.4 In Situ *Titration of the pH Fluoroprobe*

At the end of every experiment, an *in situ* calibration is performed to obtain parameters using the pH-sensitive ratios (530/488) (*see***Notes 12** and **13**).

1. Stop acquisition after steady-state pH measurements (typically 5–10 min) but continue superfusion.
2. Exchange the CSB superfusate for high K^+ buffer pH_{ex} 5.5 containing 6.8 μM nigericin and 2 μM valinomycin and superfuse for 10 min. These ionophores allow equilibration of $pH_{ex} = pH_{cyt}$ and $pH_{ex} = pH_{nuc}$; nigericin sets the H^+ gradient equal to the K^+ gradient and valinomycin completes collapse of the K^+ gradient (*see***Note 12**).

3. Acquire ratio images for 1 min with 100 ms exposures at 5 s intervals to obtain the first data point in the titration.
4. Exchange the perfusate (pH_{ex} 5.5) for the next pH_{ex} in the titration (e.g., pH 6.0) and superfuse for 5 min without acquisition (*see***Note 14**).
5. Acquire ratio images for 1 min to obtain the second point of the titration.
6. Stop data acquisition and superfuse for 5 min with the next pH buffer (e.g., pH 6.5).
7. Acquire ratio images for 1 min to obtain the third point of the titration.
8. Repeat **steps 4–7** of this section for a total of at least 6 points to obtain a good fitting of the data. If the cells tolerate the titration you could use 9–12 points, but 6 points should suffice (*see* Fig. 1) (*see***Note 15**).
9. Wash the cells with CSB and then incubate them for 1–2 min with DAPI to localize the nucleus and select the ROIs (nuclear region and cytosol) for post-acquisition analysis, and then superfuse for 1–2 min to wash out the DAPI.
10. Visualize the cells at 60× using the XF05-2 DAPI longpass fluorescence filter set (excitation 365QM35, dichroic 400DCLP, and emission filter 400 ALP) (*see***Note 16**).
11. Acquire images using 100 ms exposure time, or longer as needed.

3.5 Data Analysis

1. Reselect the ROIs for post-acquisition analysis to clearly identify the nucleus and cytosol by the DAPI stain (*see***Note 17**).
2. Export a newly created spreadsheet to Excel to create a plot of time versus ratio.
3. Using Excel, average the ratio values from the *in situ* titration to obtain a single point for each pH buffer.
4. Create a plot of the ratio values versus the known pH_{ex} and export the data to SigmaPlot (version 10 or higher) (*see***Note 18**).
5. Fit the data using the SigmaPlot section entitled "Pharmacology" on the upper bar of the notebook worksheet.
6. Select "Simple ligand binding" and "one site saturation" from the menu to fit the data. This will provide the pK_a, R_{max}, and R_{min} values needed to convert the ratio values to pH values (*see* Fig. 2) (*see***Notes 19** and **20**).
7. Insert these parameters into the Excel spreadsheet containing the ratio values (i.e., steady-state pH). Table 1 shows an

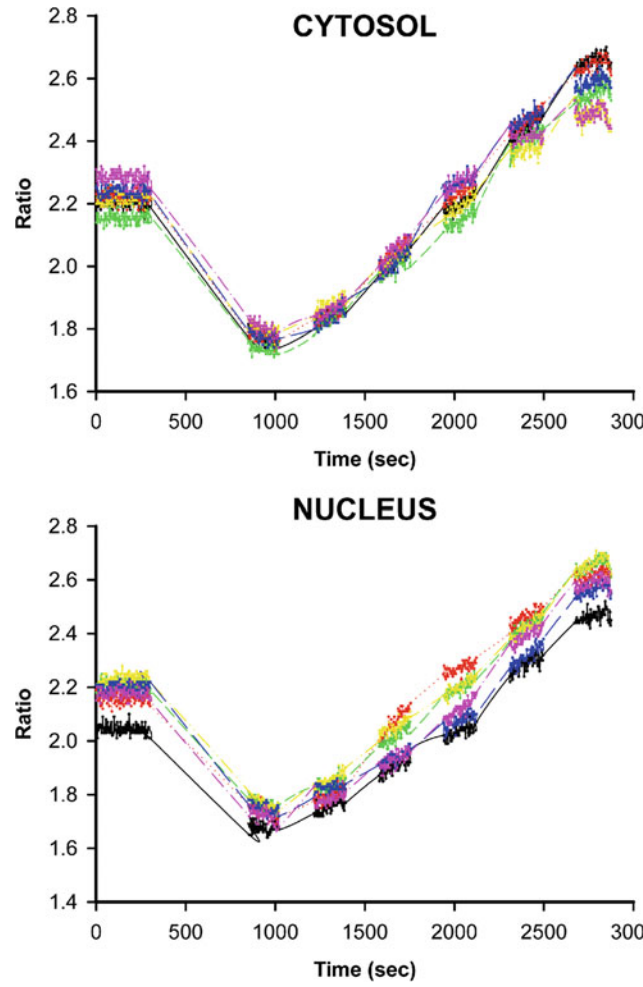

Fig. 1 Simultaneous measurement of pH in cytosol and nucleus. DU145 cells grown on coverslips were loaded with SNARF-1 AM that distributes in both cytosol and nucleus. Cells were transferred to a cell chamber with a holder and perfusion device and imaged with a 60× oil objective (1.4 NA) at 37 °C while superfused with CSB at 3.0 mL/min. ROIs corresponding to the nucleus and cytosol were selected using Metafluor software. Emission ratio images (excitation at 534 and 488 nm) were obtained at 600 nm (long bandpass filter) with 100 ms exposure at 5 s intervals for 5 min, using a system to rapidly exchange excitation filters and a CCD camera. In a typical experiment we evaluate 12–16 cells in the field of view, depending on cell size and level of confluency, but for data presentation we only show traces corresponding to 6 cells (one ROI from the cytosol and one from the nucleus). The first 5 min correspond to steady-state ratios. Then, acquisition is stopped to decrease photobleaching of the fluoroprobe and perfusion continues with high K^+ buffer pH 5.5 containing nigericin and valinomycin for 10 min. Then, acquisition starts again for 1 min (5 s intervals). The superfusate is exchanged for the next pH for 5 min (no acquisition) and then acquisition starts for 1 min. The lines (data points not shown) represent acquisition stoppage for 5 min following for 1 min acquisition at the desired pH_{ex} values. This process is repeated iteratively (*see***Note 21**)

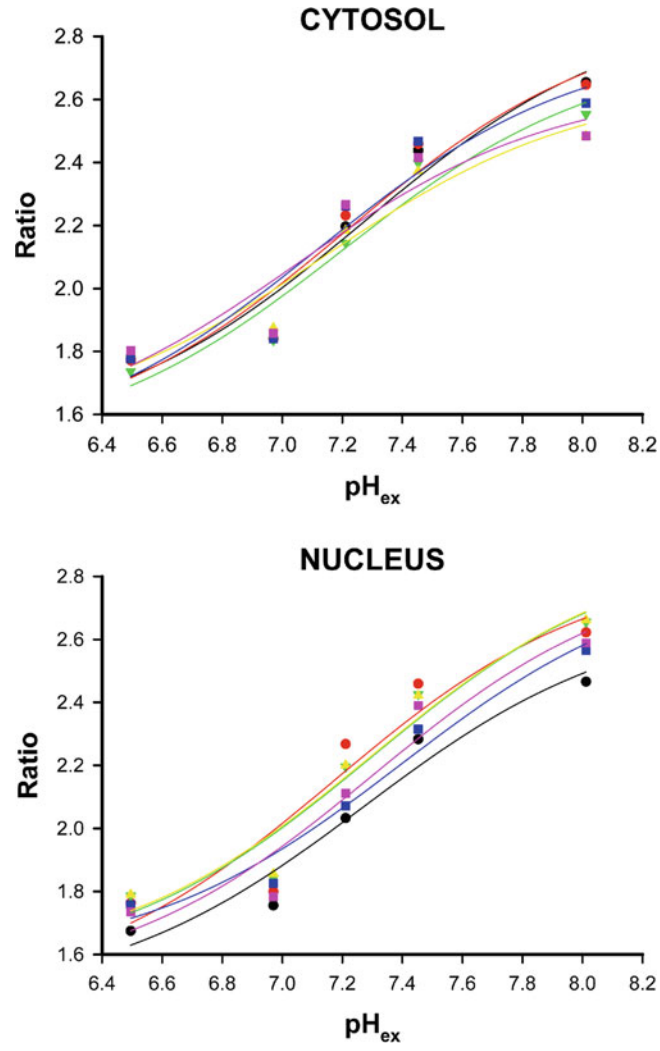

Fig. 2 Ratio versus pH_{ex} in cytosol and nucleus. Cells were loaded with SNARF as described in Fig. 1. The traces in Fig. 1 were averaged to obtain a single point (*R*) for each pH_{ex}. For purposes of presentation, only the data corresponding to 6 cells (nucleus and cytosol) are shown. The data points were fitted using a modified Henderson-Hasselbalch equation to obtain the *in situ* titration parameters needed to estimate pH for each cell (nucleus and cytosol)

example of how individual *in situ* titration parameters (R_{min}, R_{max}, and pK_a) are entered into the top rows in the Excel spreadsheet. This is done for 3 cells as a function of time (10.5 s) as an example.

8. Write equation 1 shown on the top of the Excel spreadsheet to solve for pH. This formula can be entered in the empty column to the right of ratio (column G, row 9, shown in green). The

Table 1
Converting ratio (*R*) to pH using *in situ* calibration

G9 | =C$5+LOG((C9-C$3)/(C$4-C9))

	A	B	C	D	E	F	G	H	I
1			cell #1	cell #2	cell #3				
2									
3		Rmin	1.918	2.3148	2.096				
4		Rmax	2.5476	3.0435	2.832				
5		pKa	7.5062	7.5082	7.4606				
6									
7		Time (sec)	R cell #1	R cell #2	R cell #3		pH cell #1	pH cell #2	pH cell #3
8									
9		1.5	2.11	2.56	2.32		7.15	7.21	7.10
10		4.5	2.14	2.53	2.31		7.24	7.13	7.07
11		7.5	2.13	2.53	2.32		7.21	7.13	7.10
12		10.5	2.12	2.54	2.31		7.18	7.16	7.07

This table illustrates how to convert ratio (R) to pH using *in situ* calibration parameters (R_{min}, R_{max}, and pK_a) for three cells using Excel (*see* Subheading 3.5, **steps 7** and **8**)

dollar sign in the formula anchors the pK_a, R_{max}, and R_{min}. Drag the formula from column G row 9 to copy the equation into empty rows and columns to convert ratio values to pH for all cells (*see* Tables 2 and 3).

3.6 Other Experimental Approaches to Measure pH in Living Cells

A more specific approach to label nuclei is to target a fluorescent probe such as ratiometric GFP to the inner nuclear membrane [27, 43]. Recently the ratiometric probe Hoechst-tagged fluorescein has been used to measure pH in the nucleus [44]; the Hoechst dye binds to DNA forming a complex that displays fluorescence shoulders at 460 nm and 520 nm corresponding to the emission signals of Hoechst and fluorescein, respectively, when excited at 405 nm. This probe has been used to measure pH from 5.5 to 8.3, and we have successfully used it to measure nuclear pH (unpublished results). Another approach utilizes HaloTag protein conjugated to chloroalkane-attached SNARF fused to a nuclear localization signal (NLS) [27]. Other approaches have used genetically encoded fluorescent protein-based pH sensors with a NLS [43, 45], but these require gene expression and exhibit low transfection efficiency, depending on the cell type.

Table 2
Significance of using individual *in situ* calibration parameters

	R_{min}		R_{max}		pK_a		pH	
Cells	**Cytosolic**	**Nucleoplasmic**	**Cytosolic**	**Nucleoplasmic**	**Cytosolic**	**Nucleoplasmic**	**Cytosolic**	**Nucleoplasmic**
#1	1.521	1.453	2.890	2.686	7.270	7.272	7.133	7.200
#2	1.495	1.458	2.875	2.843	7.215	7.172	7.134	6.999
#3	1.480	1.546	2.761	2.905	7.199	7.296	7.085	7.188
#4	1.548	1.554	2.650	2.908	7.135	7.298	7.119	7.174
#5	1.471	1.573	2.790	2.830	7.126	7.393	7.057	7.394
#6	1.502	1.493	2.648	2.845	7.044	7.301	7.224	7.247

These data demonstrate the significance of using individual *in situ* calibration parameters for cytosol and nucleus of each cell. These data were obtained from CL-1 prostate cancer cells. As shown, the in situ calibration parameters are different for each cell, indicating that averaging pK_a, R_{min} and R_{max} values to obtain a global set of parameters will result in either underestimation or overestimation of pH values in the cytosol and nucleus. The lack of appreciation of this need to use single *in situ* calibration parameters for cytosol and nucleus has led to erroneous conclusions regarding differences in pH between cytosol and nucleus

Table 3
***In situ* calibration parameters are distinct for each cell type**

	R_{min}		R_{max}		pK_a		
Cells	**Cytosolic**	**Nucleoplasmic**	**Cytosolic**	**Nucleoplasmic**	**Cytosolic**	**Nucleoplasmic**	**Number of cells**
RWPE-1	1.32 ± 0.02	1.36 ± 0.01	1.83 ± 0.03	1.90 ± 0.03	7.66 ± 0.02	7.64 ± 0.02	131
LNCaP	2.24 ± 0.02	2.31 ± 0.02	3.19 ± 0.04	3.33 ± 0.04	7.54 ± 0.01	7.55 ± 0.01	89
CL2	2.19 ± 0.03	2.23 ± 0.02	3.05 ± 0.06	3.11 ± 0.05	7.67 ± 0.02	7.63 ± 0.02	60
DU145	2.00 ± 0.03	2.05 ± 0.03	2.99 ± 0.07	3.22 ± 0.06	7.56 ± 0.04	7.68 ± 0.02	71

Data show the mean and the standard error of the mean for the number of cells evaluated

4 Notes

1. Be sure that filters are changed regularly and that the Total Organic Carbon (TOC) is <5 ppb.
2. You need large volumes of CSB per experiment, since perfusion at 3.0 mL/min is recommended. Prepare 25 L of buffer without glucose and glutamine to avoid contamination, which can be stored at 4 °C in the refrigerator for several months. The pH is adjusted on the day of an experiment and glucose and glutamine are added.
3. Use a new electrode to obtain reliable pH values.
4. High K^+ buffer can be prepared in large volumes (5 L) at room temperature and aliquots adjusted to the starting pH (typically pH 5.5) and in increments of ~0.5 pH units up to pH 7.0, using 10 M NaOH (avoid HCl). After that use increments of ca. 0.2 pH units. Take 500 mL from the 5 L container, this will allow 10 data points for the titration. Once you have prepared the whole set of buffers, transfer to a water bath to 37 °C, add glucose and glutamine, let them equilibrate, and measure the pH again. Write down the pH in the bottle for room temperature and 37 °C, since your experiments are done at 37 °C and the pH values to use for titration are those at 37 °C. Be sure that you use pH values (7.0, 7.2, 7.4, and 7.6) around the predicted pK_a of SNARF-1 (~7.4) as well as pH 5.5, 6.0, and 8.0.
5. Incorrect coverslip thickness can greatly reduce your ability to obtain the most information from the optical microscope. Most recent objective lenses are marked "0.17" to indicate the thickness (in mm) of the coverslips to be used; if not marked, 0.15 mm (#1) coverslips can be used. Clean all coverslips from one case in a 4 L plastic beaker with diluted phosphate-free detergent (2.1.7), then rinse 4–6× with distilled H_2O. Prepare a layer of Kimwipes (30 × 30 cm) in a glass dish (15 × 3 cm), and using tweezers place coverslips on top, close to each other. Fill the surface but do not put them on top of each other. Add another layer of Kimwipes on top and then more coverslips until the dish is filled, sterilize them in an autoclave, and transfer the dish to the oven to dry.
6. Using a shaker in the incubator helps homogeneous loading, and although it is not absolutely essential it is recommended (e.g., Mini shaker Grant Bio PS-3D, Fisher Scientific or Rocker Platform, Bellco, Vineland, NJ). The speed should be set to low.
7. Do not use cells that are >90% confluent; you need to have single cells to easily identify the cytosol and the nucleus to

select ROIs. Check the coverslips the day following plating cells and re-arrange them if needed to avoid floating and overlap.

8. It has been recognized that SNARF-1 labels the cytosol, and we have shown that it also labels nuclei [17]. Because its acetoxy methyl ester form can permeate most cellular membranes, it is expected that if esterases are located in intracellular compartments the free form of the dye would be produced, allowing us to measure pH in cytosol and nucleus.
9. Superfusion is important in that it allows to exchange buffers at different pH values and minimizes movement of the cell chamber.
10. ROIs outside the nucleus are visualized by phase contrast or DIC microscopy at the beginning of the experiment. Most image analysis software (e.g., NIS Elements, Nikon) allows you to select square or circular ROIs. Use whichever software you prefer, but use the same dimensions consistently for cytosol and nuclear regions.
11. It is important to stop acquisition to minimize photobleaching.
12. High K^+ buffer (pH 5.5–8.5 at 0.2 pH intervals) containing the ionophores 2 μM valinomycin and 6.8 μM nigericin is used to approximate the intracellular K^+ concentration. Nigericin exchanges H^+ and K^+ across the membrane, rendering the pH_{cyt} equal to the extracellular pH (pH_{ex}), while valinomycin moves K^+ across the plasma membrane and, together with nigericin, helps to equilibrate pH_{cyt} and pH_{ex}.
13. Cells are subsequently incubated for 10 min to ensure total collapse of pH gradients before the titration procedure. Thereafter, the pH is increased stepwise from 5.5 to 8.5 and cells are perfused with high K^+ for 5 min to allow for equilibration of $pH_{ex} = pH_{cyt}$ and $pH_{ex} = pH_{nu}$.
14. We allow 10 min for the first data point in the titration, but for subsequent points 5 min is sufficient to allow for $pH_{ex} = pH_{cyt}$ and $pH_{ex} = pH_{nu}$.
15. Most cells tolerate acidic pH very well, but at pH 7.6 they tend to detach and at $\geq$ pH 8.0 it is more difficult to titrate. Dye is also lost after a long titration using more than six data points.
16. DAPI allows to define the nucleus and cytosol for post-acquisition analysis. Thus, select the ROIs and re-run the acquired data for final analysis of pH in cytosol and nucleus. Most available software allow you to re-analyze the data at the end of the experiment (post-acquisition).
17. It is good practice to run the post-acquisition analysis and evaluate if the cell chamber and frame have moved, e.g., if the chamber is not firmly fastened to the microscope stage.

By evaluating frames from end to beginning of the experiment, one can easily identify if the chamber has moved. Sometimes it is possible to save an experiment by identifying the time when the frame moved; the section can be then stitched and used for analysis by adding the two sections (before and after frame movement) by selecting a new ROI.

18. These data (ratio versus pH) are fitted into the modified Henderson-Hasselbalch equation: $\mathrm{pH} = \mathrm{p}K_a + \log \frac{(R-R_{min})}{(R_{max}-R)}$ to obtain the *in situ* calibration parameters for cytosol and nucleus in individual cells. We use SigmaPlot to obtain the *in situ* calibration parameters ($\mathrm{p}K_a$, R_{min}, and R_{max}) needed to convert steady-state ratio values to pH_{cyt} and pH_{nu}.
19. Using SigmaPlot, you can insert known pH values in column 1 and ratio values in columns 2, 3, 4, etc. The software will automatically fit each column to obtain individual *in situ* calibration parameters [i.e., $\mathrm{p}K_a$, R_{max}, and R_{min} for each cell (cytosol and nucleus)].
20. From *in situ* titrations we obtain R_{min}, R_{max}, and $\mathrm{p}K_a$. R_{min} is the ratio observed when the dye is fully protonated, and R_{max} represents the ratio of fluorescence when the dye is fully unprotonated. These *in situ* calibration parameters are used to generate the pH_{cyt} and pH_{nu} values for each individual cell.
21. The slight upward drift observed in the time course of this titration is probably due to dye leakage; however, because we averaged 60 s acquisitions to plot the ratio versus pH_{ex}, this compensates for the drift.

References

1. Dernburg AF, Misteli T (2007) Nuclear architecture--an island no more. Dev Cell 12:329–334
2. Rinn J, Guttman M (2014) RNA function. RNA and dynamic nuclear organization. Science 345:1240–1241
3. Kramer A, Ludwig Y, Shahin V, Oberleithner H (2007) A pathway separate from the central channel through the nuclear pore complex for inorganic ions and small macromolecules. J Biol Chem 282:31437–31443
4. Beck M, Hurt E (2017) The nuclear pore complex: understanding its function through structural insight. Nat Rev Mol Cell Biol 18:73–89
5. Strambio-De-Castillia C, Niepel M, Rout MP (2010) The nuclear pore complex: Bridging nuclear transport and gene regulation. Nat Rev Mol Cell Biol 11:490–501
6. Bustamante JO (1993) Restricted ion flow at the nuclear envelope of cardiac myocytes. Biophys J 64:1735–1749
7. Bustamante JO, Hanover JA, Liepins A (1995) The ion channel behavior of the nuclear pore complex. J Membr Biol 146:239–251
8. Garner MH (2002) Na,K-ATPase in the nuclear envelope regulates Na^+: K^+ gradients in hepatocyte nuclei. J Membr Biol 187:97–115
9. Matzke AJ, Behensky C, Weiger T, Matzke MA (1992) A large conductance ion channel in the nuclear envelope of a higher plant cell. FEBS Lett 302:81–85
10. Bustamante JO (2006) Current concepts in nuclear pore electrophysiology. Can J Physiol Pharmacol 84:347–365
11. Matzke AJ, Weiger TM, Matzke M (2010) Ion channels at the nucleus: electrophysiology meets the genome. Mol Plant 3:642–652
12. Mazzanti M, DeFelice LJ, Cohn J, Malter H (1990) Ion channels in the nuclear envelope. Nature 343:764–767

13. Gerasimenko O, Gerasimenko J (2004) New aspects of nuclear calcium signalling. J. Cell Sci 117:3087–3094
14. Gomes DA, Leite MF, Bennett AM, Nathanson MH (2006) Calcium signaling in the nucleus. Can J Physiol Pharmacol 84:325–332
15. Mazzanti M, Bustamante JO, Oberleithner H (2001) Electrical dimension of the nuclear envelope. Physiol Rev 81:1–19
16. Resende RR, Andrade LM, Oliveira AG et al (2013) Nucleoplasmic calcium signaling and cell proliferation: calcium signaling in the nucleus. Cell Commun Signal 11:14
17. Santos JM, Martinez-Zaguilan R, Facanha AR, Hussain F, Sennoune SR (2016) Vacuolar H+-ATPase in the nuclear membranes regulates nucleo-cytosolic proton gradients. Am J Physiol Cell Physiol 311:C547–C558
18. Cuppoletti J (2016) Nuclear v-type ATPase: Focus on "vacuolar H^+-ATPase in the nuclear membranes regulates nucleo-cytosolic proton gradients". Am J Physiol Cell Physiol 311: C544–C546
19. Galva C, Artigas P, Gatto C (2012) Nuclear Na^+/K^+-ATPase plays an active role in nucleoplasmic Ca^{2+} homeostasis. J Cell Sci 125:6137–6147
20. Oliveira AG, Guimaraes ES, Andrade LM et al (2014) Decoding calcium signaling across the nucleus. Physiology 29:361–368
21. Casey JR, Grinstein S, Orlowski J (2010) Sensors and regulators of intracellular pH. Nat Rev Mol Cell Biol 11:50–61
22. Sennoune SR, Martinez-Zaguilan R (2007) Plasmalemmal vacuolar H^+-ATPases in angiogenesis, diabetes and cancer. J Bioenerg Biomembr 39:427–433
23. Boron WF (2004) Regulation of intracellular pH. Adv Physiol Educ 28:160–179
24. Shrode LD, Tapper H, Grinstein S (1997) Role of intracellular pH in proliferation, transformation, and apoptosis. J Bioenerg Biomembr 29:393–399
25. Batrakou DG, Kerr AR, Schirmer EC (2009) Comparative proteomic analyses of the nuclear envelope and pore complex suggests a wide range of heretofore unexpected functions. J Proteomics 72:56–70
26. Schirmer EC, Florens L, Guan T et al (2003) Nuclear membrane proteins with potential disease links found by subtractive proteomics. Science 301:1380–1382
27. Benink H, McDougall M, Klaubert D, Los G (2009) Direct pH measurements by using subcellular targeting of 5(and 6-) carboxyseminaphthorhodafluor in mammalian cells. Biotechniques 47:769–774
28. Masuda A, Oyamada M, Nagaoka T et al (1998) Regulation of cytosol-nucleus pH gradients by K^+/H^+ exchange mechanism in the nuclear envelope of neonatal rat astrocytes. Brain Res 807:70–77
29. Seksek O, Bolard J (1996) Nuclear pH gradient in mammalian cells revealed by laser microspectrofluorimetry. J Cell Sci 109:257–262
30. Bright GR, Fisher GW, Rogowska J, Taylor DL (1987) Fluorescence ratio imaging microscopy: Temporal and spatial measurements of cytoplasmic pH. J Cell Biol 104:1019–1033
31. Lamm G, Pack GR (1990) Acidic domains around nucleic acids. Proc Natl Acad Sci U S A 87:9033–9036
32. Lamond AI, Spector DL (2003) Nuclear speckles: a model for nuclear organelles. Nat Rev Mol Cell Biol 4:605–612
33. Avedanian L, Jacques D, Bkaily G (2011) Presence of tubular and reticular structures in the nucleus of human vascular smooth muscle cells. J Mol Cell Cardiol 50:175–186
34. Hou Z, Matherly LH (2014) Biology of the major facilitative folate transporters slc19a1 and slc46a1. Curr Top Membr 73:175–204
35. Zhao R, Diop-Bove N, Visentin M, Goldman ID (2011) Mechanisms of membrane transport of folates into cells and across epithelia. Annu Rev Nutr 31:177–201
36. Boshnjaku V, Shim KW, Tsurubuchi T et al (2012) Nuclear localization of folate receptor alpha: a new role as a transcription factor. Sci Rep 2:980
37. Chen C, Ke J, Zhou XE et al (2013) Structural basis for molecular recognition of folic acid by folate receptors. Nature 500:486–489
38. Chandler JD, Williams ED, Slavin JL, Best JD, Rogers S (2003) Expression and localization of glut1 and glut12 in prostate carcinoma. Cancer 97:2035–2042
39. Rogers S, Macheda ML, Docherty SE et al (2002) Identification of a novel glucose transporter-like protein-glut-12. Am J Physiol Endocrinol Metab 282:E733–E738
40. Sennoune SR, Bakunts K, Martinez GM et al (2004) Vacuolar H^+-ATPase in human breast cancer cells with distinct metastatic potential: distribution and functional activity. Am J Physiol Cell Physiol 286:C1443–C1452
41. Gillies RJ, Martinez-Zaguilan R (1991) Regulation of intracellular pH in balb/c 3T3 cells. Bicarbonate raises pH via $NaHCO_3/HCl$ exchange and attenuates the activation of Na^+/H^+ exchange by serum. J Biol Chem 266:1551–1556
42. Martinez-Zaguilan R, Lynch RM, Martinez GM, Gillies RJ (1993) Vacuolar-type $H^{(+)}$-

ATPases are functionally expressed in plasma membranes of human tumor cells. Am J Physiol 265:C1015–C1029

43. Bencina M (2013) Illumination of the spatial order of intracellular pH by genetically encoded pH-sensitive sensors. Sensors 13:16736–16758
44. Nakamura A, Tsukiji S (2017) Ratiometric fluorescence imaging of nuclear pH in living cells using Hoechst-tagged fluorescein. Bioorg Med Chem Lett 27:3127–3130
45. Sherman TA, Rongali SC, Matthews TA et al (2012) Identification of a nuclear carbonic anhydrase in Caenorhabditis elegans. Biochim Biophys Acta 1823:808–817

Chapter 6

COMBinatorial Oligonucleotide FISH (COMBO-FISH) with Uniquely Binding Repetitive DNA Probes

Michael Hausmann, Jin-Ho Lee, Aaron Sievers, Matthias Krufczik, and Georg Hildenbrand

Abstract

During the last decade, genome sequence databases of many species have been more and more completed so that it has become possible to further develop a recently established technique of FISH (Fluorescence In Situ Hybridization) called COMBO-FISH (COMBinatorial Oligo FISH). In contrast to standard FISH techniques, COMBO-FISH makes use of a bioinformatic search in sequence databases for probe design, so that it can be done for any species so far sequenced. In the original approach, oligonucleotide stretches of typical lengths of 15–30 nucleotides were selected in such a way that they only co-localize at the given genome target. Typical probe sets of about 20–40 stretches were used to label about 50–250 kb specifically. The probes of different lengths can be composed of purines and pyrimidines, but were often restricted to homo-purine or homo-pyrimidine probe sets because of the experimental advantage of using a protocol omitting denaturation of the target strand and triple strand binding of the probes. This allows for a better conservation of the 3D folding and arrangement of the genome. With an improved, rigorous genome sequence database analysis and sequence search according to statistical frequency and uniqueness, a novel family of probes repetitively binding to characteristic genome features like SINEs (Short Interspersed Nuclear Elements, e.g., ALU elements), LINEs (Long Interspersed Nuclear Elements, e.g., L1), or centromeres has been developed. These probes can be synthesized commercially as DNA or PNA probes with high purity and labeled by fluorescent dye molecules. Here, new protocols are described for purine-pyrimidine probes omitting heat treatment for denaturation of the target so that oligonucleotide labeling can also be combined with immune-staining by specific antibodies. If the dyes linked to the oligonucleotide stretches undergo reversible photo-bleaching (laser-induced slow blinking), the labeled cell nuclei can be further subjected to super-resolution localization microscopy for complex chromatin architecture research.

Key words Combinatorial oligonucleotide fluorescence in situ hybridization, COMBO-FISH, Computer-based probe search, DNA/PNA oligonucleotides, Unique labeling, Combination of FISH and immune-staining, Fluorescent nano-probes for super-resolution localization microscopy, Chromatin nano-architecture

1 Introduction

Specific chromatin labeling by fluorescence in situ hybridization (FISH) has become an indispensable tool in biological and

Ronald Hancock (ed.), *The Nucleus*, Methods in Molecular Biology, vol. 2175, https://doi.org/10.1007/978-1-0716-0763-3_6,

biomedical research as well as in routine medical diagnostics. FISH offers attractive possibilities to label DNA sequences in 3D-conserved cell nuclei, on metaphase chromosomes, or on chips for screening purposes with high specificity and sensitivity. FISH probes and procedures [1] cover specific labeling from whole chromosomes (also called "chromosome painting") over centromeres or telomeres and other subchromosomal regions like chromosome arms and bands, to individual genes and gene subunits for (multi-color) microscopic visualization. Specific, ready-to-use FISH kits for the detection of numerical (e.g., gene copy number changes) or structural (e.g., translocations) chromosome or gene alterations are available, which can be applied to isolated cells in suspension, blood or bone marrow cell smears, and tissue sections (fresh, frozen, fixed, or paraffin wax embedded).

Usually, the DNA probes are derived from BAC, cosmid, or YAC clones which are amplified by standard biotechnology techniques. DNA-DNA hybridization protocols using such ready-to-use commercial probes require a denaturation step of the double-stranded target in a cell nucleus in order to bind the single-stranded DNA probe to the complementary sequence. The standard denaturation process is based on heat treatment (typically over 70 °C) mostly accompanied by an extensive use of chaotropic agents like formamide to reduce the denaturation temperature [2, 3]. This treatment could induce destructive effects on chromatin architecture [4].

Whereas standard FISH probes are based on enzymatically cut and biochemically modified DNA strands, COMBO-FISH (COMBinatorial Oligo FISH) follows a completely different approach [5, 6]. The genome targets to be specifically labeled are selected in the human DNA sequence database (in principle, the procedure also works for all other species for which a DNA sequence database exists). For a gene or in general a target of up to several hundred kilobase pairs (kb), a set of 20–40 distinct singularly co-localizing oligonucleotides of typically 15–30 bases each is selected by a computer databank search. In addition, characteristic parameters like oligonucleotide length, binding energy [7], homo-purine/homo-pyrimidine sequences [8, 9], etc. can be considered for selection. Finally, the optimized set can be synthesized as PNA [10] or DNA [8, 9] probes of high purity. It has also been shown that PNA SMART probes (= a stem/loop conformation which quenches fluorescence by a closed loop until the loop is opened for binding to the target) and TINA (Twisted Intercalating Nucleic Acid) probes (= oligonucleotides with anchoring molecules incorporated) are appropriate for COMBO-FISH [10, 11].

Depending on the sequence of the oligonucleotides designed, they either bind as probe-target double strands (Watson-Crick conformation) or as triple strands (Hoogsteen configuration) against homo-purine/homo-pyrimidine sequence stretches of

intact genomic double-stranded DNA. The oligonucleotide probes carry one fluorochrome at one or even at both ends. Due to the optical diffraction of microscope lenses used in fluorescence microscopy, the fluorescence signals of these single dye molecules merge into a nearly homogeneous COMBO-FISH "spot." Detailed protocols for COMBO-FISH with duplex- or triplex-forming oligonucleotide probes are described in [6] and so far are still valid for applications, as shown by analysis of the gene for the receptor tyrosine kinase 2 (*HER2/NEU*) [7, 10], the gene for the growth factor receptor-bound protein 7 (*GRB7*) [9], the breakpoint cluster region (BCR) on chromosome 22 [9], the ABL proto-oncogene 1 (*ABL1*) on chromosome 9 [8, 9, 12], the pseudo-autosomal region 1 (PAR1) and *T-box 1* (*TBX-1*) [11], and the *AMACR* gene on chromosome 5 [13].

In the following, this chapter will focus on further developments of COMBO-FISH beyond the protocols described in [6]. With the development of super-resolution microscopy, especially single-molecule localization microscopy [14–16], COMBO-FISH probes (DNA or Peptide Nucleic Acid (PNA)) have become ideal nano-probes for nano-scale analysis of chromatin architecture in subregions of nuclei [17, 18]. Although programs for design of probe combinations were well established [19, 20], novel alignment-free investigations of *k*-mer frequencies and positioning in genome sequences [21, 22] as well as detailed statistical analyses of such *k*-mer frequency distributions found a couple of probes that uniquely bind in a given repetition rate to repetitive chromatin sequence motives. So new generations of specific oligonucleotide probes against SINEs (Short Interspersed Nuclear Elements, e.g., ALU elements [13, 23]), LINEs (Long Interspersed Nuclear Elements, e.g., L1 [13]), or centromeres [13, 17] have been developed and successfully applied, for instance in biological dosimetry [23, 24]. The use of repetitive probes binding specifically to a trinucleotide expansion region in the promoter region of the *FMR1* gene, in combination with single-molecule localization microscopy, verified the existence of a chromatin loop on the nanoscale in 3D intact cell nuclei [18]. A novel improved protocol for these repetitively occurring probes circumvents any heat treatment for target denaturation [13, 23], whereas purine-pyrimidine probes can be used that theoretically only undergo Watson-Crick double strand pairing. Moreover, this low temperature protocol offers for the first time the combination of oligonucleotide-based FISH with specific immunofluorescence staining by means of commercially available antibodies [13, 23]. This offers a toolbox of labeling combinations and strategies for chromatin architecture and other nucleus-relevant research.

2 Materials

In the following, all materials are listed for cell preparation, COMBO-FISH, and immunostaining:

1. 1× phosphate-buffered saline (PBS) + Mg/Ca: 0.1 g $CaCl_2$, 0.2 g KCl, 0.1 g $MgCl_2 \cdot 6H_2O$, 8 g NaCl, 2.16 g Na_2HPO_4; add double-distilled (dd) H_2O to 1 L and filter-sterilize.
2. 2% and 4% formaldehyde in 1× PBS + Mg/Ca for fixation (*see* **Note 1**).
3. 0.2% and 0.05% (v/v) Triton-X100 in 1× PBS + Mg/Ca for permeabilization.
4. 2× saline-sodium citrate (2× SSC): 300 mM NaCl, 30 mM Na citrate.
5. 0.1 M HCl in H_2O.
6. 50% formamide: in 2× SSC
7. 10 mM Tris–HCl.
8. 2% bovine serum albumin (BSA) in 1× PBS + Mg/Ca: blocking solution.
9. Primary antibody (diluted according to the suppliers instructions).
10. Secondary antibody (diluted according to instructions), if required.
11. COMBO-FISH DNA probe solution for each probe used: 200 ng probe in 20 μL 10 mM Tris–HCl (pH 7–8) (*see* **Note 2**).
12. DAPI solution: 100–500 ng/mL in H_2O (counterstain).
13. Embedding medium: ProLong Gold Antifade Mountant (Thermo Fisher) (*see* **Note 3**).
14. Fixogum rubber cement (Marabu, Tamm, Germany) for sealing of cover glasses.
15. Microscope: a high-quality research microscope with an objective lens with high NA (1.3–1.5) and/or a super-resolution fluorescence microscope (a commercial STED or in-house manufactured setup) for single-molecule localization microscopy.

3 Methods

Like standard FISH techniques, COMBO-FISH can be applied to any type of cells obtained from blood, fresh tissues, tissue sections embedded in paraffin wax, bone marrow smears, or established permanent cell lines. In [6], methods for the design and preparation of the probe sets are described which can be applied for all cell types and species. The COMBO-FISH protocols shown in detail in

[6] differ in some steps depending on whether the probes bind via Watson-Crick bonding or via Hoogsteen bonding. However, they are still up-to-date for labeling of gene targets by a combination of oligonucleotide stretches. Therefore, here we focus the description on additional improvements to these protocols. Here, we first describe the computer search for uniquely binding probes, then we show protocols for fixed cells from established cell lines as routinely used in research and mostly commercially available. Such protocols may be also applied to other cells. Special attention is drawn to the applications that are useful in chromatin architecture research by super-resolution microscopy.

3.1 DNA Sequence Database Analysis and Probe Search

Schmitt et al. [6, 19] have described the algorithms for designing triplex-binding COMBO-FISH probes. By now, these algorithms can also be used to identify and design Watson-Crick-binding probes [20]. In the course of using these algorithms, one has to first choose a target sequence in DNA as the genomic region of interest. Within this range of nucleotides, a set of oligonucleotides binding to this given genomic region with a minimum of accessory binding sites and no other co-localization site of the selected probes within the genome is computed. As parameters for this search a minimum and a maximum length of the oligonucleotides, the minimum number of probes, and others like binding energy or molecular potentials are considered. The algorithms which Schmitt et al. created [6, 19] can be used as well on the genomic sequence database of the human genome as provided by the NCBI as well as on other databases available. The actual procedure for the determination of uniquely binding single oligonucleotide probes is performed on the existing DNA sequence databases available at NCBI or other sources:

1. Define the genome sequences to be analyzed (*see* **Note 4**).
2. Select a given probe length (typically >15 nucleotides) and search by a sliding window operation (i.e., always shifting by one base along the given sequence) for appropriate candidates on the given genome sequence (*see* **Note 5**).
3. Determine the number of matches in the genome for each candidate probe.
4. Test the specificity of the probe candidates: determine the number of binding sites inside and outside of the given genome motive (*see* **Note 6**).
5. Find the probe candidate that is most frequently occurring inside the motive, thereby not occurring in clusters, either by itself or with others outside the motive.
6. Correlate the distribution pattern of the selected oligonucleotide probe with the distribution pattern of the chosen target region in the genome (*see* **Notes 6** and **7**).

3.2 Preparation of Oligonucleotide Probes

Although different probe types have been tested and successfully applied for COMBO-FISH, the best results concerning probe handling and hybridization efficiency were obtained by DNA or PNA oligonucleotides which are commercially available and HPLC-purified with high quality. Typically, these probes carry a dye molecule at the 5′ end of the sequence. The number of fluorescence dyes on the target is thus equal to the number of binding probes, which is recommended for single-molecule localization microscopy. In principle, probes can be labeled at both 3′ and 5′ ends in order to further increase the fluorescence signal on the target when standard microscopic techniques are used.

3.3 Multicolor COMBO-FISH with Uniquely Binding Oligonucleotide Probes

1. Drop or grow cells on cover glasses.
2. Fix the cells in 4% formaldehyde solution (in 1× PBS + Mg/Ca) at 37 °C for 10 min.
3. Wash the cells three times in 1× PBS + Mg/Ca for 5 min each.
4. Permeabilize cells in 0.1% Triton-X100 solution for 3 min.
5. Incubate cells in 0.1 M HCl for 10 min.
6. Wash cells three times in 1× PBS + Mg/Ca on a shaker for 5 min each.
7. Equilibrate cells in 2× SSC for 5 min.
8. Add 50% formamide solution.
9. Denature the cell DNA at 70 °C for 30 min.
10. Mix 200 ng of each oligonucleotide in 20 μL 10 mM Tris–HCl (*see* **Note 8**).
11. Pipette the mixture obtained in the preceding step onto a freshly cleaned microscope slide (*see* **Note 9**).
12. Put a cover glass with the cells facing down onto the hybridization mixture on the microscope slide.
13. Seal the cover glasses with Fixogum rubber cement to prevent drying.
14. Incubate the slides in a humidified environment at 37 °C for 24 h.
15. Remove the Fixogum and wash the cells in 2× SSC at 37 °C for 5 min.
16. Equilibrate cells in 1× PBS + Mg/Ca for 5 min.
17. In the case of counterstaining of the nuclei (optional), incubate the cells in DAPI solution for 1–5 min.
18. Embed the cells in 20 μL of ProLong Gold Antifade Mountant (*see* **Note 10**).
19. Seal the specimen finally with Fixogum or nail polish and store it at 4 °C in the dark.
20. Subject the cell nuclei to single-molecule localization microscopy or other super-resolution light microscopy techniques (*see* **Note 11**).

3.4 Combined COMBO-FISH and Immunostaining with Uniquely Binding Oligonucleotide Probes and Specific Antibodies

1. Drop or grow cells on cover glasses.
2. Fix cells with 4% formaldehyde solution at 37 °C for 10 min.
3. Wash cells three times in 1× PBS + Mg /Ca for 5 min each.
4. Permeabilize cells in 0.1% Triton-X in 1× PBS + Mg/Ca for 3 min.
5. Wash cells three times in 1× PBS + Mg/Ca on a shaker for 5 min each.
6. Incubate cells in blocking solution (2% BSA in 1× PBS + Mg/Ca) for 30 min.
7. Incubate the cells with the (primary) antibody solution in a humidified environment at 37 °C for 30 min.
8. Wash cells three times in 1× PBS + Mg/Ca on a shaker for 5 min each.
9. Optional: incubate the cells with the secondary antibody solution in a humidified environment at 37 °C for 30 min.
10. Optional: together with the preceding step, wash cells three times in 1× PBS + Mg/Ca on a shaker for 5 min each.
11. Fix cells with 2% formaldehyde solution (in 1× PBS + Mg/Ca) at 37 °C for 10 min.
12. Wash cells three times in 1× PBS + Mg/Ca on a shaker for 5 min each.
13. Incubate cells in 0.1 M HCl for 10 min.
14. Wash/permeabilize cells three times in 0.05% Triton-X100 in 1× PBS + Mg/Ca on a shaker for 5 min each.
15. Equilibrate cells in 2× SSC for 5 min.
16. Incubate in 50% formamide in 2× SSC at room temperature for 30 min.
17. Mix 200 ng each oligonucleotide in 20 μL 10 mM Tris–HCl (*see* **Note 8**).
18. Pipette the mixture obtained in the preceding step onto a freshly cleaned microscope slide (*see* **Note 9**).
19. Put a cover glass with the cells facing down onto the hybridization mixture on the microscope slide.
20. Seal the cover glass with Fixogum rubber cement to prevent drying.
21. Incubate slides in a humidified environment at 37 °C for 24 h.
22. Remove the Fixogum.
23. Wash the cells in 2× SSC at 37 °C on the shaker for 5 min.
24. Optional: repeat the preceding step twice.
25. Equilibrate cells in 1× PBS + Mg/Ca for 5 min.

26. In the case of counterstaining of the nuclei (optional), incubate the cells in DAPI solution for 1–5 min.
27. Wash the cells twice in 1× PBS + Mg/Ca for 5 min each.
28. Embed the cells in 20 μL ProLong Gold Antifade Mountant (*see* **Note 10**).
29. Seal the specimen finally with Fixogum or nail polish and store it at 4 °C in the dark.
30. Subject the cell nuclei to single-molecule localization microscopy or other super-resolution light microscopy techniques (*see* **Notes 12** and **13**).

4 Notes

1. Prepare formaldehyde solution freshly from paraformaldehyde and dilute in highly purified water, pH 8.0.
2. The oligonucleotide probes should be ordered from a commercial distributor and HPLC-purified, because any unspecific background must be avoided. The oligonucleotides can be labeled with fluorochrome molecules at the 5′ end of the DNA strand (standard), and optionally at the 3′ end in addition.
3. ProlongGold embedding medium is highly recommended for single-molecule localization microscopy because it is background-free. In the case of standard fluorescence microscopy, other embedding media can also be used (e.g., Vectashield, Vector Laboratories).
4. For families of interspersed sequences, it is recommended to define a consensus sequence as, for example, shown here for the ALU sequences:
   - GGCCGGGCGCGGTGGCTCACGCCGTAATCCAGC ACTTTGGGAGGCCGAGGCGGGCGGATCACCTGA GGTCAGGAGTTCGAGACCAGCCTGGCCAACATGG TGAAACCCCGTCTCTACTAAAAATACAAAAATTAG CCGGGGCGTGGTGGCGCGCGGAGGCAGGAGAA TCGCTTGAACCCGGGAGGCGGAGGTTGCAGTGA GCCGAGATCGCGCCACTGCACTCCAGCCTGGGC GACAGAGCGAGACTCCGTCTC
5. In order to save computing time and capacity, especially for larger genome motives, not all possible sequences need to be tested. The procedure can be run several times just selecting the most promising candidate and modifying it by one base at the end. By such little shifts, promising candidates can be optimized.
6. In this case, any location of the given genome motive and any location of the selected probe candidate has to be determined

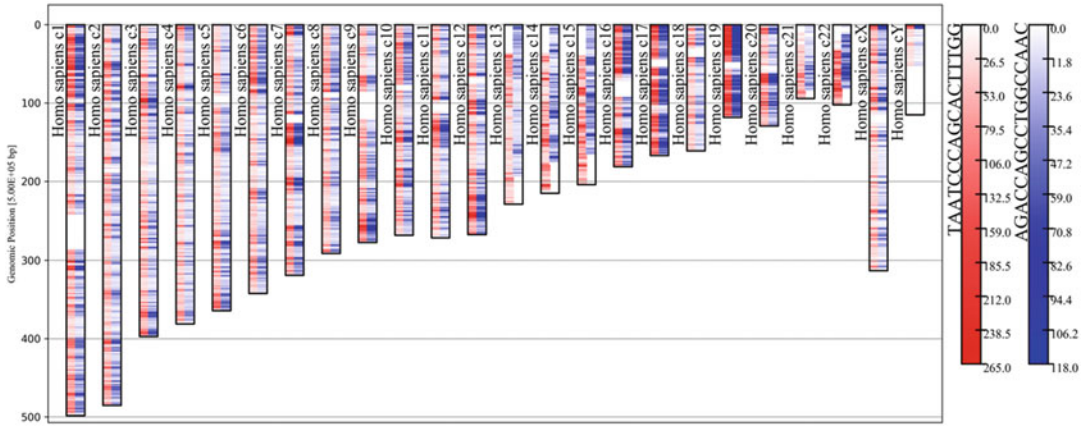

Fig. 1 ALU-oligonucleotide probe distribution along the genome. The intensity of the bars indicates the frequency within a 500 kb section of the given chromosome. Red and blue bars indicate the positions of the designed 17mer ALU probes (TAATCCCAGCACTTTGG and AGACCAGCCTGGCCAAC) indicated on the right. The sequences associated with the ALU probe appear in the entire genome at different frequency densities. The intensity (right color code) is encoded according to counts/50 kbp

in the genome database, for instance by application of BLAST algorithms.

7. A map for two candidate probes specific for the given ALU consensus sequences is presented in Fig. 1 as an example of the matching analysis.
8. Typically, one to three different DNA or PNA oligonucleotide probes labeled with different fluorochromes are used simultaneously. Applying single-molecule localization microscopy, blinking dyes are necessary. We have had good experience with dyes of the Alexa series (Invitrogen) but other dye families may also be suitable.
9. It is highly recommended to clean the microscope slides carefully, even when they are taken from a new batch. Cleaning can be done by an ethanol series, but other procedures are also possible. However, the last cleaning step should be finished with heat drying in a clean environment.
10. Be aware that ProlongGold can polymerize completely and does not form bubbles with any remaining liquid phase in it. If necessary, keep the slides at room temperature for some hours to dry.
11. Figure 2 shows an example of simultaneous labeling with two different oligonucleotides.
12. Figure 3 shows an example of simultaneous labeling with an ALU-specific oligonucleotide and an antibody (primary and secondary) against heterochromatin.

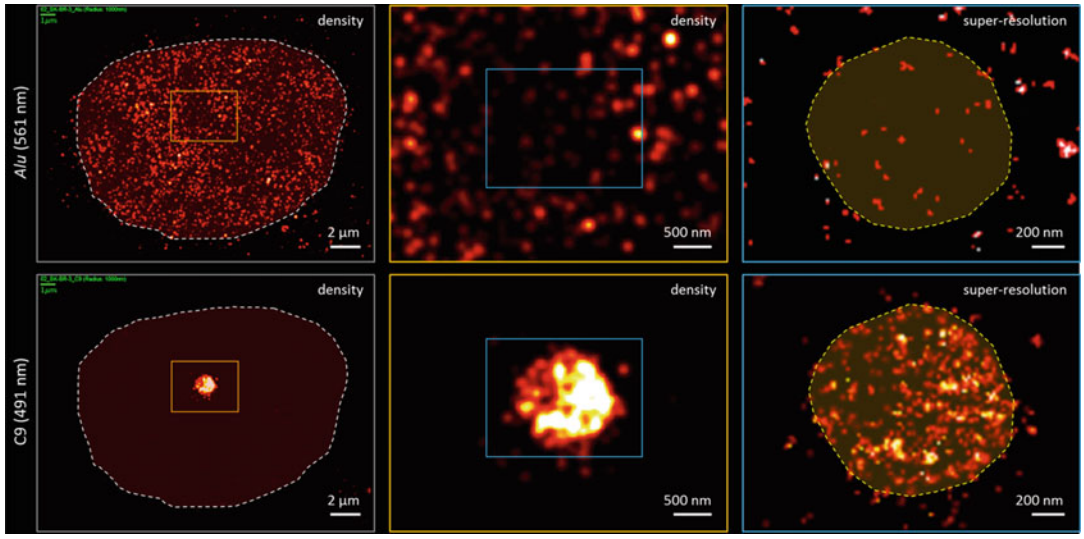

Fig. 2 Single-molecule localization microscopy image obtained from a section through a SkBr3 cell nucleus where one of the two chromosomes 9 was visualized. In this experiment the ALU-oligonucleotide probe (Alexa Fluor 568-TAATCCCAGCACTTTGG) was labeled with Alexa568 (upper row) and the centromere 9 oligonucleotide probe (Alexa Fluor 488-AATCAACCCGAGTGCAAT) with Alexa488 (lower row). For simplicity, both colors are visualized in the same false color code in order to compare the signal density by intensity. It is obvious that ALU regions and centromere 9 exclude each other

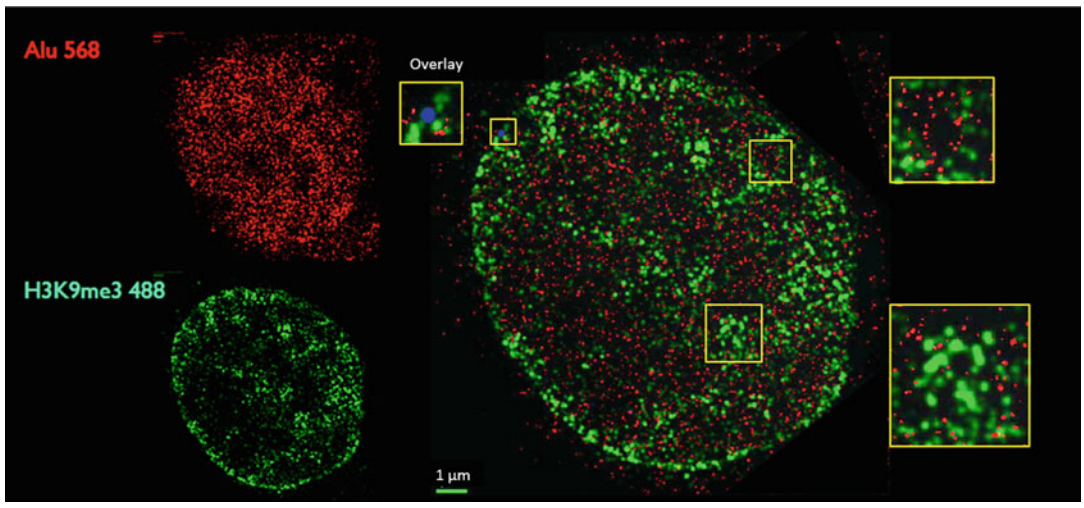

Fig. 3 Single-molecule localization microscopy image obtained from a section through a SkBr3 cell nucleus. In this experiment the ALU-oligonucleotide probes (Alexa Fluor 568-TAATCCCAGCACTTTGG) labeled with Alexa568 were applied simultaneously with anti-H3K9me3 (heterochromatin methylation site) rabbit primary antibodies and anti-rabbit Alexa Fluor 647-labeled secondary antibodies. Heterochromatin-rich regions and ALU-rich regions are shown in the enlarged image sections. At one position ("Overlay") indicated in blue, both types of signals co-localize (= signal distance below 15 nm)

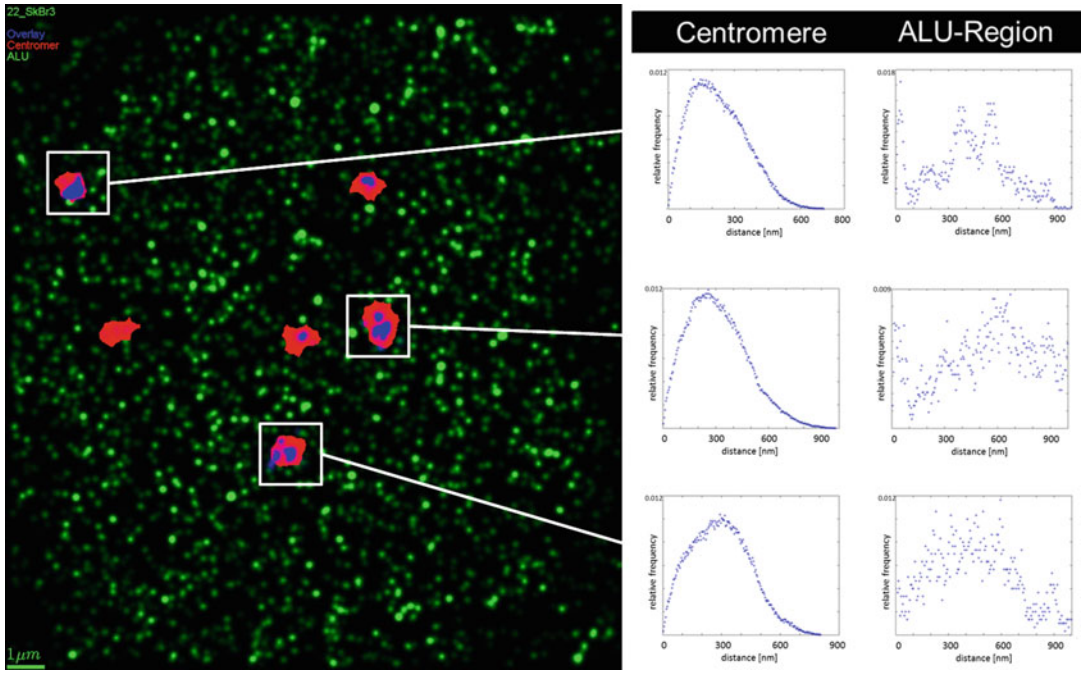

Fig. 4 Single-molecule localization microscopy image obtained from a section through a SkBr3 cell nucleus (left). In this experiment the ALU-oligonucleotide probes (Alexa Fluor 488-TAATCCCAGCACTTTGG) labeled with Alexa 488 were applied simultaneously with fluorescently labeled (Alexa 568) anti-CREST antibodies against the kinetochores of the centromeres. At positions indicated in blue, both types of signals co-localize (= signal distance below 15 nm). The distance frequency distributions (= relative frequency of distances between labeled molecules; right curves) indicate a much higher density of the centromere signals than of the ALU signals

13. Figure 4 shows an example of simultaneous labeling with an ALU-specific oligonucleotide and an antibody against centromeres.

References

1. Bridger JM, Volpi EV (eds) (2010) Fluorescence in situ hybridization (FISH) – protocols and applications. Humana Press, Springer, New York
2. Wolf D, Rauch J, Hausmann M, Cremer C (1999) Comparison of the thermal denaturation behaviour of DNA-solutions and chromosome preparations in suspension. Biophys Chem 81:207–221
3. Rauch J, Wolf D, Hausmann M, Cremer C (2000) The influence of formamide on thermal denaturation profiles of DNA and metaphase chromosomes in suspensions. Z Naturforsch C 55:737–746
4. Winkler R, Perner B, Rapp A, Durm M, Cremer C, Greulich KO, Hausmann M (2003) Labelling quality and chromosome morphology after low temperature FISH analysed by scanning far-field and scanning near-field optical microscopy. J Microsc 209:23–33
5. Hausmann M, Winkler R, Hildenbrand G, Finsterle J, Weisel A, Rapp A, Schmitt E, Janz S, Cremer C (2003) COMBO-FISH: specific labelling of nondenatured chromatin targets by computer-selected DNA oligonucleotide probe combinations. Biotechniques 35:564–577
6. Schmitt E, Schwarz-Finsterle J, Stein S, Boxler C, Müller P, Mokhir A, Krämer R,

Cremer C, Hausmann M (2010) Combinatorial Oligo FISH: directed labelling of specific genome domains in differentially fixed cell material and live cells. In: Bridger JM, Volpi EV (eds) Fluorescence in situ hybridization (FISH) – protocols and applications, Methods in molecular biology, vol 659. Humana Press, New York, pp 185–202

7. Zeller D, Kepper N, Hausmann M, Schmitt E (2013) Sequential and structural biophysical aspects of combinatorial oligo-FISH in Her2/neu breast cancer diagnostics. IFMBE Proc 38:82–85
8. Schwarz-Finsterle J, Stein S, Großmann C, Schmitt E, Trakhtenbrot L, Rechavi G, Amariglio N, Cremer C, Hausmann M (2007) Comparison of triplehelical COMBO-FISH and standard FISH by means of quantitative microscopic image analysis of abl/bcr genome organisation. J Biophys Biochem Methods 70:397–406
9. Schwarz-Finsterle J, Stein S, Großmann C, Schmitt E, Schneider H, Trakhtenbrot L, Rechavi G, Amariglio N, Cremer C, Hausmann M (2005) COMBO-FISH for focussed fluorescence labelling of gene domains: 3D-analysis of the genome architecture of abl and bcr in human blood cells. Cell Biol Int 29:1038–1046
10. Müller P, Rößler J, Schwarz-Finsterle J, Pedersen EB, Géci I, Schmitt E, Hausmann M (2016) PNA-COMBO-FISH: from combinatorial probe design in silico to vitality compatible, specific labelling of gene targets in cell nuclei. Exp Cell Res 345:51–59
11. Nolte O, Müller M, Häfner B, Knemeyer J-P, Stöhr K, Wolfrum J, Hakenbeck R, Denapaite D, Schwarz-Finsterle J, Stein S, Schmitt E, Cremer C, Herten D-P, Hausmann M, Sauer M (2006) Novel singly labelled probes for identification of microorganisms, detection of antibiotic resistance genes and mutations, and tumor diagnosis (SMART PROBES). In: Popp J, Strehle M (eds) Biophotonics. Wiley-VCH, Weinheim, pp 167–230
12. Grossmann C, Schwarz-Finsterle J, Schmitt E, Birk U, Hildenbrand G, Cremer C, Trakhtenbrot L, Hausmann M (2010) Variations of the spatial fluorescence distribution in ABL gene chromatin domains measured in blood cell nuclei by SMI microscopy after COMBO – FISH labelling. In: Méndez-Vilas A, Díaz Álvarez J (eds) Microscopy: science, technology, applications and education, vol 1. Formatex Research Center, Badajoz, pp 688–695
13. Lee J-H, Laure Djikimi Tchetgna F, Krufczik M, Schmitt E, Cremer C, Bestvater F, Hausmann M (2019) COMBO-FISH: a versatile tool beyond standard FISH to study chromatin organization by fluorescence light microscopy. OBM Genet 3(1). https://doi.org/10.21926/obm.genet.1901064
14. Cremer C, Kaufmann R, Gunkel M, Pres S, Weiland Y, Müller P, Ruckelshausen T, Lemmer P, Geiger F, Degenhard M, Wege C, Lemmermann N, Holtappels R, Strickfaden H, Hausmann M (2011) Superresolution imaging of biological nanostructures by Spectral Precision Distance Microscopy (SPDM). Review. Biotechnol J 6:1037–1051
15. Lemmer P, Gunkel M, Baddeley D, Kaufmann R, Urich A, Weiland Y, Reymann J, Müller P, Hausmann M, Cremer C (2008) SPDM – light microscopy with single molecule resolution at the nanoscale. Appl Phys B 93:1–12
16. Lemmer P, Gunkel M, Weiland Y, Müller P, Baddeley D, Kaufmann R, Urich A, Eipel H, Amberger R, Hausmann M, Cremer C (2009) Using conventional fluorescent markers for far-field fluorescence localization nanoscopy allows resolution in the 10 nm range. J Microsc 235:163–171
17. Müller P, Schmitt E, Jacob A, Hoheisel J, Kaufmann R, Cremer C, Hausmann M (2010) COMBO-FISH enables high precision localization microscopy as a prerequisite for nanostructure analysis of genome loci. Int J Mol Sci 11:4094–4105
18. Stuhlmüller M, Schwarz-Finsterle J, Fey E, Lux J, Bach M, Cremer C, Hinderhofer K, Hausmann M, Hildenbrand G (2015) In situ optical sequencing and nano-structure analysis of a trinucleotide expansion region by localization microscopy after specific COMBO-FISH labelling. Nanoscale 7:17938–17946. https://doi.org/10.1039/C5NR04141D
19. Schmitt E, Wagner J, Hausmann M (2012) Combinatorial selection of short triplex forming oligonucleotides for fluorescence in situ hybridisation COMBO-FISH. J Comput Sci 3:328–334. https://doi.org/10.1016/j.jocs.2011.10.001
20. Kepper N, Schmitt E, Lesnussa M, Weiland Y, Eussen HB, Grosveld F, Hausmann M, Knoch TA (2010) Visualization, analysis, and design of COMBO-FISH probes in the Grid-based GLOBE 3D genome platform. In: Solomonides T, Blanquer I, Breton V, Glatard T, Legré Y (eds) Healthgrid applications and core technologies. Proceedings of HealthGrid 2010, studies in health technology

and informatics, vol 159, pp 171–180. ISBN: 978-1-60750-582-2

21. Sievers A, Bosiek K, Bisch M, Dreessen C, Riedel J, Froß P, Hausmann M, Hildenbrand G (2017) Kmer content, correlation and position analysis of genome DNA sequences for identification of function and evolutionary features. Genes 8:122. https://doi.org/10.3390/genes8040122
22. Sievers A, Wenz F, Hausmann M, Hildenbrand G (2018) Conservation of k-mer composition and correlation contribution between introns and intergenic regions of animalia genomes. Genes 9:482. https://doi.org/10.3390/genes9100482
23. Krufczik M, Sievers A, Hausmann A, Lee J-H, Hildenbrand G, Schaufler W, Hausmann M (2017) Combining low temperature fluorescence DNA-hybridization, immunostaining, and super-resolution localization microscopy for nano-structure analysis of ALU elements and their influence on chromatin structure. Int J Mol Sci 18:1005. https://doi.org/10.3390/ijms18051005
24. Hausmann M, Ilić N, Pilarczyk G, Lee J-H, Logeswaran A, Borroni AP, Krufczik M, Theda F, Waltrich N, Bestvater F, Hildenbrand G, Cremer C, Blank M (2017) Challenges for super-resolution localization microscopy and biomolecular fluorescent nano-probing in cancer research. Int J Mol Sci 18:2066. https://doi.org/10.3390/ijms18102066

Chapter 7

Genome-Wide Mapping of UV-Induced DNA Damage with CPD-Seq

Peng Mao and John J. Wyrick

Abstract

Exposure to ultraviolet (UV) radiation is the major risk factor for skin cancers. UV induces helix-distorting DNA damage such as cyclobutane pyrimidine dimers (CPDs). If not repaired, CPDs can strongly block DNA and RNA polymerases and cause mutagenesis or cell death. Nucleotide excision repair (NER) is critical for the removal of UV-induced photolesions including CPDs in the cell. Investigating CPD formation and repair across the genome is important for understanding the mechanisms by which these lesions promote somatic mutations in skin cancers. Here we describe a high-throughput, single nucleotide-resolution damage mapping method named CPD sequencing (CPD-seq) for genome-wide analysis of UV-induced CPDs. Protocols for CPD-seq library preparation in yeast and human cells, as well as bioinformatics identification of the CPD damage site, are detailed below.

Key words DNA damage, DNA repair, UV damage sequencing, Single base resolution, Sequencing library, Bioinformatics analysis

1 Introduction

Ultraviolet (UV) radiation induces helix-distorting DNA damage such as cyclobutane pyrimidine dimers (CPDs). CPDs can strongly inhibit elongating DNA and RNA polymerases and are cytotoxic and mutagenic [1]. The primary DNA repair pathway for CPDs in human cells is nucleotide excision repair (NER), which involves enzymatic activities of ~30 DNA repair proteins [2]. NER plays an important role in maintaining genome stability and preventing tumorigenesis. Patients with defective NER (e.g., xeroderma pigmentosum) exhibit >1000-fold higher risk for sun-induced skin cancers [2].

Genome sequencing of melanomas, a type of highly dangerous skin cancer, has revealed that the majority of mutations are UV signature mutations, characterized by C to T transitions predominantly at dipyrimidine sites [3]. This genomic evidence is consistent with published data showing that UV-induced DNA lesions, which

Ronald Hancock (ed.), *The Nucleus*, Methods in Molecular Biology, vol. 2175, https://doi.org/10.1007/978-1-0716-0763-3_7,

mainly occur at dipyrimidines [1], are converted into mutations through error-prone translesion synthesis and/or cytosine deamination [4, 5]. The distribution of UV mutations in the melanoma genome is highly variable, and recent studies indicate that the chromatin landscape plays an important role in dictating the mutational heterogeneity across the genome [6, 7]. For example, melanoma mutation density is generally higher in closed chromatin regions relative to open regions [8, 9]. Nucleosomes, the primary building blocks of chromatin, and transcription factor binding site (TFBS), have also been shown to significantly modulate melanoma mutation distribution in local DNA sequences [6, 10–12]. To uncover the mechanism for the mutational heterogeneity widely observed in melanomas, it is important to develop genome-wide, high-resolution damage mapping methods to systematically investigate damage distribution and repair. Several genomic approaches have been developed in recent years (reviewed in [13]), which has provided an unprecedented opportunity to study UV damage, DNA repair, and their impact on cancer mutagenesis.

Cyclobutane pyrimidine dimer sequencing (CPD-seq) is a next-generation sequencing (NGS)-based CPD mapping method (*see* Fig. 1) [14]. CPD-seq is adapted from a previously published method used to map ribonucleotide lesions in yeast [15]. In CPD-seq, UV-irradiated genomic DNA is sonicated into short fragments. After ligation with the first adaptor DNA (i.e., Fig. 1, green), CPD-seq employs terminal transferase (TdT) and dideoxyATP (ddATP) to block all the free 3′-OH groups in DNA fragments. DNA repair enzymes T4 endonuclease V and AP endonuclease (APE1) are subsequently utilized to generate a new ligatable 3′-OH group precisely at the CPD damage site. After denaturing, the new 3′-OH is ligated to a sequencing adaptor DNA (*see* Fig. 1, purple). CPD-seq reads are aligned to the reference genome, the position of the two nucleotides immediately upstream of the 5′ end of the sequencing read is identified, and the dinucleotide sequence on the opposing strand is recognized as the CPD lesion site. By mapping CPDs immediately after UV irradiation and unrepaired damage at different repair time points, CPD-seq can reveal both damage formation and DNA repair kinetics across the genome at single-base resolution.

2 Materials

2.1 Growth and UV Irradiation of Yeast

1. Wild-type *Saccharomyces cerevisiae* (BY4741) available from ATCC and mutant yeast strains; essentially any yeast strain can be used.
2. 254-nm UV-C light (General Electric).

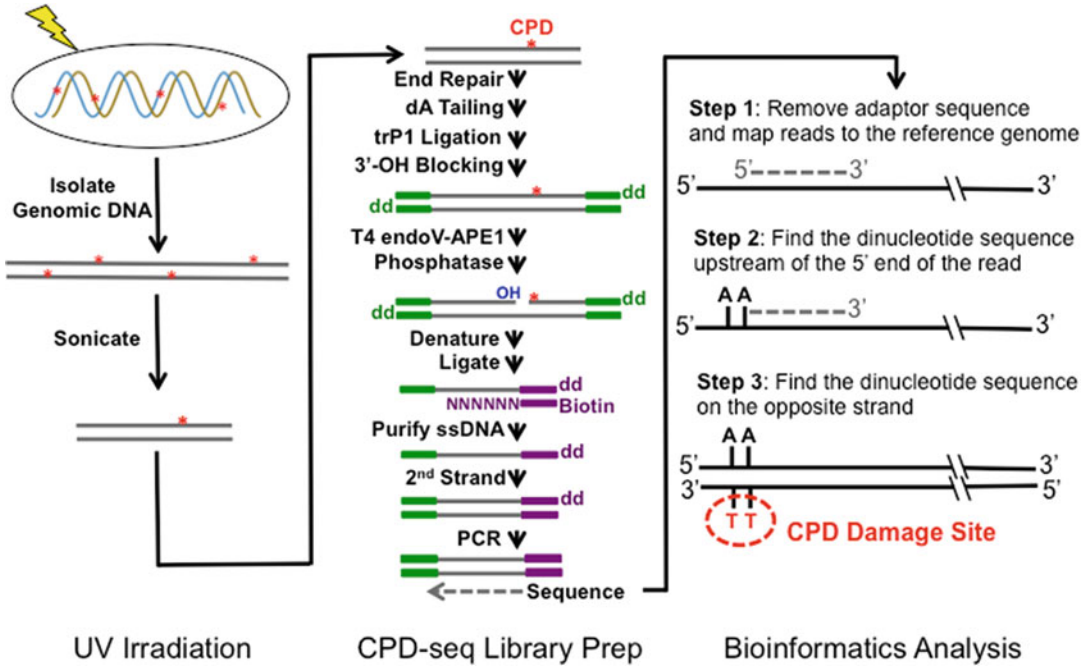

Fig. 1 CPD-seq experimental strategy. Left panel: Cultured cells are exposed to UV-C light to induce CPDs. Genomic DNA is isolated and sonicated to short fragments (~400 bp on average). Middle panel: CPD-seq library preparation procedure (*see* Subheading 3.4). Right panel: Bioinformatics analysis of CPD-seq data to identify CPD lesion sites across the genome

3. Yeast YPD medium: 1% (w/v) yeast extract (BD Bacto), 2% (w/v) peptone (BD Bacto), and 2% (w/v) dextrose (Sigma).
4. Sterile deionized water (diH_2O).

2.2 Human Cell Culture

1. Telomerase immortalized normal human fibroblast (NHF1-hTERT) cells: ATCC number BJ-5ta (ATCC CRL-4001).
2. Dulbecco's modified Eagle's medium (DMEM) with 10% fetal bovine serum (FBS).
3. 0.25% Trypsin.
4. Sterile 1× Phosphate-Buffered Saline (PBS)

2.3 Isolation of Yeast Genomic DNA

1. Yeast lysis buffer: 2% (v/v) Triton-X 100, 1% (w/v) SDS, 100 mM NaCl, 10 mM Tris–Cl pH 8.0, 1 mM EDTA.
2. 1× TE pH 8.0: 10 mM Tris–HCl, 1 mM EDTA.
3. Phenol-chloroform-isoamyl alcohol (25:24:1) (Fisher Scientific).
4. 100% and 75% ethanol.
5. RNase A/T1 (Thermo Scientific).
6. Agarose, electrophoresis grade.

7. SYBR Safe DNA gel stain.
8. Glass beads (Sigma).

2.4 Isolation of Human Genomic DNA

1. GenElute Mammalian Genomic DNA Miniprep kits (Sigma).

2.5 Reagents for CPD-seq Library Preparation

1. Glycogen (Thermo Scientific).
2. 100 bp DNA ladder (NEB).
3. NEBNext end repair module (NEB).
4. NEBNext dA tailing module (NEB).
5. NEBNext quick ligation module (NEB).
6. Terminal transferase with 10× reaction buffer and 2.5 mM $CoCl_2$ (NEB).
7. T4 Endonuclease V (NEB).
8. DNA AP endonuclease (APE1, NEB).
9. NEBuffer 4 (NEB).
10. 10× T4 DNA ligase buffer (NEB).
11. ddATP (Roche, purchased through Sigma).
12. Shrimp alkaline phosphatase (Affymetrix).
13. Dynabeads M-280 streptavidin (Life Technologies).
14. Agencourt AMPure XP beads (Beckman Coulter).
15. EconoTaq DNA Polymerase (with Mg^{++}) (VWR).
16. 3 M sodium acetate (NaOAc), pH 5.2.
17. 5 M sodium chloride (NaCl).
18. 2.5 mM $CoCl_2$.
19. 40% (w/v) PEG8000 in 1.25 M NaCl.
20. 1× biotin bind-and-wash buffer: 10 mM Tris–HCl, pH 7.5, 1 mM EDTA and 2 M NaCl.
21. 2× biotin bind-and-wash buffer: 20 mM Tris–HCl, pH 7.5, 2 mM EDTA and 4 M NaCl.
22. 1.5 M NaOH in diH_2O; store at room temperature for up to 1 month; dilute to 0.15 M with diH_2O before each use.
23. Oligonucleotides (*see* Table 1), purified by standard desalting: Integrated DNA Technologies, Coralville, IA 52241, USA

2.6 Major Equipment for Library Preparation and Sequencing

1. Benchtop centrifuges.
2. Bioruptor (Diagenode).
3. 1.5 mL Bioruptor Plus TPX microtubes.
4. Magnetic stand.
5. UV spectrophotometer for DNA quantification.

Table 1
Oligonucleotides

Name	Sequence
trP1-top	5'-CCTCTCTATGGGCAGTCGGTGATphosphorothioate-T-3'
trP1-bottom	5'-phosphate-ATCACCGACTGCCCATAGAGAGGC-dideoxy-3'
A1-top	5'-phosphate-ATCCTCTTCTGAGTCGGAGACACGCAGGGATGAGATGGC-dideoxy-3'
A1-bottom	5'-biotin-GCCATCTCATCCCTGCGTGTCTCCGACTCAGAAGAGGATNNNNNN-C3 phosphoramidite-3'
A2-top	5'-phosphate-ATCACGAACTGAGTCGGAGACACGCAGGGATGAGATGGC-dideoxy-3'
A2-bottom	5'-biotin-GCCATCTCATCCCTGCGTGTCTCCGACTCAGTTCGTGATNNNNNN-C3 phosphoramidite-3'
A3-top	5'-phosphate-ATCTCAGGCTGAGTCGGAGACACGCAGGGATGAGATGGC-dideoxy-3'
A3-bottom	5'-biotin-GCCATCTCATCCCTGCGTGTCTCCGACTCAGCCTGAGATNNNNNN-C3 phosphoramidite-3'
A4-top	5'-phosphate-ATCGCGATCTGAGTCGGAGACACGCAGGGATGAGATGGC-dideoxy-3'
A4-bottom	5'-biotin-GCCATCTCATCCCTGCGTGTCTCCGACTCAGATCGCGATNNNNNN-C3 phosphoramidite-3'
A5-top	5'-phosphate-ATCCAGTACTGAGTCGGAGACACGCAGGGATGAGATGGC-dideoxy-3'
A5-bottom	5'-biotin-GCCATCTCATCCCTGCGTGTCTCCGACTCAGTACTGGATNNNNNN-C3 phosphoramidite-3'
A6-top	5'-phosphate-ATCAGTTCCTGAGTCGGAGACACGCAGGGATGAGATGGC-dideoxy-3'
A6-bottom	5'-biotin-GCCATCTCATCCCTGCGTGTCTCCGACTCAGGAACTGATNNNNNN-C3 phosphoramidite-3'
Primer trP1	5'-CCTCTCTATGGGCAGTCGGTGATT-3'
Primer A	5'-CCATCTCATCCCTGCGTGTCTCCGAC-3'

6. Gel imaging system.
7. Ion Proton sequencer (Life Technologies); CPD-seq can be adapted for other sequencers such as the Illumina.

3 Methods

3.1 Cell Growth, UV Irradiation, and Repair Incubation

3.1.1 Growth and UV Irradiation of Yeast Cells

1. Pick a single yeast colony and grow cells into 5 mL of YPD medium in a 30 °C shaker overnight.
2. The next morning, subculture at a 1:10 ratio to 40 mL of fresh YPD so that the starting OD_{600} is ~0.1. Grow the subculture for 3–4 h until the OD_{600} reaches ~0.8.
3. Aliquot 10 mL of the yeast culture into a 15 mL Falcon tube as the "No UV" sample. Spin down the yeast cells at ~2700 × *g* for 2 min, remove the medium, and store the cell pellet at −80 °C. Spin down the remaining (30 mL) yeast cells and completely remove the medium.
4. Resuspend the cells in 30 mL of diH_2O by vortexing. Transfer the cells to a plastic tray so that the tray is covered with a thin layer of water. Expose the tray to 125 J/m^2 of UV-C light. After UV irradiation, keep the cells in the "dark" (*see* **Note 1**) to reduce photolyase activity.
5. Immediately aliquot 10 mL of cells for a 0 h repair time point. Spin down the cells, remove the supernatant, and keep the pellet at −80 °C.
6. Pellet the remaining UV-treated cells (20 mL) and resuspend them in 20 mL of fresh YPD for repair incubation in the 30 °C shaker.

7. Aliquot 10 mL of the culture at 1 h and 2 h repair time points, respectively. Keep the cell pellets at −80 °C.

3.1.2 Growth and UV Treatment of Human Fibroblasts

1. Grow NHF1-hTERT cells to ~90% confluence in 10-cm petri dishes in DMEM containing 10% FBS at 37 °C and in 5% CO_2.
2. Remove the medium and rinse off residual medium with 2 mL of 1× PBS. Discard this PBS.
3. Harvest the cells from one petri dish for a "No UV" control. To harvest cells, add 2 mL of 0.25% Trypsin and incubate at 37 °C for 5 min until the cells are detached from the dish. Spin down the cells at 400 × *g* for 5 min at RT and freeze them at −20 °C.
4. For UV irradiation, add 2 mL of fresh 1× PBS to the dish to keep the cells wet. Expose the dish to the UV-C light (e.g., 20 J/m^2). Remove the PBS and immediately harvest the cells from one dish for assay of initial damage (0 h repair). For repair, discard the PBS and add fresh prewarmed DMEM and incubate at 37 °C for different times (e.g., 1, 2, 4, and 12 h) in the incubator.

3.2 Isolation of Genomic DNA

3.2.1 Isolation of Yeast Genomic DNA

1. Thaw frozen yeast cells at RT in the "dark" (*see* **Note 1**).
2. Add 250 μL of yeast lysis buffer, 150 μL of acid-washed glass beads, and 250 μL of phenol-chloroform-isoamyl alcohol to the 15 mL Falcon tube. Vortex at top speed for 2 min. Repeat once.
3. Add 200 μL of 1× TE and mix well. Centrifuge at ~2700 × *g* for 5 min.
4. Transfer the lysate to a 1.5 mL Eppendorf tube and centrifuge at ~18,000 × *g* for 10 min.
5. Transfer the aqueous (top) layer (~400 μL) to a new 1.5 mL tube and mix with 1000 μL of 100% ethanol. Incubate at RT for 5 min.
6. Centrifuge at ~18,000 × *g* for 5 min. Discard the supernatant and rinse the DNA pellet with 75% ethanol.
7. Air-dry the DNA pellet for 10 min in a fume hood.
8. Dissolve the DNA pellet in 200 μL of 1× TE with gentle pipetting. Add 2 μL of RNase A/T1. Incubate at 37 °C for 30 min.
9. Electrophorese 5 μL of DNA on a 1% agarose gel to visualize the DNA and verify the disappearance of RNA.
10. Remove RNase: mix the DNA with 200 μL of phenol-chloroform-isoamyl alcohol, vortex for 30 s at top speed, add 300 μL of 1× TE and mix. Centrifuge in a microfuge at 18,000 × *g* for 10 min and transfer the top layer to a new

tube. Add 50 μL of 3M NaOAc (pH 5.2) and mix the DNA with 1000 μL of 100% ethanol and incubate at −20 °C for 10 min. Centrifuge in a microfuge at top speed for 5 min. Wash the DNA pellet with 75% ethanol, air-dry it, and dissolve the DNA in 400 μL of diH_2O. Measure the DNA concentration with a UV spectrophotometer.

3.2.2 Isolation of Genomic DNA from Human Cells

1. Isolate genomic DNA from NHF1 cells using a GenElute Mammalian Genomic DNA Miniprep kit, following the manufacturer's instructions.
2. Load 5 μL of DNA onto a 1% agarose gel to visualize genomic DNA.
3. Measure the DNA concentration with a UV spectrophotometer.

3.3 DNA Sonication and Purification on AMPure XP Beads

1. Prepare four 100 μL aliquots of ~30 ng/μL DNA in diH_2O in 1.5 mL Bioruptor microtubes. The total volume is 400 μL with ~12 μg of DNA in total.
2. Shear the DNA in the Bioruptor by 15 cycles of 30 s ON/30 s OFF at HIGH power setting (position H). Keep the samples at 4 °C while sonicating using the Bioruptor Water cooling system. In our experience, we typically obtain an average DNA fragment length of ~400 bp.
3. Pool the sonicated DNA into a fresh tube. Load 10 μL of DNA and a 100 bp DNA ladder onto a 2% agarose gel to confirm the fragment size distribution by gel electrophoresis. Figure 2a shows an example of a gel of sonicated DNA.
4. After the desired DNA length is achieved, precipitate the DNA by adding 40 μL of 3 M NaOAc, 2 μL of glycogen, and 1000 μL of 100% ethanol.
5. Incubate at −20 °C overnight and centrifuge at ~21,000 × *g* for 30 min. Rinse the DNA pellet with 75% ethanol. Air-dry the DNA pellet and dissolve it in 100 μL of diH_2O.
6. Add 120 μL of AMPure XP beads to the DNA from the previous step and mix them thoroughly by pipetting ten times.
7. Incubate at RT for 1 min.
8. Briefly centrifuge to collect droplets. Place the tubes on a magnetic stand for 1 min to collect the beads. The supernatant should turn clear.
9. Discard the supernatant. Add 500 μL of 75% ethanol to wash the beads thoroughly; hold the magnetic stand and rotate ten times. It is unnecessary to remove the tubes from the stand for washing.

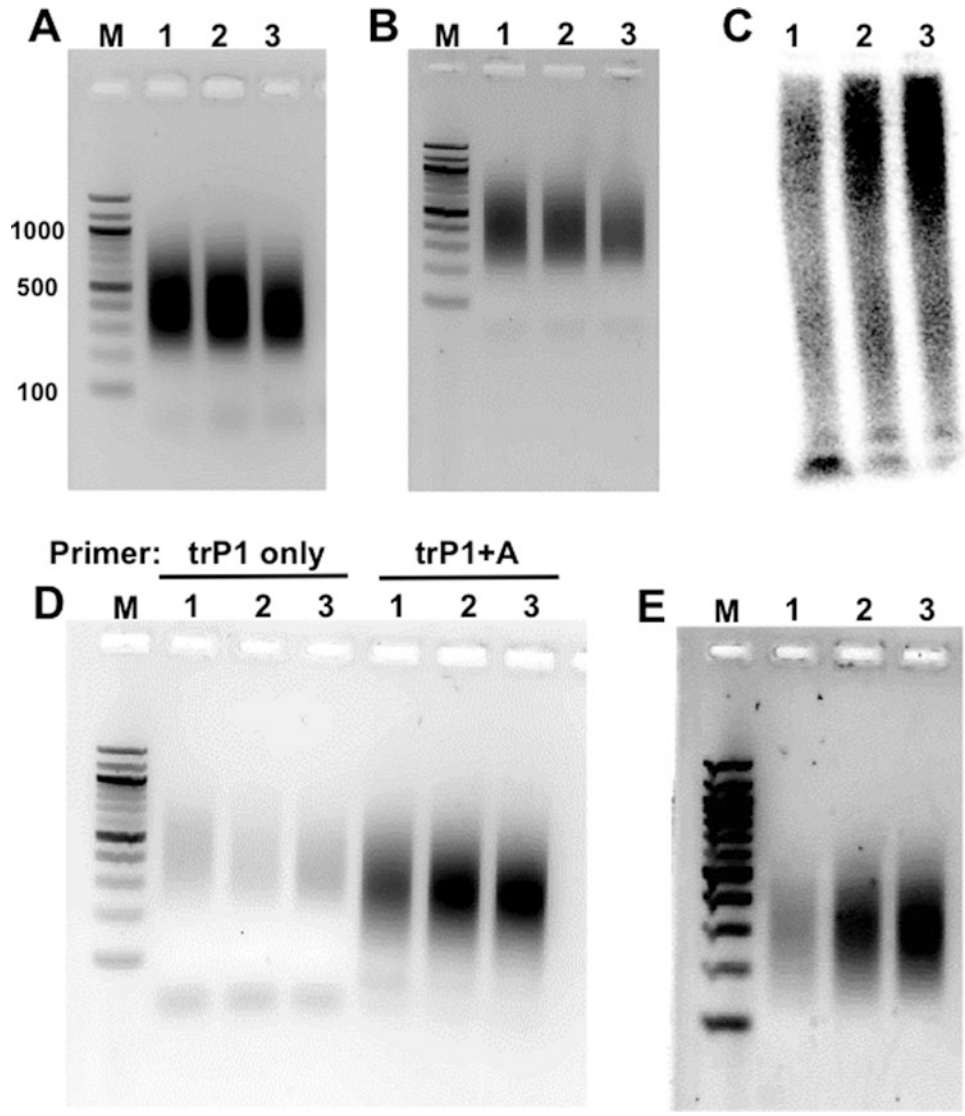

Fig. 2 Intermediate results confirming several critical steps in CPD-seq. The results were obtained from a CPD-seq experiment conducted in human fibroblast NHF1 cells. (**a**) Gel electrophoresis (2% agarose) of sonicated genomic DNA. A 100-bp marker (M) was added. DNA was stained with SYBR Safe. Sample 1 is No UV control. Sample 2 is naked genomic DNA irradiated with UV (*in vitro*—80 J/m^2). Sample 3 is DNA isolated from UV-irradiated cells (*in vivo*—100 J/m^2). (**b**) PCR confirmation of trP1 adaptor ligation. The ligation product was amplified by PCR with a single primer (Primer trP1) for eight cycles. The three samples are shown in the same order as in (**a**). (**c**) PCR confirmation of A adaptor ligation using ^{32}P-labeled Primer A and unlabeled Primer trP1. DNA was amplified for eight cycles and separated on an 8% polyacrylamide gel in 1$\times$ TBE. Samples are shown in the same order as in (**a**). The stronger DNA signal in samples 2 and 3 relative to sample 1 (negative control) suggests that the A adaptor DNA was specifically ligated to CPD damage sites. (**d**) PCR confirmation of A adaptor ligation after streptavidin bead purification and second strand synthesis. DNA was amplified for eight cycles with Primer trP1 only (left) or Primer trP1 and A (right). After PCR, DNA was separated on a 2% agarose gel and stained with SYBR Safe. The stronger DNA signal in UV-irradiated (i.e., 2 and 3) on the right side, but not on the left side, further confirms ligation of A adaptors to CPD lesion sites. (**e**) PCR amplification of the final CPD-seq libraries. Libraries were amplified for five cycles with Primer trP1 and

10. Discard the supernatant and add another 500 μL of 75% ethanol to wash again. After this second wash, centrifuge briefly to collect all the beads. Place the tubes on the magnet for 1 min. Use a pipette to remove ethanol until no droplets remain in the tube.
11. Air-dry the beads for ~10 min. Check to confirm they are dry (*see* **Note 2**).
12. Elute the DNA: add 90 μL of diH_2O and resuspend the beads thoroughly by pipetting ten times. Incubate at RT for 1 min.
13. Place the tubes on the magnetic stand for 1 min to pull down the beads. Transfer the eluates to fresh tubes.
14. Measure the DNA concentration using a UV spectrophotometer. In our experience, we usually retain >5 μg of DNA fragments at this step.

3.4 CPD-seq Library Preparation

1. Prepare the following reaction in 0.5 mL PCR tubes. Add 5 μg (*see* **Note 3**) of bead-purified DNA fragments, 10 μL of 10× end repair buffer, and 5 μL of enzyme mix from the NEBNext end repair module. Mix well and briefly centrifuge to collect droplets. Add diH_2O up to a final reaction volume of 100 μL. Incubate at 20 °C for 1 h in a PCR thermocycler.
2. Transfer the end repair products to 1.5 mL tubes. Purify the DNA by repeating **steps 6–12** of Subheading 3.3, using 120 μL of AMPure XP beads. After air-drying, add 42 μL of diH_2O to elute the DNA. The AMPure XP beads are not separated from the DNA (*see* **Note 4**).
3. Add 5 μL of 10× dA tailing reaction buffer and 3 μL of Klenow Fragment (3′→5′ exo$^-$) from the NEBNext dA tailing module. Briefly centrifuge and then incubate at 37 °C for 1 h.
4. Add 17 μL of 5 M NaCl and 30 μL of 40% PEG 8000 with 1.25 M NaCl (*see* **Note 5**) to each sample after the dA tailing reaction. Mix thoroughly by pipetting for ten times. Since the AMPure XP beads were retained in the dA tailing reaction, no new beads are required.
5. Repeat **steps 7–12** of Subheading 3.3 to purify the DNA. Add 20 μL of H_2O for DNA elution. Beads can be retained with the DNA; transfer the DNA with beads to fresh 0.5 mL PCR tubes.
6. Anneal double-stranded trP1 adaptor DNA (ds-trP1). Mix 40 μL of trP1-top (100 μM), 40 μL of trP1-bottom (100 μM) (*see* Table 1), 10 μL of diH_2O, and 10 μL of 10×

Fig. 2 (continued) A. Equal volumes of each library were mixed for sequencing. The three samples were ligated with A4, A5, and A6 adaptors and they can be demultiplexed using their specific barcodes during bioinformatic analysis

T4 DNA ligase buffer in a 0.5 mL PCR tube. Anneal in a PCR thermocycler by first incubating at 95 °C for 6 min and then decreasing the temperature by 1 °C/1 min cycle for 70 cycles to reach 25 °C. The annealed adaptor DNA can be stored at −20 °C for up to 6 months.

7. Add 15 μL of ds-trP1, 10 μL of 5× quick ligase buffer, and 5 μL of quick ligase from the NEB NEBNext quick ligation module to the dA-tailed DNA. Mix the components in the ligation reaction by gently pipetting 3–5 times.
8. Incubate at 20 °C in a PCR thermocycler for 2 h (*see* **Note 6**).
9. Add 17 μL of 5 M NaCl and 30 μL of 40% PEG 8000 with 1.25 M NaCl to each sample. Follow **steps 7–13** of Subheading 3.3 to purify the DNA. Elute the DNA with 100 μL of diH_2O and transfer it to a fresh 1.5 mL tube to separate it from beads.
10. Confirm the ligation of the trP1 adaptor by PCR using a single primer (i.e., Primer trP1) (*see* Table 1) with the following steps: (a) 94 °C for 3 min; (b) 94 °C for 30 s; (c) 55 °C for 30 s; (d) 72 °C for 30 s. PCR amplification for eight cycles (**steps b–d**) is usually sufficient to detect ligation products. Visualize the PCR products by electrophoresis on a 2% agarose gel. Figure 2b shows an example of PCR confirmation of trP1 adaptor ligation.
11. After confirmation of trP1 adaptor ligation, add 96 μL of diH_2O to each DNA sample to increase the volume to 195 μL. Add 25 μL of 10× terminal transferase reaction buffer, 25 μL of 2.5 mM $CoCl_2$, 2.5 μL of ddATP (*see* **Note 7**), and 2.5 μL of terminal transferase to the DNA. The total reaction volume is 250 μL. Incubate at 37 °C for 2 h.
12. Add 300 μL of AMPure XP beads and follow **steps 6–13** of Subheading 3.3 to purify the DNA. Elute the DNA with 60 μL of H_2O and separate DNA from beads.
13. Use 51.5 μL of DNA for T4 Endonuclease V and APE1 digestion. The remaining DNA (~8.5 μL) is used for ligation with the A adaptor DNA to confirm efficient blockage of free 3′ ends (*see* **Note 8**). Add 6 μL of 10× NEBuffer 4, 2 μL of T4 Endonuclease V, and 0.5 μL of APE1 to the DNA and incubate at 37 °C for 1.5 h. The total reaction volume is 60 μL.
14. Add 72 μL of AMPure XP beads and follow **steps 6–12** of Subheading 3.3 to purify DNA. Elute the DNA with 85 μL of diH_2O and retain beads with DNA.
15. Add 10 μL of 10× shrimp alkaline phosphatase buffer and 5 μL of SAP to the DNA and incubate at 37 °C for 1 h. The presence of AMPure XP beads does not affect the phosphatase activity.

16. Add 34 μL of 5 M NaCl and 60 μL of 40% PEG 8000 in 1.25 M NaCl to the DNA. Mix the beads and other components thoroughly by pipetting ten times. Follow **steps 7–13** of Subheading 3.3 to purify DNA. Add 29 μL of diH_2O to elute the DNA. Transfer DNA to a 0.5 mL PCR tube and discard the beads.
17. Anneal barcoded A adaptors (dsA) using the protocol described in **step 6** of Subheading 3.4.
18. Use a PCR thermocycler to heat the DNA from **step 16** at 95 °C for 5 min. Snap-cool DNA on ice to ensure DNA stays denatured. Immediately add 6 μL of precooled dsA adaptor DNA, 10 μL of 5× quick ligase buffer, and 5 μL of quick ligase from the NEB NEBNext quick ligation module. Incubate at 20 °C for 2 h using a PCR machine.
19. After ligation, add 90 μL of AMPure XP beads and follow **steps 6–13** of Subheading 3.3 to purify DNA. Add 41 μL of diH_2O for DNA elution. Transfer DNA to a fresh 1.5 mL tube and discard beads.
20. Check the ligation of dsA adaptors by PCR using ^{32}P- or Cy3-labeled Primer A (*see* Table 1). Add 1 μL of labeled Primer A (5 μM), 1 μL of unlabeled Primer trP1 (5 μM), and 1 μL of purified ligation product in a 20 μL PCR tube. Set the PCR program: (a) 94 °C for 3 min; (b) 94 °C for 30 s; (c) 55 °C for 30 s; (d) 72 °C for 30 s for 5–8 cycles. PCR products with radioactive label are assessed by polyacrylamide gel electrophoresis. Load 10 μL of PCR product onto a 1× TBE, 8% polyacrylamide gel. Scan the gel. Figure 2c shows an example of PCR products after dsA adaptor ligation. Cy3-labeled DNA can be separated by electrophoresis on a 2% agarose gel and visualized with a scanner.
21. Use M-280 streptavidin beads to purify the single-stranded CPD-seq library. Transfer 20 μL of streptavidin beads to a fresh tube. Add 50 μL of 1× biotin bind-and-wash buffer to wash beads. Place the tube into a magnetic stand to collect the beads. Discard the supernatant.
22. Resuspend the beads in 40 μL of 2×biotin bind-and-wash buffer. Add 40 μL of DNA from **step 19** and incubate on a rotator at RT for 15 min. Briefly centrifuge and collect beads using the magnet stand. Discard the supernatant.
23. Add 50 μL of 1× SSC and resuspend the beads by pipetting. Incubate on the rotator for 5 min at RT. Briefly centrifuge, and collect beads on the magnetic stand. Discard the supernatant. Repeat this wash step once to remove all unbound DNA fragments.

24. After completely removing the supernatant, add 40 μL of fresh 0.15 M NaOH and resuspend the beads by pipetting. Incubate on a rotator at RT for 10 min.
25. Collect the beads with the magnetic stand. Transfer the supernatant, which contains the single-stranded CPD-seq library, to a fresh 1.5 mL tube.
26. Add another 40 μL of fresh 0.15 M NaOH to the beads and incubate for 5 min. Elute again and combine both eluates.
27. Use the magnetic stand to pull down any carryover beads in the combined eluate, and transfer the DNA to another tube.
28. Add 120 μL of diH_2O, 20 μL of 3 M NaOAc, and 2 μL of glycogen. Mix and then add 800 μL of 100% ethanol. Incubate at −20 °C overnight to precipitate DNA.
29. Centrifuge at ~21,000 × *g* for 30 min at 4 °C. Wash the DNA pellet with 75% ethanol and air-dry it.
30. Prepare a master mix for the second strand synthesis. The master mix (for each reaction) contains 14.5 μL of diH_2O, 2 μL of 10× EconoTaq reaction buffer, 1 μL of 3 mM dNTPs, and 1 μL of 5 μM Primer A.
31. Add 18.5 μL of this master mix to each DNA pellet and incubate at 37 °C for 10 min to dissolve the DNA.
32. Dilute EconoTaq DNA Polymerase 10 times with 1× EconoTaq reaction buffer and add 1.5 μL of this diluted polymerase to the DNA. Transfer the mixture to a PCR tube.
33. Synthesize the second strand in a PCR thermocycler by sequentially incubating at 94 °C for 3 min, 55 °C for 30 s, and 72 °C for 1 min.
34. Add 36 μL of AMPure XR beads (1.8×) to purify the DNA. Elute DNA with 32 μL of diH_2O. Separate the DNA from the beads.
35. Set up two parallel PCRs (1 and 2) to assess the CPD-seq libraries. For PCR 1, only add Primer trP1 to estimate the background signal (i.e., the abundance of DNA fragments with the trP1 adaptor on both ends). For PCR 2, include both Primer trP1 and Primer A. Each PCR has 1 μL of DNA from the previous step as the template and is amplified for 5–8 cycles. The PCR program is the same as that described in **step 20**. Figure 2d shows an example of PCR results.
36. Prepare the final products for sequencing. Set up a PCR master mix using the following recipe (for each reaction): 22 μL of diH_2O, 5 μL of 10× EconoTaq reaction buffer, 2.5 μL of 3 mM dNTPs, 2.5 μL of 5 μM Primer A, 2.5 μL of 5 μM Primer trP1, and 0.5 μL of EconoTaq DNA Polymerase. Split this master mix to 0.5 mL PCR tubes, 35 μL in each, and add

15 μL of DNA from **step 34**. Incubate in a PCR thermocycler at 94 °C for 3 min, 94 °C for 30 s, 55 °C for 30 s, and 72 °C for 30 s. Repeat from the second step for a total of five cycles (*see* **Note 9**).

37. Add 90 μL of AMPure XR beads (1.8×) to purify the DNA (*see* **Note 10**). Elute DNA with 30 μL of diH_2O. Load 5 μL of DNA from each sample and a 100 bp DNA ladder onto a 2% agarose gel. Visualize DNA abundance and fragment size distribution by gel electrophoresis. Figure 2e shows an example of the final products ready for DNA sequencing.
38. After confirming an enriched CPD-seq signal in UV-damaged samples, combine the different CPD-seq libraries with distinct barcodes at equal volumes (e.g., 5 μL of each library). After further confirmation of DNA concentration and size distribution, e.g., using a Fragment Analyzer (Agilent), the combined library can be sequenced (*see* **Note 11**).

3.5 Bioinformatics Analysis of CPD-seq Data

1. Demultiplex the sequencing reads. We use custom Python scripts to demultiplex the fastq file and remove barcodes and the last nucleotide added by the dA tailing step from sequencing reads. Below is an example of our scripts (using A1 barcode as the example):

```
# Remove barcodes and the last nucleotide
input=open('sequencing_dataset.fastq')
output=open('A1_file.fastq','w')
for line1 in input:
    line2=input.next().rstrip()
    line3=input.next()
    line4=input.next().rstrip()
    if line2.startswith('AAGAGGAT'):#A1
        output.write(line1)
        output.write(line2[8:-1]+'\n')
        output.write(line3)
        output.write(line4[8:-1]+'\n')
output.close()
```

2. After removing barcodes, sequencing reads can be aligned to the reference genome (e.g., sacCer3 for yeast or hg19 for human) using the software Bowtie2 (*see* **Note 12**) [16]. The alignment commands are:

```
bowtie2 -x genome_index_file -U A1_file.fastq -S A1_alignment.sam
```

3. The alignment file, which is typically in the SAM format [17], can be converted to BAM and BED files using the following commands (*see* **Note 13**):

```
samtools view -b -S A1_alignment.sam > A1_alignment.bam
bamToBed -i A1_alignment.bam > A1_alignment.bed
```

4. The BED file contains the starting and ending positions of sequencing reads that are mapped to the reference genome (*see* **Note 14**). The two nucleotides immediately upstream of the 5′ end of each sequencing read on the opposing strand are the putative damage site. Use BEDTools to search for the damage sites and obtain the dinucleotide sequences from the genome:

```
bedtools flank -i A1_alignment.bed -g chromosome_size_file
-l 2 -r 0 -s > dinu_A1_alignment.bed
bedtools getfasta -fi genome_seq_file -bed dinu_A1_align-
ment.bed -s -fo A1_dinucleotide.fa
```

4 Notes

1. In yeast cells, we conduct all steps from UV irradiation to DNA extraction in a yellow light room to prevent undesired photolyase activity. UV experiments with human cells can be conducted under normal light.
2. We usually air-dry beads in a fume hood for no more than 10 min. Overdrying may reduce DNA recovery.
3. The maximal amount of DNA for end repair is 5 μg. We have used as low as 2 μg of sonicated DNA for a CPD-seq library preparation.
4. AMPure XP beads can be reused at several steps of CPD-seq library preparation. They do not interfere with the subsequent enzymatic reaction.
5. PEG 8000 solution is sticky and hard to pipette. It is suggested to use wide pipette tips in this step.
6. Ligation at 16 °C overnight works the same as at 20 °C for 2 h.
7. We have also tested ddGTP for 3′-OH blocking and it works the same as ddATP.
8. Complete blockage of free 3′-OHs is critical for CPD-seq experiments. It is necessary to confirm that the majority of 3′ ends are blocked. We usually use a small fraction of the blocked DNA products to conduct a ligation reaction with dsA adaptors. After ligation, purify the DNA with AMPure XP beads. Add 1 μL of DNA to a PCR reaction containing ^{32}P-labeled Primer A and non-labeled Primer trP1. Visualize PCR products by electrophoresis on an 8% polyacrylamide gel. The blocked DNA should give significantly fewer ligation products relative to DNA without TdT and ddATP treatment.

9. We have also tried six PCR cycles in some experiments and the result is consistent with that for five cycles. In general, the number of PCR cycles should be minimized in order to maintain the sequencing library complexity.
10. A size selection can be added with AMPure XP beads if large DNA fragments are present in the final products. Size selection with a 0.6×volume of beads (i.e., add 30 μL of beads to 50 μL of PCR product) can efficiently remove fragments >500 bp. After bead binding, discard the beads and add 60 μL of fresh beads to the supernatant. Follow **steps 7–13** of Subheading 3.3 to purify small DNA fragments.
11. The adaptors shown in this protocol are designed for the Ion Proton sequencing platform (Life Technologies). CPD-seq can be adapted for other sequencers such as the Illumina sequencer.
12. Installation of Bowtie2 software and generation of index files can be found at http://bowtie-bio.sourceforge.net/bowtie2/index.shtml.
13. SAMtools information can be found at http://samtools.sourceforge.net/.
14. BEDTools information is available at https://bedtools.readthedocs.io/en/latest/.

Acknowledgments

We thank Drs. Mingrui Duan and Kathiresan Selvam for critical reading of this manuscript. Research related to this work is supported by grants from NIEHS (R03ES027945 to P.M., R21ES029302 to P.M. and J.J.W., R01ES028698, R21ES029655, and R21ES027937 to J.J.W). Yeast strains and custom scripts for CPD-seq data analysis will be shared with interested readers upon request.

References

1. Friedberg EC, Walker GC, Siede W et al (2006) DNA repair and mutagenesis. In: DNA repair and mutagenesis, 2nd edn. ASM Press, Washington, DC
2. Marteijn JA, Lans H, Vermeulen W, Hoeijmakers JHJ (2014) Understanding nucleotide excision repair and its roles in cancer and ageing. Nat Rev Mol Cell Biol 15:465–481. https://doi.org/10.1038/nrm3822
3. Hayward NK, Wilmott JS, Waddell N et al (2017) Whole-genome landscapes of major melanoma subtypes. Nature 545:175–180. https://doi.org/10.1038/nature22071
4. Sugiyama T, Chen Y (2019) Biochemical reconstitution of UV-induced mutational processes. Nucleic Acids Res 47:6769–6782. https://doi.org/10.1093/nar/gkz335
5. Ikehata H, Ono T (2011) The mechanisms of UV mutagenesis. J Radiat Res 52:115–125. https://doi.org/10.1269/jrr.10175
6. Mao P, Wyrick JJ, Roberts SA, Smerdon MJ (2017) UV-induced DNA damage and mutagenesis in chromatin. Photochem Photobiol

93:216–228. https://doi.org/10.1111/php.12646

7. Schuster-Böckler B, Lehner B (2012) Chromatin organization is a major influence on regional mutation rates in human cancer cells. Nature 488:504–507. https://doi.org/10.1038/nature11273
8. Adar S, Hu J, Lieb JD, Sancar A (2016) Genome-wide kinetics of DNA excision repair in relation to chromatin state and mutagenesis. Proc Natl Acad Sci USA 113:E2124–E2133. https://doi.org/10.1073/pnas.1603388113
9. Polak P, Karlić R, Koren A et al (2015) Cell-of-origin chromatin organization shapes the mutational landscape of cancer. Nature 518:360–364. https://doi.org/10.1038/nature14221
10. Mao P, Brown AJ, Esaki S et al (2018) ETS transcription factors induce a unique UV damage signature that drives recurrent mutagenesis in melanoma. Nat Commun 9:2626. https://doi.org/10.1038/s41467-018-05064-0
11. Pich O, Muiños F, Sabarinathan R et al (2018) Somatic and germline mutation periodicity follow the orientation of the DNA minor groove around nucleosomes. Cell 175:1074–1087.e18. https://doi.org/10.1016/j.cell.2018.10.004
12. Brown AJ, Mao P, Smerdon MJ, Wyrick JJ, Roberts SA (2018) Nucleosome positions establish an extended mutation signature in melanoma. PLoS Genet 14:e1007823. https://doi.org/10.1371/journal.pgen.1007823
13. Wyrick JJ, Roberts SA (2015) Genomic approaches to DNA repair and mutagenesis. DNA Repair 36:146–155. https://doi.org/10.1016/j.dnarep.2015.09.018
14. Mao P, Smerdon MJ, Roberts SA, Wyrick JJ (2016) Chromosomal landscape of UV damage formation and repair at single-nucleotide resolution. Proc Natl Acad Sci USA 113:9057–9062. https://doi.org/10.1073/pnas.1606667113
15. Ding J, Taylor MS, Jackson AP, Reijns MAM (2015) Genome-wide mapping of embedded ribonucleotides and other noncanonical nucleotides using emRiboSeq and EndoSeq. Nat Protoc 10:1433–1444. https://doi.org/10.1038/nprot.2015.099
16. Langmead B, Salzberg SL (2012) Fast gapped-read alignment with Bowtie 2. Nat Methods 9:357–359. https://doi.org/10.1038/nmeth.1923
17. Li H, Handsaker B, Wysoker A et al (2009) The Sequence Alignment/Map format and SAMtools. Bioinformatics 25:2078–2079. https://doi.org/10.1093/bioinformatics/btp352

Chapter 8

AP-Seq: A Method to Measure Apurinic Sites and Small Base Adducts Genome-Wide

Anna R. Poetsch

Abstract

DNA is constantly challenged by chemical modification and spontaneous loss of its bases, which results in apurinic sites (AP-sites). In addition to the direct route, modified bases may be converted into AP-sites through enzymatic removal of the base as part of the base excision repair pathway. Here we present the method AP-seq, which allows enriching and sequencing AP-sites genome-wide. Quantification of DNA recovery (AP-quant) allows for relative quantification of global AP-sites, and AP-site pulldown followed by qPCR (AP-qPCR) allows for site-specific damage assessment. Taking advantage of glycosylases that specifically excise modified bases also *in vitro*, this method allows not only to address the genomic distribution of AP-sites but also to detect base modifications, e.g., 8-oxo-7,8-dihydroguanine (8-oxoG). AP-quant, AP-qPCR, and AP-seq can be applied to investigate quantitatively the relative amount and genome specificity of DNA damage and repair, effects of radiation, as well as multiple other questions around AP-sites and base modifications.

Key words AP-sites, DNA damage, Genomics, Epigenomics, 8-oxoG, Base modification, DNA repair, Radiation, Base excision repair

1 Introduction

Apurinic or abasic sites (AP-sites) are a type of DNA damage, which is caused when a base is removed from the DNA. This can occur either through spontaneous depurination and depyrimidination or through enzymatic excision of modified or damaged bases as part of the base excision repair (BER) pathway (*see* Fig. 1).

Damage types that are typically repaired through this process are oxidatively damaged base such as 8-oxo-7,8-dihydroguanine (8-oxoG), but also methyl adducts and uracil. Upon excision, the bond between the base and the backbone-ribose is broken, which leaves an accessible aldehyde at the AP-site. The AP-site can present with a non-interrupted backbone or as a single-strand break via beta-elimination. In 1992, Kubo *et al.* developed an aldehyde reactive probe (ARP) that specifically tags this site in both variations

Ronald Hancock (ed.), *The Nucleus*, Methods in Molecular Biology, vol. 2175, https://doi.org/10.1007/978-1-0716-0763-3_8,

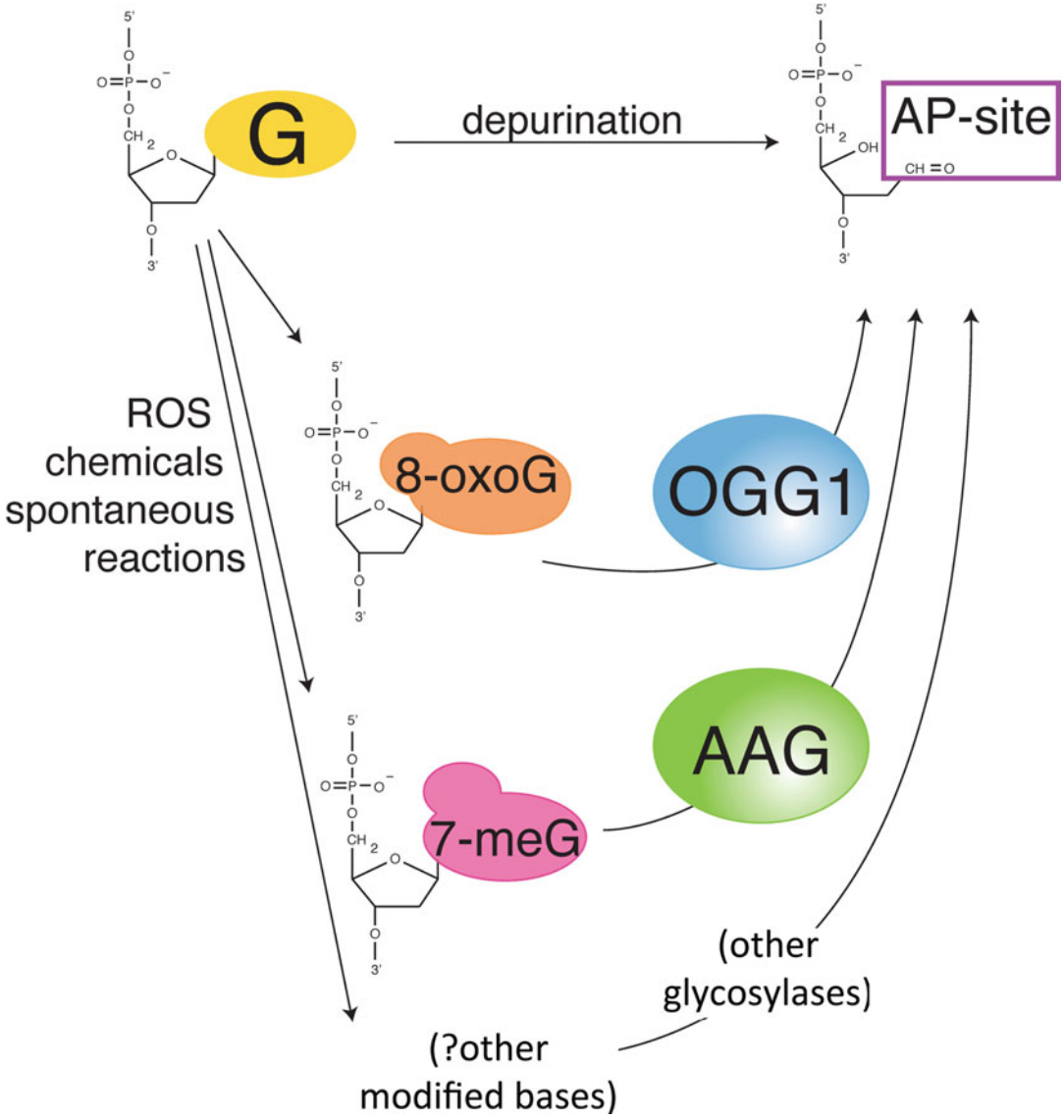

Fig. 1 Routes to apurinic sites (AP-sites). Loss of a base through depurination leads to breakage of the bond between the ribose in the backbone and the base, which reveals an accessible aldehyde at the resulting AP-site. In addition to this direct route, base modifications represent an indirect route to AP-sites. Base modifications are the result of reactions with reactive oxygen species, chemicals, and spontaneous reactions such as deamination. The repair via the base excision repair pathway is initiated through excision of the modified base such as 8-oxo-7,8-dihydroguanine (8-oxoG) and 7-methyl-guanine (7-meG) by specific glycosylases, such as 8-oxoguanine DNA glycosylase (OGG1) and alkyladenine DNA glycosylase (AAG), respectively. Potentially, other types of modified base could be studied using other glycosylases

with biotin and allows for specific detection of AP-sites through biotin-streptavidin interactions [1] (*see* Fig. 2).

This chemical reaction was then used mainly for colorimetric assays and mass spectrometry-based strategies [2–6]. Through this

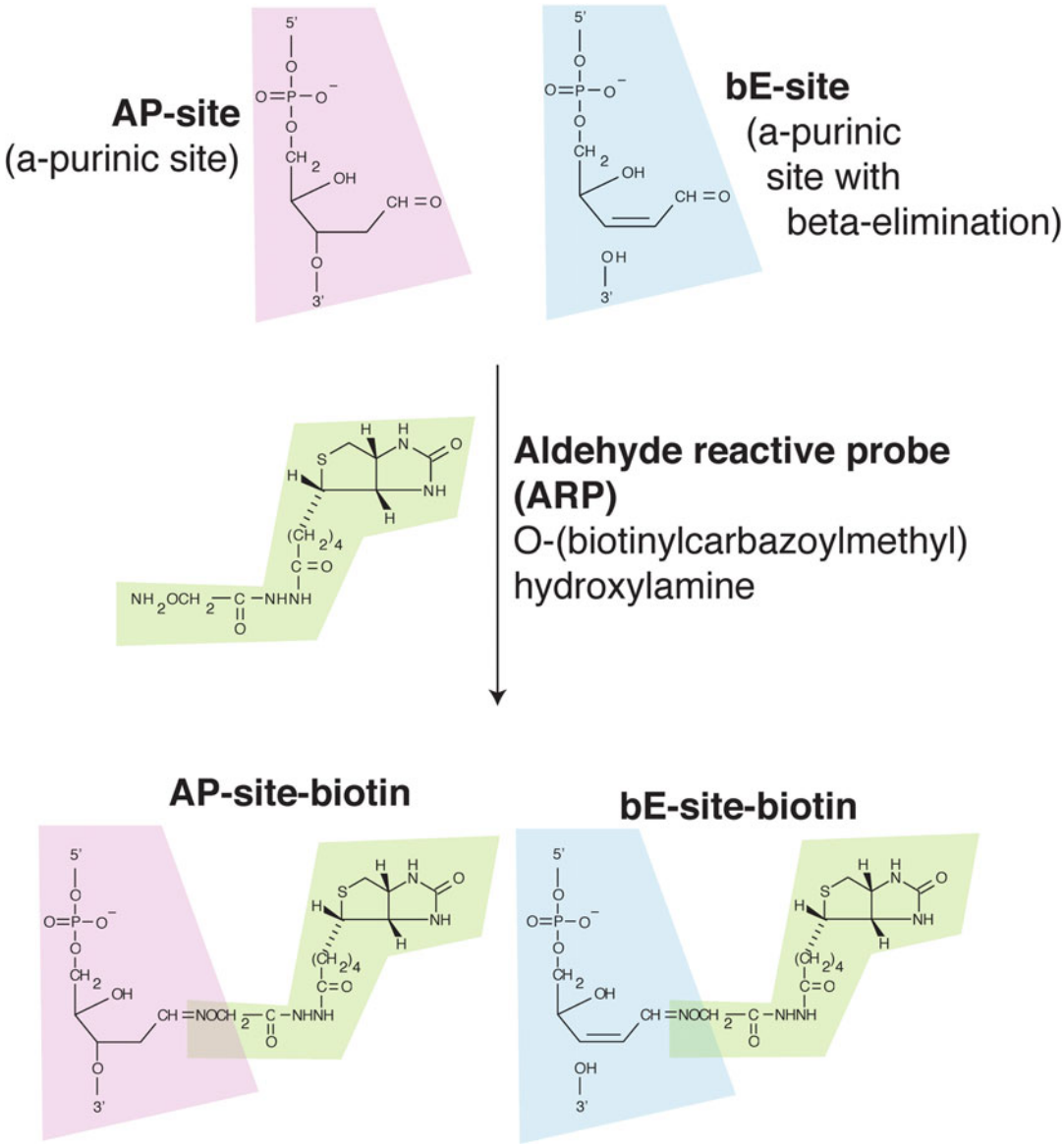

Fig. 2 The chemical principle behind the aldehyde reactive probe (ARP). AP-sites come in two flavors, one with the backbone intact and the second as a beta-elimination product (bE-site) which interrupts the bond between the deoxyribose and the backbone phosphate. Both AP-site types react with ARP, chemically N-(aminooxyacetyl)-N'-(D-Biotinoyl) hydrazine. The reaction between aldehyde and the probe's hydroxylamide leads to covalent tagging with biotin

and other approaches [5, 7] it could be determined that total AP-site levels range from ~15,000 to 30,000 per cell at a steady state.

We adapted this chemical biology approach to enrich genomic DNA containing AP-sites via its biotin tag. Through measuring DNA recovery, qPCR, and DNA sequencing, this method can

detect relative global AP-site levels (AP-quant), AP-sites at specific genomic loci (AP-qPCR), and genome-wide distribution (AP-seq), respectively [5]. Interestingly, their distribution over the genome is highly heterogeneous, with reduced damage levels at sites of high GC content and genomic regions of high functional importance such as promoters and coding sequence [5]. Using enzymatic glycosylation, we used the same method to measure the genomic distribution of 8-oxoG in response to ionizing radiation. We found it to specifically accumulate at potential non-B-DNA structures, such as telomeres, G-quadruplexes, and simple repeats of a specific sequence content [5]. Using ionizing radiation treatment as damage source (*see* **Note 1**) and HepG2 cells as a model system, we present here the workflows to measure AP-sites, i.e., AP-quant for relative quantification of global AP-site levels, AP-qPCR for site-specific AP-site levels, and AP-seq for assessment of AP-sites genome-wide (*see* Fig. 3).

We also describe how to use this method to assess 8-oxoG. By using different glycosylases to produce the AP-site, the method is also easily adaptable to measure additional base modifications, e.g., using uracil DNA glycosylase (UDG) to measure uracil, or alkyladenine DNA glycosylase (AAG) to address methyl adducts.

The strength of this method is the genome-wide quantification of AP-sites, oxidative DNA damage, and other base modifications. This method is suitable to measure AP-sites globally (AP-quant), at specific genomic loci (AP-qPCR), or genome-wide (AP-seq). The latter gives an enrichment pattern over the genome (*see* Fig. 4) similar to a ChIP-seq experiment and can be analyzed downstream with similar strategies dependent on the biological question. While this protocol is focused on detection of oxidative DNA damage, this versatile method would also be suitable to address other base modifications and is therefore applicable to a variety of questions beyond oxidative DNA damage.

2 Materials

Prepare all solutions using ultrapure water and store at room temperature unless indicated otherwise. Where a recommendation is given to prepare a certain volume of solution per sample, please include an appropriate overhead to account for liquid loss during pipetting.

2.1 Oxidative DNA Damage Treatment

1. Growth medium for HepG2 cells: Dulbecco's modified Eagle medium (DMEM) with 1% essential amino acids, 1% pyruvate, 2% penicillin/streptomycin, and 10% heat inactivated fetal bovine serum (FBS) (*see* **Note 2**).

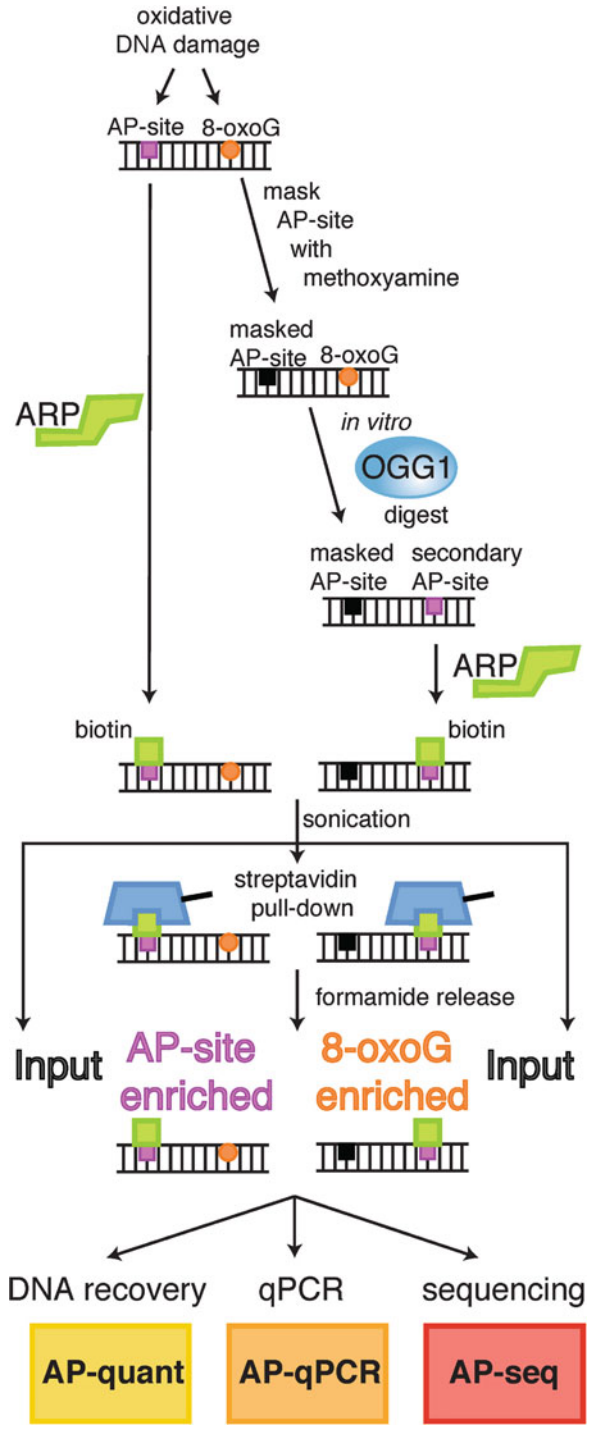

Fig. 3 Workflow to measure AP-sites and 8-oxoG. Oxidative DNA damage results both in AP-sites and 8-oxoG, which can be measured separately. While AP-sites can be directly tagged with biotin using the aldehyde reactive probe, 8-oxoG first needs to be processed. AP-sites are first masked with methoxyamine to avoid their detection instead of 8-oxoG. Then the glycosylase OGG1 is used to excise 8-oxoG to form a secondary

2. X-ray machine able to irradiate to 6 Gy (e.g., SOFTEX M-150WE). There are alternative methods for causing oxidative DNA damage (*see* **Note 3**).

2.2 DNA Extraction and Processing

1. Instrument to precisely determine gDNA concentrations (e.g., Qubit or NanoDrop, ThermoFisher).
2. Ethanol: 70% (v/v).
3. TE buffer: 10 mM Tris, 1 mM EDTA, bring to pH 8.0 with HCl, prepare several mL per sample.
4. 1 M NaCl in TE buffer: prepare >600 µL per sample.
5. 2 M NaCl in TE buffer: prepare 100 µL per sample.
6. 10 mM ARP (Aldehyde-Reactive Probe) (Life Technologies) in TE buffer: Prepare 50 µL per sample; this can be stored either at 4 °C or −20 °C but ideally should be prepared fresh.

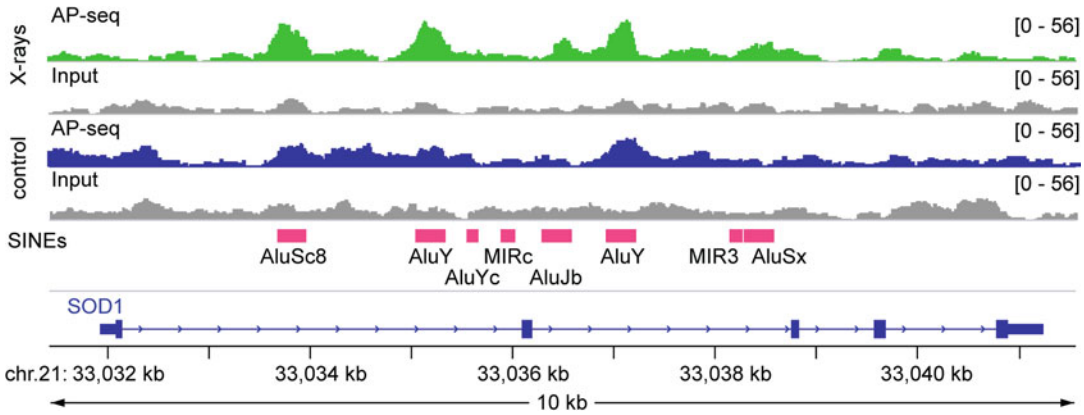

Fig. 4 Genome browser track obtained by AP-seq in the body of the oxidative stress-response gene *SOD1*. AP-sites accumulate specifically in the Alu elements in the control sample and are augmented upon ionizing radiation treatment. Displayed is the unnormalized raw read coverage pooled from three replicates [5]. HepG2 cells were exposed to 6 Gy X-rays and gDNA was extracted after 30 min and processed for AP-seq

Fig. 3 (continued) AP-site. This secondary AP-site is tagged with biotin using ARP. Consequently, in one branch of the experiment, the probe specifically tags original AP-sites and in the other branch, secondary AP-sites that are derived from 8-oxoG. After sonication, part of the tagged DNA is retained as input that does not undergo enrichment. Pulldown is performed with streptavidin-loaded magnetic beads that retain the biotin-tagged DNA. After release with formamide, we obtain two types of enriched DNA, one that originally harbored an AP-site and the second that originally harbored 8-oxoG. This enriched DNA can be quantified and a recovery score calculated. This represents a relative quantification of total AP-sites and 8-oxoG levels (AP-quant). Alternatively, the enriched DNA can be used for qPCR to interrogate specific loci (AP-qPCR). For genome-wide AP-site and 8-oxoG distribution levels, the enriched DNA and input are sequenced (AP-seq)

7. Kits to extract genomic DNA: we use Blood and Tissue Kits (Qiagen) (*see* **Note 4**).
8. AMPure beads (Agencourt: Beckman Coulter): count 360 μL per AP-site sample and 540 μL per 8-oxoG sample.
9. Low-bind 96-well plates (*see* **Note 5**).
10. Low-bind 1.5 mL tubes.
11. 96-well format magnetic separator.
12. 1.5 mL tube magnetic separator.

2.3 8-oxoG-Specific Material

1. 1.5 M methoxyamine (Sigma) in TE buffer: stock solution (*see* **Note 6**).
2. 10 mM methoxyamine in TE buffer: prepare 50 μL per sample.
3. OGG1 enzyme (NEB): plan 1 unit per sample (*see* **Note 7**).
4. 10× NEB buffer 2.
5. Bovine serum albumin (BSA).
6. OA buffer: 10 mM ARP, 1 unit OGG 1, and 10 μL of NEB buffer 2 in 50 μL TE buffer. The purpose of OA buffer is OGG1 digestion and ARP labeling of your DNA samples. Always prepare fresh. Prepare 50 μL per sample.

2.4 Pulldown

1. DNA fractionator (Covaris or other) with 130 μL tubes (1 per sample).
2. Sample rotator (dependent on availability for tubes or 96-well format).
3. Biotin beads: MyOne Dynabeads (Life Technologies): count to use 10 μL per sample.
4. 95% formamide with 10 mM EDTA: always prepare fresh, count 100 μL per sample.

2.5 AP-Quant

1. No special equipment is required.

2.6 AP-qPCR

1. qPCR machine.
2. Standard qPCR reagents (e.g., 2× Maxima SYBR Mastermix; Thermo Fisher).
3. Primer pair of interest (0.3 μM per sample).

2.7 AP-Seq: Library Preparation and Sequencing

1. *In vitro* DNA repair Kit: PreCR (NEB).
2. Library preparation Kit: 125-bp paired-end (KAPA Biosystems, Roche Diagnostics).
3. Sequencing kit: Illumina HiSeq 2000.

2.8 Software and Data for Core Data Processing

1. Sequencing quality control: FastQC (https://www.bioinformatics.babraham.ac.uk/projects/fastqc/).
2. Alignment: Bowtie2 (http://bowtiebio.sourceforge.net/bowtie2/index.shtml).
3. Read duplicate assessments: Picard Tools, (https://broadinstitute.github.io/picard/).
4. Filtering: SAMtools (http://samtools.sourceforge.net/).
5. Visualization: Integrative Genomics Viewer (http://software.broadinstitute.org/software/igv/).
6. Appropriate reference genome (*see* **Note 8**).
7. Downstream analyses and visualization: R/Bioconductor (*see* **Note 9**).

3 Methods

3.1 Experimental Design

If you plan to perform AP-seq, please communicate the experimental plan with the person who is going to analyze the sequencing data before you start the experiments. Functional genomics experiments of this kind usually require replicates to use the appropriate data analysis methods; triplicates would be recommended. Data analysis also requires a matched input control, sequenced to a similar depth as the pulldown. Therefore, a simple experiment addressing AP-sites with a comparison of an untreated to a treated condition already requires twelve sequencing samples:

3× pulldown of the treated condition

3× input (treated condition)

3× pulldown of the untreated condition

3× input (untreated condition)

Measurement of 8-oxoG together with AP-sites requires a total of 24 samples.

All samples should be processed side by side. If, for practical reasons, this is not possible, conditions should be randomized into batches and batch effects need to be assessed subsequently in the data analysis. A summary of the workflow is presented in Fig. 3. For changes in the method since the original publication [8], *see* **Note 10**.

3.2 Preparation of Cells

1. Seed the cells at 50% density in 6 cm ∅ dishes 24 h prior to the experiment to achieve 80% confluency at the time of the experiment. For HepG2 cells, approximately 1×10^6 cells should yield 12.5 μg genomic DNA (gDNA), and 10 μg are required. Considering the multiplication factor for controls, seed the HepG2 cells using an appropriate number of dishes.

2. Treat the cells according to your experimental design. For maximal oxidative DNA damage, expose cells to 6 Gy of X-rays (*see* **Note 2**) and keep them at 37 °C for 30 min. Treat the control cells in parallel to the irradiated cells but without radiation exposure. Treatment success can be addressed through measuring standard DNA damage markers such as γH2AX.

3.3 Genomic DNA Extraction and Processing

1. Transfer the cells on ice and extract genomic DNA (gDNA) following the Kit's instructions. Elute the genomic DNA in 50 μL TE buffer.
2. Proceed with 10 μg gDNA per sample.
3. Leave the gDNA on ice after extraction. Try to continue processing the samples directly so that storage and freeze-thaw cycles do not affect DNA damage levels.

3.4 Sample Processing for 8-oxoG

Skip this section if you are measuring AP-sites only.

1. Separate the samples that are to be processed for 8-oxoG and leave the samples for AP-sites on ice or at 4 °C.
2. Mask preexisting AP-sites in the 8-oxoG samples by adding 50 μL of 10 mM methoxyamine in TE buffer to a final concentration of 5 mM methoxyamine.
3. Incubate at 37 °C for 30 min.
4. Purify the gDNA using AMPure beads with 1.8× bead solution and 2× 70% ethanol washing (*see* **Note 11**).
5. Elute the AP-site-masked gDNA in 50 μL TE buffer.
6. Simultaneously digest the AP-site-masked DNA with OGG1 and tag with ARP (*see* **Note 12**), i.e., add to each sample 50 μL OA buffer and incubate at 37 °C for 2 h. This step may be performed in parallel to Subheading 3.5, **step 1**. Further sample processing is equivalent to Subheading 3.5, **step 2** onwards.

3.5 Sample Processing for AP-Sites

1. Add 50 μL of 10 mM ARP to each sample and incubate at 37 °C for 2 h, possibly in parallel with Subheading 3.4, **step 6**.
2. Purify the tagged gDNA from **step 1** and Subheading 3.4, **step 6** with beads as described in Subheading 3.4, **step 4**, using 2× 70% ethanol and eluting in 130 μL TE buffer (*see***Note 11**).
3. Fragment the tagged gDNA into 300 bp fragments in 130 μL TE buffer, following the instructions of the manufacturer of your fragmenter or a previously optimized fragmentation protocol.
4. Adjust the DNA concentration using TE buffer to be equal in each sample, separate 100 μL for the pulldown, and keep the rest (>30 μL) as input (*see* **Note 13**).

3.6 Pulldown of ARP-Tagged gDNA

The pulldown is performed in 200 µL and is therefore suitable for both 1.5 mL tubes and 96-well plate format.

1. Wash 10 µL of streptavidin beads per sample three times with 1 M NaCl in TE buffer following the manufacturer's instructions (1 mL for ~12 samples).
2. Resuspend the beads in 100 µL of 2 M NaCl in TE buffer per sample (i.e., 1200 µL of 2 M NaCl in TE for 12 samples). Prepare some extra to account for pipetting losses.
3. Add 100 µL of bead solution to the 100 µL tagged gDNA sample.
4. Rotate at room temperature for ~10 h.
5. Wash the beads three times with 1 M NaCl in TE buffer.
6. Release the DNA from the beads with 100 µL 95% formamide and 10 mM EDTA for 10 min at 65 °C (*see* **Note 14**).
7. Purify the DNA with AMPure beads as described in Subheading 3.4, **step 4** (*see* **Note 11**) with 2× 70% ethanol and elute the DNA in 50 µL of TE buffer.
8. Measure the yield of the DNA pulldown and calculate the recovery (AP-quant). This gives you a measure of relative DNA damage levels in your experiment. This information can also be used in the data analysis to normalize for sequencing depth.

3.7 AP-qPCR

Skip this step for performing AP-seq. To robustly perform AP-qPCR it is important to first optimize the primer conditions and the amount of input. This can be done on pure genomic DNA. The amount of pulldown used in the qPCR reaction can then be adjusted based on the percentage of recovery measured in Subheading 3.8, **step 8**.

1. In 25 µL qPCR format, use 0.3 µM primers of your choice and the appropriate amount of template DNA as determined in the pre-experiments specific to your primers. Perform qPCR using the recommended temperatures and instructions for your qPCR reagents.

3.8 Library Preparation and Sequencing

1. To improve data quality, an *in vitro* DNA repair step using the PreCR Kit before library preparation can be added following the manufacturer's instructions.
2. Library preparation can be performed with any short-read library preparation kit that is suitable for ChiP-Seq experiments. It is highly recommended to use paired-end sequencing and 125 bp fragments, as DNA damage tends to enrich in repetitive sequences and retrotransposons [5]. Longer paired reads can therefore substantially improve the robustness of the analysis.

3. Due to the broad distribution of AP-sites over the genome, a minimum of 60 million reads should be sequenced (125-bp paired end) both for the input and for the pulldown.

3.9 Core Data Processing

1. Assess data quality with Fastqc to assure sufficient quality of the sequencing run.
2. Align reads to the reference genome using Bowtie2 with standard settings.
3. Assess read duplication with Picard tools. Due to the expected high damage levels in repetitive DNA, sorting out duplicate reads is generally not recommended unless there is a particular reason to do so. Key results should however be confirmed, excluding duplicate reads and repetitive regions.
4. Normalize data to account for differences in sequencing depth. The results from AP-quant may be used to adjust sequencing depth per library dependent on the total recovery of the pulldown.
5. Downstream processing is dependent on the specific questions to be asked. It is recommended to assess batch effects through dimensionality reduction with a binning approach. Possible further routes include assessing GC and trinucleotide content, the relation to genes and retrotransposons, simple repeats and telomeres, as well as chromatin architecture.

4 Notes

1. X-rays act mainly through ionization of water molecules. Ionizing radiation will also cause double-strand breaks. While double-strand breaks are more deleterious to the cell, the number of 8-oxoG, other base modifications, and AP-sites can be estimated to exceed double-strand breaks by several orders of magnitude.
2. Depending on the experiment, it may improve data quality to add antioxidants to the cell culture medium to reduce background levels of oxidative DNA damage. Similarly, it may be advisable to keep the cells under low oxygen conditions (e.g., 5%).
3. Alternative methods to induce oxidative DNA damage would be the use of $KBrO_3$ or K_2CrO_4. I would advise against the use of H_2O_2, as it leads to high variation in DNA damage measurements in our hands.
4. While we use the Blood and Tissue Kit by Qiagen, other kits to extract genomic DNA may be suitable for the same task. It is however important to keep in mind that the DNA should not acquire additional base lesions and base adducts, so any harsh

conditions and heat will impact data quality. We decided not to include antioxidants during gDNA processing, as this may cause sequence-specific artifacts. It is however possible to include these during DNA extraction and subsequent steps.

5. Ninety-six-well plates that do not bind DNA and are usually used for DNA sequencing should be suitable. Compatibility with the 96-well magnet should be assessed ahead of the experiment and the scientist should make her- or himself familiar with handling magnetic beads in the 96-well plate-magnet combination. Similarly, any low-binding 1.5 mL tubes should be suitable and every kind of tube- and 96-well plate magnets. Combinations of the respective pairs should however be tested beforehand and the handling of magnetic beads should be practiced.
6. Methoxyamine is a dangerous chemical; please familiarize yourself with the safety recommendations of the manufacturer.
7. FpG (which also recognizes 8-oxoG) was hypothesized to potentially serve as a glycosylase instead of OGG1. However, its additional AP lyase activity also leads to a single-strand break, which in experiments with standardized DNA sequences lead to much poorer pulldown efficiencies as compared to OGG1.
8. The selection of the reference genome depends on the application. Keep in mind that you may want to integrate additional data. These may only be available with a particular reference genome, so it may be advisable to stick to the same, even if it is not the newest.
9. Downstream analysis is very dependent on the question asked, and other tools may be used than those recommended here. For further analyses, please *see* [5].
10. Some parts of this protocol have been changed since the method was first published [5]. These changes are based on optimization experiments on synthesized DNA, particularly the masking of AP-sites using methoxyamine which was not yet performed in the original study. Also, library preparation for sequencing was performed on beads, without prior release of the DNA with formamide. Such release is however necessary to quantify DNA pulldown recovery and to perform qPCR, and is therefore introduced into the protocol.
11. To wash the DNA solution with AMPure beads, the total working volume needed will be 280 μL. If using 96-well plates, please make sure that there is enough volume and otherwise use tubes with an appropriate magnet. Add 180 μL of beads (1.8×) to the solution. For washing, follow the instructions of the manufacturer's protocol. Use two washing cycles with 70% ethanol. Make sure that the beads do not dry during the process, as you may lose the high molecular weight DNA.

12. Initially, these steps were separate with a purification step in between. However, using synthetic standard DNA it was tested whether the pulldown efficiency is affected by performing the digest and tagging simultaneously, and it was concluded that this shortcut has no adverse effects but saves one purification step.
13. From this step onwards the DNA can be frozen and stored, as the damaged sites are tagged and additional DNA damage, while possibly affecting sample quality, will not be detected.
14. Make sure to remove the DNA solution from the beads swiftly, as cooling down may re-establish the streptavidin-biotin bond.

Acknowledgments

This work was supported by the St. Anna Children's Cancer Research Institute, the Okinawa Institute of Science and Technology Graduate University, University College London, and the Francis Crick Institute which receives its core funding from Cancer Research UK (FC001110, FC001048), the UK Medical Research Council (FC001110, FC001048), and the Wellcome Trust (FC001110, FC001048). It was partially performed in the laboratories of Simon Boulton at the Francis Crick Institute and Nicholas Luscombe at the Francis Crick Institute and the Okinawa Institute of Science and Technology. ARP was also supported by a postdoctoral fellowship from the Peter and Traudl Engelhorn Foundation and a Wellcome Trust Investigator Award to Nicholas Luscombe.

I am most grateful to the Luscombe and Boulton labs, in particular Lorea Blazquez, Mary Bonks, and Panagiotis Kotsantis, for helpful advice and discussions throughout the establishment of the method. For careful reading of the manuscript, I thank Suzana Pascoal, Boris Kovacic, Adrian Stütz, and Claudia Gebhard.

References

1. Atamna H, Cheung I, Ames BN (2000) A method for detecting abasic sites in living cells: age-dependent changes in base excision repair. Proc Natl Acad Sci U S A 97:686–691
2. Kubo K, Ide H, Wallace SS et al (1992) A novel, sensitive, and specific assay for abasic sites, the most commonly produced DNA lesion. Biochemistry 31:3703–3708
3. Nakamura J, Walker VE, Upton PB et al (1998) Highly sensitive apurinic/apyrimidinic site assay can detect spontaneous and chemically induced depurination under physiological conditions. Cancer Res 58:222–225
4. Nakano T, Terato H, Yoshioka Y et al (2002) Detection of NO-induced DNA lesions by the modified aldehyde reactive probe (ARP) assay. Nucleic Acids Res Suppl (2):239–240
5. Poetsch AR, Boulton SJ, Luscombe NM (2018) Genomic landscape of oxidative DNA damage and repair reveals regioselective protection from mutagenesis. Genome Biol 19:215
6. Rahimoff R, Kosmatchev O, Kirchner A et al (2017) 5-Formyl- and 5-carboxydeoxycytidines do not cause accumulation of harmful repair intermediates in stem cells. J Am Chem Soc 139:10359–10364

7. Roberts KP, Sobrino JA, Payton J et al (2006) Determination of apurinic/apyrimidinic lesions in DNA with high-performance liquid chromatography and tandem mass spectrometry. Chem Res Toxicol 19:300–309

8. Swenberg JA, Moeller BC, Lu K et al (2013) Formaldehyde carcinogenicity research: 30 years and counting for mode of action, epidemiology, and cancer risk assessment. Toxicol Pathol 41:181–189

Chapter 9

Locus-Specific Chromatin Proteome Revealed by Mass Spectrometry-Based CasID

Enes Ugur, Michael D. Bartoschek, and Heinrich Leonhardt

Abstract

Biotin proximity labeling has largely extended the toolbox of mass spectrometry-based interactomics. To date, BirA, engineered BirA variants, or other biotinylating enzymes have been widely applied to characterize protein interactions. By implementing chromatin purification-based methods the genome-wide interactome of proteins can be defined. However, acquiring a high-resolution interactome of a single genomic locus preferably by multiplexed measurements of several distinct genomic loci in parallel remains challenging. We recently developed CasID, a novel approach where the catalytically inactive Cas9 (dCas9) is coupled to the promiscuous biotin ligase BirA (BirA∗). With CasID, first the local proteome at repetitive telomeric, major satellite, and minor satellite regions was determined. With more efficient biotin ligases and sensitive mass spectrometry, others have successfully identified the chromatin composition at even smaller genomic, non-repetitive regions of a few hundred base pairs in length. Here, we summarize the most recent developments towards interactomics at a single genomic locus and provide a step-by-step protocol based on the CasID approach.

Key words BioID, CasID, Mass spectrometry, Chromatin composition, Locus-specific interactomics

1 Introduction

A variety of mass spectrometry (MS)-based methods focus on protein interactomes to investigate genome organization and chromatin proteome composition. These approaches are mostly based on chromatin immunoprecipitation (ChIP) or affinity purification (AP) coupled to MS. Therefore, identification of interactors is largely dependent on effective antibody-bead-mediated purification of intact protein complexes with or without prior formaldehyde crosslinking. In addition, progress in high-sensitivity MS enables the identification of even low abundant chromatin-associated proteins such as transcription factors [1].

Whereas ChIP-MS and AP-MS experiments are well established and often used to characterize a single protein's interactome in its genome-wide context, the global chromatin composition is

Ronald Hancock (ed.), *The Nucleus*, Methods in Molecular Biology, vol. 2175, https://doi.org/10.1007/978-1-0716-0763-3_9,

not directly revealed. Recently, three methods to study global chromatin-associated proteins were published: (i) chromatin enrichment for proteomics (ChEP, [2]) to measure genome-wide chromatin proteomes allowing the comparison of different biological conditions and their effect on chromatin composition; (ii) density-based enrichment for mass spectrometry analysis of chromatin (DEMAC, [3]) to determine cell cycle-dependent chromatin proteomes; and (iii) chromatin enrichment by salt separation followed by data-independent acquisition (ChESS-DIA, [4]) to discriminate between nucleoplasmic proteomes as well as heterochromatic and euchromatic proteomes.

Although these methods allow a deep coverage of global chromatin composition, the local proteome is not resolved. However, since molecular changes at defined genomic regions are critical regulatory factors, in-depth analysis of the locus-specific proteomic microenvironment is essential to precisely unravel molecular mechanisms. Representing one of the first strategies to specifically purify a genomic region, proteomics of isolated chromatin segments (PiCh, [5]) relies on DNA oligomers that hybridize with target telomeric regions of crosslinked cells. Furthermore, engineered DNA-binding molecule-mediated chromatin immunoprecipitation (enChIP, [6]) applies the catalytically inactive Cas9 (dCas9) fused to a purification tag for subsequent targeted ChIP-MS on dCas9-bound chromatin that is defined by the co-expressed guide RNA (gRNA). However, to what extent nonspecific interactors are also captured as a consequence of crosslinking is not clear.

To capture transient interactions in living cells, we developed CasID [7], a method that combines dCas9 with the promiscuous biotin ligase BirA (BirA∗) to label proteins in the vicinity of specific genomic loci rendering crosslinking unnecessary (*see* Fig. 1). Since BirA∗ has an estimated labeling radius of 10 nm, the chromatin area that is subjected to biotinylation can be inferred [8]. The development of CasID greatly benefited from BioID, a strategy that applies BirA∗ fused to a protein of interest to directly capture its protein-protein interactions [9]. To perform CasID, first stable BirA∗-dCas9/gRNA expressing cells are generated. These cell lines are then supplemented with 50 μM biotin for 24 h to ensure proper labeling. Since BirA∗-dCas9 binds to genomic loci specified by the gRNA, predominantly proteins that colocalize to the targeted genomic region are biotinylated by BirA∗. Subsequently, nuclei are isolated to reduce levels of endogenously biotinylated proteins that are mainly found in cytosolic compartments [10]. Finally, biotinylated proteins are enriched by streptavidin pulldown and analyzed by LC-MS/MS.

CasID, as any other method based on BirA∗, requires thorough controls due to free-floating BirA∗-dCas9 resulting in nonspecific background biotinylation. In particular, we recommend two controls. First, a stable cell line expressing BirA∗-dCas9 with

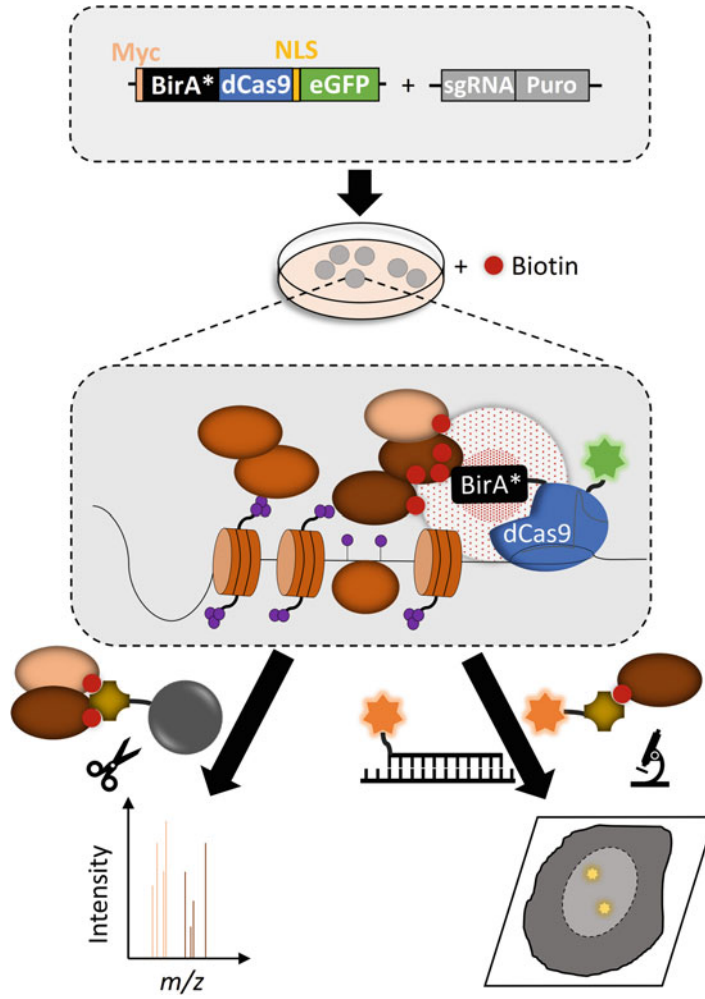

Fig. 1 Summary of CasID workflow. The BirA∗-dCas9-eGFP fusion construct is cotransfected with a vector harboring a single guide RNA (sgRNA). Biotinylation of interactors is induced by addition of biotin. After 24 h of labeling, nuclei are isolated and nuclear lysates are subjected to streptavidin-based affinity purification to enrich for biotinylated proteins. Purified protein samples are analyzed by mass spectrometry to determine local proteomes. In addition, transfected cells can be validated for proper nuclear localization of BirA∗-dCas9-eGFP by standard confocal microscopy. Correct localization to genomic targets can be validated by FISH and biotinylation can be assessed with fluorescently labeled streptavidin probes

a nuclear localization signal (NLS) but lacking a gRNA to generally capture nuclear background biotinylation as well as off-target genomic loci. Second, a stable cell line expressing BirA∗-dCas9 targeted to a distinctly different genomic locus via its gRNA to control for chromatin-associated proteins that would otherwise be selected as false positives due to their general high abundance. Additionally,

depending on the number and genomic regions to be probed, generated stable cell lines should be thoroughly characterized before commencing pulldown experiments. Since high BirA∗-dCas9 expression can lead to high background biotinylation whereas too low expression can result in poor enrichment, expression levels of BirA∗-dCas9/gRNA have to be carefully balanced. Furthermore, correct nuclear localization of BirA∗-dCas9 to target genomic loci should be confirmed. Fusion of BirA∗-dCas9 to eGFP allows validation of nuclear localization by standard confocal microscopy. In addition, biotinylation efficiency can be assessed by fluorescently labeled streptavidin probes and locus-specific binding can be further verified by fluorescence in situ hybridization (FISH) at target loci followed by high-resolution microscopy (*see* Fig. 1).

Besides thorough controls, choosing the appropriate biotin ligase is a key factor in proximity labeling-based proteomics and depends on the experimental setup and target regions. With the recent development of the engineered BirA variants miniTurbo and TurboID as well as the soybean ascorbate peroxidase-derived APEX2, more efficient biotin ligases compared to BirA∗ became available. These ligases differ in labeling reaction dynamics, labeling efficiencies, and organelle-dependent activities. APEX2, for instance, labels peptides in an estimated 20 nm radius. In contrast to BirA∗ and its variants, APEX2-mediated biotinylation requires biotin-phenol and H_2O_2 and not biotin that is also endogenously present. The catalytic activity of APEX2 is the most efficient among the currently known biotinylating enzymes and requires 1 min of reaction time. Moreover, the biotinylation reaction can be easily quenched to acquire interactomes over defined timeframes [11]. The advantages and disadvantages of each engineered biotin ligase have been reported and summarized in detail in the original publications and several reviews [12–15].

Applying APEX2 instead of BirA∗, the CasID approach has been further enhanced to define high-resolution telomere- and centromeric α-satellite-associated proteomes (C-BERST, [16]) as well as chromatin compositions at non-repetitive genomic regions (GLoPro and CAPLOCUS [17, 18]). In particular, chromatin composition of a 1.5 kb region on the human TERT promoter [17] or of a single-copy 233 bp region by recruiting multiple APEX2 molecules to one dCas9 [18] was identified.

Despite these recent improvements, the accuracy and sensitivity of capturing locus-specific chromatin composition by proximity labeling still has to be validated. Furthermore, whether these methods could be easily applied to any genomic locus of interest without labor-intensive optimization for each individual region remains unclear. In addition, the required input material and the amount of streptavidin beads and trypsin per replicate are still far above standard biotin-labeling-based interactome studies rendering the approach very cost-intensive, especially for multiple screens.

Therefore, improving the signal-to-noise ratio of measurements by comparing different multiple targeting strategies will be critical to decrease overall costs and enable multiplexed measurements of distinct single loci with high resolution. In summary, we envision single-locus interactomics by proximity labeling as a promising tool to monitor dynamic changes in the chromatin microenvironment and unravel molecular mechanisms in diverse biological contexts.

2 Materials

The experimental outcome is largely determined by gRNA specificity, biotin pulldown efficiency, and sensitivity of the mass spectrometer detection. All plasmids mentioned in this chapter or in the original publication [7] can be acquired from the Corresponding Author upon request.

2.1 Choice of Biotin Ligase and Cloning Steps

Based on our original CasID approach, we use the BirA∗ biotin ligase in the following protocols. However, for increased biotinylation efficiency we recommend replacing BirA∗ with TurboID, miniTurbo, or APEX2 that have been published recently [14, 15]. Please note that labeling reactions of these biotin ligases differ from those of BirA∗ and have to be optimized separately.

1. BirA∗-dCas9-eGFP containing plasmid.
2. gRNA containing plasmid.
3. Gibson assembly master mix (New England Biolabs).

2.2 Generation of Stable BirA∗-dCas9-eGFP/gRNA Cell Lines

1. Dulbecco's modified Eagle's medium (DMEM).
2. 20% fetal bovine serum.
3. Penicillin/Streptomycin.
4. L-glutamine.
5. Cultured cells of choice.
6. Biotin.
7. Lipofectamine® 3000 (Thermo Fisher Scientific).
8. 10 mg/mL blasticidin S.
9. 2 mg/mL puromycin.
10. Phosphate-buffered saline (PBS).

2.3 Immunofluorescence Staining and Image Acquisition

1. Coverslips (Marienfeld Superior, Lauda-Königshofen, Germany).
2. 16% formaldehyde (Thermo Fisher Scientific).
3. Triton X-100.
4. Tween 20.
5. Bovine serum albumin (BSA).

6. Phosphate-buffered saline (PBS, Sigma).
7. Blocking buffer (5% BSA and 0.02% Tween 20 in PBS).
8. Streptavidin, Alexa Fluor 594 conjugate (Invitrogen).
9. 4′,6-diamidino-2-phenylindole dihydrochloride (DAPI, Invitrogen).
10. Antifade medium (Vectashield, Vector Laboratories).

2.4 Biotin Pulldown and Sample Preparation for Mass Spectrometry

1. M-280 Streptavidin Dynabeads (Invitrogen).
2. Cell lysis buffer (10 mM HEPES/KOH pH 7.9, 10 mM KCl, 1.5 mM $MgCl_2$, 0.15% NP-40; freshly add 1× protease inhibitor cocktail (PIC, Roche)).
3. BioID lysis buffer (0.2% SDS, 50 mM Tris/HCl pH 7.4, 500 mM NaCl; freshly add 1 mM DTT, 1× PIC).
4. 50 mM Tris/HCl pH 7.4.
5. Wash buffer 1 (2% SDS).
6. Wash buffer 2 (0.1% deoxycholic acid, 1% Triton X-100, 1 mM EDTA, 500 mM NaCl, 50 mM HEPES/KOH pH 7.5).
7. Wash buffer 3 (0.5% deoxycholic acid, 0.5% NP-40, 1 mM EDTA, 500 mM NaCl, 10 mM Tris/HCl pH 7.4).
8. Digestion buffer (2 M urea in Tris/HCl pH 7.5).
9. Dithiothreitol (DTT, Sigma).
10. Chloroacetamide (CAA, Sigma).
11. Trypsin (MS grade Pierce Trypsin Protease) (Thermo Fisher Scientific).

2.5 LC-MS/MS Measurements

1. Buffer A (2% v/v acetonitrile, 0.1% v/v formic acid).
2. Buffer B (98% v/v acetonitrile, 0.1% v/v formic acid).

2.6 General Equipment (Recommendations)

1. nano-HPLC system: EASY-nLC 1200 with C18-based elution column (Thermo Scientific).
2. Mass spectrometer: Q Exactive HF-X Quadrupole-Orbitrap (Thermo Scientific).
3. Confocal microscope: Leica SP8 or similar.
4. Sonicator: Diagenode Bioruptor Plus.
5. Magnetic rack for 1.5 mL tubes for biotin pulldown with magnetic streptavidin beads.

3 Methods

Briefly, generate a suitable cell line that expresses the BirA∗-dCas9-eGFP construct and the gRNA plasmid targeting the genomic

region of interest. We recommend to establish a stable cell line that expresses the BirA∗-dCas9-eGFP construct (*see* **Note 1**). Check successful transfection and localization of the fusion construct by fluorescence microscopy. Initiate the biotinylation reaction by adding biotin-phenol if APEX is used as a biotin ligase or boost the biotinylation reaction by supplementing the media with biotin in case BirA∗ or BirA∗-derived biotin ligases (BioID2, TurboID, miniTurbo) are used. Perform biotin pulldown and digest purified proteins to subject the samples to MS. Analyze data with established MS software and perform statistical analysis to identify significantly enriched chromatin-associated proteins in the region of interest.

3.1 Choice of Biotin Ligase and Cloning Steps

Selection of an appropriate biotin ligase is of crucial importance. The underlying study was performed with the promiscuous biotin ligase BirA∗ (also used in BioID). All plasmid and primer sequences are listed in Supplementary Tables S2 and S3 of the original publication [7] and can be obtained upon request.

1. To generate a fusion construct of dCas9-eGFP and a respective biotin ligase, amplify the biotin ligase from a plasmid with approximately 20 bp overhangs complementary to the pCAG-dCas9-eGFP plasmid [19]. Linearize the pCAG-dCas9-eGFP vector with compatible overhangs and ligate the construct by Gibson Assembly to generate pCAG-BirA∗--dCas9-eGFP.
2. Next, assemble the gRNA plasmid. One possibility is to amplify a PGK-Puro cassette and ligate it with pEX-A-sgRNA [19]. The gRNA sequence(s) can be introduced into the vector by standard circular amplification.

3.2 Generation of Stable BirA∗-dCas9-eGFP/gRNA Cell Lines

Here, we describe the generation of stable cell lines by random integration of the pCAG-BirA∗-dCas9-eGFP/gRNA vectors solely by positive selection for 2 weeks and additional enrichment of positive clones by fluorescent activated cell sorting (FACS). However, the efficiency of this method varies highly between cell lines and can lead to a poor outcome, especially for delicate cell lines like mouse embryonic stem cells. Therefore, we recommend the PiggyBac or Sleeping Beauty systems for transposon-mediated incorporation of the vectors at genomic recognition motifs of the respective transposase [20, 21].

1. Grow C2C12 cells (or other cell lines of choice) under standard conditions (37 °C, 5% CO_2). For C2C12 cells, supplement Dulbecco's modified Eagle's medium with 20% fetal bovine serum, 100 U/mL penicillin, 100 mg/mL streptomycin, and 2 mM L-glutamine.
2. For transient transfections, seed 10^6 cells in a 6-well plate 1 day before transfection. Perform transfection with pCAG-

BirA∗-dCas9-eGFP/gRNA plasmids according to standard protocols (*see* **Note 2**).

3. Transfect C2C12 cells with pCAG-BirA∗-dCas9-eGFP. After 1 day, select for transfected cells by supplementing the cell culture medium with 10 mg/mL blasticidin S (concentration may vary for other cell lines). Grow cells for 2 weeks under constant selection pressure and enrich afterwards for GFP-positive cells by FACS. Isolate a single clone expressing pCAG-BirA∗-dCas9-eGFP and after cell outgrowth transfect with the gRNA plasmid. Select for gRNA-positive cells with 2 μg/mL puromycin (concentration may vary for other cell lines) for 2 weeks and analyze individual clones for correct and homogeneous expression as well as nuclear localization of BirA∗-dCas9-eGFP by confocal microscopy.
4. One day before harvesting, supplement the medium with 50 μM biotin to initiate the biotinylation reaction.

3.3 Immunofluorescence Staining and Image Acquisition

Transfected cells can be validated for proper nuclear localization of BirA∗-dCas9-eGFP by standard confocal microscopy. In addition, localization to correct genomic targets can be analyzed by FISH as described previously [19]. Furthermore, biotinylation efficiency can be assessed by fluorescently labeled streptavidin probes. Here, we focus on the validation of nuclear localization of BirA∗-dCas9-eGFP.

1. Grow BirA∗-dCas9-eGFP/gRNA-positive cells on coverslips. One day before fixation, add 50 μM biotin to cultured cells.
2. Wash cells once with PBS and crosslink with 3.7% formaldehyde for precisely 10 min (crosslinking time may vary for other cell lines). Then wash cells two more times with PBS.
3. Add Triton X-100 at a final concentration of 0.2% (diluted in PBS) and incubate for 10 min to permeabilize cells. Then wash cells twice with PBS.
4. Transfer coverslips to blocking buffer. After 1 h wash cells three times with PBS and add fluorescently labeled streptavidin probe in a 1:500 dilution in blocking buffer. Incubate for 1 h at room temperature (RT) in a dark humidified chamber.
5. Wash cells once with PBS.
6. Stain nuclei by, e.g., DAPI with a final concentration of 300 nM for 1–5 min. Wash two more times with PBS. Shortly dip coverslips into H_2O to dilute out PBS.
7. Mount coverslips in antifade medium and seal with nail polish.
8. Image cells by standard confocal microscopy.

3.4 Biotin Pulldown and Sample Preparation for Mass Spectrometry

For proper statistical analysis we recommend performing the biotin pulldown in at least triplicates. Each replicate should originate from independently cultured cells.

1. Seed 4 × 10^7BirA∗-dCas9-eGFP/gRNA-positive cells and culture for 24 h with 50 μM biotin (*see* **Note 3**). Seed also the first control cell line with a gRNA targeting a distinctly different genomic locus and the second control cell line lacking a gRNA to control for nuclear background biotinylation.
2. Harvest cells, wash pellets twice with PBS, and flash freeze in liquid nitrogen. Store at −80 °C or directly proceed to **step 3**.
3. Lyse cell pellet in cell lysis buffer to isolate nuclei (*see* **Note 4**). Use a douncer (size B) with 20 strokes and pellet nuclei by centrifugation (3200 × *g*, 15 min).
4. Carefully wash nuclear pellet twice with cell lysis buffer without NP-40.
5. Resuspend nuclei in BioID lysis buffer and shear chromatin by sonication for 15 min (30 s "on"/30 s "off" at highest intensity). Alternatively, chromatin can be digested with MNase followed by short sonication (*see* **Note 5**).
6. Dilute lysates twofold with 50 mM Tris/HCl pH 7.4 and pellet unsoluble fraction by centrifugation (16,000 × *g*, 10 min). Save the supernatant and adjust protein concentrations across samples by BCA assay to approximately 2 mg/mL. Save 1% of total protein input (here 20 μg) for Western blot analysis. Incubate 1 mL of each sample with 50 μL M-280 Streptavidin Dynabeads at 4 °C overnight on a rotator (*see* **Note 6**).
7. Prior to the first wash, save an aliquot of the unbound fraction for Western blot analysis. Wash magnetic beads successively once with 1 mL of wash buffers 1–3. Then, wash twice with 1 mL of 50 mM Tris/HCl pH 7.4. During the last wash, transfer samples to fresh 1.5 mL tubes and save 10% of bead slurry for Western blot.
8. Resuspend beads in 200 μL digestion buffer containing 10 mM DTT. Incubate samples for 20 min at RT with rigorous shaking (1100 rpm, Eppendorf ThermoMixer). Add 40 mM CAA and incubate for another 20 min at RT with rigorous shaking. Finally, add 0.35 mg trypsin per sample and digest overnight at RT with rigorous shaking.
9. Desalt peptides using C18-based StageTips and according to standard protocols [22].
10. For Western blot analysis of biotinylation efficiency and streptavidin pulldown, boil input, flowthrough, and elution fractions in 1× SDS loading buffer supplemented with 20 mM DTT and 2 mM biotin for 5 min at 95 °C. Perform standard SDS-PAGE and Western blot using streptavidin-HRP (*see* **Note 7**).

3.5 LC-MS/MS Analysis

1. Perform LC-MS/MS analysis according to well-established protocols for bottom-up shotgun proteomics of complex eukaryotic samples as described before (*see* **Note 8**). Briefly, separate peptides by liquid chromatography before MS. For this, an Easy-nLC 1200 can be used with a 50 cm C18 column. By this, reconstituted peptides are eluted successively in an acetonitrile gradient for 120 min at a flow rate of around 300 nL/min.
2. Inject samples through a nanoelectrospray source into the mass spectrometer. Keep the oven temperature constantly at 60 °C. Real-time monitoring of the operational parameters is crucial for quality control. Here, SprayQc [23] can be used (*see* **Note 9**).
3. Schedule a washing step after measuring the triplicates of each condition. Operate in a top 10–15 shotgun proteomics-based method in data-dependent MS/MS mode with an MS1 scan resolution of 60,000. Adjust the target value for the full scan MS spectra to 3×10^6. Set the m/z range to 400–1650 m/z and the maximum injection time to 20 ms.

3.6 Computational Analysis of MS Data

1. Download the latest version of the MaxQuant software package available at https://www.maxquant.org/ [24].
2. Start the MaxQuant.exe and configure the required protein sequence databases. In addition, configure a FASTA file including the BirA∗-dCas9-eGFP fusion construct protein sequence (*see* **Note 10**). For identification of contaminants, using the database provided by the Andromeda search engine is recommended [25].
3. Load the raw files into MaxQuant and adjust experimental parameters depending on sample fractions and experiment names. Set Trypsin/P digestion to a maximum of three missed cleavages. For an initial search, set carbamidomethylation of cysteine residues as a fixed modification and biotinylation, oxidation of methionine, and protein N-terminal acetylation as variable modifications. Enable label-free quantification and match between runs [26]. Set the false discovery rate to 1% for both peptides (minimum length of seven amino acids) and proteins.
4. For downstream analysis of the MaxQuant output, the software Perseus [27] (version 1.6.0.9) can be used. Filter data for common contaminants, group replicates, and perform Student's *t*-test between control samples without gRNA and samples with gRNA with a permutation-based FDR of 0.05 and an additional constant s0 of 1. Visualize results in a scatter plot.

4 Notes

1. Depending on the cell line used, transient transfections can be very inefficient or efficiencies might vary for each transfection. To obtain consistent and homogeneously high expression levels, we recommend generation of stable cell lines for each gRNA.
2. We recommend an initial transient transfection to validate expression and localization of BirA∗-dCas9-eGFP by microscopy. In addition, BirA∗-dCas9-eGFP fusion protein size and expression levels should be analyzed by Western blot. After verifying the construct, stable cell lines can be generated.
3. This step can be omitted depending on the used biotin ligase. In the case of APEX2 that uses biotin-phenol as a substrate instead of biotin, we recommend to deplete the cell culture medium from biotin for 72 h to reduce background biotinylation [8].
4. In our original protocol we used 0.15% NP-40. Strouboulis et al. [10] have systematically analyzed the effect of nuclear isolation by NP-40 on the biotin background after streptavidin pulldown and proteomic analysis. According to their findings, 0.5% NP-40 is recommended to obtain clean nuclear extracts with as little cytoplasmic contamination as possible. As the majority of endogenously biotinylated proteins are cytoplasmic, this nuclear isolation step might help to further reduce the background. However, nuclear isolation efficiency varies between cell lines and therefore should be optimized for each cell line.
5. For MNase digestion, supplement cell lysis buffer without NP-40 with 5 mM $CaCl_2$. Incubate nuclear extracts at 37 °C under gentle shaking with an appropriate amount of MNase. Quench the reaction with 50 mM EGTA to predominantly obtain mono- and dinucleosomes. MNase amount and digestion time have to be empirically tested and depend largely on cell number. The advantage of an MNase digestion over sonication is that especially large complexes might be preserved since single proteins can even degrade upon sonication. However, short sonication is still required to gain more solubilized protein amounts (3 min at 30 s "on"/30 s "off" and highest intensity).
6. Recent publications that apply APEX2 in combination with dCas9 also use higher bead volumes per replicate (e.g., 400 μL of Dynabeads MyOne streptavidin T1 [16]). We recommend optimization of protein input and bead volumes depending on BirA∗-dCas9-eGFP/gRNA target sequence abundance for each experiment.

7. For successful Western blot analysis, biotin contamination should be avoided. For instance, the blocking solution should not be based on milk powder as milk contains biotin.
8. To successfully identify interactomes by CasID, mass spectrometers have to be regularly maintained and monitored by experts regarding the quality of measurements.
9. The raw MS data can be analyzed using a variety of available software. Here, we describe the analysis of raw files using the MaxQuant software package as it is freely available, well established in the MS community, and user-friendly.
10. The sequence database of the target organism can be downloaded as a FASTA file from UniProt. An additional FASTA file including computationally annotated proteins can also be obtained from UniProt and included as a reference proteome to extend the search space. For the FASTA file of BirA∗--dCas9-eGFP include a unique protein name in the FASTA header. To add a new reference proteome to MaxQuant, open "Configuration", click on "Sequence databases", and then "Add". Add the FASTA file and fill in the taxonomy information. Note that the identifier parse rule is critical to read out the FASTA header. For standard UniProt proteomes usually ">.∗\|(.∗)\|" is used. Test the rules, then click on modify table and save changes. Now restart MaxQuant.

Acknowledgments

EU and MDB are fellows of the International Max Planck Research School for Molecular Life Sciences (IMPRS-LS). EU is supported by the research training group 1721 (RTG 1721), a graduate school of the Deutsche Forschungsgemeinschaft (DFG). The work on chromatin composition is supported by the DFG (SFB 1064/A17 to HL).

References

1. Wierer M, Mann M (2016) Proteomics to study DNA-bound and chromatin-associated gene regulatory complexes. Hum Mol Genet 25:R106–R114. https://doi.org/10.1093/hmg/ddw208
2. Kustatscher G, KLH W, Furlan C, Rappsilber J (2014) Chromatin enrichment for proteomics. Nat Protoc 9:2090–2099. https://doi.org/10.1038/nprot.2014.142
3. Ginno PA, Burger L, Seebacher J et al (2018) Cell cycle-resolved chromatin proteomics reveals the extent of mitotic preservation of the genomic regulatory landscape. Nat Commun 9:4048. https://doi.org/10.1038/s41467-018-06007-5
4. Federation AJ, Nandakumar V, Wang H et al (2018) Quantification of nuclear protein dynamics reveals chromatin remodeling during acute protein degradation.bioRxiv 345686. https://doi.org/10.1101/345686.
5. Déjardin J, Kingston RE (2009) Purification of proteins associated with specific genomic Loci. Cell 136:175–186. https://doi.org/10.1016/j.cell.2008.11.045
6. Fujita T, Asano Y, Ohtsuka J et al (2013) Identification of telomere-associated molecules by

engineered DNA-binding molecule-mediated chromatin immunoprecipitation (enChIP). Sci Rep 3:3171. https://doi.org/10.1038/srep03171

7. Schmidtmann E, Anton T, Rombaut P et al (2016) Determination of local chromatin composition by CasID. Nucleus 7:476–484. https://doi.org/10.1080/19491034.2016.1239000
8. Kim DI, Jensen SC, Noble KA et al (2016) An improved smaller biotin ligase for BioID proximity labeling. Mol Biol Cell 27:1188–1196. https://doi.org/10.1091/mbc.E15-12-0844
9. Roux KJ, Kim DI, Raida M, Burke B (2012) A promiscuous biotin ligase fusion protein identifies proximal and interacting proteins in mammalian cells. J Cell Biol 196:801–810. https://doi.org/10.1083/jcb.201112098
10. Papageorgiou DN, Demmers J, Strouboulis J (2013) NP-40 reduces contamination by endogenous biotinylated carboxylases during purification of biotin tagged nuclear proteins. Protein Expr Purif 89:80–83. https://doi.org/10.1016/j.pep.2013.02.015
11. Lobingier BT, Hüttenhain R, Eichel K et al (2017) An approach to spatiotemporally resolve protein interaction networks in living cells. Cell 169:350–360.e12. https://doi.org/10.1016/j.cell.2017.03.022
12. Trinkle-Mulcahy L (2019) Recent advances in proximity-based labeling methods for interactome mapping. F1000Res 8. https://doi.org/10.12688/f1000research.16903.1
13. Lambert J-P, Tucholska M, Go C et al (2015) Proximity biotinylation and affinity purification are complementary approaches for the interactome mapping of chromatin-associated protein complexes. J Proteomics 118:81–94. https://doi.org/10.1016/j.jprot.2014.09.011
14. Lam SS, Martell JD, Kamer KJ et al (2015) Directed evolution of APEX2 for electron microscopy and proximity labeling. Nat Methods 12:51–54. https://doi.org/10.1038/nmeth.3179
15. Branon TC, Bosch JA, Sanchez AD et al (2018) Efficient proximity labeling in living cells and organisms with TurboID. Nat Biotechnol 36:880–887. https://doi.org/10.1038/nbt.4201
16. Gao XD, Tu L-C, Mir A et al (2018) C-BERST: defining subnuclear proteomic landscapes at genomic elements with dCas9-APEX2. Nat Methods 15:433–436. https://doi.org/10.1038/s41592-018-0006-2
17. Myers SA, Wright J, Peckner R et al (2018) Discovery of proteins associated with a predefined genomic locus via dCas9-APEX-mediated proximity labeling. Nat Methods 15:437–439. https://doi.org/10.1038/s41592-018-0007-1
18. Qiu W, Xu Z, Zhang M et al (2019) Determination of local chromatin interactions using a combined CRISPR and peroxidase APEX2 system. Nucleic Acids Res 47:e52. https://doi.org/10.1093/nar/gkz134
19. Anton T, Bultmann S, Leonhardt H, Markaki Y (2014) Visualization of specific DNA sequences in living mouse embryonic stem cells with a programmable fluorescent CRISPR/Cas system. Nucleus 5:163–172. https://doi.org/10.4161/nucl.28488
20. Li X, Burnight ER, Cooney AL et al (2013) piggyBac transposase tools for genome engineering. Proc Natl Acad Sci U S A 110:E2279–E2287. https://doi.org/10.1073/pnas.1305987110
21. Kowarz E, Löscher D, Marschalek R (2015) Optimized Sleeping Beauty transposons rapidly generate stable transgenic cell lines. Biotechnol J 10:647–653. https://doi.org/10.1002/biot.201400821
22. Rappsilber J, Mann M, Ishihama Y (2007) Protocol for micro-purification, enrichment, pre-fractionation and storage of peptides for proteomics using StageTips. Nat Protoc 2:1896–1906. https://doi.org/10.1038/nprot.2007.261
23. Scheltema RA, Mann M (2012) SprayQc: a real-time LC–MS/MS quality monitoring system to maximize uptime using off the shelf components. J Proteome Res 11:3458–3466. https://doi.org/10.1021/pr201219e
24. Cox J, Mann M (2008) MaxQuant enables high peptide identification rates, individualized ppb-range mass accuracies and proteome-wide protein quantification. Nat Biotechnol 26:1367
25. Cox J, Neuhauser N, Michalski A et al (2011) Andromeda: a peptide search engine integrated into the MaxQuant environment. J Proteome Res 10:1794–1805. https://doi.org/10.1021/pr101065j
26. Cox J, Hein MY, Luber CA et al (2014) Accurate proteome-wide label-free quantification by delayed normalization and maximal peptide ratio extraction, termed MaxLFQ. Mol Cell Proteomics 13:2513–2526. https://doi.org/10.1074/mcp.M113.031591
27. Tyanova S, Temu T, Sinitcyn P et al (2016) The Perseus computational platform for comprehensive analysis of (prote)omics data. Nat Methods 13:731

Chapter 10

Methyl Adenine Identification (MadID): High-Resolution Detection of Protein-DNA Interactions

David Umlauf, Michal Sobecki, and Laure Crabbe

Abstract

Mapping the binding sites of DNA- or chromatin-interacting proteins is essential to understand many essential biological processes. Methyl Adenine Identification (MadID) is a proximity methylation-based assay that allows the visualization, quantification, and identification of binding sites from DNA-interacting proteins in eukaryotic cells. Chromatin-binding proteins of interest are fused to the newly described bacterial methyltransferase M.EcoGII. This enzyme catalyzes the methylation of adenine residues with no sequence specificity. Consequently, adenines within and in the vicinity of the protein binding sites will be decorated with a methyl group (m6A), a modification that can be further detected using different methods. M.EcoGII-dependent DNA methylation can be monitored *in situ* using immunostaining, at the genome-wide level using a combination of m6A-specific immunoprecipitation and whole-genome sequencing, or locally at DNA regions of interest purified by chromatin immunoprecipitation or probe-based capture techniques. MadID is conceptually similar to DNA adenine methyltransferase identification (DamID) that relies on the methylation of GATC motifs. However, MadID provides a higher resolution, deeper coverage, and opens ways for identification of binding sites in genomic regions that were largely inaccessible such as telomeres, centromeres, and repeated elements.

Key words MadID, DamID, m6A, Proximity labeling, M.EcoGII, Telomeres, Centromeres, LADs, Dotblot, High-throughput sequencing

1 Introduction

During interphase, chromatin folding in the three-dimensional space of eukaryotic nuclei and the composition of the chromatin fiber itself are keys to understand genome regulation. Chromatin immunoprecipitation (ChIP) has long been the method of choice to characterize interactions between proteins and DNA, allowing access to chromatin composition [1]. However, ChIP relies entirely on the availability of ChIP-grade antibodies and is incompatible with the detection of transient interactions. Here, we present MadID, a proximity-labeling technique that circumvents these limitations and allows the mapping of protein-DNA interactions with various experimental setups [2].

Ronald Hancock (ed.), *The Nucleus*, Methods in Molecular Biology, vol. 2175, https://doi.org/10.1007/978-1-0716-0763-3_10,

MadID is an optimized method based on DNA adenine methyltransferase identification (DamID), which has emerged as a comprehensive technique to map genome-wide occupancy of proteins of interest [3]. DamID uses the ability of the bacterial Dam methyltransferase to methylate adenine residues within GATC motifs. When fused to a chromatin binding protein in an inducible system, this enzyme targets the methylation of GATC motifs residing within and in the vicinity of the protein binding sites. DamID has been instrumental in unveiling nuclear organization of specific parts of the genome such as Lamin-Associated Domains (LADs) [4–6] and has also been successfully applied to study genome organization on a global scale (see for example [7]). Overall, DamID is a powerful approach that allows the study of chromatin composition and its dynamics. However, it is inherently limited by its dependence on the distribution of the GATC tetrameric recognition site, which represents only 0.9% of the human genome [2]. In addition, several genomic regions are deprived of or poor in the GATC motifs required for Dam-dependent methylation, such as AT-rich regions, telomeres, or centromeres, which are therefore blind to DamID.

To overcome these limitations, we took advantage of the newly described M.EcoGII methyltransferase from *E. coli* to implement MadID. Unlike site-specific methyltransferases such as Dam, M.EcoGII methylates adenine residues in any DNA sequence context with a high efficiency [8]. Consequently, GATC-null or GATC-poor regions are now fully accessible to MadID, which constitutes an unbiased strategy to map protein-DNA interactions with a deeper coverage and higher resolution [2]. Fused to a protein of interest, M.EcoGII drives adenine methylation (m6A) at the protein binding site, methylation that can be further analyzed by a variety of methods. M.EcoGII was successfully targeted in human cells to telomeres, centromeres, and the nuclear envelope using fusion proteins with TRF1, Centromeric Protein C, and LaminB1, respectively [2] (plasmids available from Addgene, *see* Subheading 2). However, MadID can be implemented in any model organism in which transgenesis is feasible and for any protein of interest, provided that the fusion with M.EcoGII remains functional.

In this chapter, we present a detailed protocol for MadID from the generation of cells expressing the M.EcoGII-fusion proteins using retroviral transduction to the different readouts available to assess, quantify, or map DNA methylation: (1) m6A detection *in situ* by indirect immunostaining using a m6A antibody, including a protocol to combine this detection with DNA-FISH; (2) genome-wide m6A detection after m6A-immunoprecipitation (m6A-IP) followed by high-throughput sequencing, and (3) detection of m6A on a dotblot (m6A-dotblot) with total genomic DNA or after purification of a particular DNA region of interest. We provide a method for telomere purification using a probe-based capture technique as an example.

2 Materials

2.1 Generation of Cells Expressing M. EcoGII Constructs

1. Plasmids described in reference [2], available from Addgene (https://www.addgene.org):
   pRetroX-PTuner-DD-linker-M.EcoGII (#122082)
   pRetroX-PTuner-DD-linker-M.EcoGII-v5-Lamin B1 (#122083)
   pRetroX-PTuner-DD-M.EcoGII-v5-TRF1 (#122084)
   pRetroX-PTuner DD-M.EcoGII-v5-Centromeric protein C (#122085)
2. 10 mM Shield-1 in 100% ethanol (Aobious, Gloucester, MA, USA). Make a working stock at 1 mM in 100% ethanol.
3. Phoenix amphotropic cell line (ATCC CRL-3213) that expresses an amphotropic envelope protein for the generation of helper-free amphotropic retroviruses.
4. Your cell line of interest and the appropriate medium and supplements for culturing it.
5. Phosphate-buffered saline (PBS) without Ca^{2+} and Mg^{2+}, pH 7.4.
6. Trypsin-EDTA solution.
7. Chloroquine.
8. Polybrene for transduction (Sigma or other).
9. 2× HBS solution: 50 mM HEPES pH 7.05, 10 mM KCl, 12 mM dextrose, 280 mM NaCl, 1.5 mM Na_2HPO_4. Filter sterilize, aliquot, and store at −20 °C for up to 6 months.
10. 2M $CaCl_2$: filter sterilize, aliquot, and store at −20 °C.

2.2 m6Adenine Immunofluorescence

1. Parafilm.
2. Coverslips (*e.g.*, 12 mm coverslips #1.5, Menzel-Gläzer).
3. Microscope slides (*e.g.*, 25 × 75 × 1.0 mm, VWR).
4. Fixation buffer: 4% paraformaldehyde in 1× PBS with no methanol, *e.g.*, prepared from aqueous 16% paraformaldehyde (Electron Microscopy Sciences, USA).
5. Permeabilization buffer: 0.5% Triton X-100 in 1× PBS.
6. 10 mg/mL RNase A.
7. RNase cocktail Enzyme Mix (Ambion, ThermoFisher).
8. Denaturation buffer: 1.5 M NaCl, 0.5 M NaOH.
9. Neutralization buffer: 0.5 M Tris–HCl pH 7.0, 3 M NaCl.

10. Blocking solution: 0.2% (w/v) cold water fish gelatin (Sigma or other) with 0.5% (w/v) bovine serum albumin (BSA) in 1× PBS: filter sterilize, aliquot, and store at −20 °C.
11. Rabbit Anti *N*6-methyladenosine antibody (Synaptic Systems, Goettingen, Germany).

2.3 DNA Fluorescence In Situ Hybridization (FISH)

1. Fixation buffer (*see* Subheading 2.2, **item 4**).
2. Ethanol, molecular biology grade.
3. PNA probe(s) complementary to the DNA sequence(s) of interest (Panagene, Daejeon 34027, South Korea).
4. Blocking solution: prepare from a commercial blocking reagent for nucleic acid hybridization and detection (e.g., Roche) using the manufacturer's recommendations.
5. Hybridization mix: 10 mM Tris–HCl pH 7.2, 70% deionized formamide, 0.5% blocking solution. Aliquot and store at −20 °C.
6. Heating block.
7. Incubation chamber (e.g., 245 mm × 245 mm dish, Corning).
8. Wash buffer I: 0.01 M Tris–HCl pH 7.2, 0.1% BSA, 70% formamide.
9. Wash buffer II: 0.01 M Tris−HCl pH 7.2, 0.15 M NaCl, 0.08% Tween 20.
10. 1 mg/mL DAPI (4′,6-diamidino-2-phenylindole) solution in water.
11. Antifade mounting medium.

2.4 Extraction of Genomic DNA

1. Blood and Cell Culture DNA Midi Kit Genomic-tip 100/G (Qiagen).
2. RNase A.
3. RNase Cocktail Enzyme Mix (Ambion).
4. Fluorometer to accurately measure DNA concentration.

2.5 m6Adenine Immunoprecipitation (m6A-IP) Followed by High-Throughput Sequencing

1. Sonication apparatus (*e.g.,* Diagenode Bioruptor) equipped with a water cooler.
2. Polypropylene tubes (TPX, Diagenode).
3. NEBNext End-repair module (NEB).
4. NEBNext A-tailing module (NEB).
5. Double-stranded TruSeq adapters (Illumina).
6. NEBNext Ligation module (NEB).
7. TE buffer: 10 mM Tris–HCl pH 8.0, 1 mM EDTA.
8. 10× m6A-IP buffer: 100 mM Na phosphate buffer pH 7.0, 3 M NaCl, 0.5% Triton X-100.

9. Rabbit Anti *N*6-methyladenosine antibody (Synaptic Systems).
10. Protein A/G Dynabeads mix (ThermoFisher).
11. Pre-blocking buffer: 1× PBS, 0.5% BSA, 0.1% (v/v) Tween20.
12. Digestion buffer: 50 mM Tris–HCl pH 8.0, 10 mM EDTA, 0.5% SDS.
13. 20 mg/mL proteinase K solution.
14. Phenol:chloroform:isoamyl alcohol 25:24:1 (v/v/v).
15. KAPA Hifi DNA polymerase (Kapa Biosystems, Roche).
16. P5 and P7 primers (Illumina).
17. AMPureXB magnetic beads (Beckmann Coulter).

2.6 m6A Immunodot (m6A-Dotblot) Detection

1. 96-well Bio-Dot apparatus (BioRad).
2. Hybond-N+ membranes (GE Healthcare).
3. Whatman filter paper (*e.g.,* Bio-Dot SF, BioRad).
4. 20× sodium chloride-sodium citrate (SSC): 3 M NaCl and 300 mM sodium citrate equilibrated at pH 7.0.
5. Thermomixer.
6. Denaturing solution: 1.5 M NaCl, 0.5 M NaOH.
7. Neutralization solution: 0.5 M Tris–HCl pH 7.0, 0.3 M NaCl.
8. UV crosslinker apparatus (*e.g.,* UVC500, Hoefer).
9. 20 mM Tris-base pH 7.4–7.6, 150 mM NaCl, 0.1% Tween20 (TBST).
10. Blocking solution: 5% nonfat dry milk in 1× TBST.
11. Anti-*N*6-methyladenosine antibody, rabbit (Synaptic Systems).
12. Goat anti-rabbit IgG, Horseradish Peroxidase (HRP)-conjugated (Promega).
13. Western ECL substrate Blot imaging System (e.g., Biorad Chemidoc).

2.7 Telomere Purification by TeloCapture

1. AluI, HinfI, HphI, and MnlI restriction enzymes (NEB).
2. 20× SSC: 3 M NaCl, 300 mM sodium citrate, pH 7.0.
3. Triton X-100.
4. Biotinylated telomere oligo: Biotin-5′-ACTCC$(CCCTAA)_3$-3′.
5. Thermocycler or programmable thermomixer.
6. Streptavidin-coated magnetic beads (Invitrogen M-280).
7. Prewash buffer: 1× PBS, 0.1% Tween 20.
8. 2% Ficoll (type-400), 2% polyvinylpyrrolidone (100× Denhardt solution), 2% BSA: filter sterilize, aliquot, and store at −20 °C.

9. End-over-end rotator.
10. Magnetic rack (*e.g.*, DynaMag-2, Life Technologies).
11. Wash buffer I: 1× SSC, 0.1% Triton X-100.
12. 0.2× SSC (wash buffer II).
13. Elution buffer: 1 mM Tris pH 7.5, 1 mM EDTA, 10 mM LiCl.
14. Fluorometer to accurately measure DNA concentration.

3 Methods

3.1 Transfection of Phoenix Packaging Cells

1. Grow Phoenix cells in 10 cm ∅ tissue culture dishes to reach about 50–80% confluency at the time of transfection. Be gentle when pipetting medium because Phoenix cells easily detach from the culture dish (*see* **Note 1**).
2. Transfect cells by calcium phosphate precipitation: prepare a mix in a 1.5 mL microtube with 20 μg of plasmid DNA, 62 μL of 2 M $CaCl_2$, and H_2O up to a total of 500 μL. Add 500 μL of 2× HBS to a 5 mL clear tube. While making bubbles in the HBS using a pipette aid, add the $CaCl_2$/DNA solution dropwise. Incubate the precipitate for 5 min at RT.
3. Prepare fresh medium containing 25 μM chloroquine for a 12 h transfection or 100 μM chloroquine for a 5 h transfection.
4. Change the medium of the Phoenix cells for 10 mL of chloroquine-containing medium. Add the precipitate drop by drop, mix, and return the dish to the incubator.
5. Incubate for 5 or 12 h depending on the chloroquine concentration used. Change into 6 mL of fresh non-chloroquine-containing media.
6. Harvest the virus three times on 2 consecutive days by collecting the cell supernatant and filter through a 0.45 μm filter. The supernatant can be stored at −80 °C for at least 1 year.

3.2 Transduction of Cells

1. Seed cells in 10 cm ∅ dishes at 1×10^6 cells per dish (*see* **Note 2**). Seeding conditions and optimal confluency at the time of transduction are cell-type dependent.
2. The next day, change the cell medium for the virus-containing supernatant complemented with 4 μg/mL polybrene and appropriate serum, and incubate overnight.
3. Repeat the preceding step twice within 48 h.
4. The day after the last transduction, add the appropriate antibiotic for selection of resistant cells.

3.3 Culture of Transduced Cells and M.EcoGII Construct Induction Using Shield-1

1. Culture the required amount of transduced cells in the appropriate growth medium. Add Shield-1 to 1 μM to stabilize the DD-tagged M.EcoGII construct. Treat the cells with Shield-1 for a minimum of 6–7 h, but we recommend 24 h induction when possible (*see* **Note 3**).
2. For m6A immunofluorescence (m6A IF), seed cells on glass coverslips using standard procedures (*e.g.,* 5×10^4 to 10^5 cells per well of a 24-well plate containing 500 μL of medium and a coverslip per well). In these conditions the cells are not confluent after induction, hence allowing optimal image acquisition following immunofluorescence.
3. For m6A immunoprecipitation followed by high-throughput sequencing (m6A-IP-seq) as well as for m6A dotblots, we recommend a minimum of 10–20 $\times$ 10^6 Shield-1 induced cells per condition (*i.e.,* a confluent 15 cm ∅ culture dish).

3.4 m6A Immunofluorescence

1. Prepare the incubation chamber (*see* Subheading 2.3, **item 7**). Cut the appropriate amount of Parafilm and lay it carefully on the surface on the chamber. On both sides of the Parafilm, place some paper tissues previously soaked in water to ensure humidification of the chamber during incubation steps.
2. Prepare the primary antibody in blocking solution. We routinely use a 1/250 dilution of the anti-m6A antibody. Unless otherwise specified, a volume of 50 μL of diluted antibody is enough to completely cover a round coverslip up to 13 mm in diameter; this volume should be adapted if larger coverslips are used. Washes are usually performed using larger volumes (e.g., 200 μL).
3. Carefully remove the medium by aspiration, slightly inclining the 24-well plate.
4. Wash the cells for 5 min in 500 μL of 1× PBS prior to fixation.
5. Remove the PBS.
6. Add 500 μL of fixation buffer to each well and fix for 10 min at room temperature (RT) (*see* **Note 4**).
7. Wash the cells three times for 5 min in 500 μL of 1× PBS; remove the PBS between washes.
8. Add 500 μL of permeabilization buffer and incubate for 10 min at RT.
9. Repeat **step 7**.
10. After the last wash, transfer the coverslips onto the parafilm in the incubation chamber with fine tweezers, making sure that the cells are facing up. Add 200 μL of blocking solution supplemented with 200 μg/mL of RNase A and RNase Cocktail Enzyme Mix to a final concentration of 2.5 U/mL of RNaseA

and 100 U/mL of RNaseT1. Incubate for 1 h at 37 °C (*see* **Note 5**). From this step onward, it is advisable to add and aspirate solutions from the side of the coverslips.

11. Remove the solution by aspiration and wash the cells in 200 µL of PBS for 5 min.
12. Remove the PBS by aspiration. Denature cell DNA by adding 200 µL of denaturing solution per well and leave for 30 min at RT (*see* **Note 6**).
13. Remove the denaturing solution by aspiration.
14. Neutralize with 200 µL of neutralization solution and incubate for 5 min at RT.
15. Remove the neutralization solution.
16. Wash the cells three times for 5 min in 200 µL of 1× PBS.
17. Add 200 µL of blocking solution to each coverslip.
18. Gently aspirate the blocking solution.
19. Add the primary antibody solution to each coverslip and incubate overnight at 4 °C. Alternatively, incubation can be performed at RT for 2 h. Volumes should be as indicated in **step 2**.
20. Wash the coverslips in blocking solution three times for 5 min at RT. Between washes, carefully remove the blocking solution by aspirating from the side.
21. From this step forward, protect the coverslips from light.
22. Prepare the secondary antibody in blocking solution; the dilution of the secondary antibody is at the user's discretion. Add the secondary antibody to each coverslip and incubate for 45 min to 1 h at RT. Volumes should be as indicated in **step 2**.
23. If you intend to perform DNA-FISH, proceed now to Subheading 3.5.
24. Wash the coverslips in blocking solution twice for 5 min at RT, including 100 ng/mL DAPI in the second wash, then wash one additional time in PBS. Between washes, carefully remove the solution by aspirating from the side.
25. For mounting coverslips for microscopy we describe here the steps which we use routinely, but the reader should be aware that other procedures exist. Pick up each coverslip with fine tweezers, rinse briefly in ddH_2O, drain excess water using a paper tissue, and place the coverslip (cell side facing down) onto a 20 µL drop of Mowiol mounting medium on a microscope slide. Try to avoid trapping air bubbles.
26. Drain excess mounting medium with paper tissue. Leave at RT overnight for the Mowiol to dry and then store at 4 °C. Examples of m6A staining can be found in Fig. 1 and reference [2].

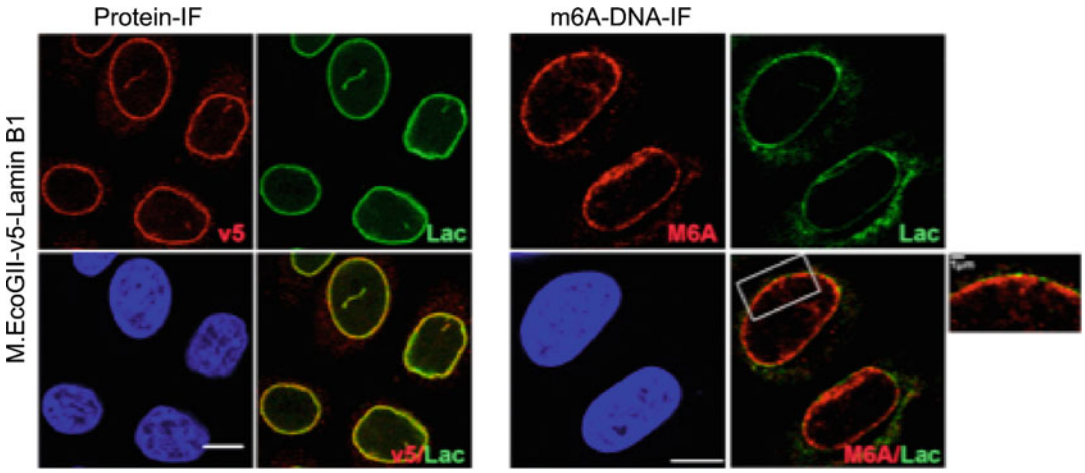

Fig. 1 Example of immunofluorescence of HeLa 1.2.11 cells induced to express M.EcoGII-v5-Lamin B1. V5 tag (left panel) or m6A (right panel) (red), Lamin A/C (green), DNA (blue), and merged. Scale bar, 10 μm. An enlarged part of the nucleus after m6A and Lamin A/C staining is shown. Scale bar, 1 μm. This figure is adapted from Figure 4 of ref. 2, an open-access article under the CC BY-NC-ND license (http://creativecommons.org/licenses/by-nc-nd/4.0/)

3.5 DNA Fluorescence In Situ Hybridization (FISH) Following m6Adenine Immunofluorescence

1. Prepare the probe (*see* Subheading 2.3, **item 3**) in hybridization buffer according to the manufacturer's instructions.
2. Heat the hot plate and set the temperature to 80 °C.
3. Wash coverslips in blocking solution three times for 5 min at RT. Between washes, carefully remove the blocking solution by aspirating from the side.
4. Remove the coverslips from the parafilm with fine tweezers and place them back into wells of a 24-well plate containing 500 μL of fixation buffer per well. Fix for 10 min at RT (*see* **Note 7**).
5. Rinse the coverslips with dH_2O twice (*see* **Note 8**).
6. Perform ethanol dehydration by sequentially incubating the cells in 70%, 90%, and 100% ethanol for 5 min each.
7. Pick up the coverslips with fine tweezers and make sure they air-dry.
8. On a clean glass slide, place 20 μL of working stock of the PNA probe and place the coverslip cell side down on the PNA solution. Avoid air bubbles.
9. Denature DNA by placing the coverslips on the hot plate for 3 min before overnight incubation in the humidified chamber at RT.
10. Remove the coverslips from the chamber with fine tweezers and place them back into a 24-well plate. Wash coverslips with 500 μL per well of wash buffer I, twice 15 min.

11. Wash coverslips with 500 µL per well of wash buffer II, three times 5 min.
12. Mount the coverslips on slides as described in Subheading 3.4, **steps 25** and **26**.

3.6 Isolation of Genomic DNA for m6A-IP-seq and m6A-Dotblots

1. Collect cells from a 15 cm ∅ culture dish by trypsinization and count them using an automated cell counter (*see* **Note 9**).
2. Wash the cell pellet once in 1× PBS (*see* **Note 10**).
3. Extract genomic DNA from the cells with a Qiagen Blood and Cell Culture DNA Midi Kit Genomic-tip 100/G. Follow the manufacturer's instructions but include the following step: when the pelleted nuclei are resuspended in buffer G2, add 100 µg/mL RNase A and RNase Cocktail Enzyme Mix to a final concentration of 2.5 U/mL RNase A and 100 U/mL RNase T1, and incubate for at least 1 h at 37 °C (*see* **Note 11**).
4. Measure the DNA concentration (*see* **Note 12**).

3.7 m6A-IP-seq Procedure

1. Dilute 20 µg of genomic DNA from Subheading 3.6, **step 4** in 300 µL of ddH_2O (final concentration 66.7 ng/µL) and transfer to a 1.5 mL polypropylene TPX tube. Sonicate the DNA to fragments of 200–400 bp (*see* **Note 13**).
2. Check the sonication efficiency by electrophoresing 500 ng to 1 µg of sheared DNA on a 2% agarose gel (*see* Fig. 2a).
3. Save 1% of the sample as the input fraction.
4. If library preparation is done at a sequencing facility, go straight to **step 8** (*see* **Note 14**).
5. End-repair 10 µg of sonicated DNA using the NEBNext End-repair module (two reactions per 10 µg of DNA) according to the manufacturer's instructions with the following modification: reagent volumes are adapted for a final reaction volume of 100 µL instead of the 50 µL advised by the manufacturer.
6. Purify the end-repaired DNA using AMPureXP beads according to the manufacturer's instructions.
7. A-tail the end-repaired DNA using the NEBNext A-tailing module according to the manufacturer's instructions.
8. Repeat **step 6**.
9. Ligate double-stranded Illumina TruSeq adapters to the DNA using the NEBNext Ligation module according to the manufacturer's instructions.
10. Repeat **step 6**.
11. Pool together the 10 µg of end-repaired, A-tailed, and adapter-ligated DNA samples and dilute in TE buffer to 360 µL. Denature for 10 min at 95 °C.
12. Snap cool on ice for 10 min.

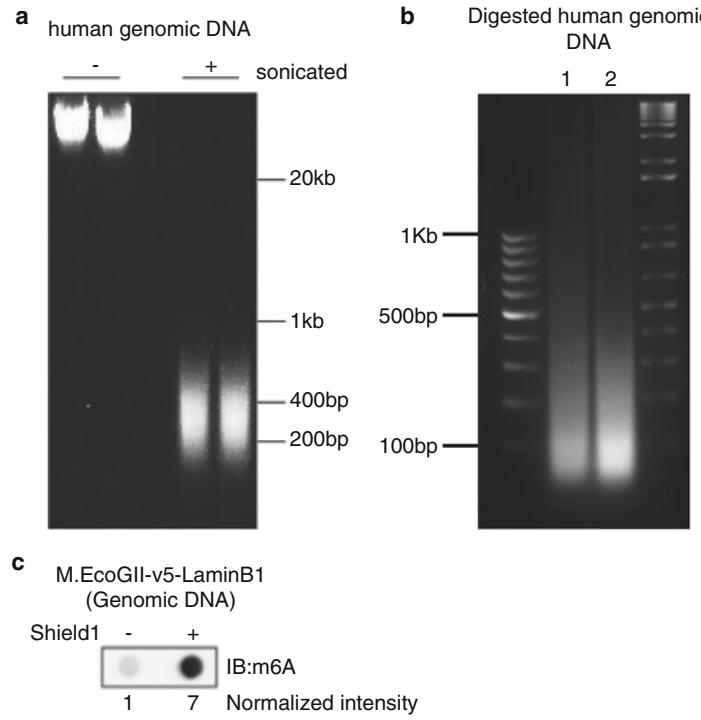

Fig. 2 (**a**) Migration patterns of sonicated human genomic DNA. One μg of human genomic DNA before (−) or after sonication (+) was loaded on a 2% agarose gel. (**b**) Migration patterns of digested human genomic DNA. 1 (lane 1) or 2 (lane 2) μg of genomic DNA was digested overnight with AluI, HinfI, HphI, and MnlI restriction enzymes (0.5 U/μg DNA) and loaded on a 2% agarose gel. (c) Representative dotblot of genomic DNA from HeLa 1.2.11 cells induced (+) or not induced (−) to express M.EcoGII-v5-Lamin B1. The membrane was probed with an m6A antibody. The normalized intensities are shown. This figure is adapted from Figure 4 of ref. 2

13. Supplement the samples with 10× m6A-IP buffer to a final concentration of 1×.
14. Add 2.5 μg of anti-m6A antibody.
15. Incubate overnight on a rotator at 4 °C.
16. If using magnetic beads, the following steps can be performed with the help of a magnetic rack.
17. Prepare protein A/G-coated magnetic beads; ensure that they are well resuspended in their buffer in the original vial. We use 20 μL of beads per sample. In a 1.5 mL Eppendorf tube, pipette enough beads for all samples. Gently remove the storage buffer and wash the beads with 1 mL of pre-blocking buffer. Rotate for 1 h at 4 °C, then gently remove the pre-blocking buffer, and resuspend the beads in the original pipetted volume of 1× m6A-IP buffer.

18. Add 20 μL of beads to each sample.
19. Rotate at 4 °C for 3 h.
20. Gently remove the unbound fraction (*see* **Note 15**).
21. Wash the beads four times with 1 mL of 1× m6A-IP buffer and invert the tube a few times between washes.
22. Resuspend the input and bead samples in 150 μL of digestion buffer supplemented with 300 μg/mL of proteinase K.
23. Incubate with shaking for 3 h at 50 °C. Remove the beads and save the eluate.
24. Purify DNA of the input and eluate fractions by standard phenol/chloroform/isoamyl alcohol extraction and resuspend in 21 μL of ddH_2O.
25. Measure the DNA concentration using a fluorometer.
26. Amplify half of the purified DNA for ten cycles using KAPA Hifi DNA polymerase and Illumina P5 and P7 primers according to the manufacturer's instructions. The amplified DNA is then purified using AMPureXP beads according to the manufacturer's instructions.
27. The libraries can subsequently be sent to a sequencing facility.

3.8 m6A-Dotblots

1. Dilute between 20 ng and 1 μg of genomic DNA from Subheading 3.5, **step 4** or isolated DNA regions (*see* Subheading 3.9) in 2× SSC to reach a volume of 100–200 μL.
2. Prepare Whatman filter paper by soaking it in 2× SSC. The paper must be of equal size to the dotblot apparatus.
3. Prepare the blotting membrane by sequential soaking in ddH_2O and then in 2× SSC for at least 5 min for equilibration. The membrane must be of equal size to the dotblot apparatus.
4. Mount the dotblot apparatus, assembling the Whatman paper and the membrane according to the manufacturer's instructions.
5. Heat denature DNA samples at 98 °C for 10 min and snap cool on ice for 10 min.
6. Load DNA samples on the membrane via vacuum blotting (*see* **Note 16**). Once the wells are empty, wash twice with 2× SSC.
7. Remove the membrane from the apparatus using tweezers and place it onto a Whatman paper (DNA facing up) saturated with denaturing solution for 10 min at RT.
8. Remove the membrane with tweezers and place it onto a Whatman paper (DNA facing up) saturated with neutralizing solution for 10 min at RT.
9. Remove excess of liquid by gently blotting on dry Whatman paper.

10. Crosslink with a UV crosslinker. We usually use 70,000 μJ/cm^2.
11. Block in 50 mL of blocking solution for 1 h at RT.
12. Incubate with m6A antibody (1/1000 in blocking solution) overnight at 4 °C.
13. Wash the membrane in PBST three times for 10 min.
14. Incubate with HRP-secondary antibody (1/5000 in blocking solution) for 45 min at RT.
15. Repeat **step 13**.
16. Reveal the signals on the membrane using Western ECL substrate according to the manufacture's instruction. Analyze the chemiluminescence signals obtained using a ChemiDoc or other imaging system. An example of a m6A-dotblot is shown in Fig. 2c.

3.9 m6A-Dotblot on Isolated DNA Regions: Example of Telomere Purification by TeloCapture

1. To release intact telomeric fragments, digest 50 μg of genomic DNA (*see* Subheading 3.6, **step 4**) with AluI, HinfI, HphI, and MnlI restriction enzymes (0.5 U/μL) in a 300 μL reaction volume at 37 °C overnight (*see* **Note 17**). An example of the resulting migration pattern is shown in Fig 2b.
2. Adjust the reaction mix to 1× SCC and 0.1% Triton X-100 by adding 15 μL of 20× SCC and 3 μL of 10%Triton X-100.
3. Add 3.5 pmoles of biotinylated telomere oligonucleotide (*see* Subheading 2.7, **item 4**) per sample. If the oligo is at the standard 100 μM concentration, we recommend to make a 1/100 dilution and then add 3.5 μL to each sample.
4. Anneal the oligo by controlled stepwise cooling from 80 to 25 °C (1 °C/min) using a thermocycler.
5. If using magnetic beads, the following steps can be performed with the help of a magnetic rack to collect the beads.
6. During the annealing step, prepare the streptavidin-coated magnetic beads. Ensure that the beads are well resuspended in their buffer in the original vial. We use 18 μL of beads per sample. In a 1.5 mL Eppendorf tube, pipette enough beads for all samples. Prewash once in 1× PBST. Block the beads by adding 1 mL of 5× Denhardt solution and incubate for 1 h at 4 °C on a rotating wheel. Resuspend the beads in the original pipetted volume of 1× PBST.
7. After annealing, save 3 or 10 μL (i.e., 3–10 % of the starting material) of the sample as input.
8. Add 18 μL of prepared beads to each sample.
9. Incubate overnight on a rotator at 4 °C.

10. Gently remove and discard the unbound fraction (*see* **Note 15**).
11. Wash the beads with 1 mL of wash buffer I four times and invert the tube a few times between washes.
12. Wash the beads once with wash buffer II.
13. Resuspend the beads in 50 μL of elution buffer and elute telomeric DNA by incubating at 50 °C for 20 min, gently rotating the tube. Remove the beads and save the eluate.
14. The preceding step may be repeated once (optional).
15. Measure the DNA concentration using a Qubit.
16. Perform a dotblot as described in Subheading 3.8 (*see* **Note 18**).

4 Notes

1. M.EcoGII constructs are stably expressed in cells using retroviral transduction. Prepare one 10 cm ∅ dish of Phoenix cells for each transduction that you wish to perform.
2. Prepare one 10 cm diameter dish for each transduction you wish to perform.
3. After retroviral cell transduction, the expression cassettes will randomly integrate into the host genome for stable expression. The M.EcoGII constructs that we generated (see material section) were cloned into the pRetroX-PTuner plasmid (Clontech) that allows the regulation of the amount of the expressed protein of interest. The vector encodes a 12 kDa destabilization domain (DD) that is expressed as a N-terminal tag on all M. EcoGII constructs and causes their rapid degradation via the proteasome. The DD-tagged protein can be rapidly stabilized by addition of Shield-1, a permeable molecule that will bind the DD tag and prevent the proteasomal degradation. Although we found that 6–7 h of induction was sufficient to induce significant methylation of genomic DNA, experiments that do not require short induction time should be carried out after 24 h of induction to increase the signal to noise ratio. It is important to note that constitutive overexpression should be avoided as it will result in permanent m6A methylation. We strongly advise to include a condition with no Shield-1 treatment to test for background methylation and efficiency of the induction. As Shield-1 is solubilized in Ethanol, add the corresponding amount of Ethanol in the non-induced samples.
4. Fixation is a crucial step. Extended fixation may result in antigen masking, thereby decreasing the primary antibody's efficiency. Also, for some specific proteins the percentage of paraformaldehyde used and/or the fixation time may be adapted.

5. m6A immunofluorescence, when used to detect methylated DNA, requires an RNase treatment. Indeed, m6A methylation of mRNA is a very abundant modification in eukaryotic cells. If not removed, it will automatically result in a high fluorescence background masking the localization of methylated DNA.
6. This step will allow a better accessibility of m6A to the anti-m6A antibody.
7. This step is required to fix the antibodies for subsequent PNA hybridization steps.
8. At this stage, the coverslips can be stored for a couple of days in 1× PBS at 4 °C in the dark.
9. Any cell counting apparatus can be used; the key point is to have a clear idea of the number of cells harvested for each condition. For example, an excess of cells may impede genomic DNA extraction by blocking the columns used. Conversely, a low starting amount of cells may result in a suboptimal DNA yield for high-throughput sequencing or a suboptimal telomere yield at the end of Telocapture, hence resulting in a poor signal on the slot-blot membrane.
10. At this stage, the cell pellets can be stored at −20 °C for up to 2 months.
11. Using commercially available kits for genomic DNA extraction is a time saver. However, standard protocols can also be used.
12. At this point, genomic DNA can be stored at −20 °C for a least a year.
13. We perform this step using a Bioruptor Plus equipped with a water cooler (Diagenode). Sonication is performed using the following settings: 40 cycles 30s ON, 60s OFF, low power.
14. As mentioned in **Note 6**, the m6A-specific antibody has a higher affinity for m6A on denatured DNA. As Illumina adaptors need to be added to double-stranded DNA, the steps of end-repair, A-tailing, and ligation need to be performed before the immunoprecipitation step.
15. The unbound fraction can be kept for further analysis if needed.
16. To load DNA on the membrane, the volume of the sample should ideally be between 100 and 200 μL. We do not recommend loading less than 50 μL, as air bubbles can form in the well that may result in unequal spreading of the DNA. The amount of genomic DNA to load can vary between experiments. We recommend loading several amounts to test the linearity of the m6A signal later on.

17. It is good practice to check the digestion efficiency by running an aliquot of digested DNA (usually 1–2 μg) on a 2% agarose gel.
18. It is possible to assess the efficiency of telomere capture using a Q-PCR approach [9].

Acknowledgments

We would like to thank all the members (past and present) of the Crabbé lab for helpful discussions, especially Sonia Stinus Ruiz de Gauna for critical reading of the manuscript. This work was supported by an ATIP starting grant from CNRS in the framework of Plan Cancer 2014–2019 (to L.C.), the ANR Tremplin ERC teloHOOK (ANR-16-TERC-0028-01 to L.C.), and a European Research Council (ERC) grant (TeloHOOK, 714653 to L.C.).

References

1. Orlando V, Strutt H, Paro R (1997) Analysis of chromatin structure by in vivo formaldehyde cross-linking. Methods 11:205–214. https://doi.org/10.1006/meth.1996.0407
2. Sobecki M, Souaid C, Boulay J et al (2018) MadID, a versatile approach to map protein-DNA interactions, highlights telomere-nuclear envelope contact sites in human cells. Cell Rep 25:2891–2903.e5. https://doi.org/10.1016/j.celrep.2018.11.027
3. van Steensel B, Delrow J, Henikoff S (2001) Chromatin profiling using targeted DNA adenine methyltransferase. Nat Genet 27:304–308. https://doi.org/10.1038/85871
4. Kind J, Pagie L, de Vries SS et al (2015) Genome-wide maps of nuclear lamina interactions in single human cells. Cell 163:134–147. https://doi.org/10.1016/j.cell.2015.08.040
5. Guelen L, Pagie L, Brasset E et al (2008) Domain organization of human chromosomes revealed by mapping of nuclear lamina interactions. Nature 453:948–951. https://doi.org/10.1038/nature06947
6. Kind J, van Steensel B (2014) Stochastic genome-nuclear lamina interactions: modulating roles of Lamin A and BAF. Nucleus 5:124–130. https://doi.org/10.4161/nucl.28825
7. Filion GJ, van Bemmel JG, Braunschweig U et al (2010) Systematic protein location mapping reveals five principal chromatin types in Drosophila cells. Cell 143:212–224. https://doi.org/10.1016/j.cell.2010.09.009
8. Murray IA, Morgan RD, Luyten Y et al (2017) The non-specific adenine DNA methyltransferase M.EcoGII. Nucleic Acids Res 46:840–848. https://doi.org/10.1093/nar/gkx1191

Chapter 11

Optimized Detection of Protein-Protein and Protein-DNA Interactions, with Particular Application to Plant Telomeres

Šárka Schořová, Jiří Fajkus, and Petra Procházková Schrumpfová

Abstract

Characterization of protein-protein and protein-DNA interactions is critical to understand mechanisms governing the biology of cells. Here we describe optimized methods and their mutual combinations for this purpose: bimolecular fluorescence complementation (BiFC), co-immunoprecipitation (Co-IP), yeast two-hybrid systems (Y2H), and chromatin immunoprecipitation (ChIP). These improved protocols detect trimeric complexes in which two proteins of interest interact indirectly via a protein sandwiched between them. They also allow isolation of low-abundance chromatin proteins and confirmation that proteins of interest are associated with specific DNA sequences, for example telomeric tracts. Here we describe these methods and their application to map interactions of several telomere- and telomerase-associated proteins and to purify a sufficient amount of chromatin from *Arabidopsis thaliana* for further investigations (e.g., next-generation sequencing, hybridization).

Key words Bimolecular fluorescence complementation, Co-immunoprecipitation, Yeast two-hybrid system, ChIP for low-abundance proteins

1 Introduction

Characterization of molecular interaction partners provides valuable information on protein function and the subcellular localization of interactions, as well as on the composition and three-dimensional architecture of protein complexes [1]. There are several efficient systems for mapping protein-protein interactions, of which two-hybrid systems (Y2H) and co-immunoprecipitation (Co-IP) are straightforward and powerful. In Y2H, separate plasmids coding for bait and prey proteins are introduced simultaneously into a mutant yeast strain, and their physical interaction is detected through the downstream activation of a reporter gene that causes a change in the cell phenotype (e.g., loss of auxotrophy). Co-IP is based on precipitation of complexes formed by proteins, usually produced in an in vitro transcription/translation system or

Ronald Hancock (ed.), *The Nucleus*, Methods in Molecular Biology, vol. 2175, https://doi.org/10.1007/978-1-0716-0763-3_11,

expressed in bacteria, using an antibody that binds to an epitope on one of them. However, the absence of interaction detectable by Y2H or Co-IP does not necessarily mean that two proteins do not interact under native conditions. Bimolecular fluorescence complementation (BiFC), another widely used method, is based on the recovery of fluorescence if putative interaction partners, each fused to a different fragment of a fluorescent protein, interact even without direct contact [2]; the presence of proteins in a complex visualized using BiFC generally indicates that they participate in the same biological process. ChIP is a powerful and versatile technique to study protein-DNA interactions in vivo and is widely used to study chromatin, but no universal protocol exists for protein sample preparation.

We use these methods to study telomeres, which as the physical ends of linear chromosomes are targets of a number of proteins and protein complexes, including telomerase which accomplishes the incomplete semiconservative replication of chromosome ends (the so-called end-replication problem). The telomerase complex, besides its core subunits TERT (Telomerase Reverse Transcriptase, a protein catalytic subunit) and TR (telomerase RNA subunit), comprises several other proteins with diverse roles in telomerase assembly, trafficking, localization, recruitment to telomeres, or processivity [3–6]. Further proteins associated with telomeres perform their other essential function, to distinguish chromosome ends from unrepaired breaks and so prevent unwanted repair events (end protection). In mammals, a complex of six proteins termed shelterin associates with telomeres and can inhibit DNA damage responses, plays a role in recruitment of telomerase, and facilitates replication fork movement through telomeres and formation of telomere loops [7]. Although several orthologues of mammalian telomere- and telomerase-associated proteins have been identified in plants [3] these may show change or loss of specific function(s), interaction partners, or localization [6, 7]. Moreover, due to frequent genome polyploidization and consecutive multiplication of genes in plant genomes, the number of homologues of telomere- and telomerase-associated proteins is higher than in their mammalian counterparts and may lead to sub-functionalization, neo-functionalization, and partial or full redundancy [8]. The conservation of domain composition of plant proteins with respect to their mammalian counterparts does not guarantee that their function is conserved; for example, no telomere maintenance functions are found in *Arabidopsis* orthologues (TRF-like or TRFL proteins) of mammalian TRF proteins where the telomeric sequence-binding domain, a myb domain of the telobox type, is located C-terminally as in human shelterin subunits TRF1 and TRF2 [9]. The only proteins with confirmed telomere localization in vivo, direct

interaction with *A. thaliana* TERT, and function in telomere maintenance are the telomere repeat binding (TRB) proteins where the myb domain resides at the N-terminus [10, 11]. Likewise, orthologues of conserved telomerase RNA scaffold proteins have been identified in plants, e.g., CBF5 (dyskerin), RuvBL1 (Pontin), and RuvBL2a (Reptin) [12, 13]. On one hand, identification of RuvBL1 and RuvBL2a in *Arabidopsis* and their conservation in humans shows that factors involved in telomerase biogenesis and function are evolutionarily ancient, but on the other hand the mechanism of action of plant RuvBL proteins differs from that in mammals; their interactions with TERT in *A. thaliana* are not direct and are rather mediated by one of the TRB proteins. Elucidation of the composition of telomeric nucleoprotein structures and molecular dissection of their components and interactions are important for understanding their roles in the complex biology of telomeres. It seems that some proteins are involved in similar biochemical pathways but their interaction partners, and consequently their potential regulatory factors, may slightly differ. A further problem when working with proteins associated with chromatin of plant cells is that their composition (e.g., cell walls) makes them very difficult to disrupt, and carbohydrate matrices that often form during homogenization must be prevented from trapping nuclei. Moreover, chloroplasts must be removed because their genomes may comprise the majority of cell DNA, and volatile compounds such as polyphenols must be prevented from interacting with the nuclear DNA. Isolation of low-abundance proteins is therefore challenging.

In this chapter, we describe improved versions of Y2H, Co-IP, and BiFC and show how proper combinations of these methods can be used to distinguish whether two proteins of interest interact directly or via a linker protein, with specific applications to plant telomeres. Our optimized BiFC protocol provides a robust tool to observe direct or indirect interactions of proteins and to distinguish a nuclear, nucleolar, or cytoplasmic localization of these interactions. Our development of "Co-Immunoprecipitation with Two or Three Proteins of Interest" allows detection of trimeric complexes where two proteins interact indirectly via a protein sandwiched between them. "ChIP for Low-Abundance Proteins" allows isolation of plant chromatin that is suitable for further investigations such as next-generation sequencing or hybridization. We have used this method to prove that candidate telomeric proteins are associated with telomeric repeats in vivo [14]. It can be used for isolation not only of telomere-associated proteins, but for any low-abundance protein recognizing any DNA sequence.

2 Materials

2.1 Bimolecular Fluorescence Complementation (BiFC)

2.1.1 Solutions and Equipment

1. Protoplasting solution (freshly prepared): 0.4% (w/v) Cellulase Onozuka R-10 (Duchefa, Haarlem, The Netherlands), 0.25% (w/v) Macerozyme R-10 (Duchefa), 0.04% (w/v) Pectolyase Y-23 (Duchefa), 0.4 M mannitol, 20 mM KCl, 20 mM 2-(*N*-morpholino)ethanesulfonic acid (MES) pH 5.5–5.7, 10 mM $CaCl_2$, 1% (w/v) bovine serum albumin (BSA). Mix mannitol (4 mL of 1 M stock solution), KCl (200 μL of 1 M stock solution), MES (2 mL of 0.5 M stock solution), 700 μL of double-distilled autoclaved water (ddH_2O) and add 0.04 g of Cellulase, 0.025 g of Macerozyme, and 0.004 g of Pectolyase. Vortex, warm at 55 °C for 10 min, and cool to room temperature (RT). Add $CaCl_2$ (100 μL of 1 M stock solution), BSA to 1 % (w/v), and ddH_2O to 10 mL.
2. Protoplast washing solution: 154 mM NaCl, 125 mM $CaCl_2$, 5 mM KCl, 2 mM MES (pH 5.5–5.7), 5 mM glucose. Mix NaCl (10.3 mL of 3 M stock solution), $CaCl_2$ (25 mL of 1 M stock solution), KCl (1 mL of 1 M stock solution), MES (800 μL of 0.5 M stock solution), glucose (2 mL of 0.5 M stock solution) and ddH_2O to 200 mL. Autoclave, store at 4 °C.
3. MMg solution: 0.4 M mannitol, 15 mM $MgCl_2$, 4 mM MES (pH 5.5–5.7). Mix mannitol (80 mL of 1 M stock solution), $MgCl_2$ (3 mL of 1 M stock solution), MES (1.6 mL of 0.5 M stock solution) and add ddH_2O to 200 mL (*see* **Note 1**). Autoclave and store at 4 °C.
4. Polyethylene glycol (PEG) solution (freshly prepared): 4 g PEG 4000 (Duchefa), 0.2 M mannitol, 0.1 M $CaCl_2$. Dissolve 4 g of PEG by vortexing in a mixture of mannitol (2 mL of 1 M stock solution), $CaCl_2$ (1 mL of 1 M stock solution), and 3.5 mL of ddH_2O. Mix until the solution becomes clear.
5. BSA: 10% (w/v) in ddH_2O.
6. Plasmid DNA isolation kit: NucleoBond Xtra Midi/Maxi (Macherey-Nagel, Düren, Germany).
7. Centrifuge for Falcon round-bottom tubes providing $\geq 150 \times g$.
8. 15-mL round-bottom Falcon tubes.
9. 5-mL or 10-mL pipets.
10. 24-well tissue culture plates (Ø 1.5 cm).
11. Petri dishes (Ø 6 cm).
12. Straight-tipped scissors.
13. White opaque tape and transparent tape.
14. Lamp with white light.

15. Epifluorescence microscope (Zeiss ZA1 AxioImager or similar).
16. Optical microscope (Zeiss Lab A1 or similar).
17. Glass microscope slides, coverslips.
18. Platform shaker.
19. Hemocytometer.

2.1.2 Plants and Growth Conditions

Grow *A. thaliana* wild-type plants in growth chambers (phytotrons) in a mix of peat, sand, and polystyrene (12:2:1) without chemical treatment, using 8 h light/16 h dark at 21 °C. Leaves from 3 to 5 weeks old plants can be used, but use only fresh and healthy plants (*see* **Note 2**).

2.1.3 DNA Constructs

Constructs to express fusion proteins are prepared using Gateway technology (Invitrogen). The entry clones pDONR/Zeo or pDONR 207 containing cDNA sequences coding for genes of interest are used for LR-recombination reactions (recombination between attL and attR sites). As destination vectors, expression vectors pSAT5-DEST-cEYFP-C1 and pSAT4-DEST-nEYFP-C1 (numbers CD3-1097 and CD3-1089, respectively, Arabidopsis Information Resource (https://www.arabidopsis.org) are used; kindly provided by Prof. Stanton Gelvin, Purdue University).

2.2 Yeast Two-Hybrid System (Y2H)

2.2.1 Solutions and Equipment

1. Yeast extract–Peptone–Glucose (YPG) liquid medium: weigh 20 g peptone (Duchefa), 10 g yeast extract (Duchefa), and add ddH_2O to 1000 mL. Autoclave, store at RT. Immediately before use add 40% (w/v) D-glucose to 2% (w/v) glucose.
2. Yeast extract–Peptone–Glucose (YPG) plates: weigh 3 g peptone (Duchefa), 1.5 g yeast extract (Duchefa), 3 g plant agar (Duchefa), and add ddH_2O to 150 mL. Autoclave, chill slightly, and add 7.5 mL of 40% (w/v) D-glucose. Store at 4 °C.
3. 100× adenine solution: dissolve 0.27 g of adenine in 100 mL ddH_2O.
4. 100× histidine solution: dissolve 0.20 g of histidine in 100 mL ddH_2O.
5. Synthetic defined (SD)-Leu, Trp plates (minimal medium lacking leucine and tryptophan) for selection of double yeast transformants: weigh 4.67 g Minimal SD (Synthetically Defined) Agar Base (TakaraBio) and 0.06 g Dropout (DO) Supplement (TakaraBio), add 1 mL 100× adenine solution, 1 mL 100× histidine solution, and ddH_2O to 100 mL (*see* **Note 3**). Autoclave and store at 4 °C.
6. SD-Leu, Trp, His plates (minimal medium lacking leucine, tryptophan, and histidine) for scoring interactions: weigh 4.67 g Minimal SD Agar Base (TakaraBio) and 0.06 g DO

Supplement (TakaraBio), add 1 mL 100× adenine solution and ddH_2O to 100 mL (*see* **Notes 3** and **4**). Autoclave and store at 4 °C.

7. SD-Leu, Trp, Ade plates (minimal medium lacking leucine, tryptophan, and adenine) for scoring interactions: weigh 4.67 g Minimal SD Agar Base (TakaraBio) and 0.06 g DO Supplement (TakaraBio), add 1 mL 100× histidine solution and ddH_2O to 100 mL (*see* **Note 3**). Autoclave and store at 4 °C.
8. 10× TE: dissolve 1.58 g of Tris-base and 0.29 g of EDTA in 100 mL ddH_2O, adjust to pH 7.5 with HCl. Sterilize through a 0.22 μm filter, store at RT.
9. 1× TE (10 mL): mix 1 mL of 10× TE with 9 mL of ddH_2O, prepare fresh.
10. 10× lithium acetate (LiAc) solution: dissolve 10.2 g of LiAc in 100 mL ddH_2O, adjust to pH 7.5 with acetic acid. Sterilize through a 0.22 μm filter, store at RT.
11. PEG solution, 50% (w/v): dissolve 125 g PEG 4000 (Duchefa) in 250 mL ddH_2O. Autoclave, store at RT.
12. PEG-LiAc solution, 40% (w/v): (10 mL): mix 1 mL of 10× TE with 8 mL of 50% (w/v) PEG, add 1 mL of 10× LiAc. Prepare fresh (*see* **Note 5**).
13. 1× TE-LiAc (10 mL): mix 1 mL of 10× TE with 8 mL of ddH_2O, add 1 mL of 10× LiAc. Prepare fresh (*see* **Note 5**).
14. 40% (w/v) D-glucose: dissolve 40 g of D-glucose in 100 mL ddH_2O. Autoclave, store at RT.
15. 1 M aminotriazole (3-amino-1,2,4-triazole) solution: dissolve 840 mg of aminotriazole in 10 mL of ddH_2O. Sterilize through a 0.22 μm filter, store at −20°C.
16. cOmplete Mini EDTA-free Protease Inhibitor Cocktail (Roche).
17. GenElute Plasmid Miniprep Kit (Sigma).
18. Petri dishes.
19. 50 mL Erlenmeyer flask.
20. Centrifuges providing ≥5000 × *g* for Falcon tubes and ≥18,000 × *g* for microcentrifuge tubes.
21. 2-mL microcentrifuge tubes and 50-mL Falcon tubes.
22. Incubator for agar plates at 30 °C.
23. Incubator/shaker at 30 °C for aerating liquid cultures.
24. Incubator/shakers or thermomixers at 30 °C and 42 °C.
25. Spectrophotometer.
26. Parafilm.

2.2.2 DNA Constructs and Yeast Strains

As described in Subheading 2.1.3, plasmid DNA constructs for the expression of bait or prey fusion proteins and empty vector controls are prepared using Gateway technology (Invitrogen). The entry clones pDONR/Zeo or pDONR 207 containing cDNA sequences coding for genes of interest are used for LR-recombination reactions. Destination vectors pGBKT7-DEST and pGADT7-DEST, coding for bait or prey, are used for these reactions (derived from Matchmaker System vectors). The yeast strain of choice is haploid *Saccharomyces cerevisiae* PJ69-4A (*MATa, trp1-901, leu2-3,112, ura3-52, his3-200, gal4Δ, gal80Δ, GAL2-ADE2, LYS2::GAL1-ADE2, LYS2::GAL1-HIS3, met2::GAL7-lacZ*), with HIS3 and ADE2 reporter genes [15], which can be obtained from the Yeast Resource Center, University of Washington.

2.3 Co-immunoprecipitation (Co-IP) with Two or Three Proteins of Interest

2.3.1 Solutions and Equipment

1. Coupled transcription/translation system: TNT T7 Quick (Promega).
2. ^{35}S-labeled L-methionine (15 mCi/mL).
3. Anti-c-Myc antibody, mouse (Sigma-Aldrich).
4. Protein G-magnetic beads (Dynabeads, Invitrogen).
5. DynaMag-5 magnet (ThermoFisher).
6. 2× Hepes buffer: 50 mM Hepes, 300 mM KCl, 10 mM $MgCl_2$, 20% (v/v) glycerol. Dissolve 0.36 g of Hepes in KCl (3 mL of 1 M stock solution), $MgCl_2$ (300 μL of 1 M stock solution), glycerol (6 mL), add ddH_2O to 30 mL and adjust to pH 7.5 by adding KOH or HCl. Sterilize through a 0.22 μm filter. Store at −20 °C. Add a protease inhibitor cocktail tablet immediately before use.
7. 1× Hepes buffer: dilute from 2× Hepes buffer with ddH_2O and add a protease inhibitor cocktail tablet.
8. 2× gel loading buffer: 100 mM Tris (pH 6.8), 4% (w/v) SDS, 20% (w/v) glycerol, and 0.2% (w/v) bromophenol blue. Mix 4 mL of 0.5 M Tris stock solution, 0.8 g of SDS, 4 g of glycerol, and 40 mg of bromophenol blue and add ddH_2O to 20 mL.
9. Electrophoresis system and transfer cell (Bio-Rad).
10. 10× SDS-PAGE running buffer: 25 mM Tris, 192 mM glycine, 0.1% (w/v) SDS. Dissolve 30.3 g of Tris and 104.3 g of glycine in <1 L ddH2O, add 10 g of SDS and ddH2O to 1 L.
11. Transfer buffer: mix 100 mL of 10× SDS-PAGE running buffer with 200 mL of methanol and add 700 mL of ddH2O.
12. Precast SDS polyacrylamide gels: 12% Mini-protean TGX (Bio-Rad).
13. Nitrocellulose membranes (Hybond ECL, GE Healthcare).
14. Phosphorimager (Fujifilm FLA-7000 or similar).
15. Storage phosphor screen.

16. Thermomixer.
17. Centrifuge for microcentrifuge tubes providing $\geq 2000 \times g$.
18. Microcentrifuge tubes, 1.5 mL.
19. Parafilm.
20. Rotating mixer.
21. Plastic food wrap.

2.3.2 In Vitro Transcription/Translation

The TNT T7 Quick Coupled Transcription/Translation System (Promega), which contains all necessary factors for easy transcription/translation, is used for protein expression. Plasmid DNAs coding for proteins of interest in proper vectors are added to the TNT Quick Master Mix according to the manufacturer's protocol. As the destination vectors pGADT7-DEST and pGBKT7-DEST (also used in Y2H assays, Subheading 2.2) contain a T7 promoter, they can be transcribed in the this TNT system. Alternatively, when clones are not available it is possible to generate linear genes or their fragments using PCR with a forward primer containing a T7 promoter at its 5′ end and to use the products as substrates in the TNT system.

2.4 Chromatin Immunoprecipitation Assay (ChIP) for Low-Abundance Proteins

2.4.1 Solutions and Equipment

1. EtOH: 70% and 95% (v/v).
2. ddH_2O: 1 L prechilled at 4 °C.
3. Agar: plant cell culture tested (Sigma or other).
4. Murashige and Skoog (MS) medium plates with 1% sucrose and 0.8% plant agar: mix 4.4 g MS salts (Duchefa), 8 g plant agar, and 10 g sucrose, add ddH_2O to 1 L, and adjust pH to 5.7 with KOH. Autoclave, store at RT.
5. 1% (v/v) formaldehyde solution in ddH_2O (prepare fresh; keep at RT).
6. Nuclei grinding buffer: 400 mM sucrose, 10 mM Tris–HCl (pH 8.0), 5 mM β-mercaptoethanol (β-ME), 0.1 mM phenylmethanesulfonyl fluoride (PMSF), leupeptin (1.0 μg/mL), and pepstatin (1.0 μg/mL). Mix sucrose (20 mL of 2 M stock solution) and Tris–HCl (1 mL of 1 M stock solution pH 8.0), make up to 100 mL with ddH_2O, and sterilize through a 0.22 μm filter. Immediately before use add β-ME (35 μL of 14.3 M stock solution), PMSF (50 μL of 0.2 M stock solution), leupeptin (100 μL of 1 mg/mL), and pepstatin A (100 μL of 1 mg/mL).
7. Nuclei wash buffer 1: 250 mM sucrose, 10 mM Tris–HCl (pH 8.0), 10 mM $MgCl_2$, 1% (v/v) Triton X-100, 5 mM β-ME, 0.1 mM PMSF, leupeptin (1.0 μg/mL), and pepstatin (1.0 μg/mL). Mix sucrose (1.25 mL of 2 M stock solution), Tris–HCl (100 μL of 1 M stock solution), $MgCl_2$ (100 μL of 1 M stock solution), and Triton X-100 (0.5 mL of 20% (v/v)

stock solution), add ddH_2O to 10 mL, and sterilize by filtration through a 0.22 μm filter. Immediately before use add β-ME (3.5 μL of 14.3 M stock solution), PMSF (5 μL of 0.2 M stock solution), leupeptin (10 μL of 1 mg/mL), and pepstatin A (10 μL of 1 mg/mL).

8. Nuclei wash buffer 2: 1.7 M sucrose, 10 mM Tris–HCl (pH 8.0), 2 mM $MgCl_2$, 0.15% (v/v) Triton X-100, 5 mM β-ME, 0.1 mM PMSF, leupeptin (1.0 μg/mL), and pepstatin (1.0 μg/mL). Mix sucrose (8.5 mL of 2 M stock solution), Tris–HCl (100 μL of 1 M stock solution), $MgCl_2$ (20 μL of 1 M stock solution), and Triton X-100 (75 μL of 20% (v/v) stock solution), add ddH_2O to 10 mL, and sterilize through a 0.22 μm filter. Immediately before use add β-ME (3.5 μL of 14.3 M stock solution), PMSF (5 μL of 0.2 M stock solution), leupeptin (10 μL of 1 mg/mL), and pepstatin A (10 μL of 1 mg/mL).
9. Nuclei lysis buffer: 50 mM Tris–HCl (pH 8.0), 10 mM EDTA, 1% (w/v) SDS, 0.1 mM PMSF, leupeptin (1.0 μg/mL), and pepstatin (1.0 μg/mL). Mix Tris–HCl (250 μL of 1 M stock solution), EDTA (100 μL of 0.5 M stock solution), SDS (250 μL of 20% (w/v) stock solution), add ddH_2O to 5 mL. Sterilize through a 0.22 μm filter. Immediately before use add PMSF (2.5 μL of 0.2 M stock solution), leupeptin (5 μL of 1 mg/mL), and pepstatin A (5 μL of 1 mg/mL).
10. ChIP dilution buffer: 16.7 mM Tris–HCl (pH 8.0), 167 mM NaCl, 1.1 mM EDTA, 0.11% (v/v) Triton X-100, 0.11 mM PMSF, leupeptin (1.1 μg/mL), and pepstatin (1.1 μg/mL). Mix Tris–HCl (167 μL of 1 M stock solution), EDTA (24 μL of 0.5 M stock solution), NaCl (334 μL of 5 M stock solution), Triton X-100 (55 μL of 20% (v/v) stock solution), add ddH_2O to 10 mL and autoclave. Immediately before use add, PMSF (5.5 μL of 0.2 M stock solution), leupeptin (11.1 μL of 1 mg/mL), and pepstatin A (11.1 μL of 1 mg/mL) (*see* **Note 6**).
11. Blocking buffer 1 (freshly prepared): 50 mM Tris–HCl (pH 8.0), 200 mM ethanolamine, and 0.1% (v/v) Tween-20. Mix Tris–HCl (1 mL of 1 M stock solution), ethanolamine (4 mL of 1 M stock solution), and Tween-20 (20 μL of 100% stock solution) and add ddH_2O to 20 mL. Adjust to pH 9.0 with 2 M NaOH.
12. Blocking buffer 2 (freshly prepared) (*see* **Note 7**): mix 15 μL of each complementary ssDNA oligonucleotide (100 μM) [14], heat at 95 °C/5 min, cool to RT, and add to 500 μL of ChIP dilution buffer. Add 20 μg of BSA powder.
13. Low salt wash buffer: 20 mM Tris–HCl (pH 8.0), 150 mM NaCl, 0.1% (v/v) Triton X-100, 2 mM EDTA. Mix Tris–HCl (1 mL of 1 M stock solution), NaCl (1.5 mL of 5 M stock

solution), Triton X-100 (50 μL of 100% stock solution), EDTA (200 μL of 0.5 M stock solution), and add ddH_2O to 50 mL.

14. High salt wash buffer: 20 mM Tris–HCl (pH 8.0), 500 mM NaCl, 0.1% (v/v) Triton X-100, 2 mM EDTA. Mix Tris–HCl (1 mL of 1 M stock solution), NaCl (5 mL of 5 M stock solution), Triton X-100 (50 μL of 100% stock solution), EDTA (200 μL of 0.5 M stock solution), and add ddH_2O to 50 mL.
15. LiCl wash buffer: 10 mM Tris–HCl (pH 8.0), 250 mM LiCl, 0.1% (v/v) Nonidet P-40 (NP-40), 0.1% (w/v) sodium deoxycholate, and 1 mM EDTA. Mix Tris–HCl (0.5 mL of 1 M stock solution), LiCl (3.12 mL of 4 M stock solution), NP-40 (250 μL of 20% (v/v) stock solution), sodium deoxycholate (50 mg), and EDTA (100 μL of 0.5 M stock solution) and add ddH_2O to 50 mL.
16. TE buffer: 10 mM Tris–HCl (pH 8.0), 1 mM EDTA. Mix Tris–HCl (0.5 mL of 1 M stock solution), EDTA (100 μL of 0.5 M stock solution) and add ddH_2O to 50 mL.
17. Elution buffer (freshly prepared): 1% (w/v) SDS, 100 mM $NaHCO_3$. Mix SDS (500 μL of 20% (w/v) stock solution) in 8mL of ddH2O, dissolve NaHCO3 (84 mg) add ddH2O to make up to 10 mL.
18. Protein G-agarose beads (Pierce, Thermo Scientific) or GFP_TRAP-agarose (ChromoTek).
19. Proteinase K: 20 mg/mL (Serva).
20. RNase A: 10 mg/mL (Serva).
21. Co-precipitant: Pellet Paint (Novagen, now Merck).
22. 1 M Tris–HCl buffer (pH 6.5): dissolve 12.1 g Tris base in 80 mL ddH_2O, adjust pH with HCl, and make up to 100 mL. Autoclave and store at RT.
23. 2 M Tris–HCl buffer (pH 8.0): dissolve 24.2 g Tris base in 80 mL ddH_2O, adjust pH with HCl, and make up to 100 mL. Autoclave and store at RT.
24. Phenol/chloroform/isoamyl alcohol (25:24:1 v/v) (pH 8.0) (Merck).
25. Chloroform/isoamyl alcohol (24:1 v/v) (Merck).
26. 3 M sodium acetate (NaAc) (pH 5.2): dissolve 24.61 g NaAc in 80 mL ddH_2O, adjust the pH with glacial acetic acid, and make up to 100 mL. Autoclave, store at RT.
27. Refrigerated centrifuges providing $\geq$12,000 $\times$ *g* for Falcon tubes and $\geq$18,000 $\times$ *g* for microcentrifuge tubes.
28. Centrifuge tubes: 1.5 mL, 2 mL, 15 mL, and 50 mL.

29. High Recovery 1.5-mL microcentrifuge tubes (Maxymum Recovery, Axygen, Corning).
30. Liquid nitrogen.
31. Glass funnel.
32. Miracloth.
33. Microscope slides.
34. Sterile filter paper.
35. Curved tip forceps.
36. Spoon.
37. Glass beaker - 250 mL.
38. Magnetic stirrer.
39. Sieve: mesh size 0.3 mm.
40. Vacuum chamber.
41. Sterile environment (hood).
42. Petri dishes: square, 120 × 120 mm.
43. Mortar and pestle.
44. Parafilm.
45. Rotator.
46. Thermoblock for 1.5-mL microcentrifuge tubes (Eppendorf).
47. Sonicator: Bioruptor UCD-200 TM-EX (Diagenode, Denville, USA).
48. Antibodies against the proteins of interest.

3 Methods

3.1 Bimolecular Fluorescence Complementation (BiFC)

BiFC is widely used to detect interactions between two interacting proteins in living cells. The protocol described here is adapted for *A. thaliana* protoplasts [13, 16] but can also be applied to *A. thaliana* culture cells or *Nicotiana tabacum* tobacco culture cells. One protein of interest is fused to the N-terminal part of the fluorescent protein YFP (nYFP) and the second protein to the C-terminal fragment (cYFP). If these two proteins interact in vivo, a fluorescence signal is produced and can be detected by epifluorescence or confocal microscopy. Advantages of this assay are detection not only of direct but also of indirect interactions [17, 18] and indication of the subcellular localization of an interaction.

For cloning genes coding for proteins of interest, the vectors pE3130 pSAT5-DEST-cEYFP-C1(B) and pE3136 pSAT4-DEST-nEYFP-C1 (*see* Subheading 2.1.3) are used. Co-transfection with a Monomeric Red Fluorescent Protein (mRFP) construct (mRFP_VirD2NLS [19] RFP fused with a nuclear localization

signal; or mRFP_AtFibrillarin 1, RFP fused with a nucleolar localization signal [12, 20]) serves as a control of successful transfection and also helps to localize the subcellular compartment where interaction occurs.

3.1.1 DNA Constructs

BiFC assays require a high concentration (≥1 μg/μL) of plasmid DNA, so each sample requires 10 μg of each construct encoding a protein of interest. NucleoBond Xtra Midi/Maxi kits (Macherey-Nagel) are appropriate for isolation of plasmid DNA constructs. Constructs are required coding for:

(a) A transfection control (e.g., mRFP_VirD2NLS or mRFP_AtFibrillarin 1) (*see* **Note 8**).

(b) The protein of interest X fused with the N- or C-terminal part of YFP (e.g., construct coding protein X cloned into pE3136 pSAT4-DEST-nEYFP-C1 or pE3130 pSAT5-DEST-cEYFP-C1(B)).

(c) The protein of interest Y fused with the N- or C-terminal part of YFP (e.g., construct coding protein Y cloned into pE3136 pSAT4-DEST-nEYFP-C1 or pE3130 pSAT5-DEST-cEYFP-C1(B)).

Each experiment requires these samples:

(a) construct coding protein of interest X (cYFP) + construct coding protein of interest Y (nYFP) + Transfection control (mRFP);

(b) construct coding protein of interest Y (cYFP) + construct coding protein of interest X (nYFP) + Transfection control (mRFP);

(c) as a negative control, a construct coding a protein that does not interact with the proteins of interest fused with either nYFP or cYFP. For experiments on plant nuclei and nucleoli, we use the protein AtGAUT10 that does not interact with telomeric proteins.

3.1.2 Isolation of A. thaliana Protoplasts

1. Prepare 6 cm Ø Petri dishes containing 10 mL of protoplasting solution (*see* **Note 9**).
2. Pick 10–20 plant leaves (*see* **Note 10**).
3. Stabilize the adaxial side of leaves (facing toward the stem) with white opaque tape and cut off leaves by scissors.
4. Stick transparent tape to the abaxial side of the leaf and press it slightly [21]. Pull the tape to peel away the lower epidermal surface cell layer.
5. Transfer the leaf to a Petri dish with the peeled side down and in contact with protoplasting solution (*see* **Note 11**).

6. Incubate on a platform shaker at 50–60 rpm in light for 45–90 min or until protoplasts are released. Check the protoplasts by microscopy every 30 min; prolonged digestion will damage them.
7. Transfer the solution into a 15-mL round-bottom Falcon tube (*see* **Note 12**) and pellet the protoplasts at 150 × *g*/5 min/RT. Remove the supernatant carefully by pipette.
8. Wash the protoplasts twice with 10 mL of freshly prepared chilled protoplast washing solution; spin at 150 × *g*/5 min/RT and remove the supernatant carefully by pipette.
9. Add 1 mL of protoplast washing solution and incubate on ice for 30 min. During this incubation, count the protoplasts using a hemocytometer (*see* **Note 13**).

3.1.3 Transfection of Protoplasts

1. Coat the wells of 24-well tissue culture plates with 10% BSA solution (500 µL/well) for at least 30 min at RT.
2. Spin down the protoplasts (150 × *g*/2 min) and resuspend them in MMg solution at a concentration of 3×10^5 protoplasts/mL.
3. Mix 10 µg of each of the three plasmid DNAs (*see* Subheading 3.1.1) in the bottom of a 15-mL round-bottom Falcon tube. Add 200 µL of protoplasts in MMg solution (6×10^4 protoplasts per tube).
4. Add an equal volume (220 µL) of freshly prepared PEG solution and mix the tube contents gently by tapping with a finger or by swirling it slightly. Incubate at RT for 15–25 min (*see* **Note 14**).
5. To stop DNA uptake, gently add 2 mL of protoplast washing solution, rubbing the micropipette tip against the inner wall of the tube. Mix gently by pipetting up and down and pellet the protoplasts at 150 × *g* for 2 min (*see* **Note 15**).
6. Wash the protoplasts gently: add 1 mL of protoplast washing solution, spin at 150 × *g* for 5 min at RT, and discard the supernatant (*see* **Note 16**).
7. Resuspend the protoplasts gently in 600 µL of protoplast washing solution.
8. Remove the BSA solution from the wells of the BSA-coated plate (*see* **step 1**), transfer the protoplasts into the wells, and incubate at RT for 16 h (maximum 18 h) with exposure to white light.
9. To visualize and score protein-protein interactions, mount 10 µL of sample on a microscope slide using a cut-off pipette tip, place a coverslip gently, and observe the signals immediately by epifluorescence with filters for YFP (AlexaFluor 488), RFP (Texas Red), and CY5 (chloroplast autofluorescence) (*see* **Note 17**) (Fig. 1a).

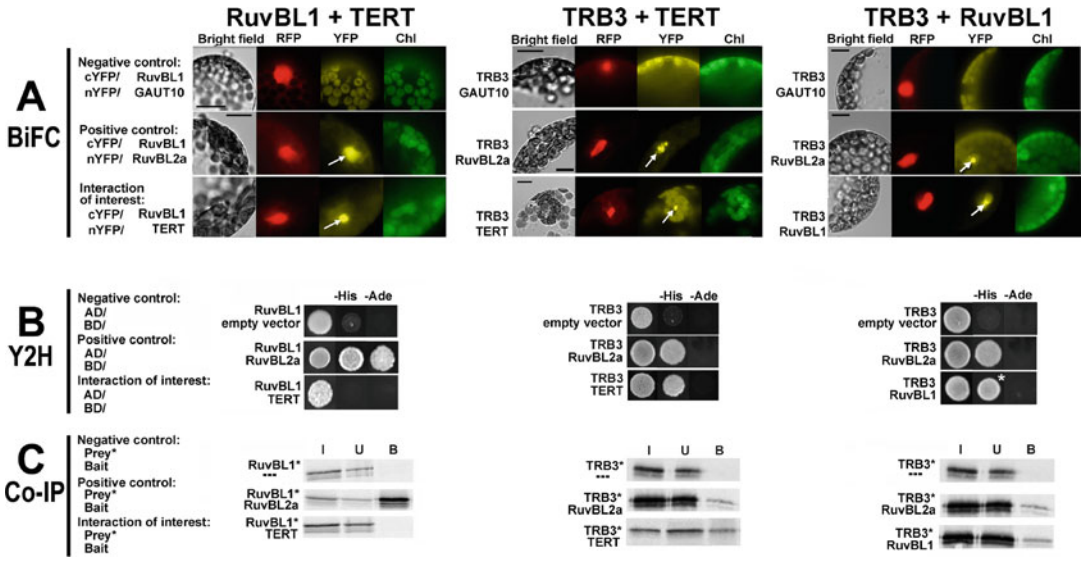

Fig. 1 A comparison of techniques to identify protein-protein interactions. Detection of a trimeric complex where two proteins of interest (TERT and RuvBL1) interact indirectly *via* a protein sandwiched between them (TRB3). Although a clear nuclear interaction between RuvBL1 and TERT is detected using bimolecular fluorescence complementation (**a**), indicating that both proteins are in the same macromolecular complex [13] this interaction is not observed in a yeast two-hybrid system (**b**) or by co-immunoprecipitation (**c**) [13]. On the other hand, direct TERT-TRB3 and RuvBL1-TRB3 interactions are confirmed using all three methods [13, 16] (**a**) For BiFC, *A. thaliana* protoplasts were co-transfected with 10 μg each of plasmids encoding cYFP-tagged or nYFP-tagged RuvBL1, TRB3, or TERT. GAUT10 clones were used as negative control and RuvBL2a as positive control. Left, bright-field images; right, RFP (mRFP-VirD2NLS, red fluorescent protein fused with a nuclear localization signal) labels nuclei and indicates transfection efficiency, and YFP (yellow fluorescent protein) signals indicate specific protein-protein interactions (white arrows). *Chl* chloroplast autofluorescence (green pseudocolor, also visible in the YFP channel). Scale bars = 10 μm. (**b**) For Y2H, two sets of plasmids coding for RuvBL1, TRB3, and TERT proteins (and RuvBL2a as positive control) fused to either the GAL4 activation domain (AD) or the GAL4 DNA-binding domain (BD) were introduced into yeast strain PJ69-4a carrying the reporter genes *His3* and *Ade2*. Co-transformation with an empty vector (AD, BD) served as a negative control. ∗ ±5 mM 3-amino-1,2,4-triazole. (**c**) Co-IP was performed with RuvBL1, TRB3, TERT, and RuvBL2a (as positive control) proteins expressed in TNT-reticulocyte lysates (TNT-RRL) where only prey proteins were radioactively labeled. In the control, the prey proteins were incubated with anti-Myc antibody and protein G-coupled magnetic beads in the absence of a partner protein. Input (I), Unbound (U), and Bound (B) fractions were collected and run in 12% SDS-PAGE gels. ∗^{35}S-labeled prey protein

3.2 Yeast Two-Hybrid System (Y2H)

We base Y2H experiments on the recovery of activity of the transcription factor (TF) GAL4 in living yeast cells, using strains in which reconstitution of a functional TF upstream of a reporter gene leads to the ability to grow on a selective medium. Media lacking leucine and tryptophan are used as selection markers to test for successful transformation. In *S. cerevisiae* PJ69-4A with *HIS3* and *ADE2* reporter genes, *HIS3* allows selection on medium lacking histidine and *ADE2* on medium lacking adenine [15]. The proteins of interest X and Y are fused either with the activating domain (AD) (prey cloned in vector pGADT7-DEST) or the

DNA-binding domain (BD) (bait cloned in vector pGBKT7-DEST) of GAL4, and association of the AD and BD domains forms active TF. Possible protein-protein interactions are reflected by growth of colonies on selective medium lacking leucine, tryptophan, and histidine or lacking leucine, tryptophan, and adenine.

3.2.1 DNA Constructs for Y2H

For isolation of plasmid DNAs coding for the prey and bait proteins, we use GenElute Plasmid Miniprep Kits (Sigma) according to the manufacturer's protocol. The destination vectors pGADT7-DEST and pGBKT7-DEST are used for DNA construct assembly. The concentration of plasmid DNA should be 100–150 ng/μL.

DNA constructs required are:

(a) Construct coding the bait protein of interest in pGBKT7-DEST.

(b) The empty vector (pGBKT7-DEST) as negative control.

(c) Construct coding the prey protein of interest in pGADT7-DEST.

(d) The empty vector (pGADT7-DEST) as negative control.

(e) Constructs coding for positive controls of the bait or prey proteins.

Each experiment requires these samples:

(a) Bait protein X (cloned in pGBKT7-DEST) + prey protein Y (cloned in pGADT7-DEST).

(b) Bait protein Y (cloned in pGBKT7-DEST) + prey protein X (cloned in pGADT7-DEST).

(c) Empty vector as a negative control.

(d) Proper DNA construct as a positive control.

3.2.2 Transformation of Yeast Cells

1. Inoculate 10 mL of YPG liquid medium in a 50 mL Erlenmeyer flask with 1–3 yeast colonies and incubate for 16–18 h at 30 °C with rotation at 200–300 rpm until the stationary phase of growth ($OD_{600} > 1.5$) (*see* **Note 18**).
2. Transfer the culture to 100 mL of YPG liquid medium to give an OD_{600} of 0.2–0.3 and incubate for 3–4 h until the OD_{600} reaches 0.5–1.0 (*see* **Note 19**).
3. Pellet the cells at 2500 × *g*/5 min/RT in 50-mL Falcon tubes, discard the supernatant.
4. Resuspend the cells in 20 mL of sterile ddH_2O, collect them at 2500 × *g*/5 min/RT, and discard the supernatant.
5. Resuspend the cells in 2 mL of freshly prepared 1x TE-LiAc solution, transfer to a 2-mL microcentrifuge tube, centrifuge at 1000 × *g*/2 min, and discard the supernatant.
6. Resuspend the cells in 1 mL of 1x TE-LiAc.

7. Place 100–150 ng of each DNA construct (bait, prey, negative and positive controls) in the bottom of a 2-mL tube, and add 50 μL of competent yeast cells prepared in the previous step.
8. Add 300 μL of PEG-LiAc solution to each tube and incubate at 30 °C/30 min with rotation at 300 rpm.
9. Heat-shock at 42 °C for 20 min with rotation at 300 rpm.
10. Pellet the cells at 1500 × *g*/15 s, remove the supernatant by pipette, and resuspend the cells in 50 μL of 1× TE buffer.
11. Spread each sample on a separate SD-Leu, Trp plate and incubate for 2–3 days at 30 °C to select double transformants (*see* **Note 20**).

3.2.3 Screening for Protein-Protein Interactions

1. Inoculate 3–5 colonies from the control SD-Leu, Trp plates into 300 μL of YPG liquid medium in 2-mL microcentrifuge tubes. Close the tubes with Parafilm and cultivate overnight at 30 °C/300 rpm (*see* **Note 21**).
2. Vortex the cultures and prepare 1:10 and 1:100 dilutions in ddH_2O.
3. Spot 5 μL of the 1:10 and 1:100 dilutions onto SD-Leu, Trp (control); SD-Leu, Trp, His (selection); and SD-Leu, Trp, Ade (selection) plates and incubate for at least 2 days at 30 °C until a positive control appears.

All the yeasts transformed with potential interaction partners have to grow on control plates (SD-Leu, Trp). The SD-Leu, Trp, His and SD-Leu, Trp, Ade plates serve for selection of protein-protein interactions. Colonies indicating strong interaction between proteins of interest grow on both selective media, while those with weaker interaction grow only on histidine-deficient plates (SD-Leu, Trp, His). Because certain baits may self-activate (produce positives without interactions so that negative controls grow), add aminotriazol (a competitive inhibitor of the *HIS3* gene product used as the reporter gene) at 1–10 mM in SD-Leu, Trp, His plates to reduce these false positives (*see* **Note 4**) (Fig. 1b).

3.3 Co-immunoprecipitation (Co-IP) with Two or Three Proteins of Interest

Co-IP is an in vitro method which serves to detect a physical interaction between two or more proteins and can be used to validate interactions observed by Y2H or BiFC. Co-IP is based on co-precipitation of putative prey proteins with a tagged bait protein expressed in an in vitro transcription/translation system. The bait protein is then isolated, via its tag, by an antibody bound to a solid matrix, for example in the case of a c-Myc-tagged bait protein by an anti-c-Myc antibody, and isolated using Protein G-magnetic beads.

The DNA constructs pGBKT7-DEST and pGADT7-DEST (*see* Subheading 3.2.1) contain a T7 promoter located just upstream of the c-Myc- or HA-tag sequence, respectively, and can

thus serve as templates for protein synthesis in a coupled transcription/translation system. Prey proteins (cloned into pGADT7-DEST) are radioactively labeled by ^{35}S-methionine during translation (*see* **Note 22**). In the case of an indirect protein-protein interaction mediated via a linker protein, two radioactively labeled proteins (prey and linker) with an HA-tag are incubated together or sequentially with a c-Myc-tagged (bait) protein that is then pulled down with a solid matrix. The bound proteins are eluted, resolved by SDS-PAGE, and transferred to a nitrocellulose membrane which is exposed to a phosphorimaging screen to detect radioactive polypeptides. Input Unbound, and Bound fractions are collected. The Input fraction serves as a control of protein translation and degradation, the Unbound fraction determines how much of the prey protein remains unbound to the bait protein, and the Bound fraction contains all prey proteins co-purified with the bait protein.

3.3.1 Transcription and Translation

1. Assemble the reaction components in 1.5-mL microcentrifuge tubes according to the manufacturer's protocol for the transcription/translation system (*see* **Note 23**). All operations must be carried out at 4 °C, either in a cold room or on ice.
2. Design of experiments:
   (a) Prey and linker proteins (radioactively labeled): perform 50 µL reactions (*see* **Note 24**).
      - 10 µL plasmid DNA (pGADT7-DEST vector with HA-tag, 100–150 ng/µL).
      - 37 µL TnT Quick Master Mix.
      - 1 µL TnT PCR Enhancer (TNT kit).
      - 30 µCi ^{35}S methionine (TNT kit).

   (b) Bait protein: perform a 25 µL reaction.
      - 5 µL plasmid DNA (pGBKT7-DEST vector with c-Myc-tag, 100–150 ng/µL).
      - 18.5 µL TnT Quick Master Mix.
      - 0.5 µL TnT PCR Enhancer (TNT kit).
      - 1 µL unlabeled methionine (TNT kit) (*see* **Note 25**).
3. Incubate the reactions for 1.5–2 h at 30 °C in a thermomixer at 300 rpm and then place them on ice.
4. Take a 3 µL aliquot from each sample into a 1.5-mL microcentrifuge tube and mix with 3 µL of 2× SDS gel loading buffer as a control of protein expression.

3.3.2 Co-immunoprecipitation

1. Prepare sample and control mixes; radioactively labeled proteins are marked with an asterisk (*see* **Note 26**):

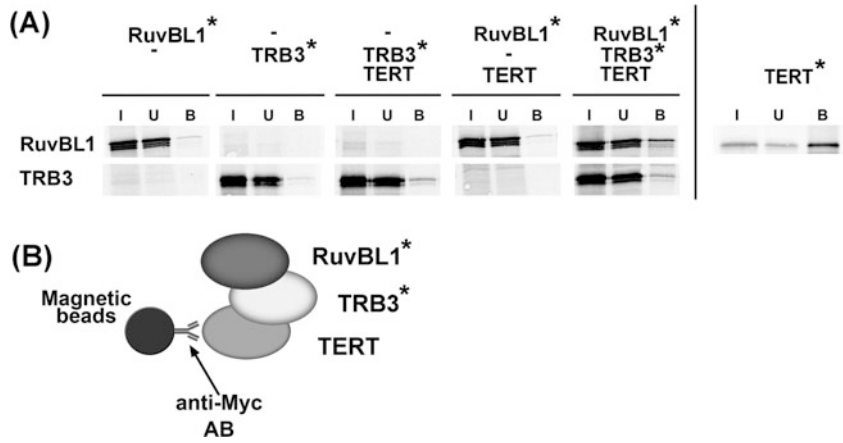

Fig. 2 Co-Immunoprecipitation with three proteins: protein TRB3 can mediate interaction between RuvBL1 and TERT. (**a**) RuvBL1 and TRB3 were labeled by ^{35}S-methionine (asterisks) during expression in a TNT-kit lysate and incubated with non-radioactive Myc-tagged TERT and anti-Myc antibody. In the control samples the proteins were incubated with anti-Myc antibody and protein G-coupled magnetic beads in the absence of one or both partner proteins. Radioactively labeled TERT was expressed in a parallel sample as a control for expression. Input (I), Unbound (U), and Bound (B) fractions were run in 12% SDS-PAGE gels. From the penultimate column it is evident that the presence of TRB3 results in a significant increase in the amount of RuvBL1 in the immunoprecipitated complex. (**b**) Schematic depiction of the putative complex formed by RuvBL1, TRB3, and TERT

   (a) Sample mix: prey∗ (47 μL) + linker∗ (47 μL) + bait (22 μL) + 75 μL 2× Hepes + 0.2 μL anti-c-Myc antibody.
   (b) Negative control mix: use the same amount of ddH_2O instead of prey, linker, or bait (Fig. 2).
2. Parafilm the tubes and incubate overnight with rotation in a cold room or fridge (*see* **Note 27**).
3. Wash the Protein G-magnetic beads (10 μL of slurry per sample; adjust the volume according to the number of samples). Add 100 μL of 1× Hepes buffer for each 10 μL of bead slurry, vortex, centrifuge at 2000 × *g*/5 s, separate beads with a DynaMag Magnet, and remove the supernatant. Repeat this wash three times.
4. After the overnight incubation of the samples, centrifuge at 2000 × *g*/5 s.
5. Input sample: remove 5 μL from the supernatant and from each of the controls and mix with 5 μL of 2× gel loading buffer. Keep on ice, or at −20 °C for longer storage.
6. Add the rest of the overnight reaction to the washed Protein G-magnetic beads and incubate for 1.5–2 h at 4 °C on a rotator (*see* **Note 28**).
7. Centrifuge the samples at 2000 × *g*/5 s.

8. Unbound sample: separate beads with a DynaMag Magnet, take 5 µL and add 5 µL of 2× gel loading buffer. Keep on ice, or at −20 °C for longer storage. Discard the rest of the supernatant.
9. Wash the pellet of beads three times with 1× Hepes buffer: add 300 µL to each tube, vortex, centrifuge at 2000 × *g* for 5 s, separate the beads with the DynaMag magnet, and discard the supernatant.
10. Add 300 µL of 1× Hepes buffer, transfer the bead slurry with a 1-mL pipet into a clean tube, and repeat **step 9** one more time.
11. Bound sample: add 10 µL of 2× gel loading buffer to the dry magnetic beads to elute proteins (*see* **Note 29**).
12. Incubate the Input, Unbound, and Bound samples at 85 °C for 10 min.

3.3.3 Analysis of Radioactively Labeled Immunoprecipitates

1. Load 5 µL of the Input and Unbound samples and the whole Bound sample (without beads) on a precast SDS polyacrylamide gel and perform standard electrophoresis (140 V/1 h).
2. Western blot the proteins onto a nitrocellulose membrane.
3. Cover the membrane with plastic food wrap and place it in a cassette with a storage phosphor screen (*see* **Note 30**).
4. Analyze the exposed storage phosphor screen on a Phosphorimager (Fig. 1c).

3.4 Chromatin Immunoprecipitation Assay (ChIP) for Low-Abundance Proteins

CHIP allows determination of proteinsassociated with specific genomic regions in vivo. Cross-linked DNA-protein complexes from chromatin are sheared to small fragments by sonication and selectively immunoprecipitated by an antibody recognizing a protein of interest.

We have developed a robust ChIP protocol suitable for low-abundance proteins using *A. thaliana* as a model system (*see* **Note 31**), which allows specific isolation of appropriate amounts of even low-abundance proteins. Specific pretreatment of immunosorbent beads allows reduction of the concentration of detergents during the washing steps. The sequence of DNA fragments associated with these proteins can be identified by direct Next-Generation DNA sequencing (ChIP-Seq), quantified by quantitative-PCR (qPCR-), hybridized with specific probes, or investigated with DNA microarrays (ChIP-on-chip). Our method is suitable for isolation of both native proteins using a specific antibody recognizing a protein of interest bound to a Protein G-agarose matrix or of proteins tagged with, for example, GFP, isolated on a GFP-TRAP-agarose matrix bearing covalently coupled small recombinant alpaca antibody fragments.

3.4.1 Preparation of Plant Material and Chromatin Cross-Linking

1. Sterilize *Arabidopsis* seeds: place ~100 μL of them in a 1.5-mL microcentrifuge tube, add 1 mL of 70% EtOH, invert the tube several times, and incubate for 5 min. Discard the supernatant and add 1 mL of 95% EtOH for 15 s. Discard the ethanol and dry the seeds on sterile filter paper in a sterile environment.
2. Sow the seeds on a square Petri dish containing 50 mL of 1/2 MS medium with 1% sucrose and 0.8% plant agar (*see* **Note 32**).
3. After 3 weeks, harvest seedlings from 4 to 5 plates with forceps to yield ~6 g, suitable for three technical replicates. Rinse the seedlings on a sieve with 200 mL of ddH_2O at RT (*see* **Note 33**).
4. Transfer the seedlings into a 250 mL glass beaker on a magnetic stirrer, add 150 mL of 1% formaldehyde, and vacuum infiltrate in a vacuum chamber for 10 min at RT (*see* **Note 34**).
5. Stop the cross-linking by adding 21 mL of 2 M Tris–HCl (pH 8.0) and apply vacuum for an additional 10 min. At this stage the seedlings should appear slightly translucent.
6. Rinse the seedlings on a sieve three times with pre-chilled ddH_2O at 4 °C.
7. Remove water by placing the seedlings on filter paper and transfer to a 50-mL Falcon tube. At this stage the cross-linked material can be frozen in liquid nitrogen and stored at −80 °C, but we recommend to continue immediately with the next step, isolation of nuclei and chromatin.

*3.4.2 Isolation of Nuclei and Chromatin (see **Note 35**)*

1. Precool a mortar and pestle by filling with liquid nitrogen. Place the seedlings and grind them to a fine powder in the rest of the liquid nitrogen.
2. Transfer the powder with a spoon precooled in liquid nitrogen into an ice precooled glass beaker and add 120 mL of nuclei grinding buffer at 4 °C.
3. Filter the mixture through three layers of Miracloth placed in a glass funnel into three 50-mL Falcon tubes and centrifuge the filtrate at 3000 × *g*/20 min at 4 °C. Stop without braking.
4. Decant the supernatant and gently resuspend each pellet in 1 mL of nuclei wash buffer 1 at 4 °C. Pool the resuspended pellets in one 15-mL Falcon tube and rinse the 50-mL tubes with 0.5 mL of nuclei wash buffer 1 to increase the yield of nuclei. Centrifuge the resuspended nuclei at 12,000 × *g*/10 min/4 °C. Repeat this step until any green color disappears.
5. Discard the supernatant, resuspend the yellowish pellet in 1 mL of nuclei wash buffer 2 at 4 °C, and transfer to a 2-mL microcentrifuge tube. Centrifuge at 16,000 × *g*/1 h/4 °C (*see* **Note 36**).

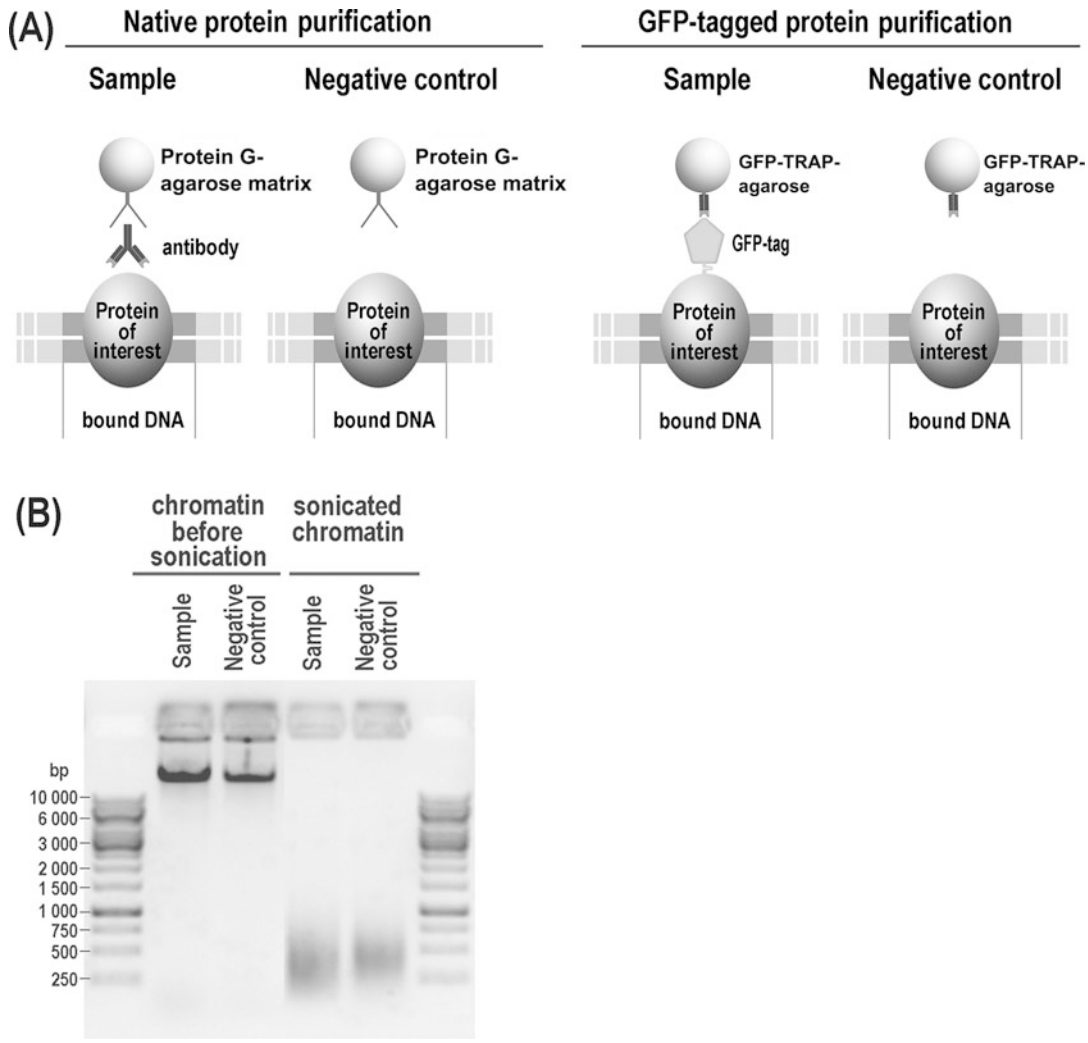

Fig. 3 Chromatin immunoprecipitation (ChIP) assay for low-abundance proteins. (**a**) Two different approaches to ChIP analysis. Left, a native protein of interest bound to DNA is isolated using an antibody followed by a Protein G-agarose matrix; the negative control is a reaction without antibody. Right, alternatively a GFP-tagged protein of interest associated with DNA is isolated using a GFP-Trap matrix. (**b**) DNA from formaldehyde-cross-linked nuclei before (left) or after (right) sonication to an average length of 250–500 bp. DNA from reverse cross-linked chromatin was separated in a 1% agarose gel containing ethidium bromide

6. Remove the supernatant and resuspend the pellet in 1 mL of nuclei lysis buffer at 4 °C by vortexing and pipetting up and down through a cut pipette tip. Transfer the resuspended pellet into a high recovery microcentrifuge tube (*see* **Note 37**). Save a 20 μL aliquot to isolate DNA for analysis on a gel as described in **steps 5–10** of **Subheading 3.4.5** (Fig. 3b).

7. Sonicate the resuspended chromatin to shear the DNA to ~250–500 bp fragments (*see* **Note 38**). The chromatin can be frozen at −80 °C or processed for immunoprecipitation (*see* Subheading 3.4.4).

3.4.3 Preparation of Immunosorbent Beads

Protein G-agarose beads are used to isolate native proteins, or GFP-TRAP-agarose beads for GFP-tagged proteins.

1. Transfer an appropriate amount of bead slurry (*see* **Note 39**) into 1.7-mL high recovery microcentrifuge tubes and centrifuge at 2000 × *g*/1 min/4 °C. Remove the supernatant, add 1 mL of ChIP dilution buffer at 4 °C, and wash the beads with gentle agitation for 30 s. Pellet the beads at 2000 × *g*/1 min/4 °C and remove the supernatant. Repeat this step three times.
2. Spin the beads at 2000 × *g*/1 min/4 °C, remove the supernatant, and add 1 mL of ChIP dilution buffer and 15 μL of antibody (1 mg/mL) against the protein of interest. A negative control without antibody should also be prepared (*see* **Note 40**). Incubate at 4 °C for 2 h with gentle agitation (*see* **Note 41**).
3. Remove the supernatant and wash the beads in 1 mL of ChIP dilution buffer at 4 °C with gentle agitation for 30 s. Pellet the beads at 2000 × *g*/1 min/4 °C, remove the supernatant, and repeat this step three times.
4. Spin the beads at 2000 × *g*/1 min/4 °C, remove the supernatant, and add 500 μL of blocking buffer 1 at 4 °C (*see* **Note 42**). Incubate overnight at 4 °C with gentle agitation.
5. Repeat the washing procedure in **step 3** three times.
6. Pellet the beads at 2000 × *g*/1 min/4 °C, remove the supernatant, and add 500 μL of blocking buffer 2. Incubate for 3 h at 4 °C with gentle agitation.
7. Repeat the washing procedure in **step 3** three times. At the final step, do not remove the supernatant.

3.4.4 Immunoprecipitation

Chromatin from 2 g of seedlings is needed for each sample.

1. Spin the sonicated chromatin from Subheading 3.4.2 at 16,000 × *g*/5 min/4 °C. Remove the supernatant into a new tube and save 20 μL for examination of the sonication efficiency (Fig. 3b).
2. Divide the 1 mL of beads prepared in **step 7** of Subheading 3.4.3 into three 15-mL Falcon tubes (330 μL in each). Pellet the beads at 2000 × *g*/1 min/4 °C and remove the supernatant.
3. To each tube add 3150 μL of ChIP dilution buffer and 350 μL of sonicated chromatin (concentration ~200 ng of DNA/uL).

4. Parafilm the tubes and incubate overnight at 4 °C with gentle agitation.
5. Pellet the beads at 2000 × *g*/1 min/4 °C, remove the supernatant, transfer the beads to a 1.7-mL high recovery microcentrifuge tube, and wash them for 10 min at 4 °C with gentle agitation in 1 mL of each of the following buffers, followed by pelleting them:
   (a) Low salt wash buffer (one wash).
   (b) High salt wash buffer (one wash).
   (c) LiCl wash buffer (one wash).
   (d) TE buffer (two washes).

   After the final wash, remove TE thoroughly.

3.4.5 Elution and Reversal of Cross-Links

1. Release bead-bound complexes by adding 250 μL of freshly prepared elution buffer to the pelleted beads.
2. Vortex briefly and incubate for 15 min at 65 °C with gentle agitation (*see* **Note 43**).
3. Spin 2000 × *g*/1 min and carefully transfer the supernatant to a fresh tube. Repeat elution of the beads and combine the two eluates.
4. To reverse cross-links, add 20 μL of 5 M NaCl to the ~500 μL of eluate and incubate overnight at 65 °C with gentle agitation (*see* **Note 44**).
5. Add 5 μL of RNase A, and incubate at 37 °C for 1 h.
6. Add 20 μL of 1 M Tris–HCl (pH 6.5), 10 μL of 0.5 M EDTA, and 1.5 μL of proteinase K and incubate for 1 h at 45 °C in a thermoblock with gentle agitation.
7. To isolate the DNA, add an equal volume (~530 μL) of phenol/chloroform/isoamyl alcohol and agitate gently for 15 s. Spin at 14,000 × *g*/5 min/RT.
8. Transfer the aqueous phase into a new tube, add 530 μL of chloroform/isoamyl alcohol , and agitate gently for 15 s. Spin at 14,000 × *g*/5 min/RT.
9. Transfer the aqueous phase into a new tube, add 2.5 volumes of ethanol at −20 °C and 1/10 volume of 3 M NaAc, and precipitate DNA for 2 h at −20 °C in the presence of Pellet Paint co-precipitant. Spin at 18,000 × *g*/45 min/4 °C.
10. Wash the DNA pellets with 70% ethanol and spin at 18,000 × *g*/45 min/4 °C.
11. Dry the pellets, resuspend in 50 μL of TE buffer.
12. The DNA may then be analyzed using ChIP-Seq, quantitative-PCR (qPCR) [14], or ChIP-dot-blot assays [16] (*see* **Note 45**).

4 Notes

1. MES with a pH between 5.5 and 5.7 is recommended for isolating protoplasts. Higher or lower pH impacts their quality and stability; for example, protoplasts isolated in solutions containing MES at pH 6.0 are very fragile and can disintegrate quickly.
2. Plants have to be in perfect condition, so avoid stresses (e.g., dry stress, strong light, parasite infections) and the leaves used for experiments must not show any damage. Use non-blooming flowers; the initial buds can be cut off. Avoid anti-parasite chemical treatment of plants or soil, which can compromise protoplast stability.
3. Autoclave medium for SD plates under mild conditions, $\leq$120 °C for 20 min.
4. If self-activation occurs (*see* Subheading 3.2.3), add aminotriazole (3-amino-1,2,4-triazole) to SD-Leu, Trp, His medium. Aminotriazole is a competitive inhibitor of the *HIS3* gene product used as the reporter gene. We use 1 mM, 3 mM, 5 mM, or 10 mM aminotriazole for studies of telomere- and telomerase-associated proteins. Aminotriazole is thermosensitive, so add it just after slight cooling of autoclaved medium.
5. To avoid precipitation, do not mix directly 10× TE buffer with 10× LiAc buffer.
6. The final concentration of ChIP dilution buffer during immunoprecipitation is 15 mM Tris–HCl (pH 8.0), 150 mM NaCl, 1 mM EDTA, 0.1% (v/v) Triton X-100, 0.1 mM PMSF, 1 μg/mL leupeptin, and 1 μg/mL pepstatin.
7. To avoid contamination of subsequent procedures (e.g., next-gen sequencing or hybridization) by nonspecific DNA, we recommend using blocking buffer containing short linear synthetic oligonucleotides with known, non-telomeric sequences instead of sheared salmon sperm DNA [16].
8. Isolate an appropriate amount of plasmids coding for transfection controls, keeping in mind that it is necessary to add this control to every sample.
9. To avoid protoplast rupture which increases with time, perform all isolation steps as quickly as possible (*see* **Note 16**).
10. Protoplasts from older or younger leaves may be more susceptible to rupture. We highly recommend to only pick the leaves in the laboratory after proceeding with **step 1** of Subheading 3.1.2.

11. Peeling the epidermal layer using tape appears to be more gentle and productive for isolation of *Arabidopsis* protoplasts than cutting leaves by a scalpel [22].
12. Falcon 15-mL round-bottom tubes are used for very careful manipulations with protoplasts; do not shake them and avoid rapid movements and shocks. Use only large or trimmed tips for 5-mL or 10-mL pipettes to avoid damage. It is not possible to pellet and wash protoplasts quantitatively in 2-mL microcentrifuge tubes (steps 6-7 of Subheading 3.1.2.), and inappropriate pelleting can cause large losses. If the protoplasts do not sediment, dilute them with a larger volume of washing solution to reduce the viscosity and density and repeat the centrifugation, but do not exceed 200 × g because protoplasts can break up at higher g-forces.
13. Make a tenfold dilution with washing solution to count the protoplasts.
14. The incubation time depends on the age and condition of the plants; younger plants need a shorter incubation than older ones, e.g., transfection time should be ~15 min for 3 weeks old plants but ~25 min for 5 weeks old material.
15. The solution for PEG-mediated DNA uptake is very dense. If the protoplasts do not sediment, dilute them with a larger volume of washing solution as in **Note 12**. Insufficient removal of PEG can lead to protoplast disintegration.
16. Use the microscope to check protoplast integrity. If they are contaminated by cell residues (e.g., chloroplasts), repeat this step. However, too extensive washing may lead to their disintegration.
17. The fluorescence decays over time, so limit the time of exposure.
18. For inoculation, use only fresh yeast already grown on plates: first inoculate from a frozen stock solution on YPG plates and incubate for 2–3 days at 30 °C. Store them at 4 °C and use only fresh (<2 weeks old) plates for inoculation of YPG medium. Incubation of plates at 28 °C instead of 30 °C prolongs the yeast growth for 1–2 days.
19. The OD_{600} should be between 0.5 and 1.0, indicating that the cells are in the log phase of growth. If growth of the overnight culture is slightly retarded, transfer the yeasts into a smaller volume (50 mL) instead of 100 mL and wait until at least one doubling.
20. Plates may be stored for several months at 4 °C as long as the medium does not dry out or become contaminated.
21. Secure the tubes with Parafilm to avoid loss of material in case an increase of internal pressure occurs when opening them.

22. The anti-HA antibodies examined in our laboratory exhibit lower specificity than anti-Myc antibodies, and we therefore recommend using a protein with a Myc-tag as bait (cloned into pGBKT7-DEST) instead of an HA-tagged protein (cloned into pGADT7-DEST). We recommend to radioactively label only the prey protein and to check the translation of the bait protein in a separate tube, to avoid overlapping of their radioactive signals.
23. Reticulocyte lysates (RRL) are often used to express proteins associated with *A. thaliana* telomeric DNA sequences in vitro. Although these proteins are expressed successfully in the TnT Coupled Wheat Germ Extract System (Promega), they show no interactions, including well-established positive controls.
24. The prey and linker proteins can be transcribed/translated in separate tubes or co-transcribed/co-translated in one reaction mix. If a larger quantity of protein is needed, achieve higher yields by performing the transcription/translation reaction in aliquots reaching a maximum volume of 50 μL. Check that both proteins in a co-translation reaction are translated equally.
25. To verify expression of the bait protein, perform a separate reaction and label the bait protein with ^{35}S-methionine.
26. If the mutual interaction of only two proteins is examined, simply avoid the linker protein in the Co-IP reactions.
27. The Parafilm cover of the tubes prevents contamination by ^{35}S-methionine. If the interaction between the proteins is strong enough, incubation for 1.5–2 h is sufficient.
28. If necessary, prolong the incubation; the samples can even be incubated overnight with Protein G-magnetic beads.
29. As most protein-protein interactions between telomere-associated proteins are weak, the elution method with the highest protein recovery (SDS buffer) is chosen.
30. Wrapping the membrane prevents contamination of the screen by radioisotope.
31. This protocol is suitable for proteins expressed and localized in the nucleus of *A. thaliana* seedlings. If the protein of interest is expressed in a different tissue, use the tissue with the highest expression for isolation of nuclei.
32. Cultivation of seedlings on MS medium with agar, in comparison to cultivation on soil covered with Miracloth [23], not only avoids contamination with soil during harvesting but also allows harvesting of entire plants containing shoot and roots. Cultivate on square 120 × 120 mm plates with the seedlings at a 70% angle to support growth of roots on the surface, which enables better seedling collection.

33. The protocol is designed for three technical replicates of one biological sample (i.e., 2 g of seedlings per technical replicate). We recommend to isolate three technical replicates in parallel and to repeat the experiment three times (three biological replicates).
34. To ensure that all floating seedlings are equally submerged in cross-linking solution, place crumpled Miracloth on top of them. Always prepare the formaldehyde solution fresh.
35. All operations must be carried out at 4 °C, either in a cold room or on ice and all solutions should be kept at 4 °C. PMSF, β-ME, leupeptin, and pepstatin should be added immediately before use to minimize their degradation.
36. Verify that the nuclei are intact before adding lysis buffer by dipping a sterile micropipette tip into the pellet and applying a very small amount onto a slide. Add 10 μL of antifade mounting medium containing DAPI and check in a fluorescence microscope whether intact nuclei are present. Do not freeze the isolated nuclei at this step; freezing can aggravate chromatin fragmentation by sonication.
37. High recovery microcentrifuge tubes are recommended to avoid binding and loss of low-abundance proteins when the lysed nuclei are poured onto the plastic tube surface.
38. To obtain the right DNA fragment size after sonicating fixed chromatin is a crucial step, and appropriate conditions have to be found for specific samples on a given sonication device in each laboratory. We ultrasonicate in 150 μL aliquots in high recovery microcentrifuge tubes using a Bioruptor and 16 cycles of 30 s ON at 200 W followed by 30 s OFF. Pausing and a proper amount of ice and cool water are crucial to avoid local sample heating.
39. If native proteins are studied, use a total amount of 240 μL of Protein G-agarose beads for three reactions (in triplicate). If GFP-tagged proteins are purified, use 180 μL of GFP-TRAP-agarose matrix for a triplicate.
40. As additional negative controls, plants that carry particular gene knockouts or null mutations can be used.
41. If the protein of interest possesses a GFP-tag, we recommend to use GFP-TRAP agarose instead of anti-GFP antibody and Protein G-agarose beads. In this case, omit **steps 2** and **3** of Subheading 3.4.3.
42. Ethanolamine blocks nonspecific binding of proteins to the beads.
43. For more efficient elution, secure the lids of tubes by Parafilm and elute at 65 °C in a hybridization oven with gentle rotation.

44. Add 220 μL of 30 mM Tris–HCl (pH 8.0) and 10 μL of 5 M NaCl to the 20 μL aliquots from **step 6** of Subheading 3.4.2 and **step 1** of Subheading 3.4.4. Reverse cross-link in these aliquots using half the recommended amount of all solutions according to **steps 5–11** of Subheading 3.4.5.
45. If the protein of interest is thought to be associated with repetitive DNA sequences, as are for example telomere DNA-associated proteins, use Next-Generation DNA sequencing (ChIP-seq) instead of a DNA microarray (ChIP-on-chip) which is not suitable for detection of homologous repetitive elements.

Acknowledgments

This work was supported by the Czech Science Foundation (project 17-09644S), by the project SYMBIT (reg. no. CZ.02.1.01/0.0/0.0/15_003/0000477) financed by the ERDF, and by the Ministry of Education, Youth and Sports of the Czech Republic under the project CEITEC 2020 (LQ1601).

References

1. Lalonde S, Ehrhardt DW, Loque D, Chen J, Rhee SY, Frommer WB (2008) Molecular and cellular approaches for the detection of protein-protein interactions: latest techniques and current limitations. Plant J 53:610–635
2. Kerppola TK (2009) Visualization of molecular interactions using bimolecular fluorescence complementation analysis: characteristics of protein fragment complementation. Chem Soc Rev 38:2876–2886
3. Schrumpfova PP, Fojtova M, Fajkus J (2019) Telomeres in plants and humans: not so different, not so similar. Cells 8(1)
4. Greider CW, Blackburn EH (1985) Identification of a specific telomere terminal transferase-activity in tetrahymena extracts. Cell 4:405–413
5. Schmidt JC, Cech TR (2015) Human telomerase: biogenesis, trafficking, recruitment, and activation. Genes Dev 29:1095–1105
6. MacNeil DE, Bensoussan HJ, Autexier C (2016) Telomerase regulation from beginning to the end. Genes (Basel) 7(9)
7. de Lange T (2005) Shelterin: the protein complex that shapes and safeguards human telomeres. Genes Dev 19:2100–2110
8. Tayale A, Parisod C (2013) Natural pathways to polyploidy in plants and consequences for genome reorganization. Cytogenet Genome Res 140:79–96
9. Fulcher N, Riha K (2016) Using centromere mediated genome elimination to elucidate the functional redundancy of candidate telomere binding proteins in Arabidopsis thaliana. Front Genet 6:349
10. Schrumpfova P, Kuchar M, Mikova G, Skrisovska L, Kubicarova T, Fajkus J (2004) Characterization of two Arabidopsis thaliana myb-like proteins showing affinity to telomeric DNA sequence. Genome 47:316–324
11. Schrumpfova PP, Schorova S, Fajkus J (2016) Telomere- and telomerase-associated proteins and their functions in the plant cell. Front Plant Sci 7:851
12. Lermontova I, Schubert V, Bornke F, Macas J, Schubert I (2007) Arabidopsis CBF5 interacts with the H/ACA snoRNP assembly factor NAF1. Plant Mol Biol 65:615–626
13. Schorova S, Fajkus J, Zaveska Drabkova L, Honys D, Schrumpfova PP (2019) The plant Pontin and Reptin homologues, RuvBL1 and RuvBL2a, colocalize with TERT and TRB proteins in vivo, and participate in telomerase biogenesis. Plant J 98:195–212
14. Schrumpfová PP, Vychodilová I, Hapala J, Schořová Š, Dvořáček V, Fajkus J. (2016) Telomere binding protein TRB1 is associated with

promoters of translation machinery genes in vivo. Plant Mol Biol 90(1-2):189-206

15. James P, Halladay J, Craig EA (1996) Genomic libraries and a host strain designed for highly efficient two-hybrid selection in yeast. Genetics 144:1425–1436
16. Schrumpfova PP, Vychodilova I, Dvorackova M, Majerska J, Dokladal L, Schorova S, Fajkus J (2014) Telomere repeat binding proteins are functional components of Arabidopsis telomeres and interact with telomerase. Plant J 77:770–781
17. Miller KE, Kim Y, Huh WK, Park HO (2015) Bimolecular Fluorescence Complementation (BiFC) analysis: advances and recent applications for genome-wide interaction studies. J Mol Biol 427:2039–2055
18. Ohad N, Shichrur K, Yalovsky S (2007) The analysis of protein-protein interactions in plants by bimolecular fluorescence complementation. Plant Physiol 145:1090–1099
19. Citovsky V, Lee LY, Vyas S, Glick E, Chen MH, Vainstein A, Gafni Y, Gelvin SB, Tzfira T (2006) Subcellular localization of interacting proteins by bimolecular fluorescence complementation in planta. J Mol Biol 362:1120–1131
20. Pih KT, Yi MJ, Liang YS, Shin BJ, Cho MJ, Hwang I, Son D (2000) Molecular cloning and targeting of a fibrillarin homolog from Arabidopsis. Plant Physiol 123:51–58
21. Lee LY, Gelvin SB (2014) Bimolecular fluorescence complementation for imaging protein interactions in plant hosts of microbial pathogens. Methods Mol Biol 1197:185–208
22. Yoo SD, Cho YH, Sheen J (2007) Arabidopsis mesophyll protoplasts: a versatile cell system for transient gene expression analysis. Nat Protoc 2:1565–1572
23. Bowler C, Benvenuto G, Laflamme P, Molino D, Probst AV, Tariq M, Paszkowski J (2004) Chromatin techniques for plant cells. Plant J 39:776–789

Chapter 12

Macromolecular Crowding Measurements with Genetically Encoded Probes Based on Förster Resonance Energy Transfer in Living Cells

Sara N. Mouton, Liesbeth M. Veenhoff, and Arnold J. Boersma

Abstract

Genetically encoded Förster resonance energy transfer (FRET)-based probes allow a sensitive readout for different or specific parameters in the living cell. We previously demonstrated how FRET-based probes could quantify macromolecular crowding with high spatio-temporal resolution and under various conditions. Here, we present a protocol developed for the use of FRET-based crowding probes in baker's yeast, but the general considerations also apply to other species, as well as other FRET-based sensors. This method allows straightforward detection of macromolecular crowding under challenging conditions often presented by living cells.

Key words Macromolecular crowding, Living cells, Sensors, Genetically encoded probes, Förster resonance energy transfer

1 Introduction

The interior of the cell is highly crowded with macromolecular concentrations in the range between 50 and 400 mg/mL [1, 2]. Macromolecular crowding induces steric effects that affect the diffusion, volumes, and shapes of biomolecules or their assemblies [3]. Most theories predict a decrease in volume of a biomacromolecule, but this depends on the crowder size, shape, and concentration. The decrease in volume is larger when the crowder is smaller than the biomolecule under investigation, but larger than water. Depending on the protein, interactions such as hydrophobic, electrostatic, and hydration effects modulate macromolecular crowding effects [4, 5]. The crowded nature has a major impact on the functioning of a cell, as exemplified by its rapid recovery upon osmotic stress and the regulation of macromolecular crowding [6, 7].

Ronald Hancock (ed.), *The Nucleus*, Methods in Molecular Biology, vol. 2175, https://doi.org/10.1007/978-1-0716-0763-3_12,

Genetically encoded probes have major advantages over chemical probes for intracellular measurements. Chemical probes generally need injection or membrane permeabilization procedures, which can be invasive and alter cellular function. Using a genetically encoded probe, an experimenter can genetically engineer the probe and control its amount and location in the cell by expressing it from an inducible promotor or fusing it to a specific target protein or sorting signal. The new generation fluorescent proteins allow sensitive measurements using fluorescence microscopy, fluorometry, or FACS.

We designed the first genetically encoded fluorescent probes to measure macromolecular crowding [8]. They are based on Förster resonance energy transfer (FRET) [9]. The FRET donor and acceptor are two fluorescent proteins fused by a long linker. Upon placing the probe in a solution with high macromolecular crowding, the probe is compressed. Compression leads to a smaller distance between the fluorescent proteins and concomitantly a higher FRET efficiency [10]. The sensitivity of the probes depends on their size, as well as the size and concentration of the macromolecular crowder. Others and we have applied them in *Escherichia coli*, HEK293 cells and *Saccharomyces cerevisiae* cells. The probes function in compartments such as the nucleus [11] and the endoplasmic reticulum [12], as well as outside cells in dense protein solutions or in gels [13]. An experimenter may probe the FRET efficiency by sensitized emission, but also by fluorescence lifetime measurements [14], single molecule [15] or time-resolved anisotropy [16].

Although execution of experiments is straightforward and widely implementable, working with cells, fluorescent proteins, and genetically encoded probes brings potential systematic errors [17, 18] that can be reduced by the following procedure. This protocol is based on yeast as a model organism, but also applies to other species as well as to other FRET sensors. Thus, following this procedure gives robust measurements of FRET in cells in a straightforward manner.

2 Materials

All solutions should be prepared using deionized water and analytical grade reagents. All reagents can be prepared at room temperature. Follow all regulations for waste disposal. Work with yeast has to be performed under sterile conditions. Clean all surfaces with 70% ethanol and use a Bunsen burner. Follow all safety guidelines for use of Bunsen burners and genetically modified organisms.

2.1 Synthetic Drop-Out Growth Medium Without Histidine

1. Weigh 6.7 g of BD Difco yeast nitrogen base without amino acids and 1.92 g of synthetic drop-out mix without histidine (Sigma). Add 800 mL of deionized water into a beaker of 1 L. Add a clean stirring bar and use a magnetic stirrer. Start adding the yeast nitrogen base and the amino acid mix in intervals until all components are completely dissolved in the water. Filter-sterilize the media in a 1 L bottle using a 0.2 μm bottle-top filter system and a vacuum pump.
2. 10% w/v D-glucose: weigh 100 g of D-glucose and add 800 mL of deionized water to a graduated cylinder. Add a clean stirring bar and use a magnetic stirrer. Add the D-glucose in intervals (*see* **Note 1**). Fill up to the 1 L mark of the cylinder with deionized water. Filter-sterilize this 10% glucose stock using a 0.2 μm bottle-top filter system and a vacuum pump.
3. SD-his, 2% glucose medium: add 200 mL of 10% w/v glucose generated in **item 2**, Subheading 2.1 to the medium generated in **item 1**, Subheading 2.1 to obtain 1 L of synthetic drop-out without histidine medium, supplemented with a final concentration of 2% glucose. Invert the bottle several times to mix the glucose with the medium.

2.2 Hyperosmotic Shock and Imaging

1. High precision glass cover slips with a thickness tolerance of 170 ± 5 μm (Marienfeld, 97922 Lauda-Königshofen, Germany).
2. 50 mM sodium phosphate at pH 7: prepare 160 mL of distilled water in a graduated cylinder. Add 3.10 g of $Na_2HPO_4{\cdot}7H_2O$ and 1.17 g of $NaH_2PO_4{\cdot}H_2O$ to the solution. Adjust the pH if needed by adding HCl or NaOH. Add distilled water until the volume is 400 mL. Prepare fresh before every experiment.
3. 5 M sodium chloride stock solution.
4. Wide-field fluorescence microscope: our experiments were performed on a DeltaVision Elite imaging system (Applied Precision (GE), Issaquah, WA, USA) composed of an inverted microscope (IX-71; Olympus), equipped with a UPlanSApo 100× (1.4 NA) oil immersion objective, InsightSSI solid-state illumination, ultimate focus, and a PCO sCMOS camera, but can be carried out on other wide-field fluorescence microscopes with a controlled temperature chamber, set at 30 °C.
5. Image analysis software: Fiji (https://imagej.net/Fiji).

3 Methods

3.1 Yeast Strain and Sensor Choice

A yeast strain expressing the CrGE2.3 version of the crowding sensor (which is equipped with the fluorophores mEGFP and mScarlet-I) under the strong constitutive TEF1 promoter will give the most reliable results [17]. This strain is derived from the haploid laboratory strain BY4741 (with the genetic background

MATa, his3Δ1, leu2Δ0, met15Δ0, ura3Δ0) where the sensor gene is integrated into the HIS locus, recovering the missing his3 gene. Therefore, this strain can grow without histidine supplementation in the growth medium. Alternatively, the sensor can be expressed from a plasmid (*see* **Note 2**) or under an inducible promoter (*see* **Note 3**), and a sensor with a different FRET couple can be used (*see* **Note 4**). In principle, the protocol can be applied to other species with a few important considerations (*see* **Note 5**).

3.2 Growing Yeast Cells and Expressing the Crowding Sensor

1. Add 5 mL of SD-his, 2% glucose media to a 14 mL culture tube.
2. Sterilize the wire inoculating loop by passing through the flame until the entire length of the wire becomes glowing red/orange from the heat. Do not lay the loop down once it is sterilized or it may become re-contaminated. Wait for the wire to attain its original color.
3. Keep agar plates upside down (lid facing the table surface) to prevent drying of the agar. Take the plate and cool the inoculating loop on an empty spot on the agar plate. Pick a quarter of a single colony to inoculate the 5 mL of medium and start the culture. Incubate overnight at 30 °C with 200 rpm shaking.
4. On the morning of the next day, take 80 μL of the culture and transfer to a 100 mL flask containing 10 mL of fresh medium. Incubate for at least 7 h at 30 °C with shaking at 200 rpm.
5. After 7–8 h, transfer 100 μL of culture using sterile pipette tips and a serological pipette to a cuvette containing 900 μL of water. Mix well with the pipette until the solution becomes homogeneous. Prepare a control cuvette with 900 μL of water and 100 μL of medium that does not contain cells. Measure the optical density of the culture at 600 nm wavelength, using a spectrophotometer. Mark down the value and multiply by 10 to correct for the dilution factor.
6. Calculate the amount of culture needed to obtain an exponentially growing culture on the following day prior to microscopy (*see* **Note 6**).

3.3 Hyperosmotic Shock and Crowding Measurements

Macromolecular crowding can be measured with high spatiotemporal resolution. However, new locations or conditions may provide biochemical or physical mechanisms that alter the readout. Therefore, we recommend calibrating the sensor in the system in which it is measured. The only way to change macromolecular crowding is to apply an osmotic up/downshift in the medium. An upshift reduces water content in the cell through osmosis, increasing the concentration of all cellular components and hence increasing macromolecular crowding.

1. Prewarm the microscopy setup, including the objective and sample stage, 30 min before the start of an experiment. Follow instructions for use of the wide-field fluorescence microscope (*see* **Notes 7** and **8**).
2. Take 1.5 mL of an exponentially growing yeast culture of $OD_{600} = 0.5$ and transfer to a clean 2 mL Eppendorf tube. Centrifuge for 5 min at 3000 × *g*. Remove the supernatant with a pipette without touching the pellet.
3. For measurements of crowding in normal conditions: add 200 μL of fresh prewarmed growth medium to the cells and gently mix with the pipette.
4. For measurements of crowding after hyperosmotic shock: add a solution of 160 μL 50 mM sodium phosphate, pH 7 with 40 μL of 5 M NaCl to achieve a final NaCl concentration of 1 M (adapt this volume to achieve other desired NaCl concentrations) and mix by pipette. As a control, add 200 μL of 50 mM sodium phosphate, pH 7 to a cell pellet and mix gently with the pipette (*see* **Notes 9** and **10**). Proceed immediately to microscopy (*see* **Note 11**).
5. Place 1.2 μL of cells onto a cover slip. Cover carefully with a clean glass microscopy slide. If there are empty corners or air bubbles (which tilt the glass slide and prevent even focus), discard the slide and cover slip and repeat.
6. Place a drop of oil or water with the correct refractive index in the center of the cover slip or directly on the objective. Observe the yeast cells at 100× magnification.
7. Insert the glass slide into the fluorescence microscope and focus with the bright-field mode (*see* **Note 12**). If the microscope has an autofocus function, it could be used at this time (*see* **Note 13**).
8. The following settings (*see* Table 1) apply to a wide-field fluorescence microscopy and the sensor variant crGE2.3 with expression controlled by the TEF1 promoter.

Table 1
Bright-field channel: standard settings

Channel	Excitation wavelength/ bandpass (λ)	Emission wavelength/ bandpass (λ)	Exposure time (ms)	Transmission (%)
Donor (mEGFP [19])	475/28	525/48	25	10
Acceptor (mScarlet-I [20])	575/25	625/45	25	100
FRET	475/28	625/45	25	100

9. The exposure times and transmission time are highly dependent on the instrumentation and those listed here are just a guideline (*see* **Notes 14** and **15**).
10. Acquire 20 *z*-stacks with 0.2 μm spacing for all channels. Begin imaging from the middle of the sample to minimize bleaching in the focal plane that will be used for analysis.
11. Collect images of at least 30 cells for each condition (control and osmotic upshift). Imaging of one slide should not continue for longer than 10 min; if the necessary number of cells in the acquired images is not collected at the end of the 10 min, prepare a new slide.

3.4 Image Data Analysis

1. Download and install Fiji image analysis software [21].
2. Open the software and insert the image file by drag and drop.
3. After the file is open, select a region of interest (ROI) by outlining each cell in the FRET channel. Try to exclude the most outer rim of the cell, for better precision (*see* Fig. 1) (*see* **Note 16**).
4. Measure the fluorescence intensity in each ROI by pressing "m." Press "m" for each fluorescent channel without changing the selection.
5. Select a ROI outside the cell and measure the background fluorescence in each channel.
6. Subtract the average background fluorescence from each channel. To eliminate additional systematic errors we correct for

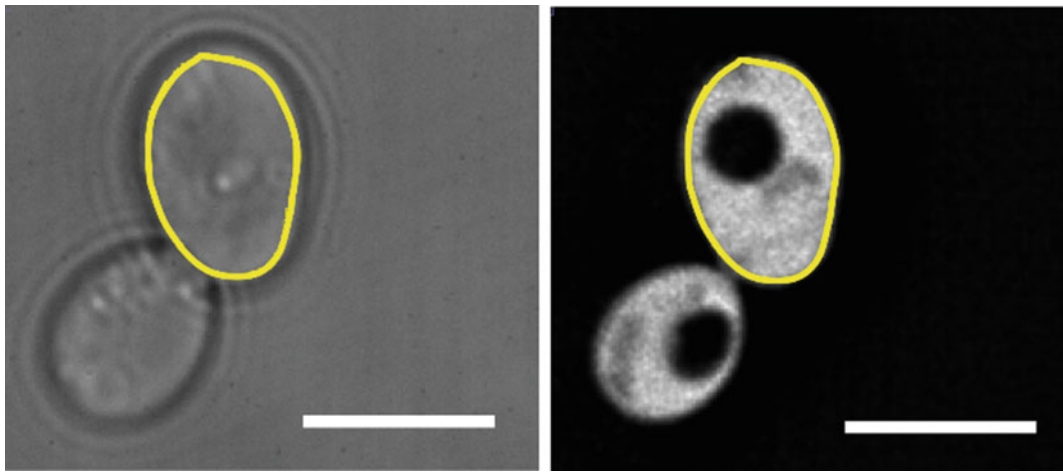

Fig. 1 Typical example of selection of the ROI (yellow line) in the fluorescence channel (right) and superimposed on the bright field (left) for comparison. Displayed is the overexpression of crGE2.3 under the TEF1 promoter. The nonfluorescent disk corresponds to the vacuole. This region can be selected with the cytoplasm and nucleus because it does not influence the final FRET values. Fluorescence (right) is from excitation and emission of mScarlet-I. Scale bar is 5 μm

unequal numbers of donors and acceptors by FRET normalization (N_{FRET}), adapted from [22] (*see* **Notes 17** and **18**):

$$N_{\mathrm{FRET}} = \frac{I_{\mathrm{FRET}}}{\sqrt{I_{\mathrm{donor}} \times I_{\mathrm{acceptor}}}}$$

7. The data can be plotted as box plots before and after osmotic upshift. Additionally, it is informative to plot the N_{FRET} versus the intensity of the acceptor channel to assess for any sensor concentration dependence.

4 Notes

1. If glucose is added at once to the water, it takes very long to dissolve. Adding glucose in intervals allows faster dissolution.
2. The sensor can alternatively be encoded on an episomal or centromeric plasmid. A drawback of plasmids is that they will eventually be lost if the strain is not grown on selective media. Another problem, specific only to episomal vectors, is varying sensor concentration and therefore variability in brightness due to the different copy number of the plasmid. If a centromeric plasmid is used in a haploid strain then this ensures a single copy of the plasmid and more consistent results. However, varying brightness between individual cells can also be beneficial for certain types of experiments. For example, if an experimenter would like to know whether the concentration of the sensor itself is affecting the intracellular crowding levels, bright and dim cells can be compared to establish whether there is difference in the crowding readout. Another advantage of expression from plasmids is that in most model systems (other than yeast) it is practically simpler than genomic integration.
3. Different promoters can be used if inducible expression is desirable. Examples are a galactose-inducible GAL1 promoter or a Cu^{2+}-inducible CUP promoter. It is important to note that work with the galactose promoter requires growth on media with a different carbon source, which inevitably affects cell physiology and potentially crowding levels. Furthermore, inducible expression is often leaky, meaning that low levels of the crowding sensor might be expressed even in conditions where an inducer is lacking. Additionally, inducible expression can exacerbate fluorescent protein maturation artifacts, which can eventually result in false observations. Therefore, we recommend using constitutive expression if the experimental setup allows for it.
4. The crowding sensor has been constructed with different FRET couples (*see* Table 2).

Table 2
Crowding sensors constructed with different FRET couples

Abbreviation	Donor	Acceptor	References
crGE	mCerulean3	mCitrine	[8]
crGE2	mTurquoise2	mCitrine	[11]
crGE2.1	mTurquoise2.1	mCitrine	[11]
crGE2.2	mEGFP	mCherry	
crGE2.3	mEGFP	mScarlet-1	[17]
–	Clover	mRuby	[23]
crH2	acGFP	mCherry	[13]

5. We recommend using the mEGFP-mScarlet-I FRET couple. According to our experience with this FRET couple, it is optimal for use in yeast under various conditions [17]. The original FRET acceptor mCitrine has increased pH sensitivity inside yeast cells, while the FRET donor mCerulean3 matures exceptionally slowly. mEGFP-mScarlet-I alleviates these artifacts, because the two FPs have similar maturation times and pH sensitivity [24]. In addition, these proteins are the brightest in their class. We observed, for example, that measurement with mCherry as an acceptor was hampered by its lack of brightness. Finally, the use of more red-shifted fluorophores reduces phototoxicity and reduces the autofluorescence.
6. This protocol can in principle be applied to any cell type that allows fluorescence measurements, taking into account the media, expression, and handling required for the species involved. In general, we find that small cells such as *E. coli* are more challenging for wide-field measurements, where separate excitations are required to obtain fluorescence, because any small misalignment gives ambiguities in area selection during data analysis. Although such alignments can be improved by calibration, we prefer confocal where the emission of a single laser excitation can be split into two emission channels, which spatially overlap better. We further suggest maintaining expression levels low (e.g., ~10× background intensity determined from cells that overexpress a nonfluorescent protein) to prevent any possible intermolecular FRET. Finally, during measurements all types of cells should be maintained in the environment in which they were cultured. When testing in a new species or environment, we recommend testing multiple different FRET couples to prevent fluorescent protein-specific behavior due to misfolding or oxidation.

7. If the culture on the next day is $OD_{600} > 0.5$ but below 1, dilute to 0.5 OD in a new flask with fresh medium and continue with the experiment. If the density is too low, wait until it reaches at least OD_{600} of 0.4. The density of the culture greatly affects cell physiology and crowding [25]. If the culture is too dilute, then the cells are still in a lag phase and not an exponential growth phase. If the culture density is too high, the nutrient availability in the medium is limited and that leads to metabolic switches and often acidification of the cytosol, which can directly affect the sensor readout. Therefore, it is important to work within a narrow range of culture density (OD_{600} between 0.4 and 0.6) to obtain reliable and reproducible results.
8. If a wide-field microscope is being used, we recommend applying deconvolution, an algorithm often available in the microscope image processing software. It is suitable to use with yeast cells expressing fluorescent biosensors, since it increases the clarity of the signal and thus facilitates ROI selection (*see* Fig. 2).
9. We have also used other methods instead of wide-field microscopy. Fluorescence confocal microscopy on a Zeiss LSM 710 and LSM 780 provided higher resolution in the *z*-axis [8]. Acquiring multiple channels from a single excitation is moreover assisted by a beam splitter, which is advantageous for smaller compartments or cells (*see* **Note 5**). Additionally, we were able to measure fluorescence from the FRET probes in bacterial cells by fluorometry [11].
10. Ideally, there should not be any supernatant left. Any remainder of supernatant will cause carryover of salts and compatible solutes that help cells to recover rapidly (*see* **Note 11**).

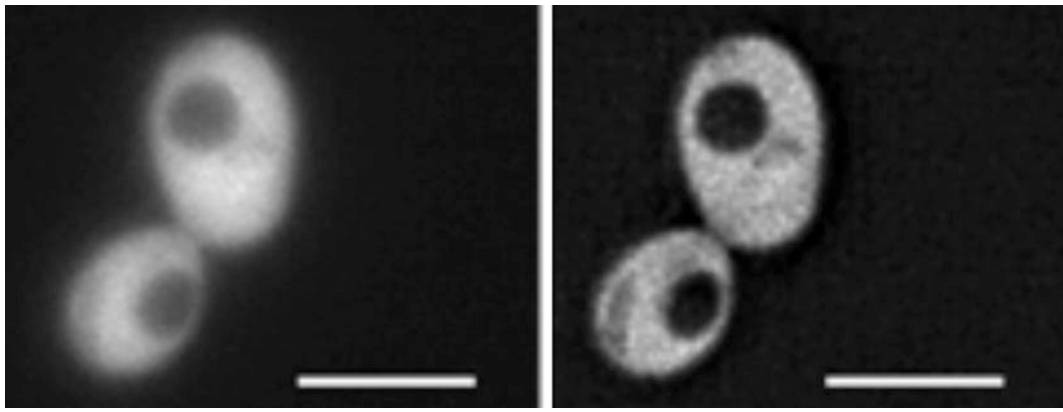

Fig. 2 Comparison of resolution before (left) and after (right) deconvolution of microscopy images. Displayed is fluorescence from excitation and emission of mScarlet-I. For clarity, we increased the thickness of the yellow ROI selection line compared to the original tool selection in Fiji. Scale bar is 5 μm

Although additional washing steps could be performed, keeping the cells in a pellet for too long or subjecting them to multiple centrifugation steps will alter their physiology. All work with live cells should be done maximally fast to avoid altering cell physiology.

11. We find that the Na phosphate solution needs to be prepared fresh before every experiment.
12. Yeast cells have very efficient ways to counteract osmotic upshift, and therefore imaging after induction of hyperosmotic shock needs to be fast. Cells counteract an osmotic upshift by immediate uptake of potassium (<1 min), and this timescale is too fast for a reliable measurement with the protocol described here. Therefore, an osmotic upshift should be measured in the absence of potassium and compatible solutes to prevent rapid recovery. The solution pH should remain buffered. If the presence of potassium is required, one can measure the rapid changes in real time by flow or microfluidics setups, either home-built or commercially available [26].
13. Use the bright field to find the cells without fluorescence to avoid bleaching the fluorescent proteins.
14. We recommend that the focus be already set on a test microscope slide to avoid spending too much time in setting up. Aim at reducing the time for handling and imaging to avoid any physiological changes that might occur due to inducing unfavorable conditions. Handling time should not take longer than a few minutes.
15. We find that these are the optimal imaging settings for our strains and system; however, the exposure needs to be adjusted to the brightness of the cells. The fluorescence signal should be at least three times the background fluorescence and pixel saturation should be avoided, since this causes an inaccurate readout.
16. We find that it is best to keep exposure time the same and vary exposure settings by tuning the transmission. The mEGFP variant is extremely bright compared to the mScarlet-I; we use 10% transmission for mEGFP, and 100% for FRET with mScarlet-I.
17. The Cell Magic Wand tool in Fiji is useful for selection of ROIs.
18. The published equation includes correction for the bleed-through of the donor emission into the FRET channel (b) and cross excitation of the FRET acceptor with the donor excitation wavelength (a):

$$N_{\mathrm{FRET}} = \frac{I_{FRET} - I_{\mathrm{acceptor}} \times a - I_{\mathrm{donor}} \times b}{\sqrt{I_{\mathrm{donor}} \times I_{\mathrm{acceptor}}}}$$

However, because of the spectral separation of mEGFP and mScarlet-I, we find the bleed-through and cross excitation to be minimal and correction is not necessary. However, using FRET pairs with high spectral overlap such as CFP/YFP of the original crGE sensor, these parameters would need to be incorporated.

19. pH-induced fluorescence quenching leads to a different number of fluorescent proteins and the same accounts for the proportion of fully matured sensors. The N_{FRET} renders excellent results, because it compensates for any pH or maturation-induced artifacts while retaining crowding sensitivity [17].

5 Requests for Materials

The genetically encoded probes or strains are available upon request.

Acknowledgments

This work was supported by The Netherlands Organization for Scientific Research Vidi grant (723.015.002) to A.J.B.

References

1. Zimmerman SB, Trach SO (1991) Estimation of macromolecule concentrations and excluded volume effects for the cytoplasm of Escherichia coli. J Mol Biol 222:599–620. https://doi.org/10.1016/0022-2836(91)90499-V
2. Cayley S, Lewis BA, Guttman HJ, Record MT (1991) Characterization of the cytoplasm of Escherichia coli K-12 as a function of external osmolarity. Implications for protein-DNA interactions in vivo. J Mol Biol 222:281–300. https://doi.org/10.1016/0022-2836(91)90212-O
3. Zhou H-X, Rivas G, Minton AP (2008) Macromolecular crowding and confinement: biochemical, biophysical, and potential physiological consequences. Annu Rev Biophys 37:375–397. https://doi.org/10.1146/annurev.biophys.37.032807.125817
4. Cohen RD, Pielak GJ (2017) A cell is more than the sum of its (dilute) parts: a brief history of quinary structure. Protein Sci 26:403–413. https://doi.org/10.1002/pro.3092
5. Gnutt D, Ebbinghaus S (2016) The macromolecular crowding effect - from in vitro into the cell. Biol Chem 397:37–44. https://doi.org/10.1515/hsz-2015-0161
6. Van Den Berg J, Boersma AJ, Poolman B (2017) Microorganisms maintain crowding homeostasis. Nat Rev Microbiol 15:309–318. https://doi.org/10.1038/nrmicro.2017.17
7. Parker JC (1993) In defense of cell volume? Am J Physiol Cell Physiol 265:c1191–c1200. https://doi.org/10.1152/ajpcell.1993.265.5.c1191
8. Boersma AJ, Zuhorn IS, Poolman B (2015) A sensor for quantification of macromolecular crowding in living cells. Nat Methods 12:227–229. https://doi.org/10.1038/nmeth.3257
9. Lakowicz JR (2006) Principles of fluorescence spectroscopy, 3rd edn. Springer, Berlin. https://doi.org/10.1007/978-0-387-46312-4
10. Liu B, Åberg C, van Eerden FJ et al (2017) Design and properties of genetically encoded probes for sensing macromolecular crowding. Biophys J 112:1929–1939. https://doi.org/10.1016/j.bpj.2017.04.004
11. Liu B, Mavrova SN, Van Den Berg J et al (2018) Influence of fluorescent protein maturation on FRET measurements in living cells.

ACS Sens 3:1735–1742. https://doi.org/10.1021/acssensors.8b00473

12. Holcman D, Parutto P, Chambers JE et al (2018) Single particle trajectories reveal active endoplasmic reticulum luminal flow. Nat Cell Biol 20:1118–1125. https://doi.org/10.1038/s41556-018-0192-2
13. Kisley L, Serrano KA, Guin D et al (2017) Direct imaging of protein stability and folding kinetics in hydrogels. ACS Appl Mater Interfaces 9:21606–21617. https://doi.org/10.1021/acsami.7b01371
14. Schwarz J, J Leopold H, Leighton R et al (2019) Macromolecular crowding effects on energy transfer efficiency and donor-acceptor distance of hetero-FRET sensors using time-resolved fluorescence. Methods Appl Fluoresc 7:025002
15. Höfig H, Otten J, Steffen V et al (2018) Genetically encoded Förster resonance energy transfer-based biosensors studied on the single-molecule level. ACS Sens 3:1462–1470. https://doi.org/10.1021/acssensors.8b00143
16. Leopold HJ, Leighton R, Schwarz J et al (2019) Crowding effects on energy-transfer efficiencies of hetero-FRET probes as measured using time-resolved fluorescence anisotropy. J Phys Chem B 123:379–393. https://doi.org/10.1021/acs.jpcb.8b09829
17. Mouton SN, Thaller S, Crane MW et al (2019) A physicochemical roadmap of yeast replicative aging. BioRxiv 858720. https://doi.org/10.1101/858720
18. Algar WR, Hildebrandt N, Vogel SS, Medintz IL (2019) FRET as a biomolecular research tool — understanding its potential while avoiding pitfalls. Nat Methods 16:815–829. https://doi.org/10.1038/s41592-019-0530-8
19. Zacharias DA, Violin JD, Newton AC, Tsien RY (2002) Partitioning of lipid-modified monomeric GFPs into membrane microdomains of live cells. Science 296:913–916. https://doi.org/10.1126/science.1068539
20. Bindels DS, Haarbosch L, Van Weeren L et al (2016) MScarlet: a bright monomeric red fluorescent protein for cellular imaging. Nat Methods 14:53–56. https://doi.org/10.1038/nmeth.4074
21. Schindelin J, Arganda-Carreras I, Frise E et al (2012) Fiji: An open-source platform for biological-image analysis. Nat Methods 9:676–682. https://doi.org/10.1038/nmeth.2019
22. Xia Z, Liu Y (2001) Reliable and global measurement of fluorescence resonance energy transfer using fluorescence microscopes. Biophys J 81:2395–2402. https://doi.org/10.1016/S0006-3495(01)75886-9
23. Gnutt D, Brylski O, Edengeiser E et al (2017) Imperfect crowding adaptation of mammalian cells towards osmotic stress and its modulation by osmolytes. Mol Biosyst 13:2218–2221. https://doi.org/10.1039/c7mb00432j
24. Botman D, de Groot DH, Schmidt P et al (2019) In vivo characterisation of fluorescent proteins in budding yeast. Sci Rep 9:2234. https://doi.org/10.1038/s41598-019-38913-z
25. Delarue M, Brittingham GP, Pfeffer S (2018) mTORC1 controls phase separation and the biophysical properties of the cytoplasm by tuning crowding. Cell 174:338–349.e20. https://doi.org/10.1016/j.cell.2018.05.042. Epub 2018 Jun 21
26. Liu B, Hasrat Z, Poolman B, Boersma AJ (2019) Decreased effective macromolecular crowding in Escherichia coli adapted to hyperosmotic stress. J Bacteriol 201. https://doi.org/10.1128/JB.00708-18

Chapter 13

Analysis of a Nuclear Intrinsically Disordered Proteome

Bozena Skupien-Rabian, Urszula Jankowska, and Sylwia Kedracka-Krok

Abstract

Intrinsically disordered proteins (IDPs) play crucial roles in cell functioning, although they do not possess defined three-dimensional architecture. They are highly abundant in the cell nucleus, and the vast majority of transcription factors (TFs) contain extended regions of intrinsic disorder. IDPs do not respond to denaturing conditions in a standard manner, and this can be used for their separation from structured proteins. Here we describe a protocol for the isolation and characterization of nuclear IDPs in which heat treatment is used for enrichment of IDPs in samples. The whole workflow comprises the following steps: nuclei isolation from HEK293 (human embryonic kidney) cells, protein extraction, enrichment of IDPs, sample preparation for mass spectrometric analysis, liquid chromatography-tandem mass spectrometry (LC-MS/MS) analysis, *in silico* assessment of protein disorder, and Gene Ontology analysis.

Key words Intrinsically disordered proteins, Nuclear proteome, Nuclear subproteome, Transcription factors

1 Introduction

Intrinsically disordered proteins (IDPs) are biologically active molecules that do not possess a defined three-dimensional (3D) structure under physiological conditions [1] and constitute a major component of the so-called dark proteome [2]. Interestingly, such proteins are more prevalent in eukaryotic than prokaryotic proteomes [3], and they are primarily involved in signaling and regulation [1]. Bioinformatic studies have shown that IDPs are especially abundant in the cell nucleus [4–7] and that even 94% of transcription factors (TFs) contain extended regions of intrinsic disorder [8]. TFs represent about 8% of all human genes and about 25% of the human nuclear subproteome [9]. Twenty-nine percent of human TFs are tissue-specific, and these TFs generally occur at lower concentration than TFs found in all tissues [10]. In line with the above, IDPs, especially those playing regulatory roles, appear less abundant than ordered proteins because of an increased decay rates of the mRNAs encoding IDPs, lower rates of IDP protein synthesis, and shorter half-lives of IDPs [11]. Therefore,

Ronald Hancock (ed.), *The Nucleus*, Methods in Molecular Biology, vol. 2175, https://doi.org/10.1007/978-1-0716-0763-3_13,

the functions of many TFs still remain uncharacterized. Importantly, IDPs usually bind multiple partners with high specificity and low affinity [12]. Additionally, many IDPs serve as hubs in cellular protein interaction networks [13]. In the crowded environment of the nucleus, IDPs also play a crucial role in the biogenesis of proteinaceous membrane-less organelles [14].

Due to their lack of rigid 3D structure, high proteolytic sensitivity, propensity for multiple post-translational modifications, and low abundance, the IDPs remain inaccessible for traditional techniques of structural biology and biochemistry. On the other hand, IDPs are resistant to harsh environmental conditions. Unlike globular proteins, IDPs keep their functionality under extreme conditions or almost immediately restore their functional state as soon as normal conditions are restored [15, 16]. IDPs are characterized by highly biased amino acid composition; they are depleted in hydrophobic residues but enriched in charged and polar residues. Thus, in contrast to globular proteins, IDPs fold partially upon an increase in temperature. This effect is attributed to the temperature-driven increase in the strength of hydrophobic interactions [17]. IDPs remain soluble at high temperatures and many of them are resistant to treatment with acids [18]. These features can be used in experimental studies to separate IDPs from structured proteins, as was the case in previous proteomic studies of the intrinsically disordered proteome (IDP-ome) [19–22]. Cortese et al. [19] found that a supernatant after treatment with trichloroacetic and perchloric acid was enriched in IDPs, while Csizmók [22] and Galea [20, 21] employed heat treatment in their research. These studies examined the whole cell IDP-ome. In our research [23] we have focused on IDPs expressed in the cell nucleus and provided experimental evidence that IDPs are overrepresented in nuclei and that nuclear IDPs are enriched in proteins involved in transcription regulation, including TFs [23].

IDPs are commonly involved in human diseases. According to the "disorder in disorders" or D2 concept, when IDPs get out of tight cellular control they easily undergo misfolding, loss of normal function, gain of toxic function, and/or protein aggregation. Particularly, misfolding and aggregation of IDPs accompany neurodegenerative diseases [13].

Here we describe methods we used in the first large-scale experimental analysis of the nuclear IDP subproteome [23]. The workflow begins with isolation of nuclei from HEK293 cells by hypotonic shock, followed by sedimentation in high density sucrose solution for purification. The next step is protein extraction with the use of a high salt buffer. Then, sample enrichment in IDPs with a heat treatment method is described. The protocol also includes sample preparation for mass spectrometric analysis using a filter-aided sample preparation (FASP) approach [24] as well as examples of conditions for liquid chromatography-tandem mass

spectrometry (LC-MS/MS) analysis together with data processing parameters. Our published data [23] were acquired with a micrOTOF–Q II mass spectrometer (Bruker Daltonics), and here we describe measurements with a more state-of-the-art instrument, a Q Exactive (Thermo Fisher). The final steps of the protocol include *in silico* assessment of protein disorder and functional characterization of the identified proteins using Gene Ontology analysis.

2 Materials

2.1 Cell Culture

1. HEK293 cells (ATCC, Manassas, VA, USA).
2. Complete medium: Minimum Essential Medium (MEM) supplemented with 10% fetal bovine serum.
3. Cell culture dishes with a diameter of 150 mm.

2.2 Isolation of Nuclei

1. Cell scraper, 50 mL conical tubes.
2. Phosphate-buffered saline (PBS).
3. Phenylmethylsulfonyl fluoride (PMSF): 100 mM stock solution in isopropanol.
4. Dithiothreitol (DTT): 2 M stock in ultrapure water.
5. Nonidet P-40: was used to prepare nuclei in our report [23] but is no longer available. Suppliers have replaced it by IGEPAL CA-630, described by Sigma as "chemically indistinguishable." Prepare a 10% (v/v) solution in buffer A.
6. Buffer A: 10 mM Tris–HCl pH 7.5, 10 mM NaCl, 3 mM $MgCl_2$, 0.2 mM PMSF, 1 mM DTT. Prepare a solution containing Tris, NaCl, and $MgCl_2$, adjust the pH, and store at 4 °C. Add PMSF and freshly defrosted DTT right before use.
7. Buffer B: 1 mM $MgCl_2$, 1 mM KH_2PO_4, pH 6.5, 320 mM sucrose, 1 mM PMSF. Prepare a solution containing 1 mM $MgCl_2$, 1 mM KH_2PO_4, adjust the pH. Add sucrose while stirring. Store at 4 °C, but only for a maximum of a few days. Add PMSF right before use while stirring. Initial precipitation of PMSF may appear, but stirring should improve solubilization.
8. Buffer C: 1 mM $MgCl_2$, 1 mM KH_2PO_4, pH 6.5, 2.23 M sucrose, 1 mM PMSF. Prepare a solution containing 1 mM $MgCl_2$, 1 mM KH_2PO_4, and adjust the pH. Put the beaker into a container with warm water on a magnetic stirrer and add sucrose while stirring. Store at 4 °C, but only for a maximum of a few days. Add PMSF right before use while stirring. Initial precipitation of PMSF may appear, but stirring should improve solubilization.

9. Ultracentrifuge (e.g., Thermo Scientific Sorvall WX80 with SureSpin 630 17 mL swinging bucket rotor, or similar), ultracentrifuge tubes (*see***Note 1**).
10. Trypan blue solution (0.4% in PBS), glass slides, and cover glasses (*see***Note 2**).

2.3 Isolation of Proteins from Nuclei

1. Protein extraction buffer: 10 mM HEPES, 0.35 M NaCl, pH 7.5, 1 mM EDTA, 1 mM DTT, 0.2 mM PMSF. Prepare a solution containing HEPES and NaCl, adjust the pH, and store at 4 °C. Add EDTA (powder, or from a 100 mM stock solution), DTT (from a freshly defrosted 2 M stock in ultrapure water), and PMSF right before use.
2. Reagents for measurement of protein concentration, e.g., Bradford assay reagent.

2.4 Enrichment of Intrinsically Disordered Proteins

1. Cold acetone (−20 °C).
2. 50 mM ammonium bicarbonate (ABC): take 198 mg of ABC, add ultrapure water to a volume of 50 mL, mix gently. Store at room temperature.
3. Urea solution: 8 M urea in 50 mM ABC. Prepare on the day of use. Add 1 mL of 50 mM ABC into 0.75 g of urea and vortex intensively.

2.5 Sample Preparation for Mass Spectrometric Analysis

1. Urea solution (**item 3** in Subheading 2.4).
2. 2 M stock of DTT in ultrapure water: store aliquots at -20 C, defrost o just before use.
3. Centrifugal concentrator with a 30-kDa membrane cutoff (e.g., Vivacon 500, Sartorius, Göttingen, Germany).
4. Iodoacetamide solution (100 mg/mL): dissolve iodoacetamide in urea solution (**item 3** in Subheading 2.4). Prepare right before use and protect from light.
5. 50 mM ABC (**item 2** in Subheading 2.4).
6. Sequencing-grade trypsin: resuspend in 50 mM ABC. Use an enzyme:protein ratio of 1:100. If you used 60 μg of starting material, prepare trypsin solution at a concentration of 0.8 μg/100 μL. Check the pH using pH test strips, it should be around 8 for proper digestion. Prepare the trypsin solution right before use.
7. 100% trifluoroacetic acid (TFA).

2.6 LC-MS/MS Analysis

1. HPLC vials.
2. Loading buffer: 2% acetonitrile, 0.05% trifluoroacetic acid (TFA) in H_2O.
3. Acetonitrile with 0.05% formic acid.

4. Water with 0.05% formic acid.
5. C18 trap column (e.g., AcclaimPepMap100 C18, Thermo Scientific, ID 75 μm, length 20 mm, particle size 3 μm, pore size 100 Å).
6. C18 analytical column (e.g., AcclaimPepMapRLSC C18, Thermo Scientific; ID 75 μm, length 500 mm, particle size 2 μm, pore size 100 Å).
7. Mass spectrometer coupled with a nanoHPLC (e.g., Q Exactive Quadrupole-Orbitrap, Thermo Fisher) coupled with a nanoHPLC (e.g., UltiMate 3000 RSLCnano System, Thermo Scientific) through a Digital PicoView 550 ion source (New Objective, Woburn, MA, USA).
8. Mass spectrometric data processing tool, e.g., Proteome Discoverer (Thermo Scientific) and database search engine, e.g., Mascot (Matrix Science, http://www.matrixscience.com).

3 Methods

3.1 Cell Culture

1. Seed the HEK293 cells on eight 150-mm ∅ culture dishes (*see* **Note 1**).
2. Grow the cells to confluency in complete medium at 37 °C in an atmosphere containing 5% CO_2.

3.2 Preparation of Cell Nuclei

Work on ice. To avoid losses of cells or nuclei, it is recommended to use pipetting to remove supernatants.

1. Decant a part of the growth medium and scrape the cells into the remaining solution. Collect the cell suspension in a 50 mL conical tube.
2. Centrifuge the cell suspension (300 × *g*, 8 min, 4 °C).
3. Discard the supernatant. Add PBS up to 40 mL and suspend the cell pellet by gentle agitation of the tube. Centrifuge the cell suspension (300 × *g*, 8 min, 4 °C).
4. Repeat **step 3**.
5. Add 40 mL of buffer A. Vortex gently, incubate for 10 min on ice.
6. Add 2.5 mL of 10% Nonidet P-40. Vortex the sample for 10 s and leave it for 3 min on ice.
7. Centrifuge (850 × *g*, 10 min, 4 °C).
8. Discard the supernatant. Add 3.75 mL of buffer B, suspend the pellet by agitation of the tube.
9. Centrifuge (850 × *g*, 10 min, 4 °C).
10. Repeat **step 2**.

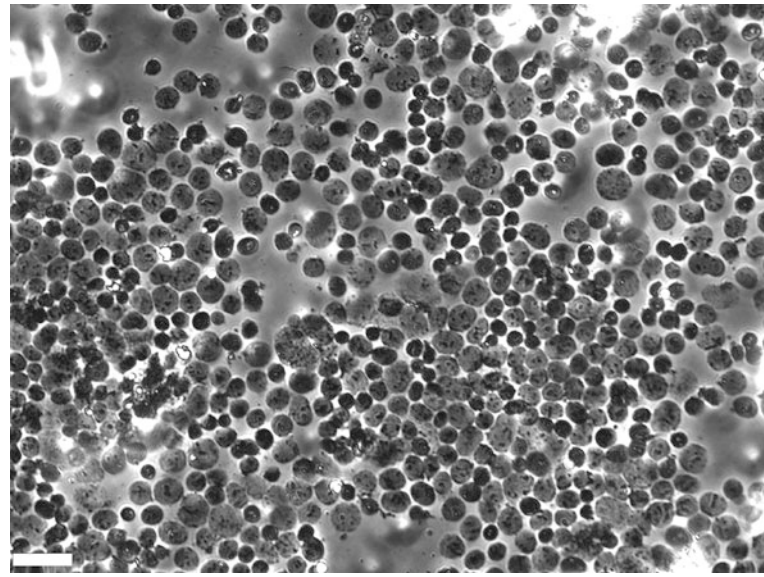

Fig. 1 Representative phase contrast image of isolated nuclei from HEK293 cells. Bar = 50 μm

11. Centrifuge (600 × *g*, 8 min, 4 °C). Discard the supernatant (*see* **Note 2**).
12. Suspend the pellet in 2.7 mL of buffer B by gentle agitation of the tube (*see* **Note 3**).
13. Prepare 13.8 mL of buffer C in a 50 mL conical tube (*see* **Note 4**) and pour the suspension into this tube.
14. Mix the sample by gentle agitation until the sucrose concentration is equalized.
15. Pour the sample into an ultracentrifuge tube and place the tube in a chilled bucket of the swinging bucket rotor.
16. Ultracentrifuge at 53,500 × *g*, 2 h, 4 °C, acceleration/deceleration rates = 9 for the rotor described in **item 7**, Subheading 2.2.
17. Remove the supernatant. Cell nuclei are in the pellet (*see* **Note 5**).
18. Suspend the nuclei in buffer B (a few hundred microliters, as needed) and transfer them into a microcentrifuge tube. Take a few microliters of nuclei suspension for microscopic observation (*see* **Note 6**). Figure 1 presents a representative image of the isolated nuclei.
19. Centrifuge (850 × *g*, 10 min, 4 °C). Discard the supernatant.
20. Proceed to the isolation of proteins from the cell nuclei in the pellet.

3.3 Isolation of Proteins from Cell Nuclei

1. Add 1.2 mL of protein extraction buffer to the pellet of nuclei (*see* **Note 7**).
2. Vortex the sample intensively and incubate it for 25 min on ice. Shake the tube every few minutes during this incubation (*see* **Note 8**).
3. Centrifuge (40,000 × *g*, 20 min, 4 °C).
4. Collect the supernatant (mixture of nuclear proteins).
5. Measure the protein concentration, e.g., with Bradford assay.
6. Conserve a part of the sample (e.g., ~100 μg protein) for analysis of the non-IDP-enriched fraction, store at −80 °C. For the rest of the sample, proceed to IDP enrichment.

3.4 Enrichment of Intrinsically Disordered Proteins

1. Dilute the mixture of nuclear proteins with protein extraction buffer to a concentration of 1 mg/mL.
2. Incubate the sample for 1 h at 98 °C. Then, cool it down by a 15 min incubation on ice.
3. Centrifuge (16,000 × *g*, 30 min, 20 °C).
4. Collect the supernatant, which is a mixture of nuclear proteins enriched in IDPs.
5. Precipitate the proteins in the supernatant (*see* **Note 9**): add six volumes of cold (−20 °C) acetone, vortex intensively, incubate at −20 °C overnight. Centrifuge to collect the protein precipitate (15,000 × *g*, 15 min, 4 °C).
6. Dissolve the proteins in urea solution and store at −80 °C until further processing.

3.5 Sample Preparation for Mass Spectrometric Analysis

The following protocol describes sample preparation using the filter-aided sample preparation (FASP) method [24] and is based on Protocol 1 from the FASP Protein Digestion Kit Use and Storage Instructions (Expedeon, San Diego, CA, USA). However, other procedures for sample preparation for LC-MS/MS analysis may be employed, e.g., the SP3 protocol [25].

1. Take 60 μg of protein mixture and bring it to 300 μL with urea solution.
2. Add DTT to a final concentration of 50 mM. Shake for 15 min at RT.
3. Centrifuge (21,000 × *g*, 15 min, 20 °C) in order to pellet potential precipitates.
4. Transfer the solution into a centrifugal concentrator. Centrifuge (14,000 × *g*, 15 min, 20 °C) (*see* **Note 10**).
5. Add 200 μL of urea solution and centrifuge (14,000 × *g*, 15 min, 20 °C). Discard the flow-through.

6. Add 10 μL of iodoacetamide solution (100 mg/mL) and 90 μL of urea solution. Mix gently by tapping the tube.
7. Incubate for 20 min at room temperature, in the dark. Centrifuge (14,000 × *g*, 10 min, 20 °C).
8. Add 100 μL of urea solution and centrifuge (14,000 × *g*, 10 min, 20 °C).
9. Repeat the preceding step twice. Discard the flow-through.
10. Add 100 μL of 50 mM ABC and centrifuge (14,000 × *g*, 10 min, 20 °C).
11. Repeat the preceding step twice. Do not discard the flow-through.
12. Add 75 μL of trypsin solution (0.8 μg/100 μL, prepared in 50 mM ABC, enzyme to protein ratio 1:100). Mix gently by tapping the tube. Wrap the tube with parafilm to prevent evaporation and incubate overnight at 37 °C for digestion.
13. The next day, transfer the column into a fresh tube and collect peptides in subsequent washing steps.
14. Add 40 μL of 50 mM ABC to the column and centrifuge (14,000 × *g*, 10 min, 20 °C).
15. Repeat the preceding step.
16. Add 50 μL of 0.5 M NaCl and centrifuge (14,000 × *g*, 10 min, 20 °C).
17. Transfer the filtrate containing collected peptides into a fresh tube.
18. Add 2 μL of 100% trifluoroacetic acid (TFA), mix gently by tapping the tube.
19. Analyze directly or store at −20 °C or −80 °C until analysis.

3.6 LC-MS/MS Analysis

This protocol presents an example of peptide separation conditions and the data acquisition method, as well as the instruments and data processing tools.

1. Transfer the peptide mixture into HPLC vials.
2. Load the peptides onto a trap column in the loading buffer at a flow rate of 5 μL/min.
3. Perform peptide separation on analytical column using a 4 h gradient of acetonitrile from 2 to 40% in the presence of 0.05% formic acid at a flow rate of 300 nL/min.
4. Acquire MS signals in a data-dependent mode. Record a full MS spectra in the range of 300–2000 m/z with a resolution of 70,000. Perform up to 12 subsequent MS/MS scans after one full MS scan (Top12 method). Acquire MS/MS spectra with a resolution of 17,500. Set maximum ion injection time (IT) to 120 ms for full MS and to 60 ms for MS/MS scans. Use 30 s of dynamic exclusion for already fragmented peptide ions.

5. Process the collected data with Proteome Discoverer 1.4 (Thermo Fisher Scientific) according to the following workflow:
   (a) Spectrum selection: precursor mass range of 350–5000 Da and signal to noise threshold of 1.5.
   (b) Protein database search: search SwissProt database restricted to *Homo sapiens* taxonomy with the use of the Mascot server (Matrix Science). Use the following parameters: enzyme = trypsin, maximum missed cleavage sites = 1, precursor mass tolerance = 10 ppm, fragment mass tolerance = 20 mmu, dynamic modification = oxidation (M), static modification = carbamidomethyl (C).
   (c) Statistical validation—use the Percolator algorithm [26], set the *q*-value below 1%.
6. Filter the list of proteins obtained: exclude contaminants (e.g., keratins, serum albumin, and trypsin), exclude proteins identified by only one peptide.

3.7 Analysis of Protein Disorder

Among several tools that predict protein disorder (e.g., IUPred [27] or PONDR-FIT [28]), RAPID [6] is a webserver convenient for proteomic-scale analyses.

1. Download fasta files for the list of identified proteins from the UniProt database [29].
2. Upload the fasta files to the RAPID server (http://biomine.cs.vcu.edu/servers/RAPID) and run the prediction.
3. Analyze the RAPID results—classify proteins according to the content of disordered residues (DRs), e.g., up to 25% of DRs and more than or equal to 25% of DRs.

3.8 Gene Ontology Analysis

There are many tools for protein functional characterization. Here, we describe examples of workflows for the GO Term Mapper (Princeton) GO tool, which uses GO Term Finder [30] and map2slim [31] and the DAVID Functional Annotation Tool [32, 33]. The GO Term Mapper allows for searching the uploaded list for proteins that have a given term assigned, while the DAVID Functional Annotation Tool classifies the uploaded list of proteins and identifies enriched annotation terms.

1. Analysis with the GO Term Mapper:
   (a) Go to the GO Term Mapper website:
   - https://go.princeton.edu/cgi-bin/GOTermMapper
   (b) Input gene names of the identified proteins.
   (c) Choose the ontology aspect that you are interested in: Process, Function, or Component.

(d) Choose an organism and annotation databases, e.g., Homo sapiens (GOA @EBI + Ensembl).

(e) Choose ontology, e.g., Generic slim.

(f) Choose output format, e.g., HTML table.

(g) In the advanced options section, input a GO term you are interested in, e.g., nucleus (GO:0005634) or DNA-binding transcription factor activity (GO:0003700). Be consistent with the ontology aspect chosen in point (c) above.

(h) Press the "Search for GO Terms" button.

2. Analysis with the DAVID Functional Annotation Tool:

(a) Go to the DAVID Functional Annotation Tool website:
- https://david.ncifcrf.gov/

(b) Upload UniProtKB accession numbers of the identified proteins as a gene list.

(c) Select species (here: *Homo sapiens*) and background (here: *Homo sapiens* or UniProtKB accession numbers of the proteins identified in a non-enriched sample).

(d) Check annotations you are interested in, e.g., GOTERM_MF_DIRECT. Display Functional Annotation Chart.

(e) Show "Options" and use your thresholds for data filtering. Default thresholds: count: 2, EASE: 0.1; the EASE score is a *p*-value of a modified Fisher's exact test for gene-term enrichment analysis [32].

3.9 Examples of Results

The described protocol was applied to HEK293 cells. The experiment was done in three replicates using cells from subsequent passages. Data for nuclear fractions (N) as well as nuclear fractions enriched in IDPs (N_IDPs) were collected. The content of nuclear proteins in N and N_IDPs samples was estimated at about 76.6% and 81.2%, respectively (Fig. 2). As expected, a higher content of proteins with 25% or more disordered residues (DRs) was found in N_IDPs samples (Fig. 3). The list of proteins identified in a given fraction in three subsequent replications was combined and analyzed with the DAVID Functional Annotation Tool. The N_IDP dataset was analyzed relative to the non-enriched nuclear fraction [the N dataset was used as a background proteome]. Binding was the prevalent molecular function enriched in N_IDPs (Fig. 4).

This function included RNA binding (RNA binding, poly (A) RNA binding, mRNA binding) as well as diverse DNA and chromatin region binding (DNA binding; chromatin binding; transcription regulatory region DNA binding; double-stranded DNA binding; transcriptional repressor activity, RNA polymerase II core promoter proximal region sequence-specific binding), including

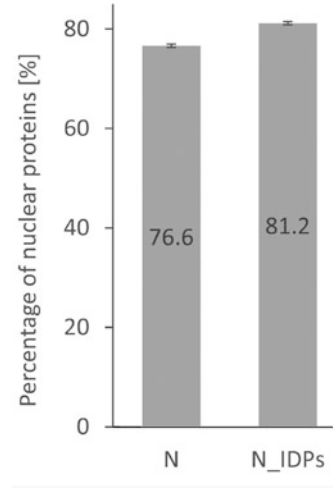

Fig. 2 Nuclear protein content in isolated fractions assigned by the GO Term Mapper. Each list of identified proteins was searched for the nucleus GO term (GO:0005634, cellular component ontology). The difference in the mean values obtained for the fractions is statistically significant (p-value <0.001)

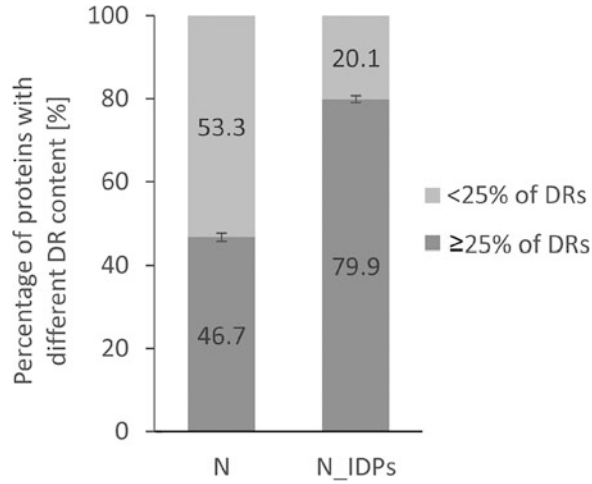

Fig. 3 Classification of proteins according to their content of disordered residues (DRs) predicted by RAPID. The difference in the mean values obtained for the fractions is statistically significant (p-value <0.001)

transcription factors (transcription factor activity, sequence-specific DNA binding). Nucleic acid binding was reported previously as a feature correlated with predicted disorder [7, 34]. The same was found for zinc-finger domains [5] and here we can observe enrichment in zinc-binding proteins in N_IDPs samples. Finally, the function of nucleotide binding was enriched as well. Apart from binding terms, cadherin binding involved in the GO term cell-cell adhesion was also enriched, which is clearly a non-nuclear function

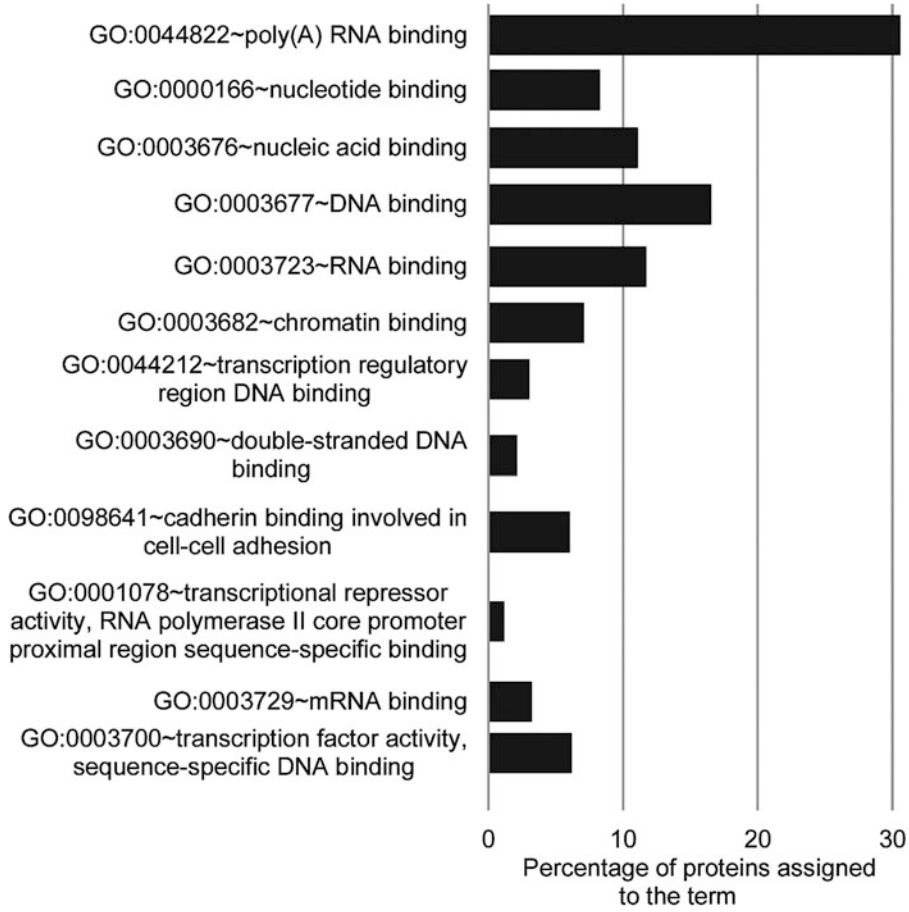

Fig. 4 Results of analysis performed with the DAVID Functional Annotation Tool. The N_IDP dataset was analyzed, while the N dataset was used as a background. A functional annotation chart was displayed for GOTERM_MF_DIRECT and results were filtered for EASE <0.01. Terms are sorted according to EASE score, from the lowest (most significant) at the top to the highest at the bottom

most likely coming from fraction cross-contamination. The content of transcription factors in two nuclear fractions was additionally examined using GO Term Mapper, and as expected a higher percentage of TFs was found in IDP-enriched samples (Fig. 5).

4 Notes

1. Sedimentation of nuclei in high-density solution is an additional purification step that might be omitted for nuclei isolation from cells in culture (after **step 11**, Subheading 3.2, continue with **step 18**, Subheading 3.2), but it is recommended for nuclei isolation from tissue.

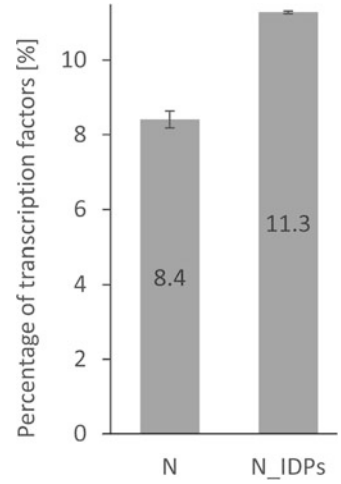

Fig. 5 The content of transcription factors in isolated fractions assigned by the GO Term Mapper. Each list of identified proteins was searched for the DNA-binding transcription factor activity GO term (GO:0003700, molecular function ontology). The difference in the mean values obtained for the fractions is statistically significant (p-value <0.001)

2. Microscopic observation can be performed to confirm that nuclei have been isolated. The following protocol might be applied: (1) mix nuclei suspension with trypan blue solution in a 1:1 ratio; (2) place a drop of the mix on a glass slide and put a cover glass; (3) observe the slide with a light microscope. Note that the osmotic strength of the solution will influence the shape of nuclei. Fluorescent dyes that stain DNA, like DAPI or Hoechst, can be used as well.
3. Eight confluent 150-mm dishes yield about 1.6×10^8 cells. This amount of starting material provides about 1 mg of nuclear proteins and roughly 200 μg of nuclear IDPs.
4. Gentle agitation is recommended to prevent nuclei damage, and it is usually not easy to completely suspend the pellet. The procedure can be continued despite visible white clumps.
5. The buffer volumes are adjusted to the volume of the ultracentrifuge tubes, as these should be completely filled to prevent damage during centrifugation.
6. The pellet of nuclei is rather firm after high-speed centrifugation and sometimes gentle scraping with a pipette tip is needed to collect it. However, careful removal of the supernatant by pipetting is recommended, as part of the pellet might be loosely attached. When a small amount of biological material is used, the pellet may appear as a white ring or small patches close to the bottom of the tube.

7. The volume of protein extraction buffer has to be adjusted to the size of the nuclei pellet. A smaller volume is recommended when less biological material is used.
8. At the step of protein isolation from nuclei, a sonication step may be added to fragment DNA and lower sample viscosity (e.g., Bioruptor UCD-200, Diagenode, Liège, Belgium; 10 min at 320 W, intensity setting high, time interval 30 s ON/30 s OFF).
9. Be careful when changing the method of precipitation of IDP proteins, as they can remain soluble, e.g., when treated with acids [19].
10. If needed, extend centrifugation time during sample preparation with the FASP protocol to ensure complete solution exchange.

Acknowledgments

SKK acknowledges financial support by the Polish National Science Centre [(UMO-2017/25/B/NZ4/01403)]. BSR acknowledges financial support by the Polish National Science Centre (UMO-2017/24/T/NZ3/00294).

References

1. Xie H, Vucetic S, Iakoucheva LM et al (2007) Functional anthology of intrinsic disorder. 1. Biological processes and functions of proteins with long disordered regions. J Proteome Res 6:1882–1898. https://doi.org/10.1021/pr060392u
2. Kulkarni P, Uversky VN (2018) Intrinsically disordered proteins: the dark horse of the dark proteome. Proteomics 18:1–11. https://doi.org/10.1002/pmic.201800061
3. Xue B, Dunker AK, Uversky VN (2012) Orderly order in protein intrinsic disorder distribution: disorder in 3500 proteomes from viruses and the three domains of life. J Biomol Struct Dyn 30:137–149. https://doi.org/10.1080/07391102.2012.675145
4. Ward JJ, Sodhi JS, McGuffin LJ et al (2004) Prediction and functional analysis of native disorder in proteins from the three kingdoms of life. J Mol Biol 337:635–645. https://doi.org/10.1016/j.jmb.2004.02.002
5. Vucetic S, Xie H, Iakoucheva LM et al (2007) Functional anthology of intrinsic disorder. 2. cellular components, domains, technical terms, developmental processes, and coding sequence diversities correlated with long disordered regions. J Proteome Res 6:1899–1916. https://doi.org/10.1021/pr060393m
6. Yan J, Mizianty MJ, Filipow PL et al (2013) RAPID: Fast and accurate sequence-based prediction of intrinsic disorder content on proteomic scale. Biochim Biophys Acta 1834:1671–1680. https://doi.org/10.1016/j.bbapap.2013.05.022
7. Peng Z, Yan J, Fan X et al (2015) Exceptionally abundant exceptions: comprehensive characterization of intrinsic disorder in all domains of life. Cell Mol Life Sci 72:137–151. https://doi.org/10.1007/s00018-014-1661-9
8. Liu J, Permal N, Oldfield CJ et al (2006) Intrinsic disorder in transcription factors. Biochemistry 45:6873–6888. https://doi.org/10.1021/bi0602718
9. Lambert SA, Jolma A, Campitelli LF et al (2018) The human transcription factors. Cell 172:650–665. https://doi.org/10.1016/j.cell.2018.01.029

10. Uhlén M, Fagerberg L, Hallström BM et al (2015) Tissue-based map of the human proteome. Science 347:1260419. https://doi.org/10.1126/science.1260419
11. Gsponer J, Futschik ME, Teichmann SA, Babu MM (2008) Tight regulation of unstructured proteins: from transcript synthesis to protein degradation. Science 322:1365–1368. https://doi.org/10.1126/science.1163581
12. Liu Z, Huang Y (2014) Advantages of proteins being disordered. Protein Sci 23:539–550. https://doi.org/10.1002/pro.2443
13. Uversky VN, Dave V, Iakoucheva LM et al (2014) Pathological unfoldomics of uncontrolled chaos: intrinsically disordered proteins and human diseases. Chem Rev 114 (13):6844–6879. https://doi.org/10.1021/cr400713r
14. Darling AL, Zaslavsky BY, Uversky VN (2019) Intrinsic disorder-based emergence in cellular biology: physiological and pathological liquid-liquid phase transitions in cells. Polymers (Basel) 11:1–23. https://doi.org/10.3390/polym11060990
15. Uversky VN (2013) Unusual biophysics of intrinsically disordered proteins. Biochim Biophys Acta 1834:932–951. https://doi.org/10.1016/j.bbapap.2012.12.008
16. Uversky VN (2019) Intrinsically disordered proteins and their "mysterious" (meta) physics. Front Physiol 7:1–23. https://doi.org/10.3389/fphy.2019.00010
17. Uversky VN (2002) What does it mean to be natively unfolded? Eur J Biochem 269:2–12. https://doi.org/10.1046/j.0014-2956.2001.02649.x
18. Receveur-Bréchot V, Bourhis J-M, Uversky VN et al (2006) Assessing protein disorder and induced folding. Proteins 62:24–45. https://doi.org/10.1002/prot.20750
19. Cortese MS, Baird JP, Uversky VN, Dunker AK (2005) Uncovering the unfoldome: enriching cell extracts for unstructured proteins by acid treatment. J Proteome Res 4:1610–1618. https://doi.org/10.1021/pr050119c
20. Galea CA, Pagala VR, Obenauer JC et al (2006) Proteomic studies of the intrinsically unstructured mammalian proteome. J Proteome Res 5:2839–2848. https://doi.org/10.1021/pr060328c
21. Galea CA, High AA, Obenauer JC et al (2009) Large-scale analysis of thermostable, mammalian proteins provides insights into the intrinsically disordered proteome. J Proteome Res 8:211–226. https://doi.org/10.1021/pr800308v
22. Csizmók V, Szollosi E, Friedrich P, Tompa P (2006) A novel two-dimensional electrophoresis technique for the identification of intrinsically unstructured proteins. Mol Cell Proteomics 5:265–273. https://doi.org/10.1074/mcp.M500181-MCP200
23. Skupien-Rabian B, Jankowska U, Swiderska B et al (2016) Proteomic and bioinformatic analysis of a nuclear intrinsically disordered proteome. J Proteomics 130:76–84. https://doi.org/10.1016/j.jprot.2015.09.004
24. Wiśniewski JR, Zougman A, Nagaraj N, Mann M (2009) Universal sample preparation method for proteome analysis. Nat Methods 6:359–362. https://doi.org/10.1038/NMETH.1322
25. Hughes CS, Foehr S, Garfield DA et al (2014) Ultrasensitive proteome analysis using paramagnetic bead technology. Mol Syst Biol 10:757. https://doi.org/10.15252/msb.20145625
26. Käll L, Canterbury JD, Weston J et al (2007) Semi-supervised learning for peptide identification from shotgun proteomics datasets. Nat Methods 4:923–925. https://doi.org/10.1038/nmeth1113
27. Dosztányi Z, Csizmok V, Tompa P, Simon I (2005) IUPred: web server for the prediction of intrinsically unstructured regions of proteins based on estimated energy content. Bioinformatics 21:3433–3434. https://doi.org/10.1093/bioinformatics/bti541
28. Xue B, Dunbrack RL, Williams RW et al (2010) PONDR-FIT: a meta-predictor of intrinsically disordered amino acids. Biochim Biophys Acta 1804:996–1010. https://doi.org/10.1016/j.bbapap.2010.01.011
29. The UniProt Consortium (2019) UniProt: a worldwide hub of protein knowledge. Nucleic Acids Res 47:D506–D515. https://doi.org/10.1093/nar/gky1049
30. Boyle EI, Weng S, Gollub J et al (2004) GO:: TermFinder - Open source software for accessing Gene Ontology information and finding significantly enriched Gene Ontology terms associated with a list of genes. Bioinformatics 20:3710–3715. https://doi.org/10.1093/bioinformatics/bth456
31. Gene Ontology Consortium (2004) The Gene Ontology [GO] database and informatics resource. Nucleic Acids Res 32:D258–D261. https://doi.org/10.1093/nar/gkh036
32. Huang DW, Sherman BT, Lempicki RA (2009) Systematic and integrative analysis of large gene lists using DAVID bioinformatics resources.

Nat Protoc 4:44–57. https://doi.org/10.1038/nprot.2008.211

33. Huang DW, Sherman BT, Lempicki RA (2009) Bioinformatics enrichment tools: paths toward the comprehensive functional analysis of large gene lists. Nucleic Acids Res 37:1–13. https://doi.org/10.1093/nar/gkn923

34. Xie H, Vucetic S, Iakoucheva LM et al (2007) Functional anthology of intrinsic disorder. 3. Ligands, post-translational modifications, and diseases associated with intrinsically disordered proteins. J Proteome Res 6:1917–1932. https://doi.org/10.1021/pr060394e

Chapter 14

Timing of Cytosine Methylation on Newly Synthesized RNA by Electron Microscopy

Lorena Zannino, Stella Siciliani, and Marco Biggiogera

Abstract

Increasing evidence demonstrates that RNA nucleotides undergo epigenetic modifications, such as methylation on cytosine. Although the presence of modified bases on mRNA has been proven, their molecular significance is largely undefined. We describe here a methodology to dissect the timing of modification of cytosine to 5-methylcytosine (5mC or m^5C) in relation to RNA elongation and processing. To do this we use chlorouridine and iodouridine, two synthetically modified nucleotide bases which can be recognized by RNA polymerase II and incorporated into nascent RNA. These modified bases are added to a cell culture for defined intervals of time, and then immunocytochemical staining using antibodies against the modified nucleotides is carried out. This procedure allows us to identify the range of time in which 5mC is produced in nascent mRNA. This method provides the ultra-resolution of electron microscopy and allows following nascent RNA molecules during their elongation.

Key words Nascent RNA transcripts, 5-Methylcytosine, Ultrastructural localization, Halogenated RNA precursors, Immunocytochemistry, Chromatin, Transmission electron microscopy

1 Introduction

Understanding theprincipal mechanisms underlying regulation of gene expression is one of the major goals for both basic and applied biological research. In this context, the epigenetics of DNA is one of the widely studied topics in recent years. Importantly, among the different kind of epigenetic regulation DNA methylation appears to predominantly trigger the attention of the scientific community. However, the addition of a methyl group on carbon 5 of cytosine is a phenomenon that is not limited to DNA, but also involves different cellular RNAs. RNA methylation appears to be catalyzed by a family of enzymes called RNA methyltransferases, a large series of enzymes divided into subgroups depending on the substrate recognized. Indeed, all types of RNA seem to be methylated, and on each

Lorena Zannino and Stella Siciliani contributed equally with all other contributors.

Ronald Hancock (ed.), *The Nucleus*, Methods in Molecular Biology, vol. 2175, https://doi.org/10.1007/978-1-0716-0763-3_14,

of these the methylation provides a new function which, for some kinds of RNA, still needs to be elucidated [1].

tRNA is a particularly heavily modified class of RNA, and 5mC sites have been identified in numerous archaeal and eukaryotic tRNAs; generally methylation occurs around the variable region and the anticodon loop thanks to the enzyme NSUN2. This modification has been shown to stabilize tRNA secondary structure and codon recognition and to confer metabolic stability [2]. 5mC sites have also been found in rRNA, where they appear to have a role in maintaining translational fidelity and tRNA recognition [3]. Interestingly, in 1975 low levels of internal 5mC were detected in the polyA-containing mRNA of hamster for the first time [4], underlining a putative function of this modification in mRNA also. More recently, it was observed that this modification could be linked to splicing regulation [5] and to the regulation of nuclear export of mRNA [6]. These observations have reignited interest in the occurrence and function of 5mC in mRNA and noncoding RNAs.

Methods to study methylation on DNA are many, such as thin layer chromatography, bisulfite-conversion sequencing, methylated-DNA immunoprecipitation (MeIP), immunofluorescence, and immuno-gold labeling of 5mC [7]. In the case of RNA, the techniques to observe methylation level are 5mC-RNA immunoprecipitation (5mC-RIP), aza-immunoprecipitation (Aza-IP), or immune-gold labeling against 5mC which we described recently [8]. Here we describe a new method to follow methylation of RNA, using a temporal transcriptional window given by the incorporation of two halogenated RNA precursors, chlorouridine and iodouridine (Cl-U and I-U), at different times [9].

2 Materials

Use freshly distilled water for the preparation of reagents.

2.1 Solutions

1. Sörensen buffer: prepare Solution A by dissolving 11.88 g $Na_2HPO_4{\cdot}2H_2O$ in 1 L of dH_2O; prepare Solution B by dissolving 9.08 g of KH_2PO_4 in 1 L of dH_2O. Mix 81.8 mL of Solution A and 18.2 mL of Solution B to obtain the final reagent (pH 7.4).
2. 20% formaldehyde solution (*see***Note 1**): dissolve 1 g of paraformaldehyde in 20 mL of boiling dH_2O under a fume hood, stirring continuously; add some drops of 1 N NaOH to completely dissolve the powder. Store the 20% solution only at 4 °C for 1–2 months (*see***Note 2**). Dilute the 20% solution in Sörensen buffer before use to a final concentration of 4%.
3. Phosphate-Buffered Saline (1× PBS): prepare 10× PBS by dissolving with continuous stirring 2 g of KCl, 2 g of

KH_2PO_4, 80 g of NaCl, and 14.24 g of $Na_2HPO_4{\cdot}2H_2O$ in 1 L of dH_2O. Dilute ten times in freshly distilled water and store at room temperature.

4. 0.5 M NH_4Cl solution: dissolve 0.54 g of NH_4Cl in 20 mL of 1× PBS by gently stirring; store at 4 °C.
5. 2% agarose (*see***Note 3**): add 1 g of agarose slowly with stirring into 50 mL of warm dH_2O; this can be stored at 4 °C.
6. 30%, 50%, 70%, and 90% (v/v) ethanol solutions and absolute ethanol. Store at room temperature.
7. Embedding resin: LR-White (Agar Scientific) (*see***Note 4**).
8. Normal goat serum (NGS): prepare fresh by diluting NGS 1:50 in 1× PBS (*see***Note 5**); do not keep this solution.
9. PBS, 0.05% Tween 20 (PBT): dissolve 50 µL of Tween 20 in 100 mL of 1× PBS.
10. PBS, 0.05% Tween 20, 0.1% BSA (PBTB): dissolve 10 mg of bovine serum albumin (BSA; Grade V) in 10 mL of PBT; the solution can be aliquoted and kept frozen at −20 °C for months and thawed just before use (*see***Note 6**).
11. 1 N NaOH: dissolve 0.4 g of NaOH in 10 mL of dH_2O; keep at RT.
12. 1 mM 5-iodouridine (I-U) (Sigma): dissolve 0.074 g of I-U in 20 mL of dH_2O; store at 4 °C.
13. 4 µM 5-chlorouridine (Cl-U) (BioLog, Bremen, Germany): dissolve 0.056 mg of Cl-U in 50 mL of dH_2O; store at 4 °C.
14. 5% uranyl acetate: aqueous solution.
15. 0.2 M EDTA (for staining): add 7.44 g of Na_2-EDTA to 50 mL of dH_2O, stir continuously and add 1 N NaOH drop by drop until the mixture starts to clarify. Add 1 N NaOH until pH is 7.0, the solution should be transparent. Fill to 100 mL with dH_2O to obtain a 0.2 M solution. Keep for 1 week at 4 °C to stabilize before using; the solution can be kept at 4 °C for months.
16. Lead citrate solution (for staining): prepare 1.33 g of Pb $(NO_3)_2$, 1.76 g of sodium citrate $(Na_3(C_6H_5O_7){\cdot}2H_2O)$, and 30 mL of dH_2O in a 50 mL flask. Shake vigorously for 1 min and stand with intermittent shaking to insure complete conversion of lead nitrate to lead citrate. After 30 min add 8.0 mL of 1 N NaOH, dilute to 50 mL with dH_2O, and mix by inversion to dissolve the lead citrate. The pH is routinely 12.0 and the solution is stable for up to 6 months [10].
17. Terbium citrate solution (for staining): add 5 mL of 0.2 M terbium nitrate (Sigma) dropwise to 5 mL of 0.2 M sodium citrate with continuous stirring. Remove the white precipitate by adding 1 N NaOH drop by drop while gently stirring until

the flocculates dissolve completely; the solution must become transparent. Adjust the pH to 8.2–8.5 with 1 N NaOH and control the pH after 24 h to readjust it if necessary (*see***Note 7**). The staining solution is stable for several weeks at RT.

2.2 Equipment

1. Electron microscope grids: 300 mesh nickel formvar-carbon coated.
2. Tweezers and embryo dishes for rinsing grids.
3. Filter paper to dry grids during the procedure.
4. Parafilm sheet as a support for immunoreactions and staining procedures.

2.3 Antibodies

1. Monoclonal antibodies against bromodeoxyuridine (BrdU) selected for their high affinity for IdUrd (purified mouse anti-BrdU antibody, Becton-Dickinson) or for CldUrd (rat antibody BU1/75 (ICR1) ab6326, Abcam). Each of these antibodies recognizes specifically only one of the two RNA precursors and they do not cross-react [11, 12]. Dilute 1:5 in PBTB.
2. Rabbit polyclonal antibody against 5mC (GeneTex, Irvine, CA, USA): dilute 1:500 in PBTB.
3. Secondary antibodies coupled with colloidal gold particles: 6 nm gold-goat anti-mouse IgG and 12 nm gold-goat anti-rat (Aurion, Wageningen, The Netherlands), and 18 nm gold-goat anti-rabbit (Jackson ImmunoResearch). Dilute 1:20 in PBS.

3 Methods

The procedure is described here for HeLa cells, but any transcriptionally active cells or tissues may be used.

3.1 Sample Preparation

1. Grow HeLa cells in Dulbecco's minimal essential medium (DMEM) supplemented with 10% fetal bovine serum, 1% glutamine, 100 U/mL penicillin and streptomycin, in 25 cm^2 plastic flasks at 37 °C in a 5% CO_2-humidified atmosphere.
2. After trypsinization collect the cells into tubes with 900 μL of medium. Add 100 μL of 1 mM I-U for 15 min at 37 °C followed by centrifugation at 800 × *g*.
3. Replace the medium by fresh medium without precursors for 15 min. Centrifuge the cells for 3 min at 125 × *g* and resuspend them in 0.5 mL of medium containing 4 μM Cl-U for 15 min.
4. Centrifuge the cells for 3 min at 125 × *g* and resuspend them in Sörensen buffer containing 4% paraformaldehyde for 90 min at room temperature (*see***Note 1**).

5. Embed the cells in 2% agar: add warm, molten 2% agar in dH_2O to the cell pellet, allow it to solidify, and remove the pellet from the tube.
6. Dehydrate the agarose block following the schedule: 30% ethanol (2 × 5 min at RT); 50% ethanol (2 × 10 min at RT); 70% ethanol (2 × 10 min at RT); 90% ethanol (2 × 15 min at 4 °C); and then 100% ethanol (3 × 10 min at 4 °C).
7. Embed the cells in LR-White resin for 24 h (not more) at 60 °C.
8. Cut 70–80 nm sections with an ultramicrotome and collect them on 300 Mesh formvar-carbon-coated nickel grids.

3.2 EM Immunocytochemistry

In all the following steps, the grids must be incubated so that the sections are in direct contact with the solution.

1. Float the grids on a drop of NGS diluted 1:100 in PBS for 3 min at RT on a parafilm sheet.
2. Remove excess NGS with a filter paper and incubate the grids overnight at 4 °C in a humid chamber with the primary antibodies diluted 1:5 in PBTB in the same reaction mix.
3. The following day, fill two embryo dishes with PBT and another two with PBS.
4. Blot the grids with filter paper to remove excess solution and rinse the sections twice with PBT for 5 min.
5. Repeat the washing using 1× PBS (*see***Note 8**). Do not forget to blot the grids when they are moved from one vessel to another. Avoid drying the grids: this disturbs the binding of the primary antibody.
6. Float the grids on a drop of NGS diluted 1:50 in PBS for 3 min at RT on a parafilm sheet.
7. Incubate the grids with the secondary antibodies coupled to colloidal gold particles which specifically recognize the primary antibodies against I-U or Cl-U for 30 min at RT. Both secondary antibodies are diluted 1:20 in PBS in the same reaction mix.
8. Rinse the sections twice with 1× PBS for 5 min and then twice with dH_2O for 5 min at RT.
9. Float the grids on a drop of NGS diluted 1:50 in PBS for 3 min at RT on a parafilm sheet.
10. Remove the excess NGS with a filter paper and incubate the sections overnight at 4 °C with the anti-5mC antibody diluted 1:500 in PBTB.
11. Blot the grids with filter paper to remove excess solution and rinse the sections twice with PBT for 5 min.

12. Repeat the washing using 1× PBS (*see***Note 8**). Do not forget to blot the grids when they are moved from one vessel to another.
13. Float the grids on a drop of NGS diluted 1:50 in PBS for 3 min at RT on a parafilm sheet.
14. Incubate the grids for 30 min at RT with the secondary antibody against 5mC coupled with 18 nm colloidal gold.
15. Rinse the sections twice with 1× PBS for 5 min and then twice with dH_2O for 5 min at RT.
16. Allow the grids to dry for at least 30 min before staining.

3.3 Staining

1. Sections are stained with the regressive EDTA technique for ribonucleoproteins [13] with the following steps. Place the grids with the sections facing down and do not forget to thoroughly rinse them after each incubation, especially after the lead citrate (*see***Note 9**).
2. Incubate in uranyl acetate for 2 min.
3. Incubate in EDTA for 30 s to remove uranyl from DNA (*see***Note 10**).
4. Incubate in lead citrate for 2 min.
5. Allow to dry for at least 30 min.
6. If desired, following this procedure sections can be stained with terbium citrate which contrasts RNA, in order to highlight the RNA nascent fibrils. This staining shows a high precision despite its very low contrast [14, 15] (*see***Note 11**). Float the specimen on a 50 µL drop of terbium citrate on parafilm for 30 min at RT. Without drying, wash the grid in 100–150 µL drops of dH_2O for 10 s and immediately afterwards for 5 s at RT. Allow to dry for at least 30 min.

3.4 Analysis of Antibody Distribution

The samples are observed in a transmission electron microscope operating at 80–120 kV. In the nucleus, areas of condensed chromatin (heterochromatin) are clearly visible, as well as euchromatic zones where chromatin is looser. Moreover, in the perichromatin region near the periphery of heterochromatin it is possible to observe RNA fibrils termed perichromatin fibrils (PF). The presence of Cl-U or I-U is negligible in the cytoplasm: a very weak labeling is present due to the fact that the antibody can also recognize the free halogenated bases.

By evaluating the incorporation of the two precursors, we can define a temporal transcription window in which RNA methylation occurs. For instance, if the PF are marked with 5mC and only one of the two halogenated markers, in particular Cl-U, we can say that the methylation already occurred in those PFs transcribed very early (in less than 15 min). On the other hand, if the methylation label

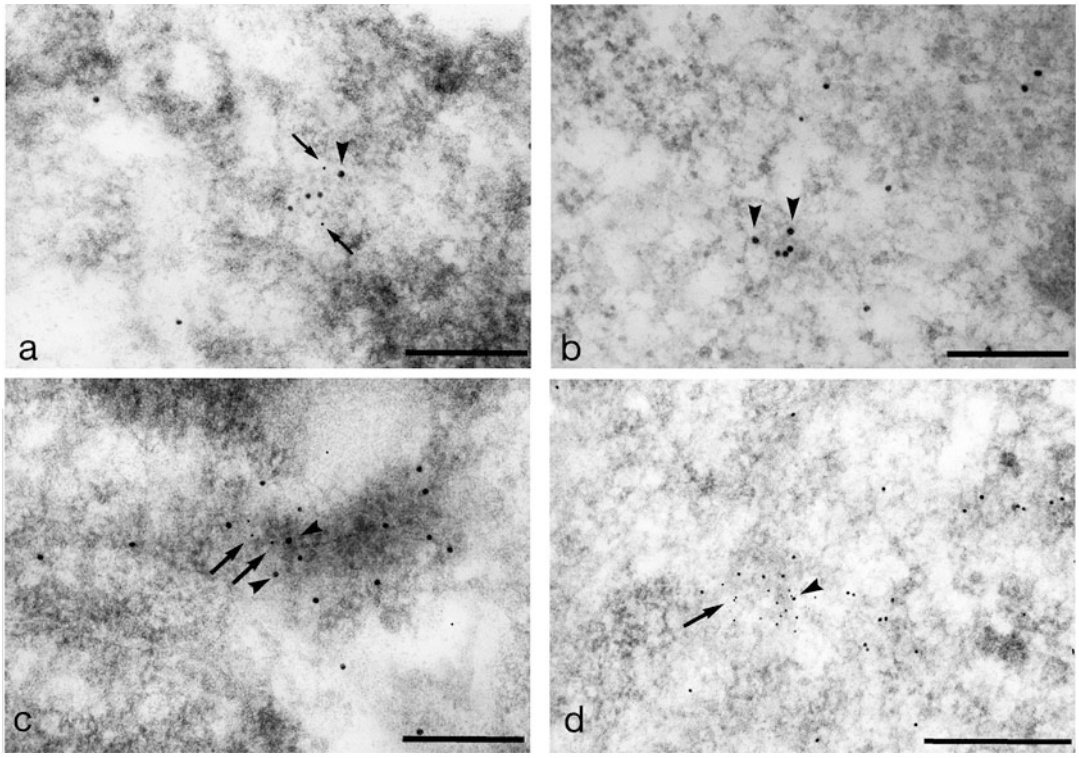

Fig. 1 Sections of Hela cells stained with the EDTA-regressive technique. (**a**) Triple labeling: 5mC (18 nm dots, arrowheads) co-localizes with I-U (6 nm dots, arrows) and with Cl-U (12 nm dots). Bar = 200 nm. (**b**) 5mC (18 nm dots, arrowheads) co-localizes with Cl-U (12 nm dots). Bar = 200 nm. (**c**) 5mC (18 nm dots, arrowheads) co-localizes with both Cl-U (12 nm dots) and I-U (6 nm dots, arrows). Bar = 200 nm. (**d**) Double labeling. Cl-U (12 nm dots, arrows) and 5mC (18 nm dots, arrowheads). Bar = 500 nm. The contrast of the 6 nm gold particles was enhanced by using Paint Shop Pro software

appears together with both markers we can conclude that methylation also occurs tardively on those PF transcribed in more than 15 min (*see* Fig. 1). The advantage of this technique is the possibility to reveal 5mC on nascent or mature RNA by double/triple labeling with specific RNA precursors, performed at very high resolution by electron microscopy. This allows one to observe single RNA fibrils, their modification, and the time of their synthesis.

4 Notes

1. Paraformaldehyde fixation is preferred for immunocytochemistry because it modifies antigens less, avoiding false negative results due to alteration of epitopes. Glutaraldehyde at even low concentrations can leave free aldehyde groups which cause

false positive results. The use of paraformaldehyde only is therefore mandatory.

2. Check the possible presence of precipitates in the fixative solution: in this case, discard it and prepare fresh fixative.
3. This is only necessary when working with isolated cells.
4. The use of acrylic resins instead of epoxy resins may allow better antigen retrieval for immunocytochemistry: in fact, epoxy resins form smooth sections in which epitopes are less exposed. If necessary, activate LR-White resin by adding benzoyl peroxide catalyst as specified by the supplier and store at 4 °C.
5. The NGS concentration can be modulated if necessary according to the type of background signal.
6. As for NGS, the BSA concentration in which the primary antibody is diluted can be increased to correct the background signal. Discard the PBTB solution if precipitates are found to avoid their deposition on sections and possible false negative results.
7. At pH lower than 8.0, terbium precipitates are formed within 2–3 days. Therefore, it is very important to check the pH after 24 h and the possible presence of precipitates before use.
8. The number and timing of the rinses can be increased to facilitate the removal of background.
9. When lead citrate is used, we recommend to avoid the formation of bubbles and to increase the number of washes to avoid and remove lead precipitates.
10. The EDTA incubation time can be changed to obtain correct chromatin bleaching, considering the type of sample, the section thickness, and the temperature.
11. Basic water (pH 9) can be used to increase terbium contrast; however, it seems to us that then the staining is less stable (unpublished data). The washing step is the most critical in this procedure due to the weak binding of Tb to RNA; therefore, longer rinsing and blotting are not recommended.

Acknowledgments

The authors would like to thank Ms. Francine Flach and Ms. Gloria Milanesi for excellent technical skill in preparing the ultrathin sections. This research was supported by the Italian Ministry of Education, University and Research (MIUR): Dipartimenti di Eccellenza Program (2018–2022)—Dept. of Biology and Biotechnology "L. Spallanzani," University of Pavia (to M.B.).

References

1. Motorin Y, Lyko F, Helm M (2009) 5-methylcytosine in RNA: detection, enzymatic formation and biological functions. Nucleic Acids Res 38:1415–1430. https://doi.org/10.1093/nar/gkp1117
2. Schaefer M, Pollex T, Hanna K et al (2010) RNA methylation by Dnmt2 protects transfer RNAs against stress-induced cleavage. Genes Dev 24:1590–1595. https://doi.org/10.1101/gad.586710
3. Chow CS, Lamichhane TN, Mahto SK (2007) Expanding the nucleotide repertoire of the ribosome with post-transcriptional modifications. ACS Chem Biol 2:610–619. https://doi.org/10.1021/cb7001494
4. Dubin DT, Taylor RH (1975) The methylation state of poly A-containing messenger RNA from cultured hamster cells. Nucleic Acids Res 2:1653–1668. https://doi.org/10.1093/nar/2.10.1653
5. Young JI, Hong EP, Castle JC et al (2005) Regulation of RNA splicing by the methylation-dependent transcriptional repressor methyl-CpG binding protein 2. Proc Natl Acad Sci U S A 102:17551–17558. https://doi.org/10.1073/pnas.0507856102
6. Dominissini D, Rechavi G (2017) 5-methylcytosine mediates nuclear export of mRNA. Cell Res 27:717–719. https://doi.org/10.1038/cr.2017.73
7. Masiello I, Biggiogera M (2017) Ultrastructural localization of 5-methylcytosine on DNA and RNA. Cell Mol Life Sci 74:3057–3064. https://doi.org/10.1007/s00018-017-2521-1
8. Masiello I, Biggiogera M (2019) Electron microscope detection of 5-methylcytosine on DNA and RNA. Methods Mol Biol 1870:165–177. https://doi.org/10.1007/978-1-4939-8808-2_12
9. Spedito A, Cisterna B, Malatesta M et al (2014) Use of halogenated precursors to define a transcription time window after treatment with hypometabolizing molecules. Histochem Cell Biol 141:243–249. https://doi.org/10.1007/s00418-014-1180-7
10. Reynolds ES (1963) The use of lead citrate at high pH as an electron-opaque stain in electron microscopy. J Cell Biol 17:208–212. https://doi.org/10.1083/jcb.17.1.208
11. Jaunin F, Visser AE, Cmarko D, Aten JA, Fakan S (1998) A new immunocytochemical technique for ultrastructural analysis of DNA replication in proliferating cells after application of two halogenated deoxyuridines. J Histochem Cytochem 46:1203–1209
12. Vecchio L, Solimando L, Biggiogera M et al (2008) Use of halogenated precursors for simultaneous DNA and RNA detection by means of immunoelectron and immunofluorescence microscopy. J Histochem Cytochem 56:45–55. https://doi.org/10.1369/jhc.7A7225.2007
13. Bernhard W (1969) A new staining procedure for electron microscopical cytology. J Ultrastruct Res 27:250–265. https://doi.org/10.1016/S0022-5320(69)80016-X
14. Biggiogera M, Fakan S (1998) Fine structural specific visualization of RNA on ultrathin sections. J Histochem Cytochem 46:389–395
15. Biggiogera M, Masiello I (2017) Visualizing RNA at electron microscopy by terbium citrate. In: Pellicciari C, Biggiogera M (eds) Histochemistry of single molecules, 1st edn. Springer, Pavia, pp 277–283

Chapter 15

The Nucleus of Intestinal Cells of the Bacterivore Nematode *Caenorhabditis elegans* as a Sensitive Sensor of Environmental Pollutants

Annette Piechulek, Lutz Berwanger, Peter Hemmerich, and Anna von Mikecz

Abstract

Prevalent environmental challenges are climate change, the biodiversity crisis, and the global scale of environmental pollution. We identified the cell nucleus as a sensitive sensor for bio-effects of pollutants such as mercury and nanoparticles. As a major route of pollutant uptake into organisms is ingestion, we have developed a test system that uses single intestinal cells of the nematode roundworm *Caenorhabditis elegans*. Microscopic observation of the cell nucleus in reporter worms for the methyltransferase fibrillarin (FIB-1::GFP) revealed nuclear staining patterns that are specific for pollutants such as silica nanoparticles, BULK silica particles, silver nanoparticles, ionic $AgNO_3$, and inorganic mercury ($HgCl_2$). While the underlying molecular mechanisms need further investigation, cultivation of the reporter worms in liquid culture on microtiter plates now enables cost-effective screening of more pollutants and samples from the environment, *e.g.*, mesocosm analyses. As *C. elegans* leads a dual life in the lab and in ecosystems, alteration of nuclear structure and function may likewise explain how environmental pollutants reduce the fitness of wild worms and thus may negatively affect biodiversity.

Key words Nematodes, Cell nucleus, Gut, Environment, Global change, Pollutants, Nanomaterial, Mercury, Food, Mesocosm

1 Introduction

Our environment faces the three interrelated crises of global change: climate change, fading biodiversity, and the global distribution of pollutants. Global inventories reveal that mercury mobilized by human activities occurs throughout the Atlantic and Pacific oceans in significant concentrations and enters the marine food chain [1, 2]. Consistently, elevated levels of mercury are identified in large human cohorts such as the female US population [3]. Like mercury, microplastics or emerging pollutants such as engineered nanoparticles accumulate in the environmental sinks air, surface waters, soil, and sediments. The environmental concentrations of

Ronald Hancock (ed.), *The Nucleus*, Methods in Molecular Biology, vol. 2175, https://doi.org/10.1007/978-1-0716-0763-3_15,

the widely used nano silica and nano silver particles in sediments are modeled at 4.1–210 μg/kg and 43.3 μg/kg, respectively [4, 5]. In contrast to mercury, the exposition pathways of particles and effects on human health are largely unknown.

The nematode roundworm *Caenorhabditis elegans* represents a relevant animal model in ecotoxicology. Its dual life as a bacterivore on rotting plant material in the wild and a top animal model in the laboratory explains the growing relevance of the worm in the investigation of adverse pollutant effects. *C. elegans* is genetically tractable, amenable to biochemistry, and suitable for whole-life toxicology due to its short adult life span of 2–3 weeks [6, 7]. The ease of cultivating the nematode in high numbers enables the study of individuals or populations, generating data with high statistical relevance [8, 9]. Adult hermaphrodite *C. elegans* possess 959 cells that form organs such as body wall muscles, vulva, spermatheca, pharynx, and the gut. Three hundred and two cells are neurons and 56 are glial cells, constituting the neural system of the worm that harbors all the major neurotransmission pathways and simple neural circuits for complex neuromuscular behaviors and sensation [10].

C. elegans is likewise a surrogate animal model for the intestine. Twenty to 21 epithelial cells with 30–34 visible large nuclei are aligned pairwise along the intestinal lumen [11]. They enable investigation of nutritional uptake pathways and intestinal function as well as effects of pollutants on the nucleus of intestinal epithelial cells. Thus, the intestine of the worm represents a sensitive sensor for xenobiotics that undergo oral uptake [12]. The transparency of *C. elegans* allows for analyses and quantification of specific intestinal epithelial cells and nuclei by differential interference contrast (DIC) microscopy as well as by epifluorescence microscopy of DNA dye-stained nuclei. Also, worms carrying a reporter gene for nuclear proteins such as fibrillarin, the methyltransferase for pre-RNA processing and modification, are available that can be used in expression and localization experiments. The example of the *C. elegans* strain cguIs001 (FIB-1::GFP) [13] is described in this step-by-step protocol.

The cell nucleus is a highly dynamic subcellular structure where form follows function and vice versa. Nuclear architecture tightly reflects environmental stimuli, stress, and disease pathology [14]. A paradigm for this notion is the nucleolus that builds in response to the activity of RNA-polymerase I-dependent transcription of ribosomal RNA (rRNA) [15]. Twenty years ago we showed that concentrations of inorganic mercury (I-Hg) $\geq$5 μM specifically inhibit transcription of rRNA and induce redistribution of fibrillarin from the nucleolus to the nucleoplasm in cultures of human epithelial cells and spleen cells from I-Hg-exposed mice [16]. The idea emerged that specific alteration of nuclear structure and function

identifies effects of pollutants and that the nucleus is a sensitive sensor of environmental pollution.

Meanwhile, other environmental pollutants were discovered to target the nucleus, e.g., the nucleolus. I-Hg as well as silica nanomaterials that are produced in large quantities and widely deposited in environmental sinks [5, 17] induce amyloid protein aggregation in the nucleus [18, 19]. By means of anti-amyloid antibodies and stains such as Congo red or Thioflavin T, amyloid structures were detected especially in the nucleoli of neural cell lines and in epithelial cells of the *C. elegans* intestine [20, 21]. In addition to this local amyloid aggregation, mass spectrometry-based proteomics revealed that nucleolar proteins such as fibrillarin participate in specific aggregomes of I-Hg- and nano silica-exposed or aging *C. elegans* [22, 23]. Neurotoxic pollutants such as I-Hg and nano silica induce widespread amyloid aggregation that includes axons of single neurons, disturbs neurotransmission, and ultimately elicits premature defects of neuromuscular behaviors such as reduced locomotion that normally occur in old *C. elegans* [7].

Naturally, studies of invertebrate animal models such as *C. elegans* raise the question of cross-species translation, i.e., if results concerning toxic effects obtained in a nematode are of any value or concern to humans. Notably, approximately 20,000 genes encode the nematode's proteins and the majority (60–80%), including disease genes, have a counterpart/homologue in the worm [24]. Key pathways and signaling molecules are conserved between worms and mammals [25]. Consistently, *C. elegans* is used as a tool for reliable and cost-effective medium-throughput screening of neuroprotective compounds, some of which are running in phase 3 clinical trials [26]. Moreover, the basics of intestinal cell architecture are strikingly similar in worms and humans [27, 28], which justifies *C. elegans* as a relevant surrogate animal model for the human intestine. In this chapter we introduce methods to use monitoring of single intestinal epithelial cells as a tool for detection of pollutant effects in *C. elegans* (*see* Fig. 1).

Investigation of cell nuclei provides the platform to analyze wild worms isolated from contaminated environments or for treatment of laboratory worms with soil, sediment, and surface water probes which represent mesocosm studies. The ongoing global change crises (*see* Fig. 2) urgently require respective innovation of environmental research that is reliable, statistically relevant, cost-effective, and practicable in medium- to high-throughput formats.

2 Materials

2.1 Strains

1. *C. elegans* SJL1 received from Prof. Szecheng J. Lo, Department of Biomedical Sciences, College of Medicine, Chang Gung University, TaoYuan 333, Taiwan. This strain carries

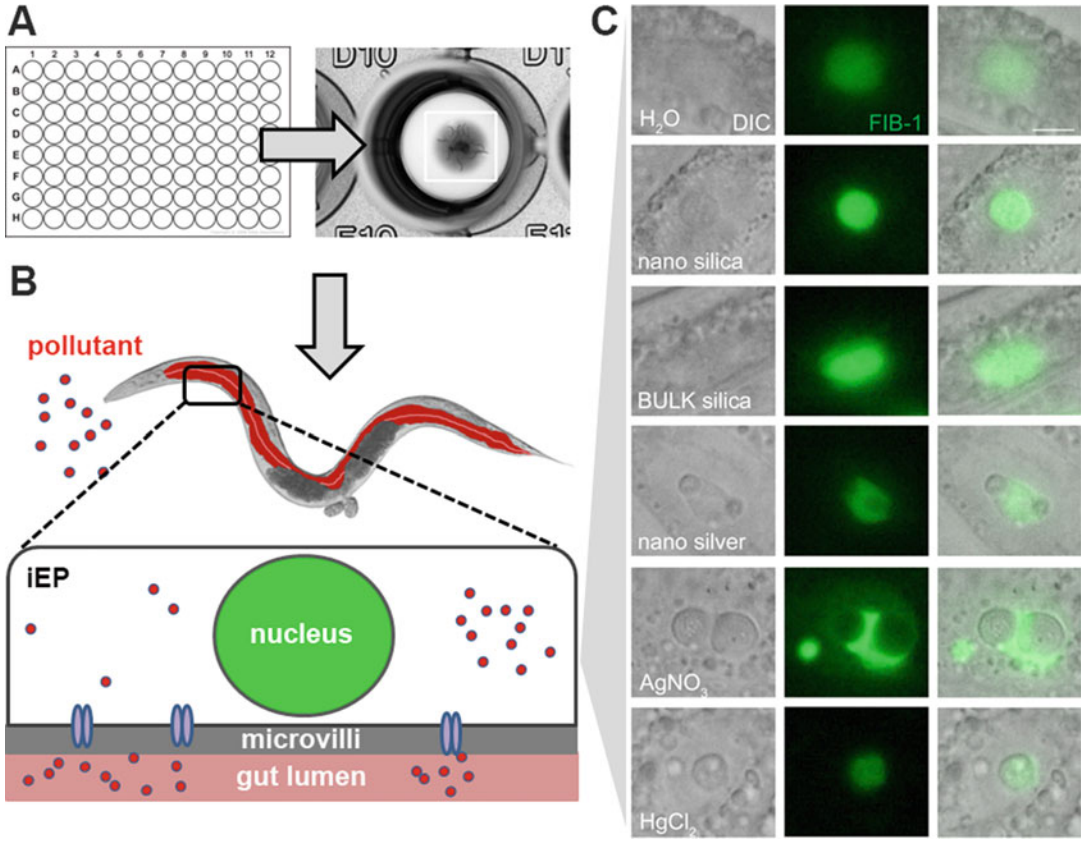

Fig. 1 Analysis of the localization of FIB-1::GFP in nuclei of intestinal cells in reporter *C. elegans*. (**a**) Schematic of *C. elegans* cultivation in a liquid medium microtiter plate format. The single well shows the microtiter habitat with bacteria as food supply and 10–15 worms. (**b**) Schematic of an adult hermaphrodite worm and blow-up of one single intestinal epithelial cell. The cell nucleus is depicted in green. (**c**) Differential interference contrast micrographs (DICs, left column), fluorescence of FIB-1::GFP (green, middle column), or combined DIC and FIB-1::GFP fluorescence (right column) of hermaphrodite adult worms that were left untreated (H_2O) or treated for 72 h at 20 °C with nano-sized silica particles, BULK-sized silica particles, nano-sized silver particles, the silver salt $AgNO_3$, or inorganic mercury ($HgCl_2$). Each micrograph shows one representative nucleus of an intestinal cell and the nuclear localization of FIB-1::GFP (green). *FIB-1* fibrillarin, *iEP* intestinal epithelial cell. Bar, 5 μm

the transgene *cguIs1* ($P_{fib\text{-}1}$::fib-1::gfp::3′ UTR $_{fib\text{-}1}$) stably integrated in the genome. The *gfp* gene was inserted into the last codon of the *fibrillarin-1* (fib-1) open reading frame to obtain a translational reporter encoding the fusion protein FIB-1::GFP. Worms stably express the reporter protein in cell nuclei under the control of the fib-1 promoter [13, 29]. This strain is available from the Corresponding Author upon request.

2. *Escherichia coli* (*E. coli*) strain OP50.

Fig. 2 Schematic of the interrelated global change crises

2.2 Reagents, Buffers, and Solutions

1. Nematode Growth Medium (NGM) plates: Add 750 mL distilled H_2O (dH_2O) to 15 g of BD Bacto Agar, 2.25 g NaCl, and 1.9 g BD Bacto Proteose No.3. Supplement the NGM agar for culturing with 3.75 g BD Bacto yeast extract. Autoclave to sterilize, cool down to 55 °C, and add 750 µL of solution A, 375 µL of solution B, 750 µL of solution C, and 18.75 mL of solution D. Mix carefully by shaking the flask and pour into 9 cm ∅ Petri dishes under sterile conditions. After drying overnight, spread 500 µL of an overnight culture of *E. coli* OP50 with an inoculation spreader in the center of the plate [30] (*see* **Note 1**).
2. Solution A: add 0.5 g cholesterol to 100 mL of absolute (>99.5%) ethanol.
3. Solution B: add 11.08 g $CaCl_2$ to 100 mL dH_2O, autoclave.
4. Solution C: add 24.65 g $MgSO_4 \cdot 7H_2O$ to 100 mL dH_2O, autoclave.
5. Solution D: 108.3 g KH_2PO_4, 36 g K_2HPO_4 in 1 L dH_2O, autoclave.
6. Liquid medium (S medium): add 2.93 g NaCl, 0.5 g K_2PO_4, and 3 g KH_2PO_4 to 500 mL dH_2O and autoclave to sterilize. Cool down to 4 °C and add 0.5 mL solution A, 5 mL 1 M potassium citrate pH 6.0, 5 mL trace metals solution, 1.5 mL 1 M $CaCl_2$, and 1.5 mL 1 M $MgSO_4$. To prevent the growth of unwanted bacteria and fungi add 205 µL of Fungizone antimycotic (Amphotericin B, stock solution 250 µg/mL) and 515 µL Carbenicillin (50 mg/mL stock in dH_2O). Mix carefully by shaking the flask. Next, overnight cultures of *E. coli* OP50 grown in LB-Medium are used to make a concentrated

pellet of bacteria. Pour 50 mL of OP50 culture into a 50 mL sterile conical centrifuge tube and spin at 2000 × *g* for 10 min at 4 °C. Discard the supernatant and suspend the pellet in S Medium [30–32]

7. 1 M potassium citrate pH 6.0: add 20 g citric acid monohydrate and 293.5 g tri-potassium citrate monohydrate to 900 mL dH_2O and shake until the solutes have dissolved. Adjust the volume of the solution to 1 L with dH_2O, adjust the pH to 6.0, and sterilize by autoclaving.
8. Trace metals solution: add 1.86 g EDTA disodium salt dihydrate, 0.69 g $FeSO_4{\cdot}7H_2O$, 0.2 g $MnCl_2{\cdot}4H_2O$, 0.29 g $ZnSO_4{\cdot}7H_2O$, and 0.025 g $CuSO_4{\cdot}5H_2O$ to 900 mL dH_2O and shake until the solutes have dissolved. Adjust the volume of the solution to 1 L with dH_2O and sterilize by autoclaving. Store in the dark.
9. 1 M $CaCl_2$: dissolve 54 g $CaCl_2{\cdot}6H_2O$ in 150 mL dH_2O. Adjust the volume to 200 mL with dH_2O and sterilize by autoclaving.
10. 1 M $MgSO_4$: dissolve 120.4 g $MgSO_4$ (anhydrous) in 900 mL dH_2O. Adjust the volume to 1 L with dH_2O and sterilize by autoclaving.
11. 5-Fluoro-2′-deoxyuridine (FUdR): dissolve 36 µL of 6.25 mM FUdR in dH_2O, add to the S medium in 96-well microtiter plates to keep the worm culture age-synchronized.
12. Worm buffer M9: dissolve 3 g KH_2PO_4, 6 g Na_2HPO_4, 0.5 g NaCl, and 1 g NH_4Cl in 1 L dH_2O. Sterilize by autoclaving.
13. Synchronization solution (10 mL): 2 mL 4 M NaOH, 3 mL 12% NaClO (*see* **Note 2**), 5 mL dH_2O.
14. 50 nm silica nanoparticles (nano silica) and 500 nm silica particles (BULK silica), 25 mg/mL stock solutions (Kisker, Steinfurt, Germany).
15. 15 nm silver nanoparticles (nano silver): 100 mg/mL stock solution in Polyoxyethylene Glycerol Trioleate and Polyoxyethylene(20)-sorbitanmonolaurate (Tween-20) (Joint Research Centre, Brussels, Belgium) [33].
16. 100 mg/mL $AgNO_3$ stock solution in sterile dH_2O.
17. 50 mM $HgCl_2$ stock solution in sterile dH_2O.
18. 10% NaN_3 in 5% agarose solution: prepare 50 mg agarose in a 1.5 mL Eppendorf tube, add 900 µL dH_2O and 100 µL NaN_3 under the chemical hood. Mix by inverting the tube and heat at 96 °C until the agarose has dissolved and the solution is viscous. Cool it down and keep it under the hood. Agarose solidifies at room temperature (*see* **Notes 3** and **4**).

2.3 Equipment

1. Stereo microscope.
2. 96-well microtiter plates.
3. Worm picker: flame the tip of a glass Pasteur pipette to melt a 32-G platinum wire into the glass [30].
4. 9 cm ∅ Petri plates with ventilation cams.
5. Pasteur pipettes, centrifuge tubes, and Eppendorf tubes.
6. 20 °C incubator to culture *C. elegans.*
7. SuperFrost Cytoslides, uncoated (Thermo Scientific); glass coverslips 22 × 22 mm, 1.5 thickness.
8. Fluorescence microscope.
9. Thermomixer.

3 Methods

3.1 Culture and Synchronization of C. elegans

C. elegans cultures are maintained on Petri dishes with NGM at 20 °C. The plates are seeded with a lawn of OP50, a uracil-auxotroph *E. coli* strain. To obtain an age-synchronized culture for exposure to environmental pollutants, worms are treated with the synchronization solution where eggs are isolated and seeded on new plates [30, 31]. Use a worm picker to transfer around 20 adult *C. elegans* onto 2 fresh 9 cm NGM plates supplemented with yeast extract, and culture at 20 °C for ~3 days until the plates contain ~500 gravid hermaphrodites (*see* **Note 5**).

1. Harvest the worms by washing them off the plate with buffer M9, collect them in a 15 mL tube by centrifugation at 250 ×*g* for 1.5 min, and discard the supernatant.
2. Add 5 mL of synchronization solution (*see* **Note 2**) to the worm pellet, resuspend by inverting the tube 3× (*see* **Note 6**), spin down at 3000 × *g* for 30 s, and discard the supernatant (*see* **Note 7**).
3. Repeat the preceding step.
4. Wash the worm pellet 3× with dH_2O and spin down at 3000 × *g* for 30 s.
5. Discard the supernatant and distribute the egg pellet onto two new 9 cm NGM plates supplemented with yeast extract and seeded with OP50.
6. Incubate the eggs at 20 °C. They develop into L4 larvae after ~44 h [34].

3.2 Exposure of C. elegans to Environmental Pollutants

The exposure to environmental pollutants like nanomaterials, silver nitrate, or mercury occurs in liquid medium with OP50 as food source. To maintain an age-synchronous culture, FUdR is added to L4 larvae which inhibits DNA synthesis and prevents self-fertilization

Table 1
Concentrations of environmental pollutants

Pollutant	Predilution	Final concentration in each well
Nano silica (mg/mL)	2	0.2
BULK silica (mg/mL)	2	0.2
Nano silver (mg/mL)	0.5	0.05
$AgNO_3$ (mg/mL)	0.5	0.05
$HgCl_2$ (mM)	0.5	0.05

[6, 31, 35]. One-day old, age-synchronized, adult hermaphrodites are exposed to the respective pollutant and incubated in 96-well microtiter plates at 20 °C. After 3 days, an altered distribution of FIB-1::GFP is observed in nuclei of single intestinal cells.

1. Wash the L4 larvae (*see* **Note 8**) off the plate with M9 and transfer them into a 15 mL tube. Let the larvae sink to the bottom and remove the buffer with a pipette.
2. Wash the pellet 3× with M9 buffer by inverting the tube, spin down at 250 × *g* for 1.5 min, and discard the supernatant.
3. Resuspend the worm pellet in liquid medium with 18 mg/mL OP50 in a 50 mL tube by inverting the tube (*see* **Note 9**).
4. Check the number of worms in the medium by pipetting 99 μL of liquid medium with worms onto a cytoslide; this should contain ~15–20 worms (*see* **Note 10**).
5. Use a cropped pipette tip to transfer 99 μL liquid media with worms into each well of a 96-well microtiter plate. Leave the external wells out and fill them with 200 μL dH_2O to avoid desiccation of the inner wells.
6. Add 36 μL of 6.25 mM FUdR to the worms in each well to keep the culture age-synchronized over the entire experiment (*see* **Note 11**).
7. Shake the plates in the thermomixer at 1000 rpm for one min at 20 °C.
8. Incubate at 20 °C in the dark.
9. The next day, add 15 μL of each environmental pollutant to be tested to the 1-day old, adult *C. elegans* in the wells (*see* Table 1). Wells with control worms receive 15 μL of dH_2O.
10. Shake the plates in the thermomixer at 1000 rpm for 1 min at 20 °C.
11. Incubate at 20 °C for 3 days in the dark (*see* **Note 12**).

3.3 Immobilization and Microscopy of FIB-1::GFP Reporter Worms

In order to observe the localization of FIB-1::GFP in intestinal nuclei of living *C. elegans*, 4-day-old, adult hermaphrodites are immobilized on cytoslides with agarose pads including NaN_3 [36].

1. Prepare cytoslides with an agarose pad containing NaN_3 (*see* Subheading 2.2, **item 12**). Heat the 1.5 mL Eppendorf tube at 96 °C until the agarose is viscous. Before use, mix up the agarose by inverting the tube (*see* **Notes 3** and **4**). Pipette 20 μL of agarose onto a cytoslide and place a second cytoslide on top (*see* **Note 13**). Let the slides dry under the hood for 10 min.
2. Collect the worms of each treatment group with a glass pipette into one well of the microtiter plate.
3. Let them sink to the bottom and discard the supernatant.
4. Remove OP50 and pollutants by washing the worms in each well at least 3× with M9. After the last wash, discard the supernatant.
5. Pull the prepared cytoslides carefully apart so that the agarose pad on the slide appears flat without any bends.
6. Transfer the worms with a glass pipette onto the agarose pad and remove the remaining liquid.
7. Carefully place a coverslip onto the worms in order to avoid damaging their tissues (*see* **Note 14**).
8. Immobilize the worms for 30–45 min at 20 °C in the dark.
9. Detect FIB-1::GFP in the intestinal cells by fluorescence microscopy. GFP can be excited with 488 nm and emits fluorescence at 510 nm (*see* **Note 15**).

4 Notes

1. Prevent damaging the surface of the NGM or spread of *E. coli* to the edges of the plate to avoid *C. elegans* from crawling into the agar or off the plate, respectively.
2. Be aware that NaOH and NaClO are corrosive.
3. Be aware that NaN_3 disturbs the electron transport of the mitochondrial respiratory chain by inhibiting cytochrome oxidase. For appropriate protection use thick gloves, safety goggles, and a lab coat and work under the hood.
4. $AgNO_3$, $HgCl_2$, and NaN_3 are toxic and have to be handled with care and disposed of according to institutional safety regulations.
5. Avoid starvation of adult *C. elegans* hermaphrodites, because starved worms develop an internal hatch phenotype and eggs cannot be isolated anymore. Food should always be abundant.

6. Tap the tube with your fingers to loosen the pellet.
7. To control the isolation procedure, check whether the hermaphrodites released their eggs. Be careful, long incubation in synchronization solution will harm the eggs, too. Proceed when the first eggs appear outside the hermaphrodites.
8. The eggs develop after ~44 h into L4 larvae. It is important to monitor the development in every experiment. L4 larvae are distinguishable by a characteristic white triangle at the developing vulva.
9. The final concentration of OP50 in each well should be 12 mg/mL.
10. To prevent damaging worms, use a cropped pipette tip and mix the liquid media by inverting the tube before pipetting. Remove or add liquid medium in order to obtain 15–20 worms in 99 μL of liquid medium. Check the number of worms at least twice.
11. The final concentration of FUdR in each well should be 1.5 mM.
12. Shake the plate every second day to mix up the components.
13. Use a cropped pipette tip, because agarose is very viscous and easily attaches to the pipette tip.
14. Air bubbles should be avoided.
15. Be aware of autofluorescence and always include a wild-type (N2) negative control. Analyze only worms with good preservation of their tissues.

References

1. Bocharova N, Treu G, Czirják GÁ et al (2013) Correlates between feeding ecology and mercury levels in historical and modern arctic foxes (Vulpes lagopus). PLoS One 8:e60879
2. Lamborg CH, Hammerschmidt CR, Bowman KL et al (2014) A global ocean inventory of anthropogenic mercury based on water column measurements. Nature 512:65–68
3. Laks DR (2014) Mercury rising: response to the EPA assessment of mercury exposure. Biometals 27:1–4
4. Sun TY, Bornhöft NA, Hungerbühler K et al (2016) Dynamic probabilistic modeling of environmental emissions of engineered nanomaterials. Environ Sci Technol 50:4701–4711
5. Wang Y, Nowack B (2018) Dynamic probabilistic material flow analysis of nano-SiO_2, nano iron oxides, nano-CeO_2, nano-Al_2O_3, and quantum dots in seven European regions. Environ Pollut 235:589–601
6. Piechulek A, von Mikecz A (2018) Life span-resolved nanotoxicology enables identification of age-associated neuromuscular vulnerabilities in the nematode *Caenorhabditis elegans*. Environ Pollut 233:1095–1103
7. Piechulek A, von Mikecz A (2019) Aging by pollutants: introducing the aging dose $[AD]_{50}$. Environ Sci Eur 31:23
8. Jung SK, Qu X, Aleman-Meza B et al (2015) Multi-endpoint, high-throughput study of nanomaterial toxicity in Caenorhabditis elegans. Environ Sci Technol 49:2477–2485
9. von Mikecz A (2018) Lifetime eco-nanotoxicology in an adult organism: where and when is the invertebrate C. elegans vulnerable? Environ Sci Nano 5:616–622
10. Hobert O, Glenwinkel L, White J (2016) Revisiting neuronal cell type classification in Caenorhabditis elegans. Curr Biol 26: R1197–R1203

11. Dimov I, Maduro MF (2019) The C. elegans intestine: organogenesis, digestion, and physiology. Cell Tissue Res. https://doi.org/10.1007/s00441-019-03036-4. [Epub ahead of print]
12. Piechulek A, Berwanger L, von Mikecz A Silica nanoparticles disrupt OPT-2/PEP-2-dependent trafficking of nutrient peptides in the intestinal epithelium. Nanotoxicology 13:1133–1148
13. Lee LW, Lee CC, Huang CR, Lo SJ (2012) The nucleolus of *Caenorhabditis elegans*. J Biomed Biotechnol 2012:601274
14. Boulon S, Westman BJ, Hutten S et al (2010) The nucleolus under stress. Mol Cell 40:216–227
15. Lam YW, Trinkle-Mulcahy L, Lamond AI (2005) The nucleolus. J Cell Sci 118:1335–1337
16. Chen M, von Mikecz A (2000) Specific inhibition of rRNA transcription and dynamic relocation of fibrillarin induced by mercury. Exp Cell Res 259:225–238
17. Creed IF, Bergström AK, Trick CG et al (2018) Global change-driven effects on dissolved organic matter composition: Implications for food webs of northern lakes. Glob Chang Biol 24:3692–3714
18. Chen M, Singer L, Scharf A, von Mikecz A (2008) Nuclear polyglutamine-containing protein aggregates as active proteolytic centers. J Cell Biol 180:697–704
19. Scharf A, Piechulek A, von Mikecz A (2013) Effect of nanoparticles on the biochemical and behavioral aging phenotype of the nematode Caenorhabditis elegans. ACS Nano 7:10695–10703
20. Arnhold F, Gührs KH, von Mikecz A (2015a) Amyloid domains in the cell nucleus controlled by nucleoskeletal protein lamin B1 reveal a new pathway of mercury neurotoxicity. PeerJ 3: e754
21. Arnhold F, Scharf A, von Mikecz A (2015b) Imaging and quantification of amyloid fibrillation in the cell nucleus. Methods Mol Biol 1228:187–202
22. Scharf A, Gührs KH, von Mikecz A (2016) Anti-amyloid compounds protect from silica nanoparticle-induced neurotoxicity in the nematode C. elegans. Nanotoxicology 10:426–435
23. Scharf A, von Mikecz A unpublished.
24. Kaletta T, Hengartner MO (2006) Finding function in novel targets: C. elegans as a model organism. Nat Rev Drug Discov 5:387–398
25. Kim W, Underwood RS, Greenwald I et al (2018) OrthoList 2: a new comparative genomic analysis of human and Caenorhabditis elegans genes. Genetics 210:445–461
26. Wischik CM, Staff RT, Wischik DJ et al (2015) Tau aggregation inhibitor therapy: an exploratory phase 2 study in mild or moderate Alzheimer's disease. J Alzheimers Dis 44:705–720
27. McGhee JD (2007) The C. elegans intestine. WormBook 27:1–36
28. Pukkila-Worley R, Ausubel FM (2012) Immune defense mechanisms in the Caenorhabditis elegans intestinal epithelium. Curr Opin Immunol 24:3–9
29. Yi YH, Ma TH, Lee LW et al (2015) A genetic cascade of let-7-ncl-1-fib-1 modulates nucleolar size and rRNA pool in *Caenorhabditis elegans*. PLoS Genet 11(10):e1005580
30. Stiernagle T (1999) Maintenance of *C. elegans*. In: Hope IA (ed) *C. elegans*. A practical approach. Oxford University Press, Oxford, pp 51–67
31. Brenner S (1974) The genetics of *Caenorhabditis elegans*. Genetics 77:71–94
32. Petrascheck M, Ye X, Buck LB (2007) An antidepressant that extends lifespan in adult *Caenorhabditis elegans*. Nature 450:553–556
33. Klein CL, Comero S, Stahlmecke B et al (2011) NM-Series of representative manufactured nanomaterials - NM 300 silver characterisation, stability, homogeneity. JRC Scientific and Technical Reports. European Union, Luxembourg, EUR 24693 EN
34. Altun ZF, Hall DH (2020). Handbook of C. elegans Anatomy. In WormAtlas. http://www.wormatlas.org/hermaphrodite/hermaphroditehomepage.htm
35. Gandhi S, Santelli J, Mitchell DH et al (1980) A simple method for maintaining large, aging populations of *Caenorhabditis elegans*. Mech Ageing Dev 12:137–150
36. Sulston JE, Hodgkin J (1988) Methods. In: Wood WB (ed) The nematode *Caenorhabditis elegans*. Cold Spring Harbor Laboratory Press, Cold Spring Harbor, pp 587–606

INDEX

Ronald Hancock (ed.), *The Nucleus*, Methods in Molecular Biology, vol. 2175, https://doi.org/10.1007/978-1-0716-0763-3,

L

M

N

P

R

S

T

U

Y